CONTENTS

VOLUME 111
JULY SEPTEMBER NOVEMBER 1962

PUBLISHED BY
THE WISTAR INSTITUTE OF ANATOMY AND BIOLOGY
PHILADELPHIA PA

CONTENTS

No. 1 JULY 1962

No. 2 SEPTEMBER 1962

No 3 NOVEMBER 1962

The Comparative Structure of the Ureter

HIN-CHING LIU
Department of Anatomy University of Hong Kong

While the comparative anatomy of the kidney is relatively well-known, information in the literature concerning the renal excretory duct systems in vertebrates is almost exclusively confined to the mammals.

The purpose of this study was to obtain information on the gross anatomy and histology and on certain histochemical aspects, of the ureter and its branches in the different vertebrate classes.

This information is presented here, together with a brief discussion of possible structural and functional correlations.

MATERIALS AND METHODS

The following adult vertebrates occurring in South China were studied:

Fish Fresh-water — *Cyprinus carpio Ctenopharyngodon idellus Aristichthys nobilis*

Marine — *Sugaxus sp Epinephelus sp Plectorynchus pictus*

Amphibians — *Bufo asiatica Rana esculenta.*

Reptiles — The soft-shelled turtle (*Chelonia amyda*) Lizard (*Gecko gecko*) Skink (*Eumeces chinensis*)

Birds — Duck (*Melanitta deglandi*) Pigeon (*Columba livia*) Domestic fowl (*Gallus domesticus*)

Mammals — Dog (*Canis familiaris*) Cat (*Felis domesticus*) Rabbit (*Oryctolagus cuniculus*)

A. Anatomical

The animals were killed by overdosing with chloroform. Two methods were employed in studying the gross morphology

1 Carmine-gelatine was injected until the system was completely filled, the quantity of the injection mass being visually controlled. After injection the specimen was fixed in 10% formalin, and later the solidified injection mass was freed from its surrounding tissues by microdissection.

2. Vinyl acetate casts were prepared as above except that the ureters were first perfused with physiological saline to remove the urine. After solidification of the vinyl acetate in cold water a cast was prepared by corrosion with 10% KOH. In a few instances after injection with vinyl acetate, the kidney was first treated with 5% KOH overnight, and then cleared in glycerin (figs. 8 10) Ureteral lengths were measured from vinyl acetate casts and the average thickness of the periureteral smooth muscle calculated from sections of the upper middle and lower thirds of the ureters. Only those sections as close to the transverse plane as possible were selected for measurement.

B Histological

The ureters were first perfused and slightly distended with fixative (Zenker formol, SUSA, or Corrosive sublimate) and tissue blocks prepared from the intra and extra-renal portion of the duct. After embedding in paraffin wax (mp 48 C) sections of about 8 μ were cut, divided into three groups and treated as follows

Group I. Sections were stained by Masson's trichrome method, *Weigert's* elastin stain, and by azocarmine to show the general histology of the ureters.

Group II The periodic acid-Schiff reaction (Pearse '53) was employed to test sections for the presence of polysaccharide complexes. Control sections were incubated for two hours at room temperature in a 40% mixture of saliva in distilled water

Group III Sections in this group were stained for 30 seconds in 1% Alcian blue 8GS to test for acid mucopolysaccharides (Steedman, '50) and counterstained by *Ehrlich's* haematoxylin.

OBSERVATIONS

For descriptive purposes the term secondary ureteric tributary (SUT) is here used to designate the order of intra-renal tubule receiving urine from the collecting tubules of the nephron. The term primary ureteric tributary (PUT) refers to the order of tubule which conducts the urine from the SUT into the main intra renal ureteric canal. In estimating the amount of periureteral smooth muscle (fig 1) only those sections as close as possible to the transverse plane were selected for measurement.

General Anatomy

Since the figures tables etc presented here obviate much detailed verbal description this section consists of notes briefly indicating the principal differences and similarities seen in the species examined.

I Fish

Vinylacetate casts show that the intrarenal portion of the ureteric canal derives from two orders of tubule as follows:—

(1) A number of larger primary radicles (PUT) occupying the centers of the renal lobules and arising from the main ureteric duct at acute angles.

(2) A number of secondary radicles (SUT) which receive the contents of the lobular collecting tubules (figs. 4 7 8 11 14) Table 1 lists the number of renal lobules and PUT observed in casts of the ureteric systems in the different types studied.

Histology

(1) *Fresh water species.* In all three types studied the epithelium of the ureter and its radicles consists of a single layer

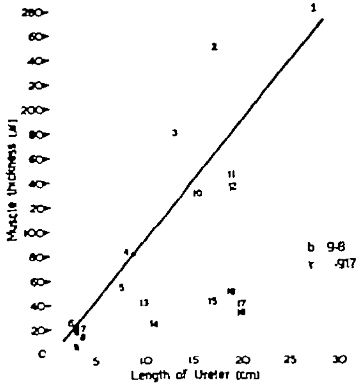


Fig. 1 The relationship between ureteral muscle thicknes and ureteral length in various species. 1 *Canis familiaris* 2 *Melanitta deglandi* 3 *Gallus domesticus*; 4 *Columba livia*; 5, *Chelonia mydas*, 6, *Eumeces chinensis* 7 *Rana esculenta*; 8 *Gecko gecko*; 9 *B f asiaticus*; 10, *Naja* tra; 11 *Oryctolagus cuniculus*; 12, *Felis domesticus*. The square points 13–15 represent the salt-water fish *Epinephelus* sp., *Siganus* sp., and *Plectorynchus pictus* respectively The points 16–18 represent the freshwater fish *Cyprinus carpio* *Aristichthys nobilis* and *Ctenopharyngodon idella* respectively The data from fish were not included in the calculation of the regression line b.

TABLE 1

Species	Fresh-water						Marine					
	Cyprinus carpio		*Ctenopharyngodon idellus*		*Aristichthys nobilis*		*Plectorhynchus pictus*		*Epinephelus* sp.		*Siganus* sp.	
	L[1]	R[1]	L	R	L	R	L	R	L	R	L	R
No. of lobules and PUT	35	33	48	36	31	20	34	33	34	34	24	19

L — left kidney.
R — right kidney

of tall columnar mucin-secreting epithelial cells with numerous goblet-forms interspersed among them. The cell nuclei are vesicular and possess a well-marked nucleolus. In the intra renal portions the fine tubules are surrounded by a delicate layer of collagenous connective tissue in which a few peritubular smooth muscle cells, and a thin layer of pigment cells occur.

In the ureter proper both longitudinal and circular smooth muscle layers occur gradually increasing in amount from the upper and middle to the lower thirds of its length. Of these two layers, however the longitudinal predominates. In all the fresh-water types examined intraepithelial parasites were commonly seen in all parts of the ureteric system and under low magnifications give the epithelial layer a pseudostratified appearance.

(2) *Marine species* Except that goblet cells are absent from the epithelium, the histology did not differ from that of the fresh-water types. Intraepithelial parasites gave the same general impression of pseudo-stratification as described above.

II Amphibians

General anatomy

(1) *Bufo asiatica* (fig. 9) The upper third of the ureter passes along the lateral edge of the kidney within which it is partly embedded. At the distal end of the kidney the ureter becomes free and abruptly enlarges to form a thin-walled tube about twice the diameter of the renal portion. Towards the cloacal end the thickness of the ureteral wall increases. Vinylacetate casts show that nine short PUT emerge from the renal portion and split into a variable number of SUT which enter the renal lobules.

(2) *Rana esculenta*. As above.

Histology

(1) *Bufo asiatica*. Within the renal portion of the ureteric system the PUT and SUT are lined by a cuboidal epithelium resting on a basement membrane and invested by a thin coat of collagenous connective tissue. In the main ureteric duct the epithelium is columnar. Mucinogen granules occupy the apical cytoplasm of the cells but there are no goblet cells present. The wall of the tube contains a few smooth muscle cells scattered within the collagenous connective tissue coat.

Although there is a distinct difference in the lumen size as between the renal and free portions, the gradual increase in the thickness of the ureteral wall is due to an increase in the thickness of the connective tissue coat and not to the development of an organized smooth muscle layer.

(2) *Rana esculenta*. As above.

III Reptilia

General anatomy

In the lizard, snake, and turtle the renal lobules do not aggregate to form lobes. Table 2 shows the number of renal lobules usually encountered in the forms studied. Vinylacetate casts indicate that the intrarenal portion of the ureteric canal is derived from two orders of tubule as follow: A variable number of SUT which receive the contents of the numerous lobular collecting tubules; and larger PUT occupying the centers of the lobules and joining the main ureteric duct at acute angles.

(1) *Gecko gecko* (fig. 10) The ureter is a slender thin-walled tube. It passes along the ventral surface of the kidney which occupies the posterior sacral region close to the cloaca.

(2) *Eumeces chinensis* As above

(3) *Naja atra* (fig. 7) While the ureters are of equal length they do not occupy the same level the left assuming a more dorsal position in the body than the right. They lie along the center of the ventral surface of the kidney and continue in free portions which pass caudally towards the cloaca.

(4) *Chelonia amyda* (fig 8) As above except that the ureters are on the same level within the body

TABLE 2

Species	*Gecko gecko*	*Eumeces chinensis*	*Naja atra*	*Chelonia amyda*
No. of lobules and PUT	8	8	18	11

Histology

(1) *Gecko gecko*

(2) *Eumeces chinensis* In these species the PUT are very short compared with those of the turtle and snake.

The ureteric tributaries and the entire length of the ureter are lined by a simple columnar epithelium which is invested by delicate lamina propria containing thin longitudinal smooth muscle fibers The epithelium rests on a delicate basement membrane Sections stained by Weigert's elastin stain show a coarse sub-epithelial elastic network whose thickest elements are longitudinally disposed. The extra-renal free position shows a histological structure similar to the foregoing but there is a general increase in the diameter of the ureter due to an increase in the thickness of its adventitial coat. The lumen is wider and the epithelial lining less folded than in the intra renal portions. Towards the cloacal end a thin layer of circular smooth muscle appears in the adventitial coat. There is an increase in the number of mucin secreting cells in the epithelial lining from the ureteric tributaries to the extra-renal portion of the ureter

(3) *Naja atra* The primary ureteric tributaries are relatively long and enter the main ureteric canal at very acute angles. The ureteric tributaries and the main ureteric duct are lined by a simple columnar epithelium containing a high proportion of mucin secreting cells. The epithelial layer rests on a delicate basement membrane and is supported by a collagenous lamina propria of which a sub-epithelial elastin lamina is a prominent feature. Tissue eosinophil cells and macrophages are often found in this zone The smooth muscle coats start in the primary tributaries as thin inner longitudinal and very delicate outer circular layers, and only in the lower third of the free portion of the ureter a third external longitudinal layer develops.

(4) *Chelonia amyda* In kidney sections cut to show the origin of the ureteric branches the collecting tubules can be identified as delicate structures lined by a simple columnar epithelium containing a few mucin secreting cells. The primary and secondary ureteric radicles have a pseudo-stratified columnar epithelium in which goblet cells are prevalent. A basement membrane is absent but the epithelial lining is supported by a thin lamina propria containing a delicate elastic net work and a thin longitudinally arranged smooth muscle. A thin adventitia of collagenous connective tissue which contains a few circularly arranged smooth muscle fibers separates the secondary tubules from the surrounding renal tissue

The intra-renal portion of the ureteric canal shows a similar structure except that there is present considerable folding of the epithelium and lamina propria and an obvious increase in the number of epithelium mucin-secreting cells.

In the extra renal free portion of the ureter the epithelial folding is more marked than in the enclosed portions and the musculature is weak and ill-defined. In this region however the adventitia is relatively thick, and the subepithelial elastic network has spread outwards to invest the muscular elements and penetrate the outer collagenous coat. The histological picture holds good for the entire length of the free portion of the ureter except that in the terminal portion close to the cloaca a few longitudinal muscle fibers and many elastin fibers may be encountered in the thick adventitial coat.

IV *Aves*

General anatomy

(1) Melanitta deglandi. (2) Columba livia. (3) Gallus domesticus Table 3 shows the number of lobules and PUT occurring in the three main renal lobes. In all three species the ureter passes through the center of the renal lobes and the ureteric tributaries connect with the ureter on its dorsal side. The duck has a thicker ureteral wall than either the pigeon or the hen.

TABLE 3

Species	*Gallus domesticus*	*Columba livia*	*Melanitta deglandi*
Upper lobe	8	6	7
Middle lobe	2	3	3
Lower lobe	3	2	8–9

Histology

(1) Melanitta deglandi The collecting tubules are lined by columnar epithelial cells, few of which appear to be mucin-secreting. There is a distinctive basement membrane and the tubules are supported by a thin collagneous connective tissue lamina. The primary and secondary ureteric tributaries and both the renal and the external portions of the main ureteric duct are lined by a pseudo-stratified columnar epithelium. There is an obvious increase in the numbers of the mucin-secreting cells from the primary down to the secondary tributaries and the main ureteric duct. In sections, secondary tubules may be found in groups each tube surrounded by a lamina propria and a few longitudinally disposed muscle fibers and the entire group ensheathed in a connective tissue coat in which a few circularly arranged muscle fibers are found. The renal portion of the ureter is surrounded by two smooth muscle layers, an inner longitudinal and an outer circular; and there is an extensive elastic network in the thick lamina propria underlying the epithelial lining The musculature increase in thickness toward the distal (free) portion of the ureter where an additional outer longitudinal layer occupies the adventitia

(2) *Columba livia* In this species the arrangement of the musculature is similar to that in the duck and hen. But individually the layers are much thinner in the pigeon, as are the *lamina propria* and subepithelial elastic lamina.

(3) Gallus domesticus. The epithelial lining of the different categories of tributary and of the ureter proper are similar to those of the duck. The main difference between the ureters of this and the previous species is to be found in the quantity and distribution of the smooth musculature. While an inner longitudinal and a middle circular layer are present in sections of the hen ureter these layers tend to be thinner than in the duck and the outer longitudinal muscle coat only developes towards the cloacal end of the ureter The quantity and distribution of the lamina propria are similar to that seen in the duck.

V *mammalia*

The gross anatomy and histology of the ureter and its tributaries are well-known and do not here require special description. For comparative purposes in this study the vinyl acetate casts and histological preparations did not reveal any new information.

The PAS and alcian blue 8GS reactions The distribution of PAS-positive material, and the results of the Alcian blue 8GS reaction for acid mucopolysaccharides in the various species studied are shown in table 5 The following additional observations were noted

Marine and fresh-water fish. In both types the actively secreting epithelial elements showed PAS-positive granules in the apical cytoplasm. Fresh-water fish were distinguished from the marine varieties by the presence of large numbers of strongly PAS-positive goblet cells (figs. 18 19)

Amphibians The PAS-positive material was concentrated at the free surface of the epithelial cells.

Reptiles All the varieties studied contained strongly-positive granules in the apical cytoplasm of the epithelial cells. The turtle however differed from others in possessing more epithelial goblet cells showing a strong PAS-positive reaction, and in the absence of a distinct basement membrane.

Birds In all three species the epithelial cells were PAS-negative or showed only a

faint diffuse reaction. Within this epithelium the goblet cells were strongly PAS-positive.

Mammals The PAS reaction in dog, cat, and rabbit are given in table 5 for comparison with the other species. Figure 17 shows the distribution of PAS-positive material in the transitional epithelium of the dog's ureter

Control sections incubated at room temperature for two hours in a 40% saliva distilled water mixture showed no change in the distribution and in the intensity of the color reaction in the epithelial PAS-positive material in fishes, reptiles, birds.

In the amphibian and the mammalian ureter however the epithelial PAS-positive material did not resist the salivary diastase and the epithelium in all the control section was PAS-negative. Alcian blue 8GS Sections stained for 30 seconds in 1% Alcian blue 8GS showed a positive reaction for acid (fig. 20) mucopolysaccharides in the ureteric epithelium in fishes reptiles and birds. In the amphibian and mammals however the epithelial cells did not take up the stain.

DISCUSSION

The products of protein metabolism and their adaptive correlation to habitat have been discussed by Prosser ('52) Delaunay ('29) Needham ('35) and others It is clear that although nitrogenous excretion in any one group of vertebrates is not confined to any single product, nevertheless the predominant excretory product can be used as a basis for a general classification Where ammonia, urea or uric acid constitute the main excretory products of protein metabolism in a given species the terms *ammonotelic ureotelic* and *uricotelic* are descriptively applied (table 4)

Embryological considerations apart, the type of urine produced (particularly in consistency and degree of toxicity) has been held to have some influence upon the structure of the channels involved in its excretion. Thus for example in *ammonoteles* the high toxicity of ammonia and its ready solubility and diffusibility in water have been contrasted with the relatively low toxicity and solubility of uric acid in the *uricotelic* types.

As a general rule this view is supportable but, as is shown in this study it would be misleading to interpret it too literally

The musculature

From a comparison of histological sections there was no evidence that the amount of musculature in the ureteric system of tubules is closely related either to the consistency of the urine excreted or to its chemical constitution. For example in the marine and freshwater *ammonoteles* which secrete a watery urine the ureters are relatively long compared with the body length and are fairly muscular In the *turtle gecko and skink, which secrete a* semi-fluid urine the ureters are comparatively short and have a relatively weak musculture; while in the snake the ureter is long and has strong muscular coat.

There is however a correlation in the reptiles birds and mammals, between the length of the ureteric system and the amount of the peri-ureteral smooth muscle (fig. 1)

In mammals muscle cells can be demonstrated in the calyces and pelvis of the

TABLE 4

Species	Urine type	Urine	Epithelium	Goblet cell
Fresh-water fish	A		c	+
Salt-water fish	A		c	0
Amphibians	U	a	c	0
Reptiles	Uco	S	c (Turtle p)	+
Birds	Uco	S	p	+
Mammals	U		t	0

A, ammonotelic; U, ureotelic; Uco, uricotelic
a, aqueous; S, semi-solid
c, columnar; p, pseudostratified; t, transitional
+, present; 0, absent

kidney (Kiil, '57) In reptiles and birds, as has been shown here the musculature begins in the finer ureteric branches. This difference is of interest. Engelmann (1869) described the movements of the ureter in laboratory mammals, and since then it has been commonly held that the urine in these species is carried by peristaltic action from the renal pelvis directly to the bladder Recent evidence, however indicates that while the sphincters of the renal calyces and the muscle layers in the mammalian renal pelvis may contract simultaneously and the pelvis and upper part of the ureter fill as a single unit, only the contents of the ureter are transported distally by the contractile waves (Kiil, '57) Should this be so the mamalian kidney may well be protected from back pressure resulting from increases in intra-abdominal pressure due to factors such as alterations in posture (Gould, '55)

In birds, in which the renal pelvis is absent, peristaltic contraction waves have been described as having a milking" effect on the urine and are said to be capable of acting against considerable pressure (Gibb '29; Sturkie '54) It has also been reported that the pressure developed by the ureteral movements can be built up to a point greater than the intra-renal secretion pressure, and this has led to the view (Gibb, '29) that in birds at any rate, renal secretion may be temporarily curtailed by this means

It has been demonstrated here that smooth muscle cells occur in the finer intra-renal ureteric radicles of fish; and it is interesting to speculate whether a mechanism similar to that postulated for birds might occur in this species, particularly in migratory types. Since it is unlikely that new glomeruli can develop and disappear again as the animal moves from salt to fresh water and *vice versa* (Baldwin 46) the possibility of upholding and releasing glomerular activity through muscular action in the fine ureteric radicles is theoretically as attractive as that of selective contraction of the renal artery and/or vein (Baldwin 46)

The epithelium

With the exception of birds and mammals, all the species studied have a simple columnar epithelium lining the ureter and its branches. The pseudo-stratified epithelium of birds, and the transitional of mammals are structures permitting a fair degree of ureteral distension without epithelial loss or damage That such distensions can occur locally in the mammalian ureter is shown by the spontaneous formation of ureteral pools (Kiil, '57 Gould, '55). While there is no evidence in the literature that similar pools form in the avian ureter the presence of a pseudo-stratified epithelium, containing many goblet cells may be associated with the type of peristaltic action by which the semi-solid urine is milked" distally towards the cloaca.

Table 4 shows in which species goblet cells were found to be most prevalent. It is noticeable that in the *uricoteles* studied goblet cells are uniformly present, whereas, in the amphibians and mammals there are none. This may be accounted for by the fact that the *uricoteles* in general secrete a semi-solid urine which is relatively toxic to epithelial tissues while, the *ureotelic* mammals and amphibians produce a more fluid urine whose urea is much less toxic than uric acid. In these forms therefore less protection is required for the epithelial surface.

Since ammonia is by far the most diffusible and toxic constitutent of all the vertebrate urines, its efficient elimination is of great importance in the *ammonoteles* On considering the fresh-water and marine fish in this study it was surprising to find that the fresh-water varieties possessed numerous ureteric gobet cells, while in the marine species these were totally absent.

A possible explanation for this may be that marine teleost secrete a good deal of waste nitrogen in the form of trimethylamine oxide which is non-toxic. In addition to this very small amounts of urine are produced daily 2-4 cc per Kg body weight (Grafflin, '31) In fresh-water forms on the other hand, the nitrogenous waste is not converted into trimethylamine oxide. There is no need therefore, to "mask ammonia, since an almost unlimited water supply is available for its excretion (Baldwin, 46) In the fresh water forms, therefore which produce relatively large amounts of ammonotelic urine (300 cc per kg per day Grafflin '31) lubricative

and protective mucin is most necessary Hence the presence of goblet cells.

Histochemistry

Of the species studied only the *ureotelic* amphibians and mammals produce ureteric PAS-positive material in the form of glycogen (Group 1A, Pearse '53) In contrast to this acid mucopolysaccharides (Group 2A, Pearse '53) predominate in the am *monoteles* and *uricoteles* (table 5) In

TABLE 5

	PAS	PAS control	Alcian blue	Group (Pearse, '56)
Fresh-water fish	+	+	+	IIA
	g	e,g	g	
Salt-water fish	+	+	+	IIA
			e	
Amphibian	+	—	—	IA
	e			
Reptiles	+	+	+	IIA
	g	g	e,g	
Birds	+	+	+	IIA
	g	g	e,g	
M mmals	+	—	—	IA

e — epithelium
g — goblet cells

formation on the comparative biochemistry of vertebrate urine is as yet insufficient to justify an explanation of the above dif ferences. It is possible however that the chemical constitution of the polysaccharide complexes adapt them to serve the functional requirements of lubrication The action of depolymerizing enzymes such as the *mucinases* can lead to loss of viscosity under certain circumstances (De Robertis '58) The structural changes induced in mucoploysaccharide complexes such as exist in the ureteric epithelial secretion may thus aid the downward flow of semi solid urines

SUMMARY

1 In reptiles birds and mammals (but not in fish) there is a correlation between ureteral length and the amount of peri ureteral smooth muscle

2. In reptiles birds and amphibians the ureteral smooth muscle extends into the finer ureteric radicles

3 The ureteral epithelial lining is col umnar in fish amphibians and reptiles (ex cept turtle) pseudo-stratified in turtle and birds and transitional in mammals

4 Epithelial goblet cells are conspicuous in fresh-water fish reptiles and birds, but absent in salt-water fish amphibians, and mammals.

5. The predominant ureteral polysaccharide complex in amphibians and mammals is glycogen. Acid mucoplysaccharide complexes predominate in the ureteral epithelium of fish reptiles and birds.

6 The possible functional significance of the above observations, particularly concerning that of the musculature in the finer ureteric radicles is discussed but too little is known of the comparative biochemistry of the urines in the different vertebrate types to speculate on the significance of their ureteral histochemistry

ACKNOWLEDGMENT

I wish to thank Prof K. S Francis Chang for his invaluable help in directing this research. I am also indebted to Mr Robin Maneely and Dr Arnold Hsieh for their assistance in the preparation of the manuscript.

LITERATURE CITED

Baldwin, E. 1948 An Introduction to Comparative Biochemistry Cambridge University Press, 35 ed., Cambridge.
Delaunay H. 1929 Nitrogen excretion in fish. C. R. Soc. Biol., 101 371
Engelman, T W 1869 Zur physiologie des Ureter Pflüg Arch. ges. Physiol., 2: 213.
Gersh, I., and H. R. Catchpole 1949 The organization of ground substance nd basement membrane and its significance in tissue injury dise se and growth. Am. J An t., 85 457
Gibb G. S. 1929 The function of the fowl s ureters. Am. J Physiol. 87 504
Gould, D W A. C. L. Hsieh and L. F Tinckler 1955 The behavior of the isolated water-buffalo ureter J Physiol., 129 425.
Graffin, A. 1931 Urine flow in marine fish. Am. J Physiol., 97 602.
Kill F 1957 The function of the ureter and renal pelvi W B. Saunders Company Philadelphia.
Needham, J J Brachet and R. J A. Brown 1935 Nitrogen excretion in Chick embryos. Exp Biol., 12: 321
Pearse A. G E. 1953 Hi tochemistry Theoretical and Applied. J and A. Churchill Ltd London.
Prosser C L. 1952 Comparative Animal Physiology W B Saunders Compa y Philadelphia
De Roberti E. D P W W Nowinski and F A Saez 19 6 General Cytology W B Saunders Company Philadelphia.
Steedman, H. F 1950 Quart. J mier Sci. 91 477

PLATES

and protective mucin is most necessary Hence the presence of goblet cells.

Histochemistry

Of the species studied, only the *ureotelic* amphibians and mammals produce ureteric PAS-positive material in the form of glycogen (Group 1A Pearse 53) In contrast to this acid mucopolysaccharides (Group 2A, Pearse '53) predominate in the *ammonoteles* and *uricoteles* (table 5) In-

TABLE 5

	PAS	PAS control	Alcian blue	Group (Pearse, '53)
Fresh-water fish	+ e,g	+ g	+ e,g	IIA
Salt-water fish	+ e	+	+ e	IIA
Amphibians	+	–	–	IA
Reptiles	+ e,g	+ e,g	+ g	IIA
Birds	+ e,g	+ g	+ e,g	IIA
Mammals	+	–	–	IA

e — epithelium
g — goblet cells

formation on the comparative biochemistry of vertebrate urine is as yet insufficient to justify an explanation of the above differences. It is possible, however that the chemical constitution of the polysaccharide complexes adapt them to serve the functional requirements of lubrication. The action of depolymerizing enzymes such as the *mucinases* can lead to loss of viscosity under certain circumstances (De Robertis, '58) The structural changes induced in mucoployaaccharide complexes such as exist in the ureteric epithelial secretion may thus aid the downward flow of semi-solid urines.

SUMMARY

1 In reptiles, birds and mammals (but not in fish) there is a correlation between ureteral length and the amount of periureteral smooth muscle.

2. In reptiles birds and amphibians the ureteral smooth muscle extends into the finer ureteric radicles.

3. The ureteral epithelial lining is columnar in fish, amphibians and reptiles (except turtle) pseudo-stratified in turtle and birds and transitional in mammals.

4 Epithelial goblet cells are conspicuous in fresh-water fish, reptiles and birds; but absent in salt water fish amphibians, and mammals.

5 The predominant ureteral polysaccharide complex in amphibians and mammals is glycogen. Acid mucoplysaccharide complexes predominate in the ureteral epithelium of fish reptiles and birds.

6. The possible functional significance of the above observations, particularly concerning that of the musculature in the finer ureteric radicles is discussed; but too little is known of the comparative biochemistry of the urines in the different vertebrate types to speculate on the significance of their ureteral histochemistry

ACKNOWLEDGMENT

I wish to thank Prof K. S Francis Chang for his invaluable help in directing this research. I am also indebted to Mr Robin Maneely and Dr Arnold Hsieh for their assistance in the preparation of the manuscript.

LITERATURE CITED

Baldwin, E. 1948 An Introduction to Comparative Biochemistry Cambridge University Press, 35 ed., Cambridge.

Delaunay H. 1929 Nitrogen excretion in fish. C. R. Soc. Biol., 101 371.

Engelman, T W 1869 Zur physiologie des Ureter Pflüg. Arch. ges. Physiol., 2: 243

Gersh, L, and H. R. Catchpole 1949 The organization of ground substance and basement membrane and its significance in tissue injury disease and growth. Am. J Anat., 85 457

Gibb, G. S. 1929 The function of the fowl ureters Am. J Physiol. 87 594

Gould, D W A. C. L. Hsieh and L. F Tinckler 1955 The behavior of the isolated water-buffalo ureter J. Physiol., 129: 425.

Grafflin, A. 1931 Urine flow in marine fish Am. J Physiol., 97 602.

Kiil, F 1957 The function of the ureter and renal pelvis. W B Saunders Company Philadelphia.

Needham, J J Brachet and R. J A. Brown 1935 Nitrogen excretion in Chick embryos. Exp Biol., 12: 321.

Pearse, A. G E. 1953 Histochemistry Theoretical and Applied. J and A. Churchill Ltd London.

Prosser C. L. 1952 Comparative Animal Physiology W B Saunders Company Philadelphia.

De Robertis, E. D P W W Nowinski and F A. Saez 1958 General Cytology W B. Saunders Company Philadelphia.

Steedman H. F 1950 Quart. J micr Sci., 91 477

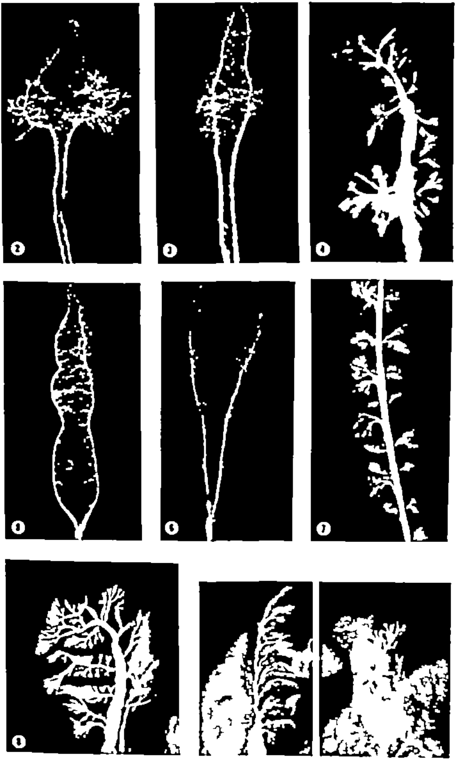

2
3
4
5
6
7
8

PLATE 2

EXPLANATION OF FIGURES

Epithelium

11 *Naja atra.* Intra-renal branches of the ureter. Lower left, primary ureteric radicle. Center, secondary ureteric radicle. Above, collecting tubule. Nonex embedding. Masson trichrome stain. × 500

12 *Columba livia.* Ureteral pseudo-stratified columnar epithelium. Paraffin wax embedding. Masson trichrome stain. × 700

13 *Chelonia amyda.* Ureteral pseudo-stratified columnar epithelium. Nonex embedding. Masson trichrome stain. × 718.

14 *Gecko gecko.* Primary ureteric radicle, left; three secondary ureteric radicles, top and center. Paraffin wax embedding. Masson trichrome stain. × 153.

15 *Gecko gecko.* Simple columnar epithelium lining the ureter. Paraffin wax embedding. Haematoxylin and Eosin. × 470

16 *Naja atra.* Ureteral simple columnar epithelium. The dark intra-epithelial bodies are mainly eosinophil leucocytes and macrophages commonly seen in this species. Paraffin embedding. Masson trichrome. × 318.

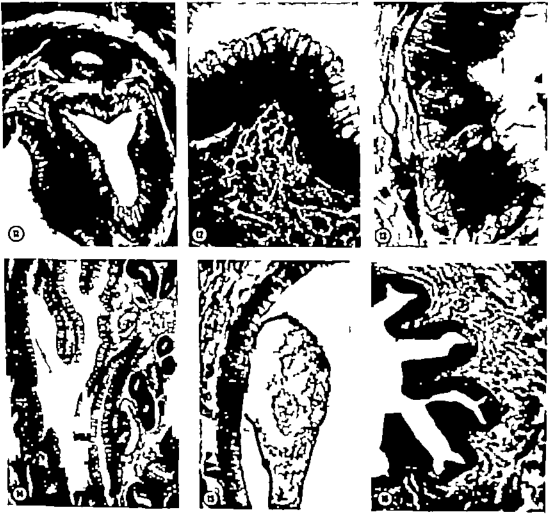


PLATE 3

EXPLANATION OF FIGURES

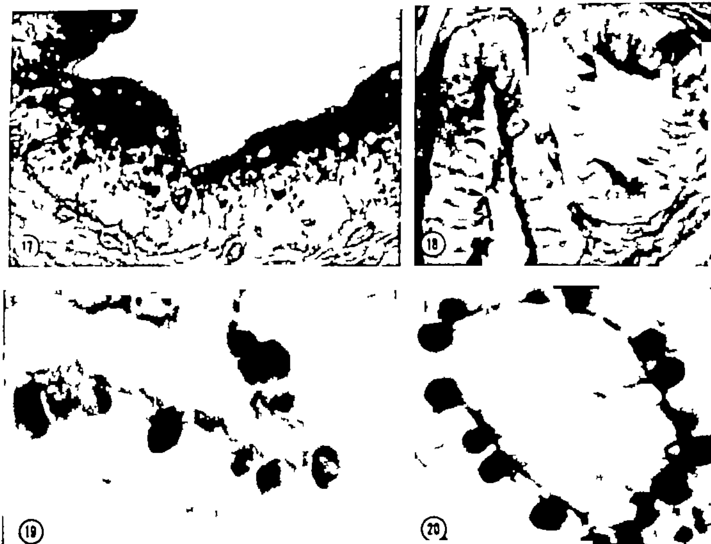
Histochemistry

17 *Caula f miliaris.* Ureteral pseudo-stratified columnar epithell m. Periodic acid-Schiff reaction Paraffin embedding. × 340

18 *Plectorynchus pictus.* Primary ureteric radicles. Periodic acid-Schiff reaction. Paraffin wa embeddi g. × 700.

19 *Cypri us carpio.* Epithelial goblet cells. Periodic acid-Schiff reaction. Paraffin wa embedding. × 800.

20 *Cypri s carpio.* Epithelial goblet cells. Alcia blue 8GS. Paraffin wax embedding. × 667


17
18
19
20

The Human Embryonic Heart in the Seventh Week[1]

DONALD G. VERNALL
The Department of Anatomy The University of Michigan, Ann Arbor Michigan

Although cardiac development has interested investigators for more than 2,500 years (see Kramer 42 and Licata, '54 for historical reviews) the discovery of many of the details of cardiogenesis awaited the development of technics for the construction of enlarged models of the embryonic heart so that its anatomy could be seen more easily Such a technic was described by Born in 1883 but the method is so pains-taking and time-consuming that many gaps still exist in the available series of models illustrating the human heart at various stages in its development. As these gaps become narrower we are confronted with the problem of the individual variability that occurs at each stage.

The present paper an attempt to fill one of the gaps in our knowledge of the embryology of the human heart, is based on an enlarged model of the heart in the seventh week of its development. This is the period during which the coronary vessels and the secondary interatrial septum appear It is also a period in which many of the structures and relationships of the adult heart are recognizable.

MATERIALS AND METHODS

The model upon which the present study is based was made from the heart of an embryo[2] with a crown-rump length of 14 5 mm. The embryo was in Streeter's Horizon early XVIII. Several factors led to the selection of this particular heart for reconstruction (1) it fits well into the existing series of reported reconstructions (2) the crucial changes that are occuring during this period have often been described on the basis of interpo' tions between more carefully obse earlier and later stages, and (3) the h was particularly well preserved tc strate internal features to best ad

Born's method of wax-plate reconstruction as modified by Kramer (42) was employed. The model, reconstructed at a magnification of 100× is dissectable at various levels in a plane coinciding with the transverse plane in which the embryo was sectioned. Figure 3 illustrates the internal structure that is evident as several succeeding segments of the model are removed. The proximal portions of the major vessels entering or leaving the heart have been included in the reconstruction (figs. 1 and 2)

Additional embryos of a comparable age examined and compared with the model are listed below:

U. of Mich. Number	Crown rump length mm	Streeter' horizon number	Plane of section
EH296	14.5	XVIII	Transverse
EH314	14.8	XVIII	Transverse
EH407	14.5	XVII	Sagittal
EH568	14.0	XVIII	Transverse
EH563	14.6	XVII	Transverse

OBSERVATIONS

External configuration

The definitive positions and interrelationships of the four chambers of the heart and the associated major vessels are externally apparent at this stage.

The pulmonary trunk crosses anterior to the ascending trunk (fig. 1) arches dorsad and to the left of it, and is connected by the temporarily robust ductus arteriosus (fig. 2) with the ventral surface of the l f dorsal aortic root.

The left f rth aortic arch and dorsal aortic root are larger than their counter parts on the right side

[1] This study wa supported in part by grant from Michigan He r ssociation.
[2] The Universi ch gan Collection No. EH-841.

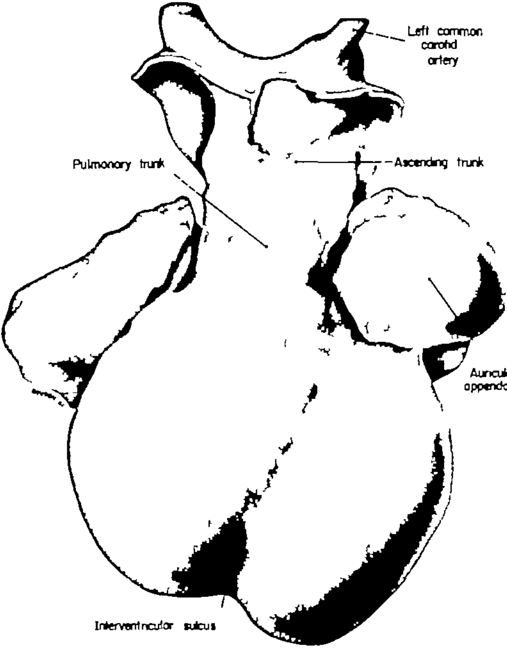


Fig. 1 Ventral view of wax-plate reconstruction of the human embryonic heart in the seventh week of development. (Reconstruction × 100 illustration × 50.)

The continuity between the primordial pulmonary arteries (fig. 2) and the right sixth aortic arch is obscured by the mass of tissue deep to the cut surface of the dorsal mesocardium, although the more distal portions of these arteries can be seen projecting from this cut surface en route to the developing lungs.

The four pulmonary veins converge into a common trunk, the pulmonary inlet, be-

fore entering the left atrium (fig 3) Los ('58) refers to this dilated pulmonary inlet as the spatium pulmonale.

The wide lumen of the left common cardinal vein and to a lesser extent that of the right narrow (fig 3) as they become continuous with the horns of the sinus venosus (venous sinus)

The left horn of the venous sinus has become more elongated than the right and

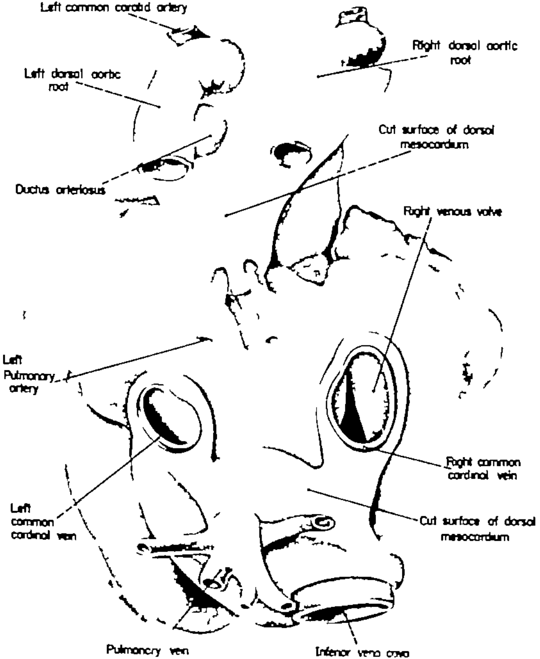


Fig. 2 Dorsal view of wax-plate re ... of the human embryonic heart in the seventh week of development. (Recor truct.on ... tion × 50.)

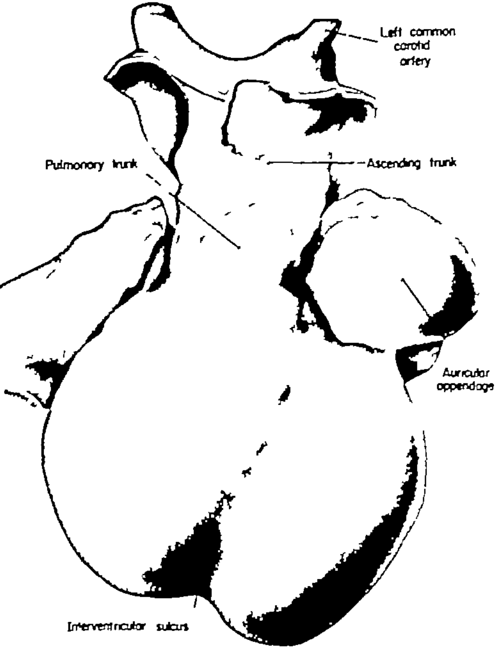


Fig. 1 Ventral view of a wax-plate reconstruction of the human embryonic heart in the seventh week of development. (Reconstruction × 100 Illustration × 50.)

The continuity between the primordial pulmonary arteries (fig. 2) and the right sixth aortic arch is obscured by the mass of tissue deep to the cut surface of the dorsal mesocardium although the more distal portions of these arteries can be seen projecting from this cut surface en route to the developing lungs.

The four pulmonary veins converge into a common trunk, the pulmonary inlet, be-

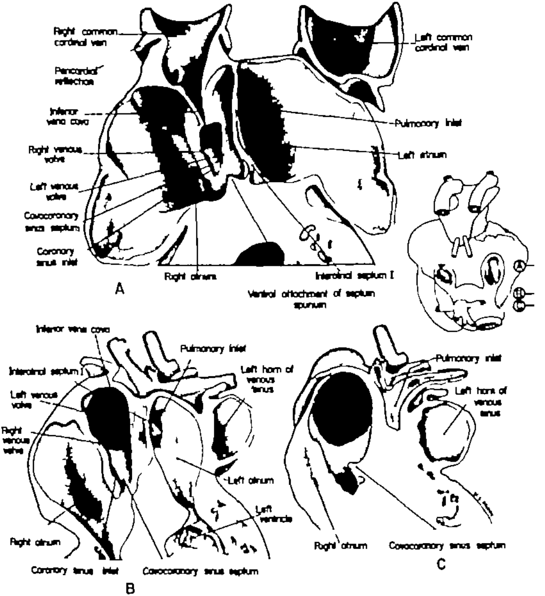


Fig. 3 Internal structure revealed as succeeding segments of the model are removed. (Reconstruction × 100, Illustration × 22.)

The lumina of the common cardial veins are surprisingly wide relative to the caliber of the anterior and posterior cardinal veins. The boundary between common cardinal vein and sinus horn is indicated by the conspicuous narrowing of the channel that has been described by Los (’78) in even younger embryos (4 4 mm c-r length)

The position and the elongation of the left sinus horn as well as its point of entry into the right atrium graphically illustrate the path followed by the venous sinus in its shift to the right of an original midline position.

The cut attachments to the ventral body wall that are visibl on the anterior surfaces of the ascending aorta and inferior

caval vein are not, according to James Baker (personal communication) remnants of a vanishing ventral mesocardium that arose from the fusion of separate lateral primordia. Examination of earlier stages of development indicates that they are actually formed by the extension of the pericardial cavity on each side of them.

The relatively broad arterial and venous segments of the dorsal mesocardium give little indication of the further narrowing of these dorsal attachments of the heart that will later occur Only in the portions proximal to the cut surfaces of the right and left sinus horns is there some suggestion of this reduction This is more apparent in the mesocardium associated with the distal portion of the left sinus horn presaging the formation of the ligamentous fold of Marshall in this area.

Internal structure

The absence in the interseptovalvular space of any evidence of the secondary l septum casts some doubt upon the validity of the predictions of some investigators such as Patten ('53) that this structure is always present at this stage Odgers ('35) and Los ('58) reported that they were unable to find any definite indication of this septum until embryos had attained a crown-rump length of 17 5 and 19 0 mm, respectively The fact, however that two of the five other hearts from 14 0 to 16 0 mm embryos examined in the current study did exhibit recognizable secondary interatrial septa confirms I feel, the prediction that this structure appears during the seventh week, but suggests that it is not so well developed as had previously been supposed The discrepancies between the various times at which the first appearance of the secondary interatrial septum has been reported emphasizes the necessity for examining more specimens at each stage of development in order to take individual variability into fuller account.

The extent of the foramen in the cephalic half of the primary interatrial septum would seem to permit the septum to offer only minimal resistance to interatrial flow The area of this orifice is many times greater than that of the inferior caval vein (fig 3) Licata ('54) reports that in the ninth week of development the area of the interatrial functional orifice is roughly equal to the area of the inferior caval inlet and Patten Sommerfield, and Paff ('29) describe this area at term as being only 40% of that of the inferior caval vein. Patten points out that this relative diminution in the size of the interatrial communication is correlated with the increasing pulmonary return to the left atrium as the lungs develop

The flow of blood from the right to the left atrium is further encouraged by the position of the well-developed right venous valve The effectiveness of this arrangement is demonstrated by the essentially similar size of the two atria in spite of the striking differences in size of the venous channels discharging into them. Some investigators were so intrigued with the efficiency of this set-up that they felt little or none of the inferior caval stream could escape being shunted into the left atrium. The various ingenious technics employed by Pohlman ('07 '09) Kellogg ('28 '30), Patten Sommerfield, and Paff ('29) and Barclay Franklin, and Prichard ('44) demonstrated conclusively however that not all of the inferior caval stream passes into the left atrium

The integrity of the right venous valve has not as yet, been violated by the thinned areas which will presage the subsequent resorption of much of this structure with the occasional persistence of strands that make up Chiari's net. Of the six human hearts of this age that were examined only one exhibited such thinned areas. There is apparent in the model, however a finger like process which projects from the dorsal wall of the right sinus horn into the lumen of the sinus venosus. Such a structure would perhaps account for those portions of Chiari's net that are occasionally encountered in a position too medial to be considered a persistence of a portion of the right venous valve.

The left venous valve which Odgers ('35) described as being more prominent than the right in the 5 mm embryo is still well-developed but is by this time smaller than the right. Its position is such

as to supplement the interatrial septum in forming a partial barrier to the flow of blood from the inferior caval vein into the left atrium.

The ridge that is present in the floor of the sinal bay of the right atrium marks the point where, in younger stages the left and right sinal horns originally met. This primordium of the venous sinus septum will continue to develop until it completely separates the inlets of the inferior vena cava and left sinus horn. In the course of this development it will meet and fuse with the medial surface of the right venous valve which is thereby subdivided into the (Eustachian) valve of the inferior vena cava and the smaller lower (Thebesian) valve of the coronary sinus. This partition is the structure that has been named the venous sinus septum by Los ('58) the cavocoronary sinus septum by Licata ('54) the sinus septum by Tandler (12) and the *Querfalte* by Born (1888).

The medial wall of the pulmonary bay of the left atrium is formed by that portion of the primary interatrial septum that has not been perforated by the interatrial orifice This arrangement serves to limit the flow of pulmonary blood across the interatrial septum into the right atrium. A further functional significance to the relationship between the orifice of the pulmonary inlet and the primary interatrial septum is pointed out by Licata ('54) who suggests that at later stages the mounting return of blood entering the heart at this point from the rapidly developing lungs would tend to crowd the primary interatrial septum against the secondary interatrial septum and encourage fusion.

The lateral wall of the pulmonary bay is formed by the left pulmonary crest. The gully like channel between this pulmonary crest and the primary interatrial septum extends in the floor of the left atrium from the pulmonary inlet to the left atrioventricular canal.

SUMMARY

1 A wax plate reconstruction of a h[illegible]rt from a human embryo in its seventh [illegible] of development with a crown-rump [illegible] of 14.5 mm and in Streeter's [illegible] mental Horizon early XVIII is de[illegible] Sections of five other embryos, of a similar age were examined and compared with the model.

External configuration

2. The four chambers of the heart and the associated major vessels are externally apparent in a close approximation to their adult positions. The pulmonary trunk arises anterior to the ascending aorta, arches around to the left of it, and connects with the anterior surface of the left dorsal aortic root via the large ductus arteriosus. The larger size of the left aortic channel presages its persistence as the dominant systemic channel accompanied by a relative reduction of the right into the proximal part of the right subclavian artery The pulmonary arteries are small but conspicuous channels which project into the dorsal body wall. The four pulmonary veins enter the left atrium via a common trunk, the pulmonary inlet. The left horn of the sinus venosus is elongated. Its diagonal position across the back of the heart approximates the position it will occupy as the coronary sinus and reflects the path of the shift of the sinus venosus to the right from an original midline position. The proximal portions of the vessels of the coronary circulation are visible in sections of the epicardium in the atrioventricular sulcus.

3. The dorsal mesocardium has separated into a venous and an arterial segment while the ventral mesocardium is absent. Ventral attachments are present on the anterior surfaces of the aortic trunk and inferior caval vein

Internal features

4 The atrial chambers conspicuously exhibit a primary interatrial septum left and right venous valves, and septum spurium. The secondary interatrial septum is absent from the model although two of the five c[illegible] hearts examined did demonstrate a rec[illegible]nizable secondary interatrial septum. A large secondary interatrial foramen occupies almost completely the cephalic half of th[illegible] primary septum The [illegible]ll-developed righ[illegible] venous valve is lo[illegible]ted so [illegible] direct [illegible]he blood entering [illegible]rom th[illegible] [illegible]ferior ca[illegible]l vein toward the

interatrial orifice. The left venous valve is also well developed but is somewhat smaller than the right.

5 The sinal bay of the right atrium is deep and sheltered by the venous valves The primordium of the cavocoronary sinus septum is present as a ridge in the floor of the sinal bay between the orifices of the inferior caval vein and the left sinal horn.

6 The inlet (spatium pulmonale) of the pulmonary veins opens into a conspicuous channel (pulmonary bay) in the floor of the left atrium.

7 The ventricles are in open continuity in the region of the unfused conus ridges but are separated in the area where the interventricular septum has become at tached to the fused endocardial cushion masses of the atrioventricular canal. There is as yet, no distinction between what will be the membranous and muscular portions of the interventricular septum. Both ventricles are similar in size thickness of and amount of trabeculation.

LITERATURE CITED

Barclay F P., K. J Franklin and M. L. Prichard 1944 The Foetal Circulation. Charles C Thomas, Springfield, Ill., XVI + 275 pp

Born, G. 1883 Die Plattenmodellirmethode. Arch f. mikr. Anat., 22: 584–599.

——— 1888 Uber die Bildung der Klappen, Ostien, und Scheidewande im Saugetierherzen. Anat. Anz., III Jahrg., 3 606–612.

Chiari, H. 1897 Ueber Netzbildungen im rechten Vorhofe des Herzens. Beitr z. path. Anat. u.z. Allg. Path., 22 1–10.

Kellogg, H. B. 1928 The course of the blood through the fetal mammalian heart. An t. Rec., 42: 443–465.

——— 1930 Studies on the fetal circulation of mammals. Am. J Physiol., 91 637–648.

Kramer T C. 1942 The partitioning of the truncus and conus and the formation of the membranous portion of the interventricular septum in the human heart. Am. J Anat., 71 343–370

Licata R. H. 1954 The human embryonic heart in the ninth week. Ibid., 94 73–125.

Los, J A. 1958 De Embryonale Ontwikkeling van der Venae Pulmonales en de Sinus Coronarius Bij de Mens. Doctoral Dissertation, Rijksuniversiteit te Leiden, Drukkerij "Luctor et Emergo — Leiden. 131 pp. + 50 figs.

Odgers, P N B 1935 The formation of the venous valves, the foramen secundum and the septum secundum in the human heart. J Anat., 69 412–422.

Patten, B M., A. Sommerfield and G. H. Paff 1929 Functional limitations of the foramen ovale in the human foetal heart. Anat. Rec., 44 165–178.

Patten, B. M. 1953 Human Embryology The Blakiston Division, McGraw Hill Book Co. Inc., New York, 2nd ed., XVII + 798 pp.

——— 1960 The Development of the Heart. Gould The P thology of the Heart. Charles C Thomas, Springfield, Ill., 2nd ed., Chap. II 24–92.

Pohlman, A. G. 1907 The fetal circulation through the heart. A review of the more important theories, together with preliminary report on personal findings. Johns Hopkins Hosp. Bull., 18 409–412.

——— 1909 The course of the blood through the heart of the fetal mammal with note on the reptilian and amphibian circulations. Anat. Rec., 3 75–109

Streeter G. L. 1948 Developmental horizons in human embryos. Description of age groups XV XVI, XVII and XVIII, being the third issue of survey of the Carnegie Collection. Contrib. to Embryol., Carnegie Inst. of Washington, 32 133–203.

Tandler J 1912 The development of the heart. In Keibel and Mall, Manual of Huma Embryology J B Lippincott Co., Philadelphia, 2 534–570.

Structure and Carbohydrate Histochemistry of Mammalian Salivary Glands

JOHN M. SHACKLEFORD AND C. E. KLAPPER
University of Alabama Medical Center Birmingham, Alabama

Systematic studies of mammalian salivary glands such as those of Zimmerman ('27) and Stormont ('28) are classics in view of the comprehensive nature of the investigations. Because of the biochemical, physiological and morphological diversity of salivary glands and their anatomical accessibility in most cases, investigators find these organs useful for a variety of research interests. Recent studies of salivary glands have resulted in an increased understanding of the biochemistry and histochemistry of mucin, the physiology of digestive enzymes mechanisms of water and electrolyte transport, relationships between exocrine and endocrine glands and many metabolic phenomena intimately associated with the secretory process. On the basis of knowledge derived from these investigations, it seemed appropriate to apply some of the more modern histochemical and morphological concepts to the salivary glands of a large group of animals with various environments and eating habits.

The present investigation deals primarily with the character and distribution of neutral and acidic carbohydrates. In view of the number of animals included in this study the structural analysis is limited to a brief description of the parenchymal elements in each of the major salivary glands e.g., the presence or absence or relative development of acini, intercalated ducts and striated ducts.

A multiplicity of terms is found in the literature to identify cell types in the major salivary glands. The secretory units, for example are described as being "homeochrome "tropochrome (Bensley '08) pseudomucous (Wimsatt, '56) serozymogenic special serous (Stormont, '28) atypical mucous (Leblond, '50); and variations of these Jacoby and Leeson ('59) point out, in particular slackness in the nomenclature referring to rodent submaxillary glands. In this paper there is no intent to discredit the terminology proposed by others. An effort is made, however to focus attention on the necessity of avoiding the use of a heterogeneous nomenclature.

METHOD AND MATERIALS

The major salivary glands of adult males and females were examined in the hamster mouse and Long Evans rat. Also studied were the major salivary glands of the rabbit, guinea pig, dog, cat, cow sheep hog, rhesus monkey and man. Adequate representation is therefore achieved in the rodents lagomorphs carnivores ungulates and primates. In addition to submaxillary sublingual and parotid glands the zygomatic gland of the dog and the molar gland of the cat were included in this work. Both the monostomatic and polystomatic portions of the dog sublingual gland were examined. In animals possessing extremely large salivary glands, e.g the cow multiple areas from each gland were studied.

Three fixatives were used in the preparation of paraffin sections. These were Bouin's, Zenker formol (10%) and 10% formalin (containing calcium carbonate) Aside from routine staining methods i.e. hematoxylin and eosin Masson and Mallory-azan, sections were also stained with the periodic acid Schiff method (PAS) alcian blue-Feulgen (AB–F) and colloidal iron-Feulgen (CI–F) (McManus and Mowry '60) Tissues were also sulfated by the method of Mowry ('58) and reacted with PAS AB–F CI–F and 0.01% toluidine blue-O solutions buffered at pH 2.6 3.6 4.5 and 6.5 In addition to sulfation, alteration of tissue components was

U. S. Public Health Service grant D-706.

accomplished by phenylhydrazine blockade of periodate oxydized 1,2-glycols (Pearse '60) acetylation and by digestion of diastase and hyaluronidase labile substances (McManus and Mowry '60)

RESULTS

One simple way to classify salivary glands is on the basis of the relative amounts of neutral and acidic polysaccharides contained in the secreting unit, or according to the presence or absence of one or the other of these types of tissue carbohydrate. Salivary gland acini by this method of classification fall into one of three categories. These are (1) mucous acini, containing large amounts of acidic carbohydrates as determinated by the colloidal iron (CI) and alcian blue (AB) methods. Upon sulfation of mucous acini, AB and CI as well as the PAS reaction are markedly blocked. (2) The serous acini contain various amounts of neutral polysaccharide but almost no acidic carbohydrate. These structures sometimes stain with AB and CI after sulfate esterification. (3) The seromucous acini possess an appreciable quantity of both neutral and acidic carbohydrate. Here, sulfation blocks AB and CI staining of the contained mucin but at the same time esterification of the neutral polysaccharides occurs. The general appearance of seromucous acini, therefore, is a structure which stains moderately with AB or CI either before or after sulfation. Sulfation produces a strong toluidine blue metachromasia in mucous and seromucous cells which persists at pH values below 2.5 whereas serous acini stain orthochromatically either before or after sulfation. In the mammals of this study salivary mucin almost invariably lacked the qualities usually associated with sulfated mucopolysaccharides (table 1). Previous workers have found CI and AB positive materials in salivary gland acini to be composed of sialic acid containing mucin (Spicer and Warren, '60 Warren and Spicer '61 Quintarelli et al. '60 '61)

The particulars of duct morphology will be discussed subsequently. In general, however the usual types found are intercalated and striated ducts (except in certain sublingual glands and in the zygomatic and molar glands of cats and dogs)

TABLE 1

The effect of sulfation on the staining of various tissue components

	Before sulfation			After sulfation		
	AB or CI	PAS	0.01% Tol. blue (pH 2.0)	AB or CI	PAS	0.01% Tol. blue (pH 2.0)
Mucous units	Positive	Positive	Negative or orthochromatic	Reduced	Reduced	Metachromatic
Serous units	Negative	Moderately positive	Negative or orthochromatic	Moderately positive	Reduced	Orthochromatic
Seromucous units	Moderately positive	Positive	Negative or orthochromatic	Moderately positive	Reduced	Metachromatic
Tracheal cartilage (hamster)	Positive	Positive	Metachromatic	Reduced	Reduced	Metachromatic
Mast cell (hamster)	Poorly stained	Poorly stained	Metachromatic	Poorly stained	Reduced	Metachromatic

granular tubules (in the submaxillary glands of the rat, mouse and hamster) and varieties of excretory ducts which, in some cases, contain large numbers of mucous secreting goblet cells.

Submaxillary glands of rodents. Submaxillary glands of the rat mouse and hamster are similar in structure and histochemical properties, i.e. the acini are according to the proposed definition, seromucous in type Moreover the submaxillary glands of these rodents possess granular tubules which appear at about the time of sexual maturity (figs. 1 2 3 4) Age, sex, and hormone disturbances are often responsible for wide biochemical and histological changes in submaxillary glands of the rat, mouse and hamster (Lacassagne, 40 Raynaud, '50 '55 '57; Grad and Leblond, 49; Junqueira et al. 49 Sreebny et al. '58 Shackleford and Klapper in press) AB and CI react moderately with the submaxillary acini of the rat, mouse and hamster After sulfation the acini still react with AB and CI (in contrast with mucous acini) and stain metachromatically with toluidine blue (in contrast to serous acini) Metachromasia, whenever present, is judged on the basis of the dehydrated tissue sections and the persistence of the color change with 0.01% toluidine blue solutions below pH 2.6. PAS staining is intense in the seromucous acini and to some extent in the granular tubules.

The rabbit is included in this group of animals although it is classified as a lagomorph. Submaxillary gland acini of the rabbit are also seromucous (fig. 6) even though there is a granular segment proximal to the intercalated ducts (Cohoe, '07) which is PAS positive but AB and CI negative. This granular segment terminates in short relatively non-granular intercalated ducts (fig. 5)

The guinea pig is the only animal included in this study which possesses purely serous submaxillary gland acini (fig. 7) According to C. Schneyer (personal communication) amylase levels are very high in this organ. Guinea pig submaxillary gland acini are moderately positive to PAS but negative to AB and CI. The striated ducts of the rabbit and guinea pig submaxillary glands contain a detectable amount of PAS positive-diastase removable material. Intercalated and striated ducts are present in the submaxillary glands of all the rodents of this study (including the rabbit) Striated ducts in the submaxillary glands of rats, mice and hamsters are not very numerous because most of them are modified into granular tubules at the time of puberty

Submaxillary glands of carnivores Multiple areas were taken from the submaxillary gland of the dog for histochemical and morphological studies. This procedure revealed a largely mucous secreting gland. Y Hashimoto and W Pigman (in press) report that the mucin of this gland contains a high percentage of sialic acid (9.2 gm/100 gm dry weight) The demilunes as well as the acini of cat and dog submaxillary glands react strongly to PAS AB and CI (figs. 8 9 10 11) If phenylhydrazine blockade is employed, demilune cells of both cat and dog submaxillary glands are highly resistant (fig. 12) With ordinary (unblocked) PAS staining of the cat submaxillary gland (fig. 11) demilunes are difficult to distinguish from acini because both secreting units stain intensely In contrast to phenylhydrazine blockade acetylation blocks PAS staining uniformly and, to a certain extent, also blocks AB staining of the mucin. Phenylhydrazine does not block AB staining to any degree. Sulfation for five minutes produces a strong toluidine blue metachromasia and blocks PAS AB and CI staining of both acini and demilunes of the cat and dog submaxillary gland (cf. the effect of sulfation on serous and seromucous elements) Though probably unrelated to the carbohydrate differences in acinar and demilune cells, Godlowski and Calandra ('61) report of the presence of argentaffin demilune cells in the submaxillary gland of the dog

Intercalated and striated ducts are well developed in the submaxillary glands of the cat and dog (fig. 8) The apical portions of striated duct cells of cat submaxillary glands are strongly positive to PAS but negative to AB and CI. This substance is not diastase labile.

Bovine and swine submaxillary glands Submaxillary glands of cows and hogs obtained at a local slaughter house contain predominantly mucous secreting acini

(fig. 13) Biochemical studies of these glands (Tsuiki et al. '61; Gottschalk, '60b) reveal high sialic acid levels as in the case of the dog submaxillary gland. Histochemical evaluation of sheep submaxillary glands is not included in this work. However Hashimoto and Pigman (in press) report that 25% of the dry weight of ovine sub maxillary glands is sialic acid. This level of sialic acid indicates a largely mucous secreting gland. With the exception of the demilunes which are more seromucous than mucous, bovine and swine submaxillary glands stain intensely with PAS AB and CI (figs. 14 15) Quintarelli et al. ('61) applied the combination AB–PAS reaction to bovine submaxillary glands. His color photomicrographs show red staining demilunes and purple acini. The effect of sulfation on AB CI, PAS and toluidine blue staining is typical of both mucous cells (the acini) and seromucous cells (the demilunes) In other words the acini stained intensely by the AB and CI methods before sulfation but were almost unstained by these ethods after sulfation. Conversely the seromucous demilunes of bovine submaxillary glands are stained moderately before and after sulfation. Toluidine blue metachromasia after sulfation is very marked in the acini and to a lesser extent in the demilunes.

In general, histochemical reactions in ruminant submaxillary glands do not vary markedly from those of swine (cf the difference in ruminant and swine parotid glands) Intercalated and striated ducts are present and well developed.

Human and rhesus monkey submaxillary glands The submaxillary glands of these primates consist of typical mucous and serous secreting acini (figs. 16 17) The serous elements usually predominate and many of the mucous acini are capped by serous demilunes Serous acini and demilunes are always orthochromatically stained either before or after sulfation and, as usual, are not stained by AB or CI. Some PAS positive material is present in all serous units. The previously described histochemical properties for mucous acini also apply to human and rhesus monkey submaxillary mucin. Sulfation reverses the CI and AB staining affinities that is, after sulfation the serous acini and demilunes are stained but the affinity of these stains for mucous acini is blocked

PAS positive material in the serous units, intercalated ducts and striated ducts of the human submaxillary gland is readily blocked by the phenylhydrazine method whereas the PAS positive material of the mucous acini requires somewhat longer incubation before blockade occurs. Intercalated and striated ducts are present and well developed in the submaxillary glands of man and the rhesus monkey

The parotid glands Histological and histochemical differences are not as great in the mammalian parotid glands of this study as compared with the variations of submaxillary glands. The most pronounced differences are seen in the parotid glands of carnivores (cat and dog) and ruminants (cow and sheep) Parotid glands of rodents lagomorphs primates and swine are similar in most respects.

The dog and cat are unique among the other animals of this study in that their parotid glands exhibit a considerable affinity for AB and CI This is true despite the morphological appearance of these glands as typically serous (figs. 18, 19) Acini of cat parotids are larger and filled with more granular material than acinar cells of the dog parotid. It might seem appropriate to employ the term pseudoserous as did Wimsatt ('58) in the case of certain cells of the principle submaxillary gland of the bat. We prefer however wherever there exists a histochemical and morphological incongruity to classify the secreting unit according to its histochemical properties In this case parotid glands of cats and dogs contain acini of the seromucous category that is, acini which histochemically resemble the seromucous elements of certain (previously described) submaxillary glands (fig 20) Accordingly cat and dog parotid gland acini stain moderately by the CI and AB methods either before or after sulfation and exhibt toluidine blue metachromasia after sulfate esterification Intercalated and striated ducts are present in parotid glands of the cat and dog. Striated ducts however are less well developed in the parotid gland of the cat.

Ruminant parotid glands are also unusual when compared with the same organ in other mammals. In these animals the outstanding difference is morphological rather than histochemical. Acini of bovine and ovine parotid glands are very long and tubular and the lining cells tend to be cuboidal rather than the usual pyramidal shape (figs. 21 22) This characteristic morphology is reminiscent of kidney tubules. Acini of sheep and cow parotid glands are only faintly AB positive but, as in typical serous cells, the affinity for AB and CI increases after sulfation. Intercalated ducts lined by very low cuboidal epithelium connect the acini with a well developed system of striated ducts. Striated ducts of bovine parotid glands often contain structures resembling mast cells. These intra-striated duct cells are strongly metachromatic (before or after sulfation) but do not stain well with PAS or AB (fig. 21)

Parotid glands from the rat, mouse hamster guinea pig, rabbit, rhesus monkey and swine are all very similar in their morphology and histochemistry (figs. 23 24 25 26 27) The cells of the parotid gland acini of the hog and guinea pig are considerably vacuolated (figs. 24 27) All the parotid glands of this investigation with the exception of the carnivores stain poorly or not at all by the AB and CI methods for acidic carbohydrates. Intercalated ducts and striated ducts are present and fairly well developed. One carnivore, the cat has relatively small and poorly developed parotid gland striated ducts. A detectable amount of PAS positive-diastase labile material was noted in the striated ducts of the rat parotid gland "Goblet cells are frequently encountered in the excretory ducts of mammalian parotid glands (fig. 28) These structures are outstanding in bovine, guinea pig and rhesus monkey parotid glands but it is entirely possible that goblet cells of other parotid glands were overlooked. When present goblet cells stain intensely with PAS AB and CI.

The sublingual glands. Mammalian sublingual glands of this study universally contain large numbers of mucous secreting acini which stain intensely by the AB CI and PAS methods. One lobule of the rhesus monkey sublingual gland contained mucous acini which stained metachromatically without previous sulfation. This metachromasia persisted when stained with 0.01% toluidine blue solutions below pH 2.6. Mucin of many sublingual glands stained metachromatically at pH values above 4.5 The unusual persistence of metachromasia in certain areas of the monkey sublingual gland compares with the toluidine blue staining of cartilage and mast cells.

Hamster and guinea pig sublingual glands consist entirely of mucous acini (figs. 1 29) while the same gland in mice and rats contain a number of acini with demilune formations. Boerner-Patzelt ('55) also noted the lack of demilunes in hamster sublingual glands.

Cat and dog sublingual glands possess a large number of non-mucous acini (fig. 30). The serous acini of carnivore sublingual glands are striking because of well developed intercellular canaliculi lined by PAS positive granules (fig. 36) The mucous secreting cells are located in tubular structures which connect the serous acini with the excretory ducts.

Bovine ovine and swine sublingual glands are almost entirely mucous with the exception of scattered demilune formations which are difficult to classify (figs 32, 34 35) These demilunes are slightly positive to PAS and to a lesser extent, to AB and CI. They would therefore fall into the serous or seromucous category but the capriciousness of the histochemical reactions makes the choice difficult. Mucous acini of the rhesus monkey are capped with typical serous demilunes.

Intercalated and striated ducts are poorly developed in the sublingual glands of the cat, dog and monkey They are almost totally absent in cat and dog sublingual glands. Intercalated and striated ducts of rodent and ungulate sublingual glands are well developed however sublingual gland intercalated ducts are most times very short as compared with the same structure in parotid glands. In two cases (bovine and swine sublingual glands) goblet cells were observed in the larger excretory ducts which gave typical

histochemical reactions for mucin (figs. 31 33)

Zygomatic and molar glands The zygomatic (infraorbital) gland in the dog is a fourth major salivary gland. The cat possesses a zygomatic and a molar gland and therefore has five major salivary glands. A description of the gross anatomy of these structures may be found in most text books of dog or cat anatomy. In our dissections of the dog a molar gland was not present but instead a series of mucous secreting minor salivary glands which nevertheless were histologically and histochemically identical to the cat molar gland.

The zygomatic and molar glands consist of extremely long branching mucous tubules (figs. 37 38) Striated and intercalated ducts are almost non-existent and the mucous tubules terminate in excretory ducts lined by low columnar to flattened cuboidal epithelium (figs 39 40) In the study of serial sections through the dog zygomatic gland one area was composed of a highly coiled series of ducts. The interstices of this area contained large numbers of plasma cells (figs 39 40)

Of all the salivary glands of this investigation the dog zygomatic gland would seem to be one of the best organs for biochemical and physiological studies of mucin. The mucin here at least histochemically is not contaminated by secretions of demilune cells and the size of the gland (about 2 gm wet weight) is sufficiently large for most research purposes

DISCUSSION

Burgen and Emmelin ('61) report the presence of amylase in the saliva of man apes guinea pig mouse rat and rabbit Amylase is absent or present in very small amounts in the submaxillary and parotid saliva of the dog cat, cow horse sheep and goat. Schneyer ('58) Schneyer and Schneyer ('60) and also C Schneyer (personal communication) report that amylase is low in concentration in submaxillary glands of the rat mouse rabbit and hamster in relation to high levels of this enzyme in the parotid glands of these animals Dr Schneyer also reported that submaxillary and parotid glands of the guinea pig exhibit considerable amylolytic activity In applying these data to the histochemical evaluations of the present investigation it appears that salivary glands composed predominantly of mucous acini, e.g. submaxillary glands of the dog, cat, cow and sheep secrete small amounts of amylase or perhaps amylase is totally absent in certain of these glands. Salivary glands containing seromucous acini, e.g. submaxillary glands of the rat, mouse, hamster and rabbit and parotid glands of the dog and cat, exhibit low concentrations of amylase as in mucous salivary glands. Relatively high amylase levels are demonstrable in salivary glands composed chiefly of serous acini, e.g. parotid glands of the rat, mouse hamster rabbit and submaxillary and parotid glands of the guinea pig.

The serous acini of bovine and ovine parotid glands and of the dog and cat sublingual gland are composed of cells which are very dissimilar to the usual type of serous cell. Salivary glands containing these atypical serous acini evidently secrete very little amylase in comparison with other serous salivary glands. In so far as this study is concerned serous simply means non-mucous.

Stormont's classification of salivary glands ('28) includes a group of cell types which he calls special serous This classification includes all cells in the submaxillary gland of the rabbit, rat mouse, muskrat and gopher; the serous cells of the dog sublingual gland; demilune cells of the cat and dog submaxillary gland, and all cells of the submaxillary glands of the hedgehog and shrew In the histochemical studies of this investigation most of the cells which Stormont names as special serous (excepting the serous cells of the dog sublingual gland and granular tubules of rodent submaxillary glands) have been designated as mucous or seromucous. Stormont also classified the parotid gland acini of most" mammals as being serozymogenic because of the structural and functional resemblance of these cells to the pancreatic acini and the chief cells of fundic stomach which as he says are well known to produce enzymes. We have characterized the parotid gland acini of the cat and dog as being seromucous and the term serozymo-

genic is not used in connection with any major salivary gland of this study Histochemical methods now in use are inadequate for the localization of digestive enzymes and do not merit the functional implications of a term such as "serozymogenic.

Recently much attention has been focused on the biochemical characterization of mucous secretions. Sialic acid (neuraminic acid) is one of the more consistently found carbohydrates which along with amino acids and other sugars makes up mucin molecules (Gottschalk, '60a, '60b; Pigman and Tsuiki, '59 Tsuiki et al., '61) According to Gottschalk, '60a, sialic acid is responsible for the viscosity of salivary mucin. With the use of the enzyme neuraminidase (Spicer and Warren, '60) and by mild acid hydrolysis (Quintarelli et al., '61) it has been established that sialic acid is responsible for most of the alcian blue and colloidal iron positive staining of salivary gland tissue sections. It is probable then, that this acidic carbohydrate is present in considerable quantities (per unit weight of gland) in the largely mucous secreting glands of this study viz. all sublingual glands (excepting those of the dog and cat which contain only scattered mucous acini) submaxillary glands of carnivores and ungulates and the zygomatic and molar glands of the cat and dog.

Granular tubules of hamsters, rats and mice (figs. 2, 3 4) contain another type of secretory cell. Some investigators believe these structures to be a source of a protease (Junqueira et al. 49 Sreebny et al. '55; Schafer et al. '59) Shackleford and Klapper (in press) have shown this enzyme-granular tubule relationship to be inconsistent in some cases or at least that granular tubules are not the only source of proteolytic enzymes in rodent salivary glands. On the basis of carbohydrate histochemistry the granular tubules are composed of serous secreting cells and are not, as Fekete (41) contends mucous elements.

Babkin ('50) lists at least 14 authors who ascribe a secretory activity to salivary gland striated ducts. In recent times electron microscopic studies of striated ducts (Scott and Pease '59; Leeson and Jacoby '59) radioautographic studies (Logothetopoulos and Myant, '56 Cohen and Logothetopoulos, '55) analysis of salivary rest transients (Burgen and Emmelin, '61) and stop-flow procedures (Langley and Brown, '60) have clarified some aspects of salivary duct physiology To a greater extent, however ductular contributions to salivary gland secretions are as yet poorly understood. In the morphological comparisons of this work, striated ducts are poorly developed in parotid glands of cats and in sublingual glands of dogs, cats and the rhesus monkey Striated ducts appear to be totally absent in the zygomatic and molar glands of cats and dogs. Correlations between the structure of certain salivary glands (those in which striated ducts are well developed, poorly developed or completely absent) and physiological studies of the secretions from these glands should be fruitful in ascribing at least a general function to striated ducts.

SUMMARY

Secreting units of mammalian salivary glands may be classified according to their content of neutral and acidic carbohydrates as determined by the alcian blue colloidal iron and periodic acid Schiff methods. Most secreting units fall into one of three categories viz. mucous serous or seromucous. Major salivary glands composed of predominantly mucous secreting acini are the submaxillary glands of the cat dog, cow and pig; zygomatic and molar glands of the cat and dog sublingual glands of all animals of this study (excepting sublingual glands of the cat and dog) Cat and dog sublingual glands contain only scattered mucous elements. Demilune formations in man and the rhesus monkey are serous secreting whereas most of the demilunes in carnivores and ungulates are either seromucous or mucous. Salivary glands which are largely seromucous are the submaxillary glands of the hamster rat, mouse and rabbit and parotid glands of the cat and dog. The submaxillary gland of the guinea pig and all the parotid glands of this investigation are composed of serous acini (with the exception of dog and cat parotid glands which contain seromucous acini) Serous acini of sheep and cow

parotid glands and those of the dog and cat sublingual glands are unusual and do not resemble the serous acini of other salivary glands. Striated ducts are absent in the zygomatic and molar glands of carnivores poorly developed in the sublingual glands of the cat dog and rhesus monkey and in parotid glands of the cat but are well developed in the other salivary glands included in the present study Striated ducts of rat mouse and hamster submaxillary glands are for the most part, modified into granular tubules.

LITERATURE CITED

Babkin, B. P 1950 Secretory Mechanism of the Digestive Glands. P ul B. Hoeber Inc., New York, Chap XXVI, p 719.

Bensley R. R. 1908 Observations on the salivary glands of mammals. Anat. Rec., 12: 105–107

Boerner-Patzelt, D 1955 Die Mundspeicheldrüsen des Goldhamsters. Anat. Anz., 102: 317–331

Burgen, A. S V and N G. Emmelin 1961 Physiology of the Salivary Glands. The Williams and Wilkins Company Baltimore.

Cohen, B., J H. Logothetopoulos and N B Myant 1955 Autoradiographic localization of Iodine-131 in the salivary glands of the hamster Nature, 176 1268–1269

Cohoe, B A. 1907 The finer structures of the glandul submaxillaris of the rabbit. Am. J Anat 6 167–190

Fekete E. 1941 Histology in Biology of the Laboratory Mouse. Dover Publications, Inc., New York.

Godlowski, Z. Z., and J C. Calandra 1961 Argentaffine cells in the submaxillary glands of dogs. Anat. Rec., 140 43–47

Gottschalk, A. 1960a Correlation between composition, structure shape and function of salivary mucoprotein. Nature, 186 949–951.

——— 1960b The Chemistry and Biology of Sialic Acid and Related Substances. Cambridge t the University Press.

Grad, B and C. P Leblond 1949 The necessity of the testis and thyroid hormones for the maintenance of the serous tubules of the submaxillary gland in the male rat Endocrinology 43 250–266.

Jacoby F and C. R. Leeson 1959 The post natal development of the rat submaxillary gland. J Anat 93 201–216.

Junqueira, L. C., A. Fajer M. Rabinovitch and L. Frankenthal 1949 Biochemical and histochemical observations on sexual dimorphisms of mice submaxillary glands. J Cell. and Comp. Physiol., 34 129–158

Lacassagne, A. 1940 Dimorphisme sexual de la glande sous-maxillaire chez la souris. C. R. Soc. Biol., Paris, 133 180–181

Langley L. L., and R. S Brown 1960 Stop-flow analysis of ionic transfer in the dog parotid gland. Amer J Physiol., 199 59–62.

Leblond, C. P 1950 Distribution of periodic acid reactive carbohydrates in the adult rat Am. J Anat., 86 1–49.

Leeson, C. R., and F Jacoby 1959 An electron microscopic study of the rat submaxillary gland during its post-natal development and in the adult. J Anat., 93 287–295.

Logothetopoulos, J H., and N B Myant 195 Concentration of radio-iodide and S35 thiocyanate by the salivary glands. J Physiol., 134 189–194

McManus, J F A., and R. W Mowry 19 Staining Methods, Histologic and Histochemical. Paul B Hoeber Inc.

Mowry R. W 1958 Observations on the use of the sulfate acid in ether for the sulfation of hydroxyl groups in tissue sections. J Histochem. Cytochem., 6 82–83.

Pearse, E. A. G 1960 Histochemistry Theoretical and Applied. J & A. Chruchill, Ltd., London.

Pigman, W and S. Tsuiki 1959 The Nature of the epithelial mucins. Int. Dent. J 9 502–516.

Quintarelli, G S. Tsuiki, Y Hashimoto and W Pigman 1960 Histochemical studies of bovine salivary gland mucins. Biochem. Biophys Res. Com., 2 423–426.

——— 1961 Studies of sialic acid containing mucins in bovine submaxillary and rat sublingual glands. J Histochem. Cytochem., 9 176–183.

Raynaud J 1950 Action de la thyroxine sur la glande sous-maxillaire de la souris castrée C. R. Soc. Biol., 144 245–248.

——— 1955 Suppression, par la surrénalectomy de l'action qu' exerce la thyroxine ur la glande sous-maxillaire des souris castrée Ibid., 149 896–900.

——— 1957 Développement du segment tubuleux de la sous-maxillaire de la souris castrée surrénalectomisée sous l'effet de la cortisone associée à la thyroxine. Ibid., 151 1061 1065

Schneyer, C. A. 1958 Genetic control of amylase levels in mouse submaxillary glands Amer J Physiol., 95 160–163.

Schneyer L. H., and C A. Schneyer 19 Regulation of salivary gland amylase activity Ann. N Y Acad. Sci., 85 189–200.

Scott, B. L. and D C. Pease 1959 Electron microscopy of the salivary and lacrimal glands of the rat. Am. J Anat., 104 115–161

Shafer W G., P G. Clark and J C. Muhler 1959 Salivary gland function in the rat. J Dent. Res., 38 121–125.

Spicer S. S., and L. Warren 1960 The histochemistry of sialic acid containing mucoproteins. J Histochem. and Cytochem., 8 13-137

Sreebny L. M., J Meyer E. Bachem and J. P Weinmann 1955 Postnatal changes in proteolytic activity and in morphology of the submaxillary gland in male and female albino rats. J Dent. Res., 34 729

Sreebny L. M., J Meyer and E. Bachem 19 Hormonal control of the proteolytic activity of

the submaxillary gland and the pancreas. Ibid., 37 485–491
Stormont, D. L. 1928 The salivary glands. Cowdry' Special Cytology 2nd Ed., P ul B. Hoeber Inc., New York.
Tsuiki, S., Y Hashimoto and W Pigman 1961 Comparison of procedures for the isolation of bovine submaxillary mucin. J Bio. Chem., 236; 2172–2178
Warren, L., and S. S. Spicer 1961 Biochemical and histochemical identification of sialic acid containing mucins of rodent vagina and salivary glands. J Histochem. Cytochem., 9 400–408.
Wimsatt, W A. 1956 Histological and histochemical observations on the parotid submaxillary and sulingual glands of the tropical American fruit bat Artibius jamaicensis Leach. J Morph., 99 169–209
Zimmerman, K. W 1927 Die Speicheldrüsen der Mündhöhle und die Bauchspeicheldrüse. von Möllendorff' Handbuch der Mikroskopischen Anatomie, Berlin. Verlag von Julius Springer

PLATE 1

EXPLANATION OF FIGURES

1 Section of hamster submaxillary-sublingual gland. Compare seromucous acini of submaxillary gland (left) with mucous acini of sublingual gland (right). Arrow indicates unstained granular tubule in submaxillary gland. Alcian blue — Feulgen stain. × 170.

2 Hamster submaxillary gland. Arrow indicates lightly stained granular tubule. Acini are darkly stained and fill most of the field. Periodic acid Schiff-hematoxylin stain. × 640

3 Mouse submaxillary gland. Granular tubule at arrow. Hematoxylin, orange-G aniline blue stain. × 640.

4 Rat submaxillary gland. Granular tubule at arrow. Hematoxylin orange-G aniline blue stain. × 640.

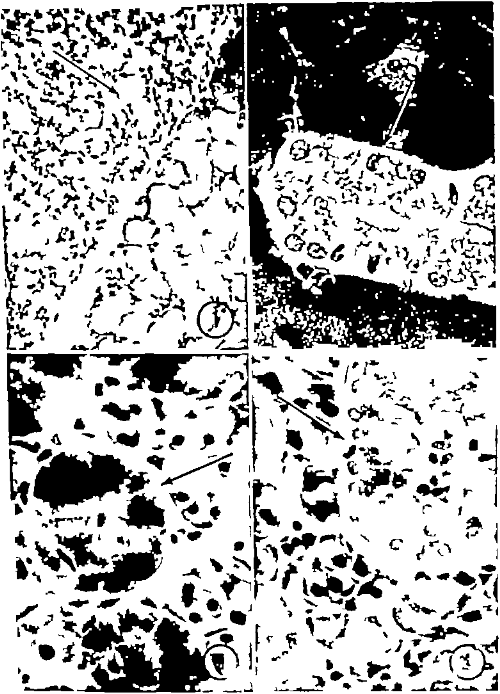


PLATE 2

EXPLANATION FIGURES

5 S bmaxillary gland f the rabbit. Arrow indicates granular segment in the ducts which connects the seromucous cells of the acini with short agranular intercalated ducts which, in turn, terminate in the striated ducts. Hematoxylin, orange-G aniline blue stain. × 640.

6 Submaxillary gland of the rabbit to show lightly stained seromucous acini. Nuclei are darkly stained by the Feulgen technique. Alcian blue — Feulgen stain. × 170.

7 Submaxillary gland of the guinea pig. Arrow indicates pigment granules in striated duct. Hematoxylin orange-G, aniline blue stain. × 640.

8 Submaxillary gland of the dog. Arrow indicates an intercalated duct terminating in striated duct. Hematoxylin, orange-G, aniline blue stain × 640.

9 Submaxillary gland of the dog. Acini are intensely stained by this method. Alcian blue-Feulgen stain. × 170.

10 Submaxillary gland of the cat. Acini are intensely stained. Alcian blue — *Feulgen stain.* × 170.

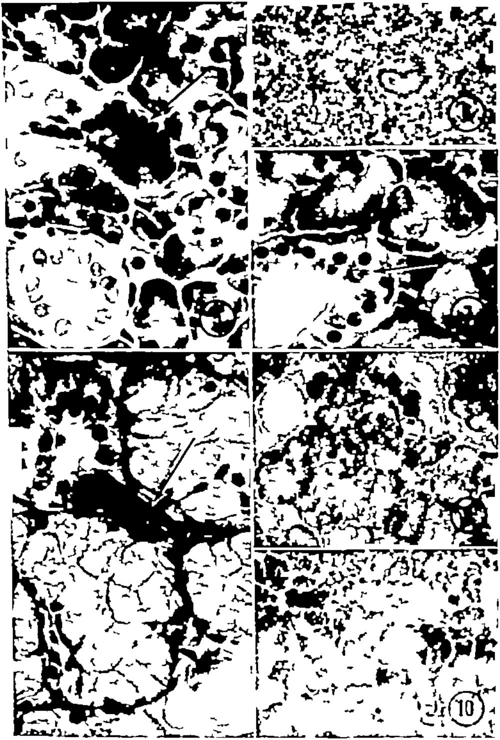

10

PLATE 2

EXPLANATION O FIGURES

5 Submaxillary gland of the rabbit. Arrow indicates granular segment in the ducts which connects the seromucous cells of the acini with short granular intercalated ducts which, in turn, terminate in the striated ducts. Hematoxylin, orange-G aniline blue stain. × 640.

6 Submaxillary gland of the rabbit to show lightly stained seromucous acini. Nuclei re darkly stained by the Feulgen technique. Alcian blue — Feulgen stain. × 170.

7 Submaxillary gland of the guinea pig. Arrow indicates pigment granules in striated duct. Hematoxylin orange-G, aniline blue stain. × 640.

8 Submaxillary gland of the dog. Arrow indicates an intercalated duct terminating in striated duct. Hematoxylin, orange-G, aniline blue stain. × 640

9 Submaxillary gland of the dog. Acini are intensely stained by this method Alcian blue-Feulgen stain × 170.

10 Submaxillary gland of the cat. Acini are intensely stained. Alcian blue — Feulgen stain. × 170.

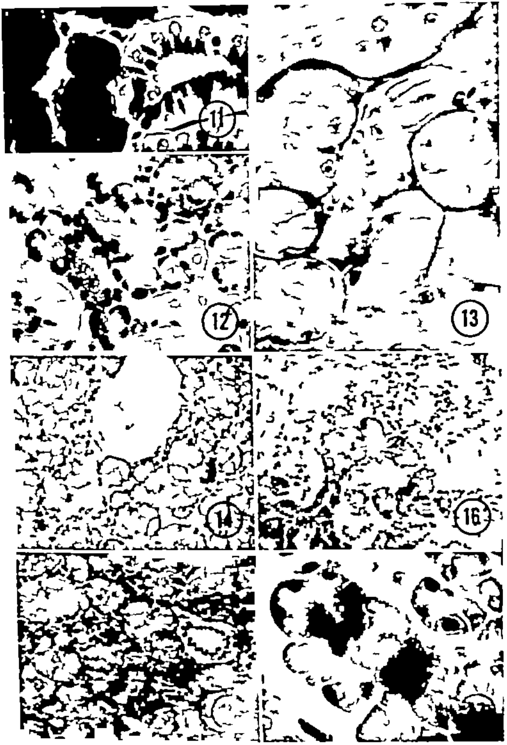

11
12
13
14
16

PLATE 4

EXPLANATION OF FIGURES

18 Parotid gland of the dog. Striated duct (left of center) is well developed. Acini are small and seromucous in type. Hematoxylin, orange-G aniline blue stain. × 640.

19 Parotid gland of the cat. Striated duct (at arrow) is poorly developed in comparison with striated ducts of other mammalian parotid glands. Seromucous acini are larger and more granular than those of the dog parotid. Hematoxylin, orange-G aniline blue stain. × 640.

20 Parotid gland of the cat. Alcian blue-Feulgen stain. × 170.

21 Parotid gland of the cow. Arrow indicates metachromatic intra-striated duct cell. Toluidine blue stain. × 640.

22 Parotid gland of the cow. Acini are atypical in comparison with other mammalian parotid glands. Note in particular the large lumina. Hematoxylin, orange-G, aniline blue stain. × 640.

23 Parotid gland of the rat. Striated duct in center of field. Hematoxylin, orange-G aniline blue stain. × 640.

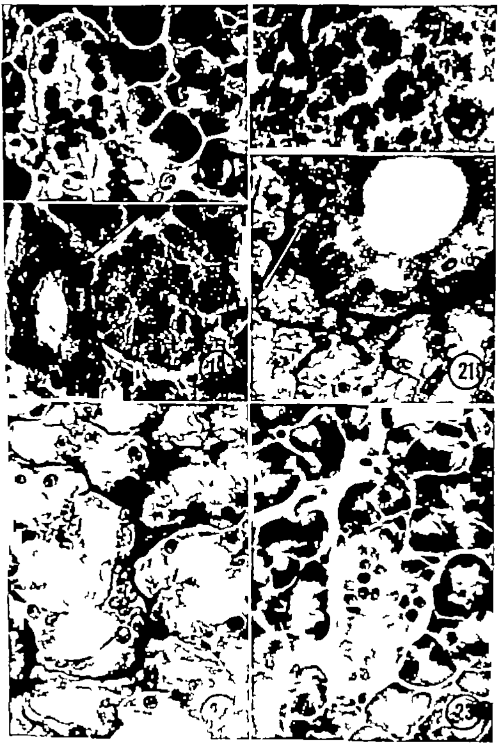


PLATE 5

EXPLANATION OF FIGURES

24 Parotid gland of the guinea pig. Striated duct crosses field diagonally Hematoxylin, orange-G aniline blue stain × 640

25 Parotid gland of the rabbit. Striated ducts are not shown. Hematoxylin, orange-G aniline blue stain. × 640

26 Parotid gland of the rhesus monkey Cross section of small striated duct in upper left corner Hematoxylin orange-G aniline blue stain. × 640

27 Parotid gland of the pig. Acini appear vacuolated Periodic acid Schiff hematoxylin stain. × 170

28 Portion of large interlobar duct of the cow parotid gland. "Goblet cells are numerous in the lining epithelium. Periodic acid Schiff hematoxylin. × 170.

29 Sublingual gland of the hamster Alcian blue-Feulgen stain. × 640.

30 Sublingual gland of the dog. Periodic acid Schiff-hematoxylin stain. × 170.

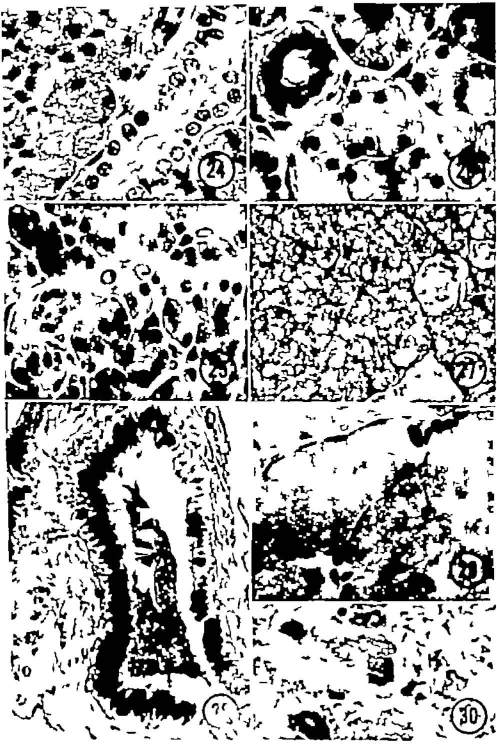

24
27
30

PLATE 6

EXPLANATION OF FIGURES

31 Portion of sublingual gland excretory duct of the cow containing mucous secreting cells in the epithelium. Periodic acid Schiff-hematoxylin stain. × 170.

32 Sublingual gland of the pig. Alcian blue-Feulgen stain. × 170.

33 Portion of large duct of pig sublingual gland containing "goblet cells Alcian blue-Feulgen stain. × 170.

34 Sublingual gland of the sheep. Alcian blue-Feulgen tain. × 170

35 Sublingual gland of the cow Striated duct in lower left corner Hematoxylin, orange-G aniline blue stain. × 640.

36 Sublingual gland of the dog. Serous acinu in center of field shows well developed intercellular canaliculi (at arrow) Periodic acid Schiff-hematoxylin stain. × 1,000.

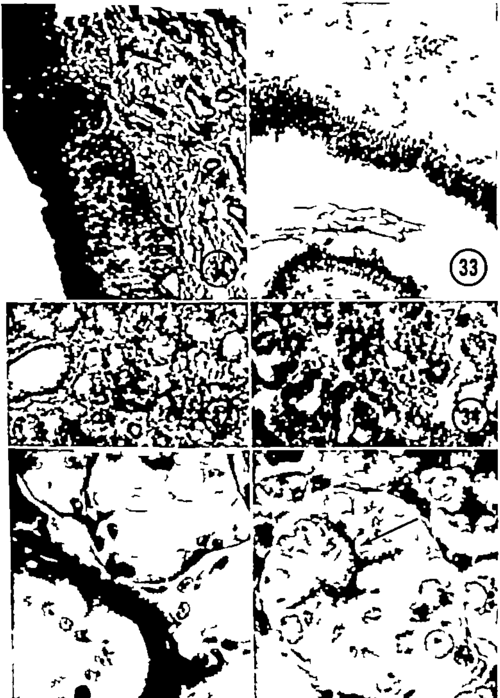

33
34
36

PLATE 7

EXPLANATION O FIGURES

37 Zygomatic gland f the dog. Secreting units composed of long m cous tubules. Alcian blue-Feulgen stain. × 170.

38 Molar gland of the cat. Interlobular duct (t arrow) lined by mucous secreting cells. Periodic acid Schiff hematoxylin stain. × 170

39 Large excretory duct of dog zygomatic gland (t arrow) Portion of zygomatic gland in upper third of picture Lower third of picture shows ductular body Periodic acid Schiff-hematoxylin stain. × 40.

40 Higher magnification of dog ductular body Large numbers of plasma cells are located in the interstices Arrow indicates excretory duct of zygomatic gland. Periodi cid Schiff-hematoxylin stain. × 170



An Histological and Histochemical Analysis of the Inner Lining and Glandular Epithelium of the Chicken Gizzard[1]

IRMA EGLITIS AND R. A. KNOUFF
Department of Anatomy, The Ohio State University
College of Medicine, Columbus, Ohio

The gizzard of the chicken as in all seed-eating birds presents two highly specialized structural features that are correlated with its grinding functions: (1) an hypertrophied muscular coat, consisting of paired disc-shaped smooth muscle masses with tendinous centers and (2) a hard relatively thick inner coat which covers the mucous membrane and serves as grinding plates.

This thick covering, a strictly avian characteristic, has been an object of interest and study for over a century. Although different views regarding its nature have been held, it is now generally regarded as a keratinized secretion of gizzard glands.

Inasmuch as the gizzard is derived from the posterior region of the embryonic stomach it would seem that the gizzard glands are the counterparts of the mammalian pyloric glands and consequently more likely to produce a muco-protein secretion than a keratinized substance which in mammals at least is not a secretion in the usual sense but a product of epithelial transformation and degeneration.

The recent development of histochemical tests which may be used to supplement the selective staining methods has prompted us to undertake a reappraisal of the nature of this remarkable structure.

Since our preliminary report (Eglitis and Knouff) given at the 1957 meeting of the American Association of Anatomists, a more extensive and detailed analysis has been completed which is presented here. The most recently reported attempts to determine its chemical nature by use of histochemical methods have been made by Aitken ('58) and Luppa ('59). Although there is general agreement in respect to the results of some tests, there are also differences more particularly in respect to the interpretation of results.

MATERIAL AND METHODS

The material used in this study was obtained from adult healthy fowls of the species Gallus domesticus. The gizzards were quickly removed from the slaughtered birds, opened by a longitudinal incision and either the lining membrane stripped off and treated as a separate specimen or narrow segments of the wall with the lining membrane *in situ* were cut out and promptly fixed. Most of the heavy muscular coat was cut away to facilitate fixation and sectioning.

Frozen sections both of fresh and fixed material were studied. For several of the histochemical reactions very small blocks were taken and fast frozen in isopentane-nitrogen at −170 C. They were then placed in an International Harris cryostat and sectioned usually at 10 μ at −18 C but thinner sections were obtained for examination with phase optics. They were mounted on coverslips and fixed in the following (1) cold −20 C acetone (2) 10% neutral formalin at room temperature, (3) formol, alcohol, acetic acid mixture. They were then washed with buffer and carried through the various histochemical procedures.

Of the several fixatives tried for general histological study 10% neutral formalin and Bouin's fluid proved best, for general histochemical tests 10% neutral formalin. Frozen section and celloidin methods were routinely employed as the hard tough

[1] Supported in part by Research Grant Number 4061 from the National Institutes of Health, Bethesda, Md.

grinding membrane made sectioning after paraffin embedding difficult. The double embedding method was used to provide thinner sections for cytological study

For routine histological study sections were stained with hematoxylin and eosin. The following more selective stains were employed hematoxylin and orcein, Ziehl-Nielsen 0 5% aqueous toluidine blue and the trichrome staining methods of Mallory and Pasini, the latter regarded as a highly selective stain for keratin and keratohyalin granules The aldehyde fuchsin staining method of Gomori ('50) and Bargman's modification of Gomori's chrome alum hematoxylin (Pearse '60 page 819) were also employed for revealing the presence of aldehyde and thiol protein-bound sulfur groups respectively

The histochemical tests chiefly employed were selected for the purpose of revealing the presence and localization of (1) carbohydrate complexes and (2) proteins and protein-bound sulfhydryl and disulfide groups as the former is a component of the mucoproteins and the latter a constituent of keratinizing substances. The presence of carbohydrates was investigated by the following methods

1 Staining with Schiff's aldehyde reagent

(a) Without prior oxidation with periodic acid-PA-control for presence of free aldehydes
(b) After oxidation with periodic acid PAS-(McManus) Pearse '60 p 832.
(c) After oxidation with lead tetra acetate LTAS-(Shimizu and Kumanoto) Pearse '60 p 833
(d) After digestion with salivary amylase followed by PA oxidation
(e) After digestion with hyaluronidase followed by PA oxidation
(f) After acetylation procedure (Lillie) Pearse p 832 followed by PA oxidation-control for (b) A negative reaction indicates that 1–2 glycol groups are responsible for the standard reaction.

2. Staining with toluidine blue to demonstrate acid mucopolysaccharides

(a) With toluidine blue below pH 5 in dilution of 0 5 and 0 01 examined for alcohol resistant metachro[masia.]
(b) With toluidine blue as in the abo[ve] but following hyaluronidase dige[s]tion.
(c) With toluidine blue as in the abo[ve] but following ribonuclease dige[s]tion.

3 Staining with alcian blue to demon[]strate acid mucopolysaccharide (Stei[d]man) Pearse '60 p 838 but withou[t] counter stains.

Protein containing material was ident[i]fied by the Ninhydrin-Schiff reaction (Y[a]suma and Itchikawa) Pearse, '60 p. 7[] and the coupled tetrazonium reaction be[]fore and after benzoylation (Pearse '6[0] p 798) Millon's reaction for tyrosi[ne] adapted to sections by Bensley and Ger[] (Pearse '60 p. 791) and Baker's modifica[]tion of the Sakaguchi reaction for argini[ne] according to the directions of Pearse '6[0] p. 799 The amino-acids revealed by th[e] above tests are abundantly found ass[o]ciated with protein bound SH– and –S–S[–] groups in keratinizing sites. Nucleopr[o]tein was tested for by staining with ba[sic] dyes and with the nucleal reaction of Feu[l]gen.

The protein bound sulfhydryl and disu[l]fide groups were especially investigated [as] these groups are involved in the keratini[z]ing process The following reactions we[re] employed:

1 The dihydroxy dinaphthyl disulf[ide] (DDD) test (Barrnett and Seligman, '[] and '54)

(a) Without prior treatment with s[o]dium thioglycollate demonstrat[es] –SH– groups alone.
(b) After treatment with sodium th[io]glycollate reveals both –SH an[d] –S–S– groups.
(c) After first blocking the –SH– group[s] with N-ethyl maleimide and the[n] reducing the disulfide group wi[th] 10% potassium cyanide — demo[n]strates the site occupied by S–S groups.

2. Staining with Schiff's reagent.

(a) Without prior oxidation (contro[l])
(b) After oxidation with performic ac[id] Pearse '60 p. 805 — PFAS reve[als] disulfide groups

3 Staining with alcian blue (Adam and Sloper) Pearse, '60 p 806
 (a) Without prior oxidation (control)
 (b) After oxidation with performic acid — also locate disulfide — PFAAB groups.

Sites of alkaline and acid phosphatases were investigated by the Gomori methods according to the directions in Pearse ('60 pp 868–869 881) For the demonstration of lipids Sudan black staining and the Schultz cholesterol tests were applied. Fresh and fixed frozen sections were examined with polarizing and phase contrast optics. Some standard qualitative chemical tests were also applied to hydrolysates of the finely ground stripped membrane for purposes of correlation with the histochemical results.

HISTOLOGICAL OBSERVATIONS

The glandular layer of the gizzard underlying the covering membrane is fairly typical of gastric mucous membranes. The superficial epithelium forms a unicellular surface layer which continues into shallow pits or crypts and forms a secreting surface of similar cells. Into each crypt open several, (5–8) narrow straight simple tubular glands. The epithelium of the simple glands is different in character from the superficial epithelium lining the crypts and the free surfaces between them.

The simple glands are arranged in groups of 10– to 30 The lamina propria between the individual glands of a group is reduced to mere slips of delicate connective tissue hardly sufficient to support capillary networks but broader bands of connective tissue are found between the groups. Sections through the glandular region parallel to the gastric surface presents a lobular arrangement of the gland tubules. Each gland consists of a neck, body and fundus and resembles more in form the peptic than the pyloric tubules of mammals The slightly expanded distal ends (fundi) reach the dense fibrous connective tissue of the submucosa. A muscularis mucosae is absent, (see figs. 1 and 2)

The hematoxylin-eosin and the toluidine blue stained vertical sections reveal clearly the composite nature of the covering layer also its mode of formation. It consists of:

(1) Arrays of vertical columns which represent secretion streams of the simple tubular gland. Each array corresponds to the secretions of a group of the glands (fig. 3)
(2) A matrix produced by the superficial cells of the crypt and free surface which appears to be deposited periodically since it presents a pattern of horizontal stria with darker stripes which would represent resting lines. The topological features are well shown in figures 1 3 7 and 16

The course of the secretion of the tubular glands passes from the gland lumens through the crypts and then vertically as columns through the entire thickness of the covering layer to its free surface where they project slightly to form a dentate surface (fig. 10) The secretion emerging from the mouths of the crypts is too rigid to spread laterally over the free surface in fact it is so inspissated and hardened within the gland lumens that upon entering the bottom of the crypts the secretion of each gland remains distinct (fig. 4) The several columns within each crypt appear to be surrounded and perhaps cemented together by the secretion of the crypt epithelium which is softer and spreads more readily around the rods and over the free surface. Stripping off the membrane pulls the already hardened rodlets out of the crypts and they remain attached to its undersurface (fig 8)

The epithelium of the tubular glands varies from a low cuboidal in the neck region to a low columnar type in the slightly expanded end portion. The nuclei are relatively large and oval and enveloped by a relatively small amount of basophilic cytoplasm. The lumens except in the fundus regions of the glands are filled with a dense homogeneous secretion that resembles the colloid of the thyroid gland in its staining reactions especially with the trichrome stains (fig. 14) The free border of the cells and the periphery of the secretion

We are indebted to Doctor Bernard Marks of the Physiological Chemistry Department for his supervision of these tests.

mass stain faintly blue with Mallory's stain (clear in the fig. 14) whereas the main central mass stains red. The columns in the crypts are markedly acidophilic, as is also the secreted membrane which staining uniformly appear as a homogeneous mass (fig. 2).

In the fundic portion of the glands the lumens often appear empty or contain fine filamentous or flocculent material. In Bouin fixed material stained with aldehyde-fuchsin these filaments are well shown. They appear to extend upward from the fundic lumen, combining with others to produce a compact mass which in the upper stretches of the tubules form the hardened columns or rodlets. The side membranes of the cells are beautifully demonstrated by this stain. They seem to participate in filament formation. In fact Wiedersheim long ago (1872) believed the basal parts of the cells also secrete and pour their secretion into the lumens by means of intercellular capillaries. These features are probably the result of the precipitating action of the fixative. The cytoplasm after toluidine blue staining in the acid pH range is basophilic with a metachromatic shade which is not observed in sections pre-treated with ribonuclease.

The superficial epithelial cells, lining the crypts and covering the free surface which secrete the matrix of the horizontal striae, are taller than the cells of the tubular glands just described. After H & orcein staining they show two distinct zones (fig. 8): a basal basophilic zone including the nucleus and a distal zone which is faintly eosinophilic staining somewhat deeper with orcein. Three zones are distinguished after toluidine blue staining: a basal basophilic zone including the nucleus, a supranuclear zone containing many deeply metachromatic granules and a narrow apical and border zone which is uncolored and appears empty (fig. 5).

Apparently the superficial cells discharge their secretion by the apocrine method. Although the details of the process are difficult to follow in our preparations, the supranuclear granules appear to swell and solubilize producing a clear substance which fills the apical poles of the cells (fig. 15). This material is refractory to most histological stains and to histochemical tests as well, so the apical pole presents an empty appearance (fig. 6). Montagna et al. ('53) have observed similar features in the apocrine sweat glands. They described supranuclear granules in the gland cells and an apical clear secreting zone, but they also described fine cytoplasmic processes projecting from the free border which by fragmentation formed spherules and granules of secretion. Granules and globules were also found in the discharged secretion of the crypt cells around the columns (fig. 6) and on the undersurface of the membrane, but we did not see the cytoplasmic extensions as described for the secreting cells of the apocrine sweat glands; perhaps they are present but of microvilli dimensions.

The tissue between the cavities of the adjacent crypts form ridges which resemble papillae-like formations with a core consisting of vascular lamina propria, the walls of crypt epithelium and crests of surface epithelium. The cells at the summit of these formations undergo pyknotic and cytoplasmic degeneration and desquamation forming a strand of nuclear and cytoplasmic debris which extends vertically through the matrix between the arrays of secreted columns (fig. 1).

Summarizing, there are two principal types of glandular cells in the chicken gizzard: (1) the cuboidal cells of the tubular glands which produce a hardened substance which is excreted in the form of rods or columns that pass vertically through the entire thickness of the covering membrane; (2) the columnar cells covering the surface and lining the crypts which secrete a softer material that spreads over the free surface before it hardens and forms the substance of the horizontal striae.

HISTOCHEMICAL OBSERVATIONS

The results of the histochemical tests are summarized in table 1. The intensity of the reaction in each case is graded as follows: absent (−), slight or trace (+), moderate (++), strong (+++), very strong (++++).

Carbohydrate reactions. The secretory material of the cells of the tubular glands

TABLE 1

Histochemical responses of secretory products of gizzard epithelium

Tests	Intracellular granules		Luminal contents				Covering membrane	
	Tubules	Surface[1]	Fundus	Body	Neck	Crypt	Columns	Matrix
Carbohydrates								
PAS	–	+++	+	++	+++	+++	++	+
LTAS	–	++++	++	+++	++++	++++	+++	+
Metachromasia	–	++++	–	–	–	–	–	±
Alcian blue	–	++++	–	–	–	–	–	±
AF[2]	–	++++	+	+++	+++	+++	–	–
Protein	Cytoplasm							
Millon	+	+	+	++	+++	+++	+++	+++
Ninhydrin-Schiff	+	+	+	++	+++	+++	++++	+++
Arginine	+	+	+	++	+++	+++	++++	+++
Coupled tetrazonium	++	+	+	++	+++	++	++++	++
DDD[3]	+	+	–	+	++	+++	+++	++
DDD[4]	–	+	–	+	++	+++	++++	++
DDD[5]	–	–	–	–	+	++	+++	++
PFAAB[6]	–	–	–	–	–	–	–	–
PFAS[7]	–	–	–	–	–	–	–	–

Includes lining cells of crypts.
Aldehyde-fuchsin.
Without pretreatment with thioglycollate –SH– group only
Pretreatment with thioglycollate –SH– and –S-S– combined.
Pretreatment with maleimide and potassium cyanide.
Performic acid, alcian blue.
Performic acid — Schiff.

is PAS and LTAS positive, but the intensity of the reaction varies from site to site. In the fundus portion of the tubule there is a very slight response, but as the material collects and condenses along the length of the tubular lumen the intensity of staining progressively increases. In the upper body and neck region where the secretion is molded into dense cylindrical rods or columns there is a strong response. In the crypts, where the columns are enveloped by a softer secretion of the crypt cells, the intensity of the staining is maintained, however at the mouth of the crypts there is an abrupt change from a strong to a moderate response.

The LTAS procedure recommended by Glegg et al. ('52) as a more specific test for carbohydrates where proteins are also present, gave parallel but somewhat stronger reactions. Neither method however demonstrated presecretion inclusions in the secretory poles of the cells of the simple glands.

The degree of basophilia after toluidine blue staining varied not only in respect to site but also to pH and strength of the staining solution. In general the material in the lumens of the fundus and lower gland regions failed to stain or was colored only slightly but in the upper regions of the glands and in the crypts the color varied from a pale blue to a bluish green. The secreted columns within the membrane were colored a light shade of blue. In general the intensity of staining with toluidine blue paralleled that of the PAS and LTAS staining methods, but at no site at a pH lower than five and a dilution of 0.5% or less did the secreted material exhibit alcohol fast metachromasia. Basophilic material with a slight metachromatic tinge was observed in the cytoplasm of the cells of the tubules. This material was present not only at the base but also at the nuclear and supranuclear level of the cells as well. The relatively large nucleus contained a single stained nucleolus. The basophilic cytoplasmic material was identified as ribonucleoprotein as it appeared to be largely removed by pretreatment with ribonuclease.

Scattered here and there among the chief cells with abundant cytoplasmic basophilia were found larger clear cells with virtually no cytoplasmic basophilia. These cells react to the basophilic stains like the parietal cells of the mammalian gastric glands. They were restricted for the most part to the fundus region of the glands. In a 10 μ section one to three of these clear cells are seen in each fundus. They probably represent a second secretory type. Gibb's method as described by Pearse ('60 p. 924) for the demonstration of argentaffin granules gave negative results.

The superficial cells including those of the crypts, also contain cytoplasmic granular material of a metachromatic nature. Pretreatment with ribonuclease removes only the material at the bases of the cells. The granules in the supranuclear position which were PAS and LTAS positive and strongly metachromatic were not affected by ribonuclease digestion. In the process of secretion, these granules undergo solubilization and apparently participate in the production of the material which collects in the apical poles of the secreting cells (fig. 19). This material is hardly colored by basophilic stains and only slightly tinged with acid dyes. The freshly discharged material appearing as fine granules and spherules on the borders of the superficial cells is also refractory to basic stains but become strongly acidophilic after it hardens and becomes incorporated into the matrix of the horizontal striae. Also to this matrix is added the cellular debris of cells desquamating from the crest of the papilla-like projection between the crypts. This cellular debris contains both basophilic and acidophilic staining material (fig. 12).

In addition to staining the elastic fibers of the tunica propria strongly and the basement membranes weakly aldehyde fuchsin (AF) stained the contents of the lumens of the simple glands and the columns in the crypts. The intensity of staining reactions at these sites paralleled those of the PAS and LTAS procedures, except that AF failed to stain columns in the secreted membrane.

A very striking positive response was seen in the side membranes and terminal bars of the secreting cells particularly

those of the superficial cells. These structures were stained very faintly by the PAS and LTAS methods. Aldehyde-fuchsin stained strongly the metachromatic granules of the superficial cells, but not the freshly discharged secretion of these cells.

Alcian blue which stained faintly the ground substance of the tunica propria and strongly the granules of mast cells, stained only the supranuclear granules of the superficial cells. The contents of the simple tubular glands the columns of secretion in the crypts and in the surface membrane d the substance of the horizontal striae all failed to stain, or at best gave only very weak responses.

Protein reactions All the carbohydrate reactive sites with the exception of the supranuclear granules of the superficial cells exhibited positive responses with the ninhydrin Schiff, Millon (tyrosine) Sakaguchi (arginine) and coupled tetrazonium reactions. The intensity of coloration in each instance paralleled in general those of the PAS LTAS and AF responses.

The hardened secretory product of the superficial cells which constitutes the substance of the horizontal striae of the covering membrane reacted positively with all the methods used to identify protein. This material is largely non-reactive to carbohydrate tests, although occasionally slight positive responses occur near the mouths of the crypts and immediately adjacent to the surface cells also slightly colored horizontal streaks alternating with non-colored layers are seen, perhaps some of the staining is due to cytoplasmic debris from the degenerated surface cells See figure 16

This histochemical behavior of the secretion product of the superficial cells raises the question of the role of the metachromatic and PAS positive supranuclear granules in the secretory process. It was pointed out earlier that the apical pole of the secreting cells is clear and free of granules but that the recently discharged secretion next to the border is composed of minute vesicles In the fresh frozen material sectioned in the cryostat and examined with the phase contrast optics apparent that the cellular granules are transformed into globules which swell and collect at the apical pole. As this process occurs they become refractory to the carbohydrate tests. However a membrane appears about each globule which reacts positively to the coupled tetrazonium arginine and DDD tests. These globules are apparently discharged from the cell by the apocrine method, and as they are compressed and condensed by secretory pressure they are gradually incorporated into the matrix of the horizontal striae.

Sulfhydryl groups were demonstrated by the dehydroxy-dinaphthyl-disulfide (DDD) reaction at all sites that exhibited positive tests with the protein and carbohydrate reactions (table 1) Pretreatment with thioglycollate to reduce disulfide to sulfhydryls revealed a greater intensity of staining of the secretion in the necks of the glands and the secretion columns in the crypts and the covering membrane which denotes the presence of disulfide at these sites (fig. 18) Localizing the disulfide groups by first blocking the sulfhydryls by maleimide and then reducing the disulfides by potassium cyanide to sulfhydryls before applying the DDD procedure also showed reactions in the secretions of the neck and in the secreted columns of the crypts and covering membrane.

Both sulfhydryls and disulfides were found also by these procedures in the matrix of the horizontal striae but the intensity of the staining here was less than in the columns however the fragments of surface cell degeneration which produces the vertical streaks in line with the tips of the papilla processes showed fairly strong reactions (fig 17) Sulfhydryls but not disulfides were found in the basal cytoplasm of the cells of the tubular glands and the cells of the crypts and free surface.

Other tests. The Schultz cholesterol test was negative except for a slight reaction on the surface of the covering membrane which is colored by the adsorption of bile Neither the substances of the membrane nor the presecretion substance was stained by Sudan black.

Very little phosphatase activity was demonstrable which indicates a very low metabolic and sluggish secretory activity perhaps of a cyclic nature The only birefringent material demonstrated was found

deep in the covering membrane in the form of crystalline material, which appeared to be a calcium compound (fig. 13)

In addition to the histochemical tests described above some chemical characterization was attempted. The fresh covering membrane contains 41 8% moisture Drying produces a brittle parchment like membrane which swells and regains its former weight when placed in water The membrane is not grossly soluble in acetone alcohol ethyl ether nor does it dissolve in salt solutions. The membrane is rendered soluble by rather prolonged hydrolysis in strong acids or bases. Attempts to solubilize the membrane by enzymatic hydrolysis with proteolytic enzymes or with hyaluronidase were not successful.

Finely minced membrane was extracted repeatedly with boiling water the extracts combined and treated with several volumes of alcohol to precipitate a white polysaccharide. This was present to the extent of approximately 6% of the fresh weight of the membrane This material gave negative qualitative tests for pentoses and but the naphthoresorcinol reaction showed the presence of a small amount of uronic acid. The presence of glycosamine was indicated by a positive Ehrlich s reaction with p-dimethylaminobenzaldehyde. N-acetyl-glycosamine was not present, as shown by no increase in the glucosamine reaction after hydrolysis. Sulfates were shown to be present in the material by the addition of barium chloride to a hydrolysate producing a copious precipitate of barium sulfate.

The membrane was hydrolyzed with 6-N hydrochloric acid, and the hydrolysate was examined qualitatively for amino-acids. Millon s test for tyrosine was positive as was the Hopkins-Cole and the aldehyde tests for tryptophane. Sullivan test for cystine was positive and typical cystine crystals were isolated by isoelectric precipitation.

DISCUSSION

Historically the concept that the hard inner covering of the gizzard is a keratin-like secretion is based on the early studies of Hedenius (1892) and Cornselius ('25) Curschmann (1866) in a still earlier report referred to the lining as a cuticula [illegible] chitinous material, however Hedenius showed by chemical methods that it contained, unlike chitin sulfur but in a lower concentration (1 13%) than in horny substances. He therefore referred to it as [illegible] keratinoid layer a term which has been generally adopted.

Cornselius in an excellent histological survey of the avian [illegible] concluded that the so-called keratinoid layer unlike epidermal keratin is a secretion product of the gizzard glands. According to his observations the secreted L[illegible] in the chicken as in other seed-eating birds consists of two secretions — one produced by the fundic portion of the gizzard glands the other by the epithelium near the mouth of the glands. The former discharges [illegible] secretion into the lining in the secretion streams or vertical columns, [illegible] latter produces an intercolumnar [illegible] stance which stains less intensely than columnar material He also noted desquamated cells were added chiefly the intercolumnar substance.

Our own histological observations [illegible] in general with this description of C[illegible] lius except he seems not to have [illegible] ated the similarity of the gizzard glands [illegible] typical gastric glands. Apparently [illegible] he termed the fundus represents the en[illegible] tire length of the simple gland tubules and the part that he refers to as near the mouth of the gland represents the crypts which are lined with the same epithelial type that covers the surface between the crypt openings. This is the cell type that produces the matrix of the horizontal striae (the intercolumnar substance of Cornselius) The chief site of cellular desquamation is the apex or crest of the papillae-like extensions of the mucosa between the crypts (fig. 8) The cellular debris is retained [illegible] the membrane and appears as vertical strands in the intercolumnar matrix paralleling the secretion column (fig. 17) This contains pyknotic and fragmented nuclei which stain with hematoxylin and the nuclear reaction also cytoplasmic debris which includes faintly metachromatic granules and material staining with chrome alum hematoxylin the latter indicating a cystine the former an acid

mucopolysaccharide component (figs 9 11 12) It appears that at this site especially death overtakes cells still filled with secretory products. This feature is especially noteworthy as it suggests that the superficial cells elaborate both a mucopolysaccharide and a protein substance containing cystine. Apparently lining cells of the crypt move upwards and onto the free ... This behavior requires a replacement by mitosis which is synchronized with the secretory processes. Since mitosis was seldom observed it would seem that ...y and mitotic activity is cyclic and related to the degree of attrition of the ...

The accumulation and hardening of the secretion in upper gland and crypt regions and the layered appearance of the secretory product of the superficial cells, also indicate a very sluggish activity The hardening of the secretion within the glands and crypts results in the formation of peg like structures (fig. 8) which would tend to hold the membrane securely to the mucosa during the grinding movements.

The histochemical analysis of the secretion of the tubular glands revealed only the presence of carbohydrates and proteins. There was a notable parallelism between the intensity of the carbohydrate and protein reactions at various levels of the secretory channels (table 1) The Sakaguchi (arginine) and coupled tetrazonium reactions as well as strong acidophilic staining denote a rich content of basic amino-acids. Staining with toluidine blue in the acid pH range gives variable results but true metachromasia was not seen. Neither salivary amylase nor hyaluronidase affected the outcome of the various reactions. These results identify the secretion as a carbohydrate-protein complex, presumably of the muco-protein variety Recently Leblond Glegg and Eidinger ('57) analyzed by chemical methods materials that stained with the PAS reaction and found that they always contained galactose and fucose as well as hexosamine and probably sialic acid often mannose and rarely glucose Most but not all of these residues carry freely reactive 1 2 glycol groups Thus the degree of reactivity at any given histological site will depend not only on the amount of carbohydrate present but also on the number of monosaccharide units combined to leave 1 2 glycol groups free to react.

The presence of metachromatic secretion granules in the lining cells of the crypts and free surface which are hyaluronidase and amylase fast, suggests that the carbohydrate moiety of the secretion is an acid mucopolysaccharide A binding of the acid groups of the polysaccharide with the basic groups of the protein would explain the weak carbohydrate staining response of the horizontal striae the secretion product of these cells. Probably most of the hexosamine and uronic acid extracted from the minced membrane by boiling water was derived from the substance of the horizontal striae, since histological sections treated with boiling water showed no appreciable reduction or PAS staining intensity of the secreted columns.

The demonstration of –SH– and –S–S groups bound to a protein rich in basic amino-acids in the secretions of both types of epithelium in our opinion does not prove that the secreted covering is keratin. It is true that it resembles keratin in respect to hardness resistance to proteolytic enzymes, insolubility in dilute acids and alkalies and organic solvents and a high content of basic amino-acids. Undoubtedly the hardening is due to the binding of –S–S groups but the amount of cystine in the membrane is relatively small in comparison with the amount in keratin. Cystine is present in small amounts in most proteins and in some it is relatively high (neuro-secretion of the hypophysis and insulin) Also the water content of the membrane is much higher than in hard keratin, but most important is the fact that complex carbohydrates are combined with protein. A carbohydrate component is absent in pure keratin. These differences in our view establishes the non-keratin nature of the membrane There is no specific histochemical test for keratin but the relative amounts of arginine and cystine as revealed by the histochemical tests are different, the arginine response being stronger in the secretion membrane and the cystine response weaker which would indicate dif

ferent sequences of amino-acids in the two substances.

Furthermore Champetier and Fauré-Fremiet ('38) in an x ray analysis of so-called secreted keratins found that the roentgenograms of the gizzard membrane and shell membrane showed none of the characteristics of keratin They behaved in regard to their fine structure as gummoides in the sense given that term by K. H Meyer Meyer (45) has also stated that many mucopolysaccharides and mucoids are quite effective inhibitors of proteolytic enzymes.

Hofmann and Pregl ('07) used the term "koilin" for this membrane for they found they were unable to recover cystine in pure form but could not prove it was absent, although if present it was only in a minimal amount, however In our chemical analysis the Sullivan test for cystine was positive and typical cystine crystals were isolated by isoelectric precipitation

Knaffl-Lenz ('07) in a study of the di amino-acids of the membrane found that arginine is present in greater concentra tion than in keratin, and in our prepara tions the Sakaguchi reaction for arginine was more intense in the membrane than in hair Moreover simple birefringence was not exhibited by either type of secretion whereas keratin and keratinizing substance shows strong birefringent proper ties

By virtue of these differences we cannot agree with Aitken ('58) who concluded on the basis of some rather non-specific staining reactions that the material secreted by the gizzard glands is a form of hard keratin, although he found in the columnar cells of the free surface meta chromatic granules which were stained with PAS and aldehyde-fuchsin and secreted material within the gland tubules and covering membrane which was PAS positive furthermore he even was unable to demonstrate sulfhydryls by the ferric ferricyanide method except at the surface where a narrow line of reactive substance may be seen.

Luppa ('59) in a histochemical study of the glandular epithelium during the embryonic development of the gizzard glands found that in early stages the secretion is metachromatic, but during later stages t metachromasia is reduced at the same ti that the intensity of the protein reac increases These changes are especi noted at the nineteenth day of incubat Positive tests for protein bound –SH a –S–S– groups also made their appear during the same incubation period. He b lieves that the loss of metachromasi explained by the binding of the acid mu polysaccharide group to the basic am acids of the protein. He concludes that so-called keratinoid layer consists of a h aluronidase resistant acid polysacchari protein complex with a cystine content

In our preliminary report (Eglitis a Knouff '57) we were of the opinion t the membrane was a composite of mu polysaccharides secreted by the gland epithelium and keratin derived from t accumulation of keratinized cells wh desquamated from the surface epithel As the granular debris stained with chr alum hematoxylin, it is possible that so true keratin is derived in this manner, b the application of the DDD tests sh that the matrix of the horizontal st which contains the desquamated mate in general shows lower cystine con than the secretion columns. We there agree in general with Luppa ('59) t the gizzard lining consists of a poly charide-protein complex containing c tine however not in the proportion fo in keratin as the PFAS and PFAAB te were negative

This histological term cuticular me brane is more preferable than kerat membrane for this structure since the l ter tends to convey a false chemical i pression.

SUMMARY

The nature of the secretions of t glandular epithelium of the gizzard of t chicken has been studied by general a selective histological and by histoche methods for demonstrating carbohydr proteins and lipids. Some chemical ch acterization was also attempted.

The hard inner covering of the muc is a composite structure consisting of (arrays of vertical columns or rods secr by simple glandular tubules (2) a ma consisting of horizontal striae or lam

secreted by the epithelial lining of the crypts and free surface. To the matrix is added desquamated surface epithelial cells which form vertical streaks between the arrays of columns.

The secretion of the simple tubular glands accumulates and hardens in the upper and neck portions and in the crypts to form rigid rods or columns which pass through the entire thickness of the lining. These hardened streams of secretion show moderate to strong PAS and LTAS responses and strong protein reaction including those for protein bound sulfhydryl and disulfide groups.

The crypt and surface epithelium representing a common type possess metachromatic supranuclear granules which are also PAS and LTAS positive. These cells produce the matrix substance of the horizontal striae. It displays negative to weak responses to the carbohydrate tests and moderate to strong responses to protein and protein bound sulfhydryl and disulfide groups.

It is concluded that the so-called keratinoid membrane consists of carbohydrate-protein complexes with a lower cystine content than that found in epidermal keratin.

LITERATURE CITED

Aitken, R. N. C. 1958 A histochemical study of the stomach and intestine of the chicken. J Anat., 92: 453–466.

Barrnett, R. J and A. M. Seligman 1952 Demonstration of protein-bound sulfhydryl and disulfide groups by two new histochemical methods. J Nat. Cancer Inst., 13 215–216.

——— 1954 Histochemical demonstration of sulfhydryl and disulfide groups of protein. Ibid 14 769–803.

Champetier G., et Emmanuel Faure-Fremiet 1938 Chimie Physique Biologique. Étude roentgénographique des kératines sécrétées. Comptes Rendus des Séances de L Académie des Sciences, 207 1133.

Cornselius, C. 1925 Morphologie Histologie und Embryologie des Muskelmagens der Vögel. Gegenbaurs Morph. Jahrbuch, 54 507–559

Curschmann, H. 1866 Zur Histologie des Muskelmagens der Vögel. Zeitschr f. Wiss. Zool. Leipzig, 16 224–235.

Eglitis, I., and R. A. Knouff 1957 Observations on the nature of the inner lining of the gizzard of the chicken. Anat. Rec., 127 287

Glegg, R. E Y Clermont and C. P Leblond 1952 The use of lead tetraacetate benzidine, o-dianisidine and "film test" in investigating the periodic acid-Schiff technic. Stain Technology 27 277–305.

Gomori, G. 1950 Aldehyde-fuchsin A new stain for elastic tissue. Am. J. Clin. Path., 20 665–666.

Hedenius, I. 1892 Chemische Untersuchung der hornartigen Schicht des Muskelmagens der Vögel. Skand. Archiv f Physiol. Leipzig, 3 244–252.

Hofmann, K. B., und Fritz Pregl 1907 Über Koilin. Hoppe Seyler Zeitschr. f. Physiol. Chemie, 52: 448–471.

Knaffl-Lenz, E. 1907 Über die Diaminosäuren des Koilins. Hoppe Seyler's Zeitschr f. Physiol. Ibid., 52: 472–473.

Leblond, C. P R. E. Glegg and D Eidinger 1957 Presence of Carbohydrates with free 1 2-glycol groups in sites stained by the periodic acid-Schiff technique. J Histochem. Cytochem., 5 445–458

Luppa, H. 1959 Histogenetische und Histochemische Untersuchungen am Epithel des Embryonalen Hühnermagens. Acta Anat., 39 51–81.

Meyer K. 1945 Mucoids and Glycoproteins. Advances in Protein Chemistry 2: 249–275. Academic Press, Inc., New York, N Y

Montagna, W H. B. Chase and W C. Lobitz, J 1953 Histology and Cytochemistry of human skin. V Axillary apocrine sweat glands. Am J Anat., 92 451–470.

Pearse, A. G. 1960 Histochemistry Theoretical and Applied. Little, Brown and Company Boston.

Wiedersheim, R. 1872 Die feineren Struktur verhältnisse im Muskelmagen der Vögel. Arch. Mikrosk. Anat., 8 435–452.

PLATE 1

EXPLANATION OF FIGURES

1 Vertical section of the inner wall of the gizzard. A, secreted membrane; B crypts C glands D epithelial caps (surface epithelium) covering extensions of tunica propria between crypts; E, desquamated epithelial cells from epithelial caps. Formalin fixation. Frozen section. Hematoxylin and eosin. × 73.

2 Mucosa of the gizzard. A, secreted membrane; B, secretion in gland lumens and in crypts. Formalin fixation. Mallory's connective tissue stain. × 69.

3 Outer part of the secreted membrane. A, arrays of secretion columns; B dentate surface C horizontal striae; D granular debris from desquamated surface epithelial cells. Formalin fixation. Toluidine blue 0.5% aqueous solution. × 295.

4 Cross section of lower portion of a crypt containing eight distinct rodlets secreted by the gizzard glands. Formalin fixation. Mallory's connective tissue stain. × 937

5 Epithelial cells lining the crypt and covering the tunica propria extensions (surface epithelium) A, secretion of the gizzard gland in the lumen of a crypt, B connective tissue of the tunica propria extensions between the crypts C, basophilic zone; D supranuclear secretion granules E, apical pole of the epithelial cell The free surface of the epithelium is shown at the lower part of the figure. Formalin fixation Toluidine blue 0.5% × 1287

6 Narrow extension of tunica propria between the crypts showing common characteristics of crypt cells and cells of the epithelial cap. A, connective tissue of the tunica propria extensions between the crypts B basophilic zone, ribonuclease labile; C, apical pole; D secreted granules and globules. Formalin fixation. Hematoxylin and orcein × 128

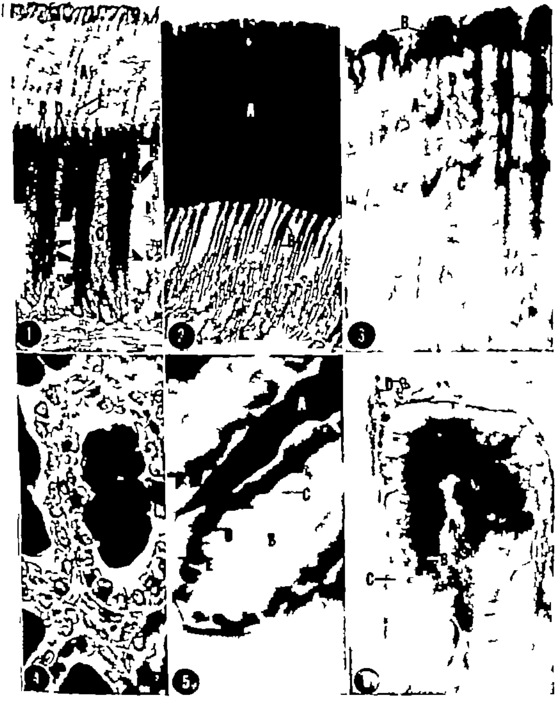


PLATE 2

EXPLANATION OF FIGURES

7 Secreted membrane and subjacent mucosa. A, secretion columns; B, surface and crypt epithelium with the secretion granules; C, horizontal striae. Formalin fixation. Toluidine blue 0.5% × 71

8 The secreted membrane detached from the underlying mucous membrane showing the hardened secretion in the mouths of the glands and crypts pulled aw y with the membrane A, hardened secretion in the gland pulled out of the crypts and glands in detached membrane; the innermost horizontal stratum represents the most recently secreted material of the crypt and surface cells. Formalin fixation. Frozen section. Hematoxylin and eosin. × 79

9 *Shows DNA of the nuclear debris of desquamated epithelial cells* which are incorporated in the secreted membrane. Formalin fix tion. Frozen section. Compare with figure 8 × 79.

10 Surface view appearance of the fresh untreated secreted membrane showing the areas of the secreted columns which project slightly above the general surface level. A, secretion columns. × 172.

11 Transverse section of the secreted membrane. Light areas represent the secreted columns and the dark area represent the cellular debris resulting from the desquamation of the surface epithelial cells. Formalin fixation. Hematoxylin and eosin. × 297

12 Vertical section of crypt region and adjacent secreted membrane. A, degenerating surface epithelial cells forming cap-like formations over the intercrypt tunica propria; B secretion of gizzard glands and its continuation through the crypt as secretory columns. Formalin fixation. Bargman modification of chrome alum hematoxylin stain. × 430.

13 Vertical section of the secreted membrane showing birefringent particles and SH and -S-S- protein bound groups. Formalin fixation. Frozen section. Ferricyanide method of Chèvremont and Frederic. × 86.

14 Cros section of the upper one-third of the tubular gizzard glands showing the dens acidophilic secretion. Note the resemblance in appearance to the small follicles of the thyroid gland. Formalin fixation. Mallory' connective tissue stain. × 937

15 Transverse section of the upper part of the crypt. Note the clear empty appearance of the apical secretory poles, resulting from the solubilization of the secretion granules. Formalin fixation. Mallory connective tissue stain. × 937 Compare with figures 5 and 6.

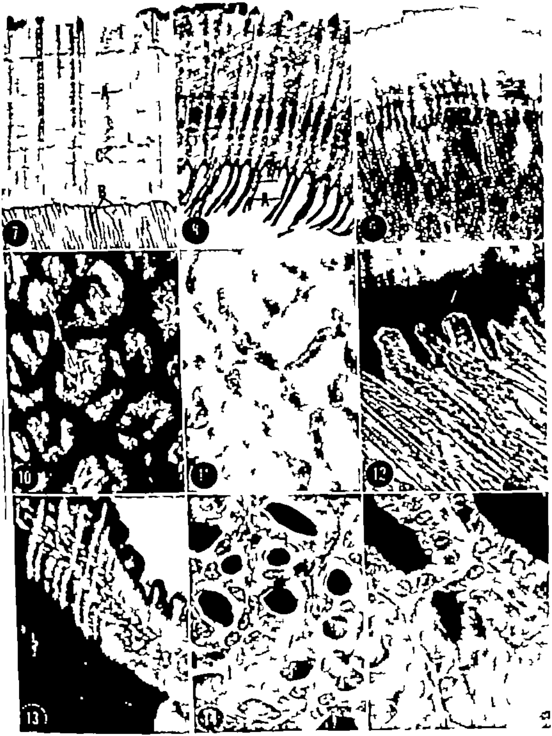


PLATE 3

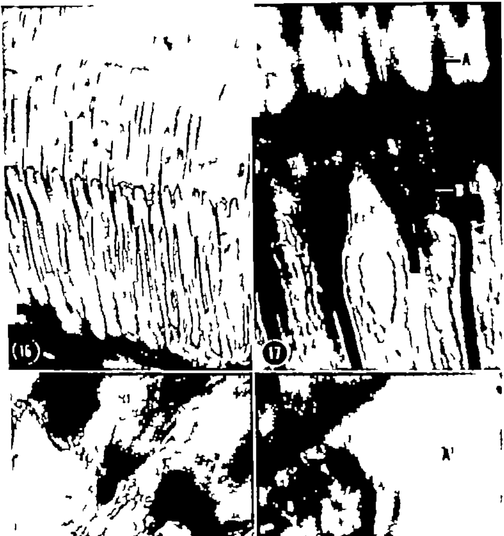
EXPLAN TION FIGURES

16 Vertical section of the mucosa including the secreted membrane showing the sites of carbohydrate complexes. Note (1) the strong positive reaction in the upper portions of the gizzard glands and their continuation into the less reactive secretion columns in the membrane; (2) the positive secretion granules in the crypt nd surface cells and (3) the slightly positive horizontal striae alternating with n reactive striae. Formalin fixation. Lead tetraacetate Schiff reaction. × 100

17 Vertical section of the crypt and adjacent secreted membrane showing strongly reactive protein ites. Note the strongly reacting secretion in the lumina of the tubular glands and crypts and their moderately reactive contin ations in the secreted columns; also the moderately reactive cellular debris which continues outward from the surface ep thelium. A secreted column ; B cellula debris. Formalin fixation Coupled Tetrazonium reaction. × 430.

18 Vertical section of crypt region and djacent secreted membrane, DDD reaction of Barrnett and Seligman showing the sites of S-S- and -SH groups. The dark colored area indicate the presence of -S-S and -SH groups Formalin fix tion. × 430.

19 Vertical section of the intercrypt surface epithelium showing solubilization of metachromatic granules. A innermost stratum of the secreted membrane; B metachromatic granules; C, pical pole. Formalin fixation. Lead tetraacetate-Schiff × 970.


16
17
A
B
A'
B
C

The Craniovertebral Veins and Sinuses of the Dog

KARL R. REINHARD, MALCOLM E. MILLER, AND HOWARD E. EVANS
National Institutes of Health, Bethesda, Maryland and New York State Veterinary College, Cornell University, Ithaca, New York

INTRODUCTION

Comprehensive study of canine anatomy is a relatively recent development in veterinary science. The increased interest in anatomy and physiology of the dog has arisen not only from the heightened veterinary clinical interest in this species but also from the fact that it has become an extremely valuable subject for teaching and research in veterinary and human medical sciences.

The veins and venous sinuses of the cranium and vertebral column are structures of considerable importance from physiological and pathological standpoints. Thus far a comprehensive study of the canine craniovertebral venous drainage has not been recorded although portions of the system were studied and described more than 60 years ago. Hofman ('01) made an extensive comparative anatomical study of the veins of the brain and spinal cord of various representative vertebrates from *Pisces* to *Perissodactyla* including *Canis familiaris*. Zimmerman ('36) published a detailed account of the anatomy of the dura mater and the venous sinuses of the canine calvarium. Drager ('37) reported anatomical studies of the canine longitudinal vertebral sinus and its relation to the venation of adjacent structures. Worthman ('56) also published an account of the canine longitudinal vertebral sinuses, including their importance as collateral venous channels. Padget ('57) recorded comparisons between human and canine cranial venation in an excellent monograph on the embryonic and fetal development of cranial venation in man. The present study was conducted to prepare an integrated description of the craniovertebral venous drainage for a forthcoming text of canine anatomy. Recent increase of interest in this region of canine anatomy on the part of experimental workers outside of the veterinary field prompted publication prior to completion of the comprehensive textbook.

MATERIALS AND METHODS

The subjects used were 28 mongrel, mesocephalic individuals weighing 15 to 20 pounds, ranging from 6 months to 6 years in age. They were obtained from private owners who wished to dispose of the animals. Intravenous injection of a lethal dose of saturated magnesium sulfate solution caused immediate insensibility and death without struggle in all instances. Blood was extravasated in the moribund subject by trocarization of the carotid artery. The subject was preserved by perfusion with 10% formalin solution.

After embalming was complete the venous system was injected with pigmented latex solution. The injection was made into one *angularis oculi vein*, and directed toward the orbit. This technique resulted in the filling of all the central and peripheral veins as far as their proximal valves. The specific latex preparation used penetrated into minute venules and polymerized to form a tough, resilient, detailed cast. The color was stable, resisting preservatives, alkali and acid treatments and clearing agents. In the first few specimens dissected, the arterial system was injected with differentially colored latex through the carotid artery to show the arterial and venous relationships of the craniovertebral circulation.

Illustrations by Marion Newsom and Pat Barrow.

Division of Research Grants, National Institutes of Health, Public Health Service, Department of Health, Education and Welfare, Bethesda, Maryland.

New York State Veterinary College, Cornell University, Ithaca, New York. Dr. Miller was formerly Professor of Anatomy and Head of the Department of Anatomy; deceased, April 1960.

Neoprene Latex 571, E. I. Dupont DeNemours Corp., Rubber Laboratory. Gratuitous supply is gratefully acknowledged.

Four of the dogs were dissected by manual methods alone They afforded valuable information on the relation of the veins to the soft structures However this approach often resulted in the destruction of the more delicate veins and the intraosseous veins and sinuses. In subsequent specimens when manual dissection reached the level of the bony structures the specimen was immersed in an aqueous solution of 10% hydrochloric acid (final concentration, 3 5% to 3 8% HCl) When the bones became leather like in consistency the specimen was washed free of acid and dissected further by hand. This minimized destruction of intraosseous veins.

To allow observation of the finer venous architecture without hazard of manual dissection ten specimens were macerated chemically All structures peripheral to the cranial and vertebral musculature were removed The specimen was then immersed in a lye solution (10 to 15%) For this technique specimens with large deposits of adipose tissue were found un- because the fat layers would and prevent deeper penetration the lye solution When the specimen ftened superficially it was placed on a non-corroding wire screen and removed daily from the lye bath for debridement of the macerated tissue. This was best accomplished, without destruction of the finer latex casts by directing a low velocity jet of water on the area to be debrided. Maceration was discontinued before the intervertebral discs were destroyed After maceration the specimen was placed in tap water Over a period of several hours the preparation was slowly neutralized with 10% hydrochloric acid. After remaining in the neutralized bath overnight the specimen was rinsed several times with tap water and placed in a 10% hydrochloric acid decalcifying bath Manual dissection was resumed when the bone could be cut easily with a knife.

The combination of maceration and decalcification greatly aided the study of venous architecture especially the intra osseous veins and sinuses The relationships between the soft tissues and the veins were destroyed but these had been determined previously in the manual dissections of the unmacerated specimens Integration of the information gained by all the dissection techniques yielded a clear picture of anatomic relationships.

OBSERVATIONS

In the following descriptions the osteologic and neuroanatomical landmarks used to describe the course of vessels will not be defined For information on these the reader is referred to Miller ('58 and '62) Ellenberger Baum ('43) Sisson and Grossman ('53) and Nickel, Schummerman and Seiferle ('54)

Veins and sinuses of the cranium

For convenience the cranial veins and sinuses are discussed as a dorsal group and a ventral group although these are not independent.

Lying along the internal parietal crest enclosed by the dorsal folds of *falx cerebri* and extending from the *foramen impar* to the dorsal end of the ethmoidal crest is the *dorsal (superior) sagittal sinus* Rostrally the sinus begins at the cribiform plate by one or two minute radicles that form in the osseous nasal septum. The sinus receives irregular tributaries along its length from the dorsal diploic circulation. Two regular emissary veins join the sinus at the rostromedial margins of the parietal bones. These veins serve the medial fronto-parietal regions exterior to the calvarium. Laterally and ventrally the sinus receives veins from the dorsal and medial surfaces of the cerebral hemispheres. The larger pair of these veins is found in the region of the lesser cruciate fissure of the brain, and the junction of these with the sinus may form a lacuna

Rostral to the *foramen impar* the dorsal sagittal sinus receives the *straight sinus* The proximal end of the straight sinus may form a large branched or circular lacuna in its junction with the sagittal sinus. The course of the straight sinus lies between the layers of the *falx cerebri* dorsal to the insertion of the latter on the *tentorium cerebelli.* The *straight sinus* is formed midway between the splenium of the corpus callosum and the foramen impar by the junction of three veins, two are veins from the medial regions of the right and left occipital lobes of the cere-

brum. The third is the large *great cerebral vein*. These veins lie together between the leaves of the falx cerebri, dorsal to the rostral half of its insertion on the tentorium cerebelli. At the rostroventral angle of the caudal attachment of the falx cerebri, the occipital cerebral veins converge from their origin in the occipital lobes. In this same area the great cerebral vein originates in the junction of the *vein of the corpus callosum* the *internal cerebral vein* and the *thalamostriate vein* The vein of the corpus callosum lies along the dorsal aspect of the corpus callosum, receiving tributaries from the ventromedial surfaces of the cerebral hemispheres and the cerebral choroid plexus. The internal cerebral vein receives tributaries from the dorsal mid-brain ventral to the corpus callosum. The thalamostriate vein serves the thalamus and *corpus striatum*. The *ventral (inferior) sagittal sinus* described by Zimmerman ('36) was not found in our dissections. Hints of a fine vessel could be seen in the ventral margin of the falx cerebri, but the existence of a vessel was not demonstrated by latex penetration.

After receiving the straight sinus the dorsal sagittal sinus enters the *foramen impar* and joins the paired *transverse sinuses* in the *confluens sinuum*. The form of the confluens sinuum is variable. Lateral to the confluens sinuum the transverse sinuses receive penetrating branches from the *occipital emissary vein*. The transverse sinuses lie in the transverse canal within the internal occipital protuberance. At the lateral orifices of the transverse canal on each side the transverse sinuses join three venous sinuses. Two tributary veins are also received at this confluence one is the *occipital diploic vein* which drains the caudolateral region of the parietal bone. The second tributary is the *lateral branch* of the *occipital emissary vein* which enters at the supramastoid foramen to join the dorsal extremity of the sigmoid sinus. The occipital emissary vein drains the nuchal area exterior to the occiput; the right and left veins anastomose medially caudal to the external occipital protuberance

The three sinuses which join the transverse sinus at its lateral extremity are the *temporal sinus* the *dorsal (superior) petrosal sinus* and the *sigmoid sinus*. The temporal sinus is an effluent vessel which courses in a rostro-ventral direction in the temporal groove and temporal canal. It leaves the skull at the postglenoid foramen, where it becomes the *retroglenoid vein*. After a short course it joins the internal maxillary vein.

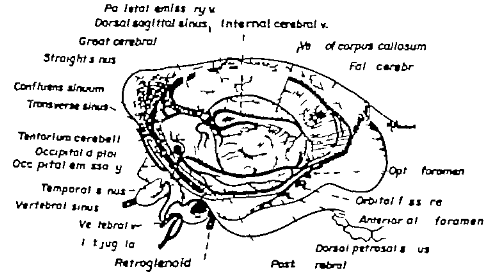


Fig. 1 Lateral view of major dorsal cranial venous channels; right half of dorsal calvarium and right cerebral hemisphere removed.

The dorsal petrosal sinus courses in the membranous *tentorium cerebelli* along the medial surface of the pyramid of the pet rous temporal bone caudoventral to the petrosal crest, arising from the area between the caudolateral surface of the midbrain and rostro medial surface of the cerebellum. It is formed by branches from the caudal, lateral and dorsal midbrain and the rostral region of the cerebellum including the vermis. These branches anastomose freely with their opposite vessels both rostral and caudal to the diencephalon. The tributaries of the dorsal petrosal sinus are longer and ramify more extensively than any other intracranial veins. On both sides a minute anastomotic branch of the dorsal petrosal sinus may be found along the crest of the pyramid contained in a minute osseous canal along the ventral half of the crest, joining the cavernous sinus ventrally The regularity of this anastomotic branch has not been ascertained. Near junction with the transverse sinus the dorsal petrosal sinus receives the *caudal cerebral vein* which ...ses in two branches from the lateral of the cerebrum. The dorsal is received from the lateral temporal region of the cerebrum. The ventral branch courses along the base of the squamous temporal bone receiving branches from the ventrolateral aspect of the cerebrum. The dorsal and ventral branches of the caudal cerebral vein may join before entering the dorsal petrosal sinus or may join the sinus separately a short distance before its termination. The *sigmoid sinus* lies caudal to the petrous temporal bone and courses ventrad to the jugular foramen. Before entering the jugular for amen the sigmoid sinus (1) receives a group of small veins which ramify to serve the dorsal and caudo-dorsal cerebel lum, the caudoventral cerebellum the choroid plexus of the fourth ventricle and the ventral region of the medulla and (2) joins the rostral end of the condyloid vein before it enters the rostral end of the condyloid canal. The sigmoid sinus ends in the jugular foramen in its anastomosis with the ventral petrosal sinus the inter nal jugular vein and the vertebral vein. These latter structures are described in the following

Ventral veins and sinuses of the cranium

The large paired *cavernous sinuses* ca be considered the central structures of th ventral cranial venation. They lie on eithe side of the floor of the middle cran fossa, from the rostral orifices of the petro basilar canals to the orbital fissures. Ro trally they communicate through the o bital fissures with the orbital venous ple uses. Ventrolaterally branches from th cavernous sinuses communicate throu the oval and round foramina with th veins lying in the alar canals. Caud the cavernous sinuses communicate w the ventral petrosal sinuses which l within the petrobasilar canals. Two co nections of the cavernous sinuses, th intercavernous sinuses are present. Th larger *caudal intercavernous sinus* l caudal to the dorsum sellae the smal *rostral intercavernous sinus* lies betwe the dorsum sellae and the hypophy Occasionally a fine vein connects the ro tral ends of the cavernous sinuses.

The cavernous sinuses do not rece tributaries from the ventromedial reg of the cerebrum. They serve to conn intimately the orbital venous plexus w the intracranial circulation. The ven *(inferior) petrosal sinus* on each sid extends from the caudal end of the cav nous sinus through the ventral petro sinus (petrobasilar) canal to the jug foramen at which point it anastomo with the sigmoid sinus. The ventral pe rosal sinus also gives off a vein wh traverses the carotid canal to join th internal maxillary vein.

The condyloid veins represent the ul mate cranial extensions of the longit dinal vertebral sinuses. The former orig nate on each side from the base of th sigmoid sinus and course caudad throu the condyloid canal, receiving a branc through the hypoglossal canal. Caud to the condyloid canal these veins beco the *ventral occipital sinuses* which tr verse the foramen magnum to the floor o the vertebral canal, where they beco the *longitudinal vertebral sinuses*

The ventral occipital sinuses are co nected by *dorsal* and *ventral interoccipit sinuses* The ventral interoccipital sin is a relatively wide flat sinus which b

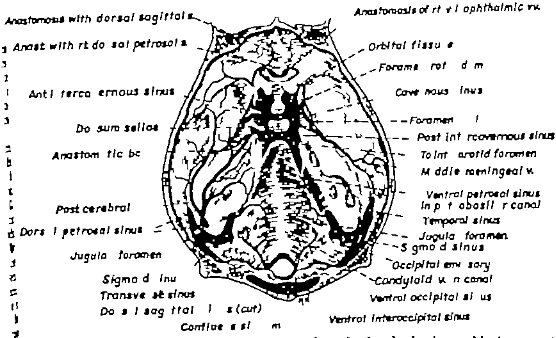


Fig. 2 Dorsal view showing position of major venous channels; dorsal calvarium and brain removed.

along the base of the occipital bone on the edge of the foramen magnum. The rostral and caudal edges of the ventral Interoc cipital sinus are irregular, sometimes fimbriate. The dorsal interoccipital sinus is not present in all specimens. When present it consists of fine channels or a rete of vessels arching along the dorsal aspect of the foramen magnum, and usually coextensive with the dorsal internal plexus of the atlas.

The return of blood from the cranial veins and sinuses towards the heart involves a number of routes. The ophthalmic veins have many junctions with the cavernous sinus via the orbital plexus and with the deep facial and angular veins which are tributaries of the external maxillary veins. The internal maxillary veins receive the retroglenoid vein and also the deep temporal veins which form anastomoses with the veins of the orbit. The middle menigeal vein, separate from the principal cranial venous system, also drains into the internal maxillary vein. Therefore by means of the numerous anastomoses of its tributaries with the cerebral veins, the external jugular vein apparently carries a major share of the cranial venous drainage.

The veins other than the external jugular system which receive blood from the brain are (1) the longitudinal vertebral sinuses, which are relatively large channels, (2) the vertebral veins, moderately large vessels which continue as the cervical vertebral veins, and (3) the small internal jugular vein. The latter is commonly supposed to have its cranial termination at the level of the thyroid. However in all specimens carefully dissected, as well as the macerated specimens, the internal jugular was found to originate in the jugular foramen in anastomosis with the sigmoid sinus, ventral petrosal sinus, vertebral vein, and a vein from the hypoglossal canal. The internal jugular vein leaves the jugular foramen in company with the vertebral vein, and proceeds caudad. From the cranial cervical region it proceeds in the sheath of the carotid artery to its termination in junction with the external jugular or brachiocephalic vein.

The general architecture of the cranial venation of the dog is similar to that of man. However marked differences in relative size of homologous structures exist.

The internal jugular in man is the largest vein draining the head in contrast to its almost vestigial nature in the dog. In the dog the temporal sinus by reason of its relatively large size receives a considerable portion of the dorsal cerebral venous blood. Only a vestige of the temporal sinus remains in man. The external jugular vein receives most of the cranial drainage in the dog the internal jugular in man. Other variations occur but those cited above seem to be of greater functional importance.

Veins and sinuses of the vertebral column

Although the internal veins of the vertebral column are continuous with the cranial venation description is facilitated by separate treatment. The largest, and most extensive vessels are the paired *longitudinal vertebral sinuses* which arise cranially as extensions of the ventral occipital sinuses. They extend caudally through the foramen magnum and along the floor of the vertebral canal, ventral to the spinal cord. The vertebral sinuses are lar[ge] flattened veins through the cervical, th[o]racic and lumbar regions. They decrea[se] rapidly in size in the sacral region an[d] terminate in fusion at the level of th[e] fourth fifth or sixth coccygeal verteb[ra]. The sinuses are multiarciform in that they diverge as they approach the intervertebral foramina but approach each other close[ly] midway along each vertebra, where each receives a *basivertebral vein* arising from the vertebral body. Occasionally anasto[mo]ses between the sinuses occur at the exits of the basivertebral veins but the number and location of these anastomoses is inconstant. At each intervertebral jun[c]tion an *intervertebral vein* arises from each longitudinal sinus and leaves the vertebral canal through the intervertebral foramen.

The intervertebral veins, on emerg[ing] from the intervertebral foramina, rec[eive] many small veins from the muscles an[d] other tissues lateral and dorsal to the vertebral column. In addition they re[ceive] small veins from the *dorsal extern[al]*

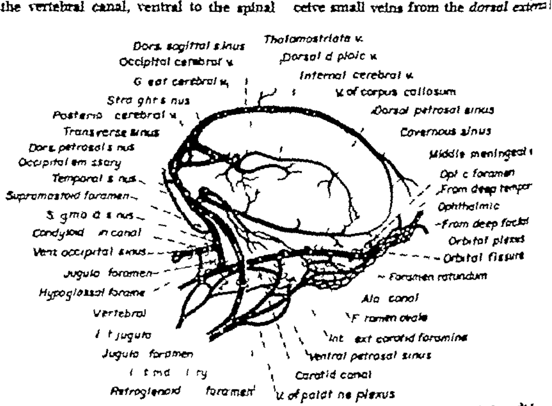


Fig. 3 Semi-diagrammatic representation of erebral venous drainage; intracranial channels connections to major efferent eins are shown.

vertebral venous plexus which forms a network around the dorsum of the vertebral column. The dorsal external vertebral venous plexus together with the veins from the structures lateral and dorsal to the vertebral column form an extensive paraxial plexus. This has many anastomoses with the tributaries of the peripheral veins which drain the paraxial region.

The intervertebral veins also receive small tributaries from the ventral surface of the body of the vertebra. These small veins anastomose ventrally and form the *ventral external vertebral venous plexus.* This is not extensive- usually only one *small vein encircles the cranial end of the* vertebral body and receives venules from it. It is joined ventrally by an unpaired median vein which receives many radicles from the vertebral body

Within the vertebral canal the vertebral sinuses receive, at the intervertebral junctions, the spinal veins which drain the spinal cord. Our injections did not fill these veins. But the plan so far as we were able to determine resembles that of man The dorsal ventral spinal veins drain into a radicular vein which follows the nerve root to the intervertebral region, and there joins the longitudinal vertebral sinus.

At the intervertebral region a small vein stems from the longitudinal sinus and courses dorsad along the interior of the vertebral arch. This transverse branch is joined to the opposite transverse branch at the apex of the internal vertebral arch. Ellenberger and Baum (43) name the combination of transverse branches the arcuate vein We have found in our specimens that this internal dorsal venous plexus is usually incomplete between the fifth and seventh cervical vertebrae, and also between the ninth thoracic and seventh lumbar vertebrae. Small transverse branches are present, but are not complete dorsally Perhaps the entire arch was present in these regions but our techniques did not effect the injection of the small vessels completing the arc. The transverse branches were not found in the coccygeal region. The vessels forming the internal dorsal plexus are generally flattened dorsoventrally They are relati el larg in the cervical and thoracic regions At the axio-atlantal and the atlanto-occipital joints they are especially massive and form arcuous retes joining the longitudinal vertebral sinuses across the vertebral arch.

The veins of the *internal dorsal vertebral plexus* did not arise regularly from the longitudinal vertebral sinus especially in the cervical and cranial thoracic regions. Instead, they joined the intervertebral vein within the intervertebral foramen or close to the origin of the latter vessel from the longitudinal sinus. Another minute but noteworthy observation on the termination of the dorsal internal vertebral veins was that they frequently divided before joining the longitudinal vertebral sinus or the intervertebral vein, thus surrounding the exit of the spinal nerve. In the cervical region the spinal ganglia lay in these orifices in a cushion of veins. In the thoracic region and caudal this venous ring occurred less regularly

Wherever the dorsal internal venous arch was complete, veins left it dorsally pierced the ligamentum flavum, passed between the margins of adjacent vertebral arches and anastomosed with the dorsal external vertebral plexus. In the cervical and lumbar regions a perforating vein left the vertebral canal on either side between the articular process and base of the spine In the thoracic region, these interspinous branches arose together beneath the base of the spinous process. They either fused or coursed together directly dorsal, between the adjacent spinous processes to the tips of the spines. Lateral branches were given off along their course to the external dorsal vertebral plexus The perforating branches in the sacral region left through the dorsal sacral foramina.

To recapitulate the dog like the human has four general vertebral plexuses; dorsal internal, ventral internal dorsal external and ventral external. The dorsal and ventral external f llow the same general plan as in m There are some differences betwee m and dog in the internal rtebral plex arrangem In man ntral internal branches nect th longudinal vertebral sinus ros th floor he vertebral canal d also receive basivertebra ns These transverse nches are lly absent n the dog d the basivertebral r the lon

gitudinal sinuses directly although basivertebral veins anastomose under the longitudinal ligament or within the body. Also, in man two retia extend along the dorsum of the vertebral canal, from the foramen magnum to the coccyx, join the transverse branches. We did not find evidence of such retia in the dog.

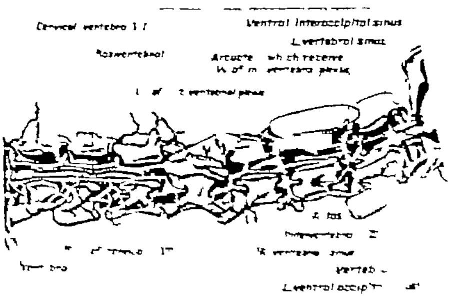


Fig. 4. Vertebral venous channels, cervical region.

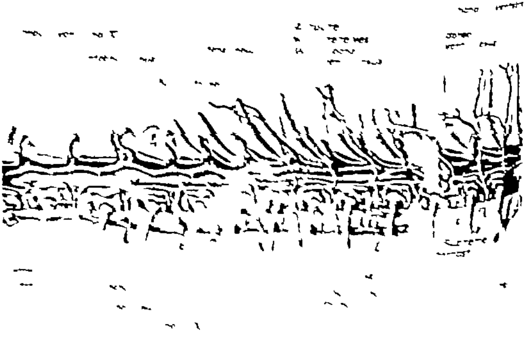


Fig. 5. Vertebral v[illegible] thoracic region.

Systemic veins draining the vertebral regions

The cervical vertebral region is drained rincipally by the vertebral veins. From he jugular foramen the *vertebral vein* of ach side courses ventral to the occipital one and passes to the ventral atlantal ossa. Here each divides into two branches.)ne the intervertebral vein of the atlanto-ccipital joint, turns dorsad, curves around ne alar notch to the dorsum of the atlantal ving, bends medially and passes through ne intervertebral foramen of the atlas, to oin the internal venous plexus. The main tem of the vertebral vein continues hrough the transverse foramen of the tlas. Within the transverse foramen, a mall vein leaves the vertebral vein and uns medially through a small canal in ne wall of the atlas to join the internal ertebral plexus. At the caudal opening f the transverse foramen of the atlas two eins are received by the vertebral vein ne from across the dorsum of the atlas rom the intervertebral foramen, and the ther the intervertebral vein from the tlanto-axial joint. The vertebral vein nen proceeds caudad to the transverse oramen of the axis. Here it receives the econd cervical intervertebral vein at the tlanto-axial junction. The vertebral veins ourse caudad through transverse foramina of the succeeding cervical vertebrae receiving the intervertebral veins at the intervertebral spaces. They continue ventrad to the transverse processes of the seventh cervical vertebrae, and join the *costocervical veins* which enter the precava. The vertebral veins collect blood directly from all of the cervical intervertebral veins. The costocervical veins collect the flow from the first, second and third thoracic intervertebral veins by the intercostalis suprema branches.

The *azygos vein* takes up vertebral drainage from the fourth thoracic intervertebral vein to the second lumbar intervertebral vein. The fourth and fifth thoracic intervertebral veins are connected by anastomotic vessels which run caudad in the spaces ventromedial to the costal tubercles to join the azygos vein. The intervertebral veins from the fifth to twelfth thoracic vertebrae, receive the intercostal veins and then drain into the azygos vein. The first lumbar intervertebral veins drain directly into the azygos vein. A small anastomotic branch of the azygos vein runs caudad along the base of the vertebral column to anastomose with the lumbar vein from the postcava. This anastomotic vein receives the second lumbar intervertebral veins. The lumbar intervertebral veins three to five are drained by the *lumbar branches* of the *postcava*. Caudad to the sixth lumbar vertebrae the lumbar and

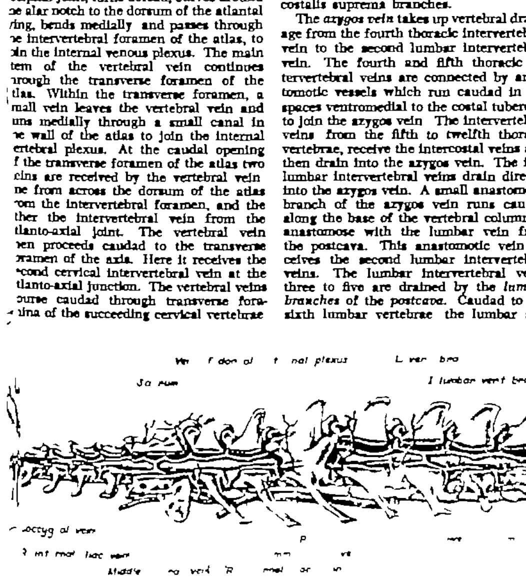


Fig. 6. Vert d u hannels, lumbar sacral, and

sacral intervertebral veins are received by tributaries of the *internal iliac veins* The small *ventral median coccygeal vein* receives the coccygeal intervertebral vein before joining the middle sacral vein. The latter joins one or both of the internal iliac veins.

DISCUSSION

Although the canine cranaxial venous *system is closely integrated and continuous*, four major drainage areas can be discerned: (1) Cranial, served mostly by the internal maxillary vein, draining into the external jugular (2) Cervical, served primarily by the vertebral veins which join the costocervical veins draining into the precava (3) Thoracic served primarily by the azygos vein, and (4) Lumbosacral-coccygeal, which drains into the iliac and lumbar veins. However the entire cranaxis is served by an intercommunicating system of internal sinuses and veins which could serve to redistribute flow should the drainage be interrupted regionally external to the cranaxis The collateral circulatory potential of the longitudinal vertebral sinuses has been explored by Worthman ('56) Anastomoses of the veins serving the brain are particularly complex and abundant. Experimental isolation of drainage from small circumscribed areas of the brain might pose difficult technical problems. Since the craniovertebral venous drainage is unvalved and closely associated with that of surrounding tissues, considerable potential exists for hematogenous extension of infection or neoplasia into the cranial and axial spaces from surrounding tissues. (Batson, 40 Worthman '56.)

LITERATURE CITED

Batson, O V 1940 Function of vertebral veins and their role in spread of metastases Am. Surg., *112* 138–149

Drager K. 1937 Uber die sinus columnae vertebralis des hundes und ihre Verbindungen zu Venen der Nachbarschaft. Morphol Jb. *80* 579–598.

Ellenberger W and H Baum 1934 Handbuch der Vergleichenden Anatomie der Haustiere 18 edition, Julius Springer, Berlin.

Hofman, M. 1901 Zur Vergleichenden Anatomie der Gehirn und Rückenmarksvenen der Vertebraten. Zeitschr f. Morphol. u. Anthropol., 3 239–299

Miller M. E. 1958 Guide t the dissection of the dog. Department of An tomy New York State Veterinary College at Cornell University

——— 1962 Anatomy of the dog (Contributed by G G Christensen and H. E. Evans). W B Saunders Co. (In preparation for publication)

Nickel, Schummerman, Seiferle 1954 Lehrbuch der Anatomie der Haustiere Band I, Bewegungsapparat. Parey Berlin.

Padget, D. H. 1957 The development of the cranial venous system in man from the viewpoint of comparative anatomy Carnegie Institute of Washington publication No. 611, Contributions to Embryology 36 79–140.

Sisson, S., and J D Grossman 1938 The anatomy of the domestic animals. 3rd ed. Rev. W B. Saunders, Philadelphia.

Worthman, R. P 1956 The longitudinal vertebral venous sinuses of the dog. Part I Anatomy Part II Functional Aspects. Am. Jour. Veterinary Research, 57 341–363.

Zimmermann, G. 1936 *Uber die Dura Mater Encephali und die Sinus der Schädelhöhle des Hundes* Zeitschr. f. Anat. u. Entwicklungsgeschichte *106* 107–137

PLATES

PLATE 1

EXPLANATION OF FIGURES

Injected specimen, showing major effluent veins of cranium.

AOV Angularis Oculi Vein
DFV Deep Facial Vein
DTV Deep Temporal Vein
EMV External Maxilliary Vein
LJV Internal J gular Vein

IMV Internal Maxillary Vein
PgV Retroglenoid Vein
VV Vertebral Vein
OV Occipital Vein

THE CRANIOVERTEBRAL VEINS AND SINUSES OF THE DOG
Karl R. Reinhard, Malcolm E. Miller and Howard E. Evans

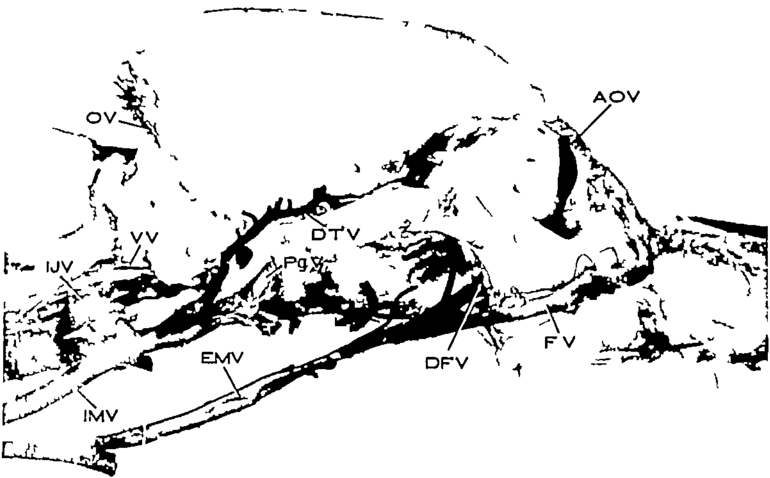


PLATE 2

EXPLANATION OF FIGURES

Injected decalcified specimen, dextrolateral view dorsal right calvarium removed

AOV A gularis Oculi Vein
CS, Confluens Si m
DCV Dorsal Cerebral Veins
DFV Deep Facial Vein
DSS, Dorsal Sagittal Sinus
DTV Deep Temporal Vein
EMV External Maxillary Vein
FV Facial Vein
IJV I ternal J gular Vein
IMV Internal Maxillary Vein

ODV Occipital Diploic Vein
OEV Lat. Occipital Emissary Vein (lateral)
OEV Med. Occipital Emissary V in (medial)
OV Occipital Vein
PEV Parietal Emissary Vein
PgV Retroglenoid Vein
TmS, Temporal Sinus
TrS, Transverse Sinu (right)
VV Vertebral Vein

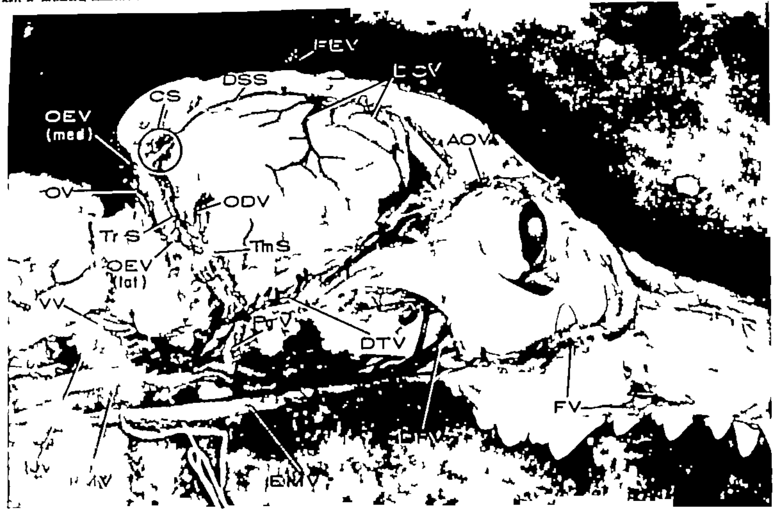

FEV
DSS
CS
OEV
(med)
OV
ODV
Tr S
TmS
OEV
(lat)
VV
PgV
DTV
AOV
FV
EMV

PLATE 3

EXPLANATION O FIGURES

I jected, decalcified specimen dorsal view right half of calvarium removed.

AOV A gularis Oculi Vein
DCV Dorsal Cerebral Veins
DSS, Dorsal Sagittal Sinus
DTV Deep Temporal V in
IMV Internal Maxillary Vein

OEV (Lat.) Occipital Emissary Vein lateral
OV Occipital Vein
PEV Parietal Emissary Vein
T.S, T ansverse Sinus

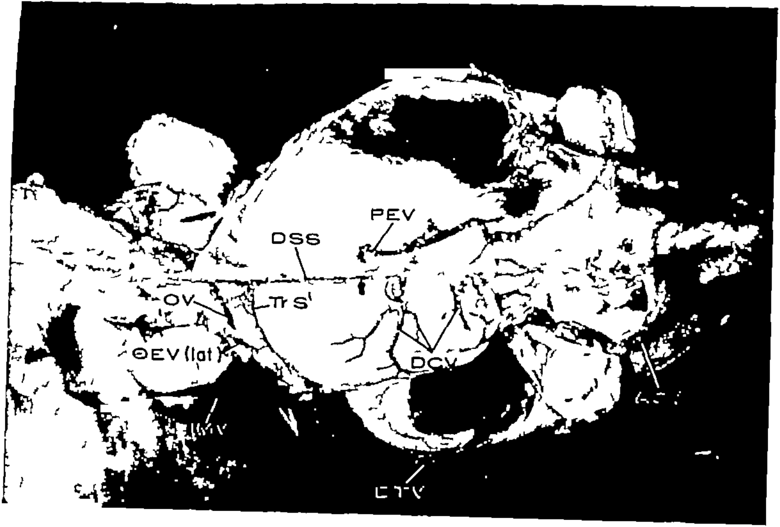

PEV
DSS
OV
Tr S
ΘEV (lat)
DCV

PLATE 4

EXPLANATION OF FIGURES

Injected, decalcified specimen, l teral view dorsal calvarium and zygoma removed.

AOV Angularis Oculi Vein
CS, Confluen Sinum
DFV Deep Facial V in
DSS, Dorsal Sagittal Sinus
DTV Deep Temporal Vein
EMV External Maxillary Vein
FV Facial Vein
ICV Internal Cerebral Vein
V Internal J gular Vein
fV Internal Maxillary Vein
JV Occipital Diploic Vein

OEV l t. — Occipital Emissary Vein (lateral)
OEV med. — Occipital Emissary Vein (medial)
OrPl, Orbital Plexu
OV Occipital Vein
PgV Retroglenoid Vein
StS, Straight Sinus
ThV Thalamostriate Vein
TrS, Transverse Sinus
VCC Vein f Corpus Callosum
VV Vertebral Vein

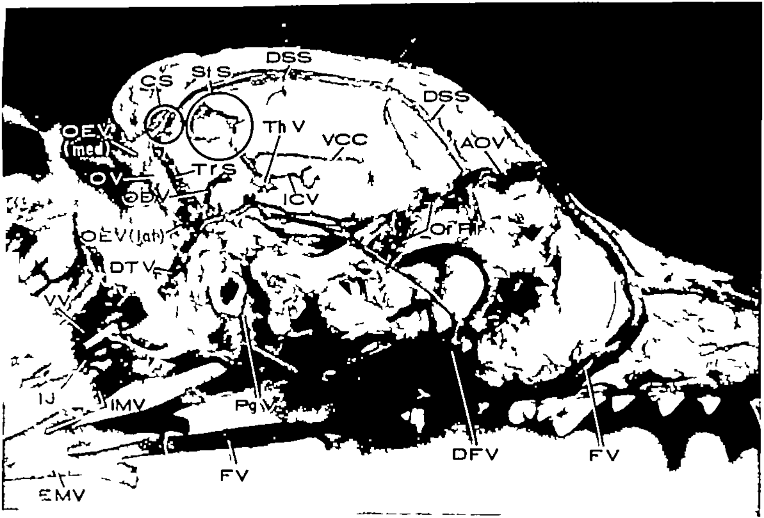
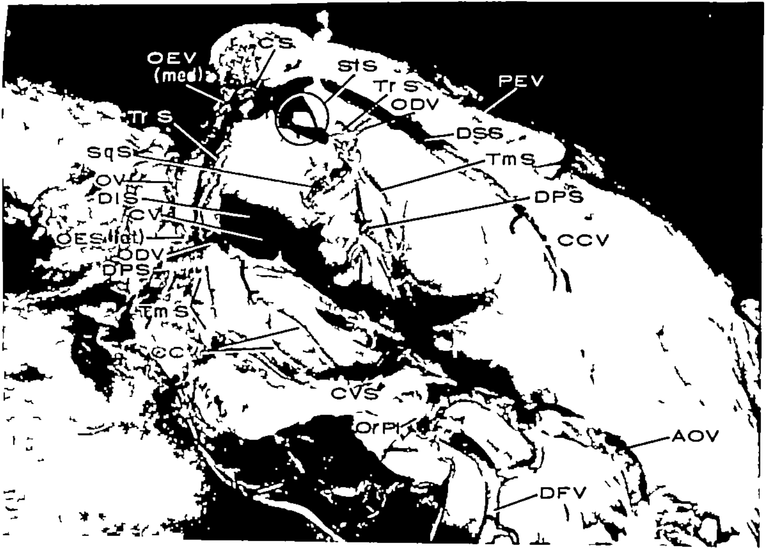

DSS
SIS
CS
DSS
OEV (med)
ThV
VCC
AOV
TrS
OV
OBV
ICV
OEV (lat)
OrFi
DTV
VV
IJ
IMV
PgV
DFV
FV
FV
EMV

PLATE 5

EXPLAN TION F FIGURES

I jected, decalcified macerated specimen dorsolaterorostral view right half f dorsal cal arium nd zygoma removed.

AOV Angularis Oculi Vein
CCV Caudal Cerebral Vein
CS Confluens Sinum
CV Condyloid Vein
CVS Cavernous Sinus
DFV Deep Facial Vein
DIS, Dorsal Interoccipital Sin
DPS, Dorsal Petrosal Sinus
DSS Dorsal Sagittal Sinus
ODV Occipital Diploic Vein
OEV l t. — Occipital Emissary Vein (lateral)
OEV med. — Occipital Emissary Vein (medial)
OrPl, Orbital Plexus
OV Occipital Vein
PEV Parietal Emissary Vein
SgS, Sigmoid Sinus
StS, Straight Sinus
TmS, Temporal Sinus
TrS, Transverse Sinus


CS
OEV
(med)
StS
Tr S
PEV
ODV
Tr S
DSS
SqS
Tm S
OV
DPS
DIS
CV
CCV
OES(lat)
ODV
DPS
Tm S
CC
CVS
Or Pl
AOV
DFV

ontinuities Between the Plasma Membrane and the ~rcoplasmic Reticulum in Crayfish Stretch Receptor ' as Revealed by Reconstructions from 1 Sections[1]

R. PRICE PETERSON
Department of Anatomy and Institute of Neurological Sciences University of Pennsylvania, Philadelphia Pennsylvania

In recent years there has occurred a derable revival in interest in the in- reticular structure of muscle, clearly described by Veratti in 1902. nis has been due primarily to its re-dis- very by electron microscopists who have med it the sarcoplasmic reticulum in malogy with the endoplasmic reticulum other cell types. The history and present iews of the structure and function of this ystem have recently been admirably re- wed in J Biochem. Biophys. Cytol., 1 10 no. 2 Suppl.

Functionally the reticulum is thought to involved in connecting the primary vent in muscle excitation, membrane de- on, with the final event, muscle ontraction. This process is referred to as xcitation-contraction coupling. This hy esis, first suggested from the work of F Huxley and co-workers ('58) rests n three primary assumptions: (1) that plasma membrane of the muscle fiber nd the membranes of the sarcoplasmic iculum (SR) are electrically continuous) that a depolarization wave can spread long the SR membranes and (3) that depolarization wave traveling along e SR membranes can initiate the chem- processes of muscle contraction. In is paper evidence will be presented in or of the first assumption for the stretch ceptor muscles of the crayfish.

In a previous communication (Peterson nd Pepe '62) incomplete evidence was resented that in the stretch receptor mus- s of the crayfish the plasma membrane component of the sarcolemma (Mauro d Adams '61) is continuous with the asmic reticulum. However this was an interpretation, and the point could not be proven from examination of single sec tions with the electron microscope Since then serial sections have been examined and reconstructions of the SR made from them. It is primarily this new evidence which will be presented here.

METHODS

Specimen preparation. The crayfish used, *Orconectes virilis* were obtained from Wisconsin and kept in the laboratory until needed. It was found that they could be maintained for several months in a common fresh water aquarium and being scavengers would eat nearly anything. The abdominal stretch receptors were dis- sected out, fixed, dehydrated, and embed- ded by essentially the same method as previously described (Peterson and Pepe '62) Two major modifications were made to facilitate study of the sarcoplasmic re ticulum of the muscles. To the fixing fluid (1 5% OsO_4 buffered to pH 7 4 with 0 2N s-collidine) was added $CaCl_2$ to a concen- tration of 0 1M. Although the concentra tion of calcium in crayfish physiological saline (van Harreveld, '36) is 0 013M, in- creasing this to 0 1M added considerable contrast to the sarcoplasmic reticulum membranes (as well as most of the other membranes) To increase further the con- trast of the specimens they were stained on the grid for 20–30 minutes with lead hydroxide according to Watson ('58) and Peachy ('59) For the staining of serial sections it was necessary first to modify

[1] This investigation was supported by U. S. Public Health grant NB-[illegible].

[2] At the suggestion of Dr Jean Paul Revel of Harvard University

the method to insure grids free of lead carbonate crystals as one crystal in the wrong place could make useless a whole series of sections. Crystals of lead carbonate were removed by washing with warm CO free water for 1–2 minutes.

The sections were cut on an LKB 4800 ultratome with glass knives and were gray to silver in color Some difficulty was encountered finding grids suitable for supporting the serial sections. At first copper grids with a single 600 micron hole were tried, but no matter what combination of parlodion formvar and carbon was used, the embedding material, Araldite would sublimate under the electron beam This produced serious disruption of morphology This problem was solved by the use of EFFA bar grids (No. 2201)[1] with a thin layer of parlodion and carbon. Using these methods seven series of cross sections ranging from 18 to 35 sections per series were prepared and photographed. Micrographs were taken on an RCA EMU-3C electron microscope at an original magnification of 13 000 diameters.

Reconstructions The method used for the reconstructions is as far as is known to the author a new one and will therefore be described in detail. The aim of the reconstructions was to establish whether or not (1) the SR is continuous with the plasma membrane and (2) whether or not the SR forms a continuous system at least from the plasma membrane past the adjacent row of myofibrils. To achieve these aims a considerable amount of accuracy was needed in that errors of 100–200 A could give misleading results. The classical methods dependent upon reconstruction with wax or lucite sheets although tried were rejected because of insufficient accuracy

The method finally arrived at is essentially a graphic one. It consists of two steps. First parallel lines are drawn on a piece of tracing paper the distance between the lines corresponding to the thickness of the sections (in this case 2 mm apart for 350 A sections) and the number of areas bounded by the lines corresponding to the number of sections in the series. A single line is then drawn perpendicular to these lines to represent the plasma membrane. The space between the first two lines on the tracing paper is then lined up over a row of the vesicular profiles on the electron micrograph with the line representing the plasma membrane coincident with the plasma membrane at the point where it is intersected by the bounded area. Wherever there is a vesicular profile within the line-bounded area the area is inked in This process is then repeated for the next section in the series utilizing the adjacent area of the tracing paper until all the micrographs in the series have been plotted. This procedure results in a reconstruction of the SR in depth i.e. an ideal longitudinal section exactly through the plane of the SR. Typical reconstructions are shown in figures 1 and 2.

From the fact that this is essentially a two-dimensional reconstruction method it follows that when the SR sheet is curved as in C in figure 7 a modification must be made to account for this variation in the third dimension. This is taken into account by simply curving the lines on the tracing paper to correspond to the curve of the SR. This modified reconstruction is shown in figure 3

There are two errors which may be introduced into this method. The first may arise from the fact that when the line-bounded area on the tracing paper is lined up over the string of vesicles, one is using the structure to be reconstructed (the SR) as a reference mark for aligning the tracing paper This means that if the string of vesicular profiles in adjacent sections did not actually coincide with one another the method would make them look as though they did. It was found that this was not the situation by drawing the plasma membranes several strings of vesicles and the mitochondrion in the series shown, onto clear glass plates. When these plates were placed on top of one another using an internal reference point independent of the vesicles under examination it was found that the strings of vesicles were coincident from section to section.

The second error is due to the fact that in most cases the sections were not there

---

[1] Available from Ernest F. Fullam, Inc. P.O. Box 444 Schenectady New York.

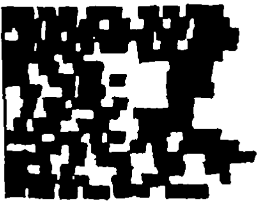


Figure 1

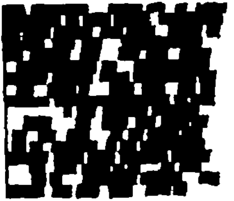


Figure 2

Fig. 1 A reconstruction, made by the method described in the text, of area A (fig. 7) as it continues from figure 7 through figure 24 (part of the reconstruction is based upon another series of micrographs which show this area more fully) In all of the reconstructions the dark areas indicate the tubules or sheets of the sarcoplasmic reticulum. The dark solid line on the left indicates the plasma membrane. From this it may be seen that the sarcoplasmic reticulum is irregularly continuous with the plasma membrane at four places. From top to bottom the reconstruction corresponds to about 0.6 μ longitudinally along the muscle fiber.

Fig. 2 A reconstruction of area B (fig. 7) It may be seen that the sarcolemma is continuous with the plasma membrane at five different places.



Fig. 3 A reconstruction of area C (fig. 7). As may be seen in figure 7 the sarcoplasmic reticulum in this area is curved forming the arc of circle. Thus, for the reconstruction, the guide lines representing the serial sections were drawn with the same curve. The continuity of sarcolemma and plasma membrane is again evident. Here it may be seen that occasionally there are invaginations of the plasma membrane which are not continuous with the sarcoplasmic reticulum (arrow).

than the width of the SR sheet. This means that the individual tubules may not be continuous completely through the section. However it must be assumed in any reconstruction method so far developed, that the structure is continuous through the section. It is for this reason that a reconstruction method must be only an approximation rather than an exact replica of the structure. This error can be reduced by using sections as thin as possible, but cannot wholly be eliminated.

On the other hand, this graphic method does offer one main advantage in accuracy over previous methods. It is essentially a one step operation involving simply tracing directly from the micrograph. Methods relying on wax or lucite plates involve at least four steps; tracing the structure onto the plate cutting it out, putting the plates together and then, invariably a certain amount of smoothing out of rough surfaces. At each of these steps some accuracy is sacrificed until by the time the reconstruction is smoothed out it may have relatively serious defects. Thus it is felt where considerable accuracy is re- d as in this study the method used is the method of choice whenever it applicable. There is the additional ad- antage over plate reconstructions of ease nd speed of application

RESULTS

The general form of the SR in the fast RM 2, Florey and Florey '55) receptor muscle of the crayfish can be seen in longitudinal section in figures 4 and 5 The SR forms a delicate reticulum of tubules and vesicles surrounding each myofibril. The membranes of the reticulum are represented by smooth agranular electron dense lines about 75 A wide (the same width as the plasma membrane) No unit membrane was resolved in this study As can be seen in figures 4 and 5 the reticulum is regular along the myofibril, and shows no interruptions along the sarcomere corresponding to dyads" (Smith '61) or triads (Porter '56) Also no evidence of intermediary vesicles (Porter '56) or separate transverse tubular systems was noted. In this respect it seems to be a somewhat less differentiated or specialized system than that found in most muscles to date (except Amphioxus, Peachy '61)

Figure 6 illustrates the form of the reticular system in cross section through the muscle. Again the reticulum may be seen forming a discontinuous sleeve around each myofibril and in addition it may be observed that the SR about each myofibril has connections with that surrounding adjacent myofibrils. These connections between adjacent sleeves do not seem to be confined to any particular part of the sarcomere but appear to be frequent and at random. The series of sections of which figure 6 is a member show that the SR appears to form a continuous system throughout the muscle fiber and in close proximity to each myofibril.

It now remains to describe the relationship of the SR to the plasma membrane In the cross section of figure 7 it may be seen that at various places the SR between the myofibrils approaches close to the plasma membrane. In several places (marked arrows) there seems to be some sort of relationship between the two. It was suspected that this relationship might be one of membrane continuity between the plasma membrane and the SR, and it was to investigate this point further that the serial sections were made (figs. 7 through 24) As can be seen in figure 7 there are at least 8 areas of interest (arrows) which can be followed through the series of sections. Three of these A, B and C were chosen for reconstruction analysis by the method described (figs. 1, 2 and 3 respectively) Unfortunately area A is not shown throughout this series. Its complete reconstruction depended in part upon another series of micrographs which more fully included this area.

From the reconstructions it may be seen that the SR is in the form of what might be described as either anastomosing tubules or fenestrated sheets. Probably the reconstruction method would tend to emphasize the sheet-like character so that anastomosing tubules would be a more apt term However the system is sheet-like in that important variations occur in two dimensions only the width of the sheet being quite constant at about 250 A.

The question regarding the relationship between the plasma membrane and the SR may be posed as follows: are there two discontinuous systems one consisting of small infolded areas of the plasma membrane and a second consisting of SR, or is there a single system composed of SR which is continuous with the plasma membrane? As may be seen from looking at a single section the impression of two discontinuous systems might arise but when reconstructed it may be seen that what appears to be a discontinuous infolding in the single section is actually continuous with the SR in adjacent sections. Thus only one system is present composed of SR which is continuous with the plasma membrane.

DISCUSSION

In this investigation we have endeavored to study the form of the SR in crayfish stretch receptor muscles and its relationship to the plasma membrane. Figures 4 5 and 6, and the series of sections from which figure 6 was taken, show that the SR is composed of anastomosing tubules and sacs which form a reticular system surrounding each myofibril, and which appears to be continuous throughout the muscle fiber. The serial sections (figs. 7 through 24) and the reconstructions made from them show that this system is also continuous at many points with the plasma membrane. The exact form of this continuity with the plasma membrane may be seen in figure 25, which is a part of figure 10 at higher magnification. Figure 25 shows that at the area of continuity the two membranes appear to be identical in morphological appearance. Although there is morphological continuity at this point, this does not preclude electrical discontinuity. However for lack of contrary evidence it is probably safe to assume that electrical continuity does exist. If this latter implication is true then it would follow that in the resting state the membranes of the SR are polarized with the space within the tubules (continuous with the extracellular space) positive with regard to the sarcoplasmic ground substance. The magnitude of this potential difference would be dependent upon membrane characteristics which are unknown. Thus it is conceivable that the depolarization of the plasma membrane could penetrate into the interior of this muscle fiber via a depolarization of the SR membranes as hypothesized for other muscles by A. F. Huxley ('58). The problem still remains as to whether this depolarization wave could or does instigate the chemical events which produce contraction at the myofilament level.

SUMMARY

Previous work, based upon examination of single sections with the electron microscope has indicated that in the muscles of the crayfish stretch receptor the sarcoplasmic reticulum might be continuous with the plasma membrane. The present investigation, utilizing serial sections, was undertaken to determine whether or not this is the case. A graphic method was devised by which the sarcoplasmic reticulum could be reconstructed with considerable accuracy. These reconstructions show that the sarcoplasmic reticulum is continuous at multiple points with the plasma membrane. The significance of this finding as related to the role of the sarcoplasmic reticulum in excitation-contraction coupling is discussed.

LITERATURE CITED

Florey, E., and E. Florey 1955 Microanatomy of the abdominal stretch receptors of the crayfish. J. Gen. Physiol., 39 69–85.

Huxley, A. F. and R. E. Taylor 1958 Local activation of striated muscles. J. Physiol. 144 426–441.

Mauro, A. and W. R. Adams 1961 The structure of the sarcolemma of the frog skeletal muscle fiber. J. Biophysic. and Biochem. Cytol. 10 No. 4 suppl. 177–185.

Peachey, L. D. 1959 A device for staining tissue sections for electron microscopy. Ibid. 5 511 153.

——— 1961 The structure of the longitudinal body muscles of amphioxus. Ibid. 10 No. 4 suppl. 159–176.

Peterson, R., and F. A. Pepe 1962 Am. J. Anat. in press.

Porter, K. R. 1956 The sarcoplasmic reticulum in muscle cells of Amblystoma larvae. J. Biophysic. Biochem. Cytol. 2 No. 4 suppl. 170.

Smith, D. S. 1961 The structure of insect ... lar flight muscle. Ibid. 10 8 suppl. 12...

van Harreveld, A. 1936 A physiological solution for freshwater crustaceans. Proc. Soc. Exp. Biol. N. Y. 34 428–432.

Veratti, E., 1902 Richerche, sulle fine struttura della fibra muscolare striata, Mem. Ist. lomb., Classe sc. mat. nat., 19 87–133 Translation ppearing in J Biophysic. and Biochem. Cytol., 1961 10 No. 4 suppl., 3–59

Watson, M. L. 1958 Staining of tissue sections for electron microscopy with heavy metals. J Biophysic. and Biochem. Cytol., 4 727–730

PLATE 1

EXPLANATION OF FIGURE

4 A longitudinal section through the crayfish stretch receptor muscle. Z, A, and M lines are clear Due to the contraction of the muscle the I bands are much reduced. The sarcoplasmic reticulum may be seen between the myofibrils as system of vesicles and tubules. 27,000 ×

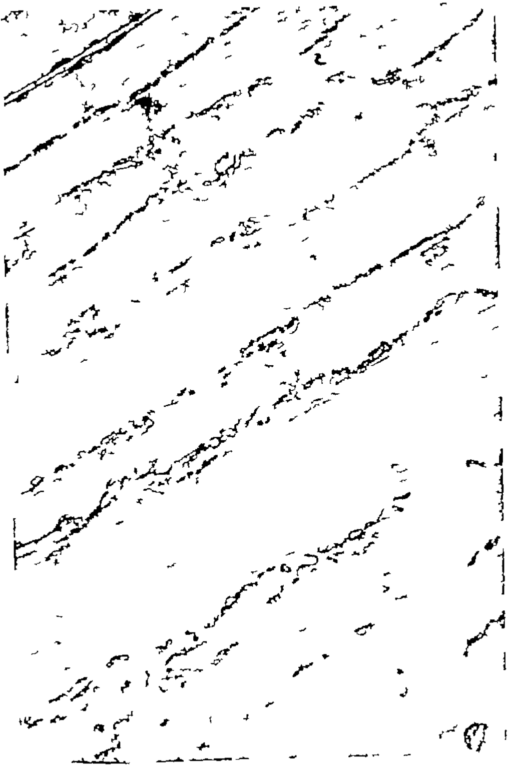


PLATE 2

EXPLANATION OF FIGURE

5 A longitudinal section showing an area similar to that in the lower left portion of figure 4. Here the myofibril has gone out of the plane of section leaving the sheet of sarcoplasmic reticulum which surrounds it. This micrograph shows clearly the anastomosing tubules which make up the sarcoplasmic reticulum. Also this and the preceding figure show the absence of any regular discontinuity of the sarcoplasmic reticulum along the sarcomere, corresponding to triad type structures. 54,000 ×

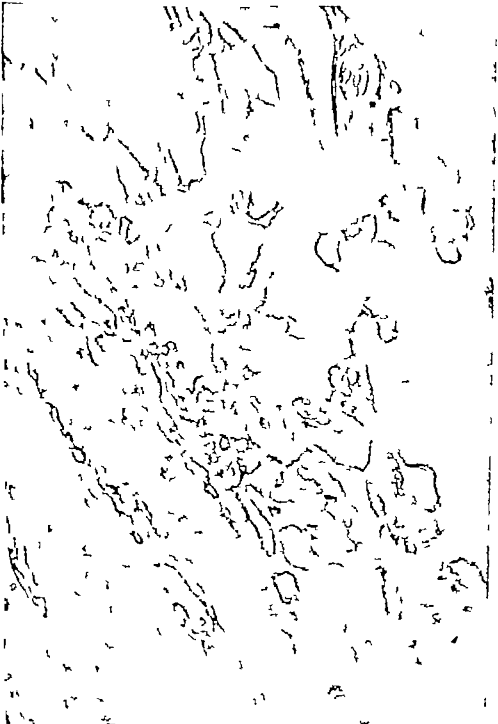
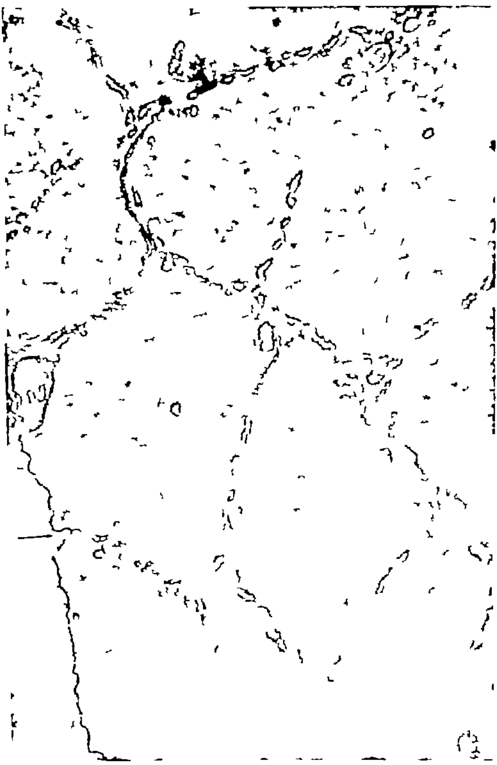


PLATE 2

EXPLANATION OF FIGURE

5 A longitudinal section showing an area similar to that in the lower left portion of figure 4. Here the myofibril has gone out of the plane of section leaving the sheet of sarcoplasmic reticulum which surrounds it. This micrograph shows clearly the anastomosing tubules which make up the sarcoplasmic reticulum. Also this and the preceding figure show the absence of any regular discontinuity of the sarcoplasmic reticulum along the sarcomere corresponding to triad type structures. 54,000 ×



PLATES 4 – 12

EXPLANATION OF FIGURES

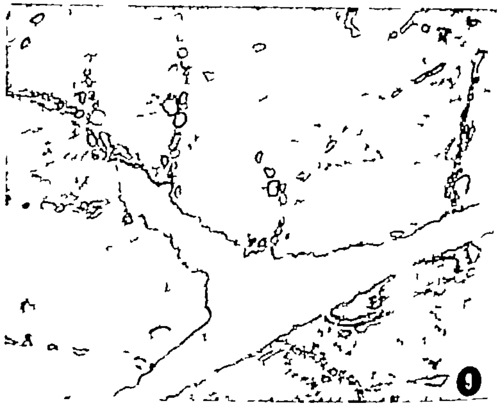
17–24 This is a series of micrographs of serial cross sections stained with lead hydroxide. Each section is approximately 350 Å thick, and the total distance covered by the series is about 0.8 μ in a longitudinal direction. Two adjacent muscle fibers are seen, the upper one with an indentation in it. In figure 7 *PM* indicates the plasma membranes of the two fibers. The unlabeled arrows indicate eight areas of particular interest where the sarcoplasmic reticulum approaches the plasma membrane. The areas indicated by A, B and C have been reconstructed in text figures 1, 2, ond 3. M indicates mitochondrion. The boxed in area of figure 10 is shown t higher magnification in figure 25. Figures 7 through 24 are t pproximately 45,000 ×



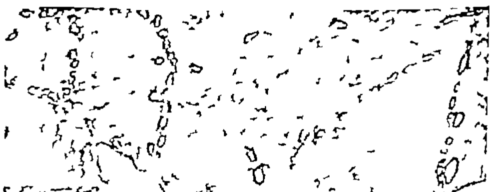
7



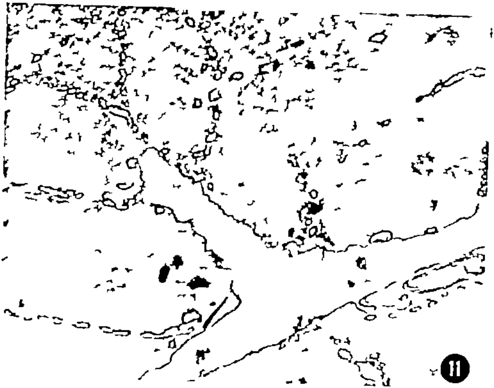
8



9



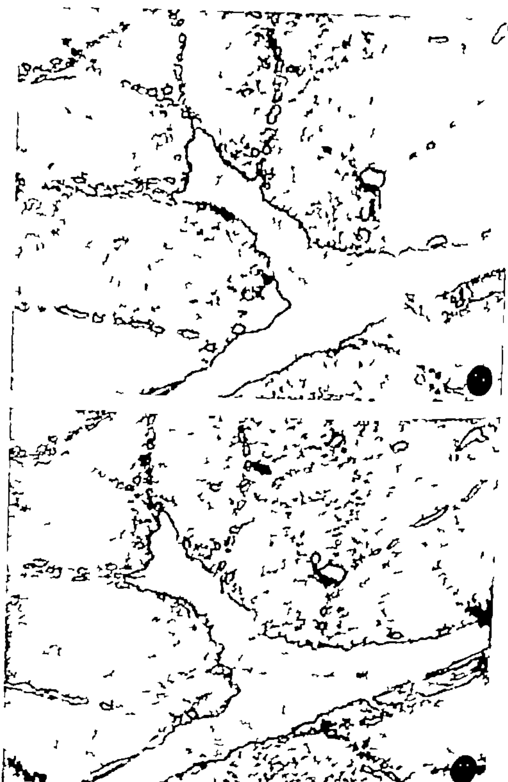
10

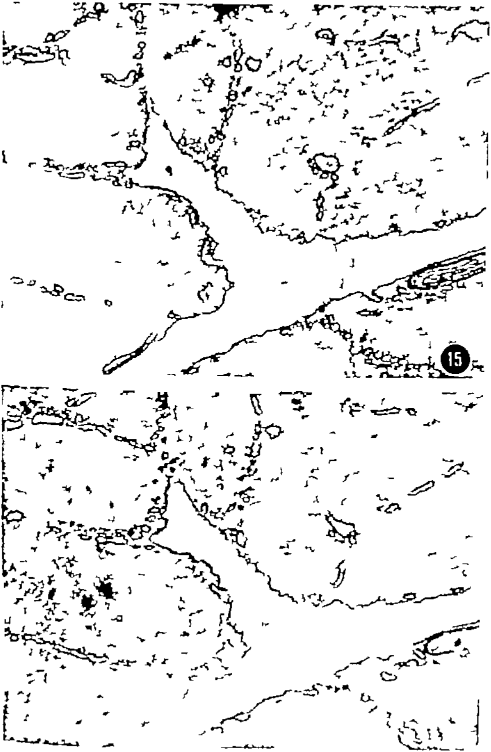


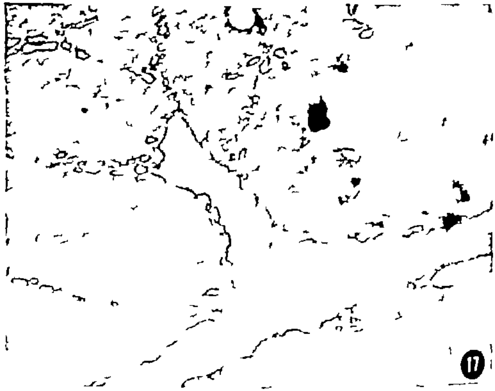
11

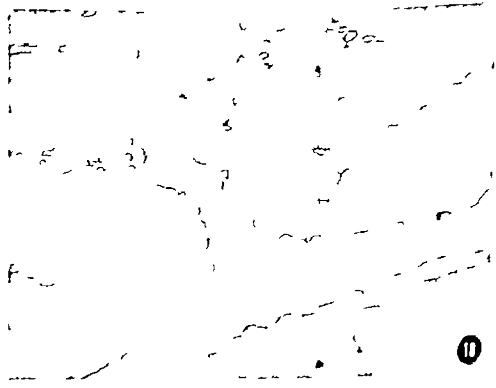


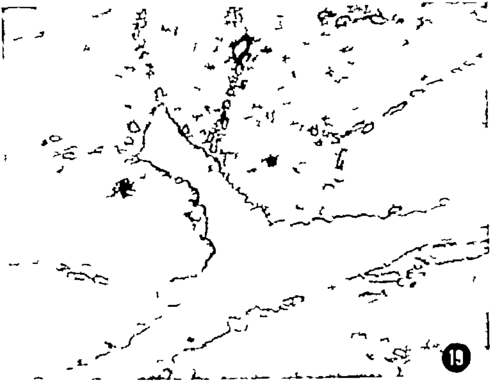
12

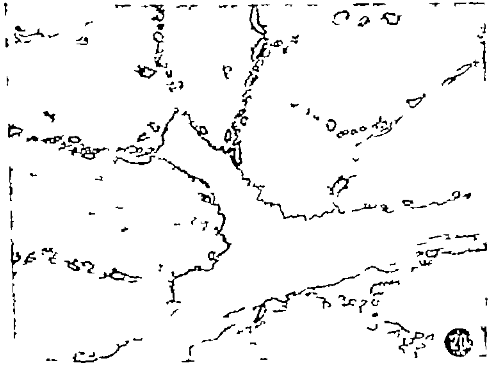


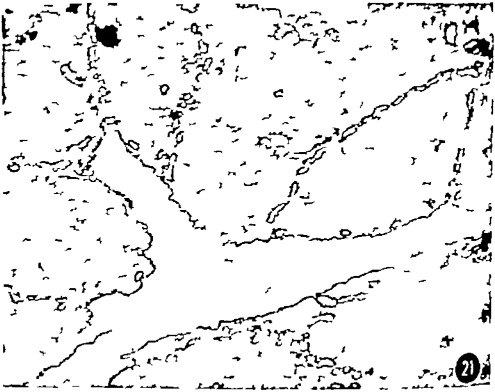

15


17

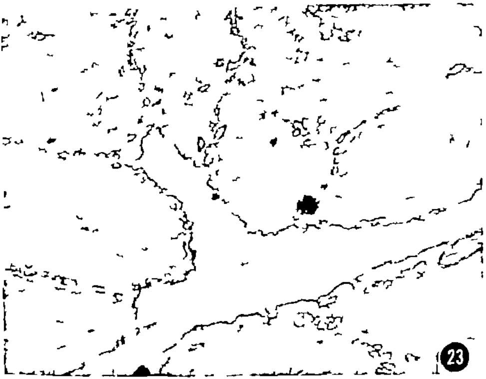




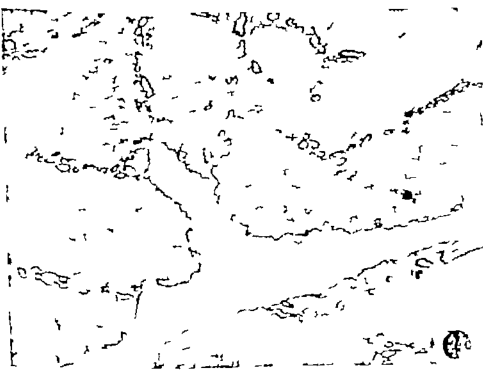



21

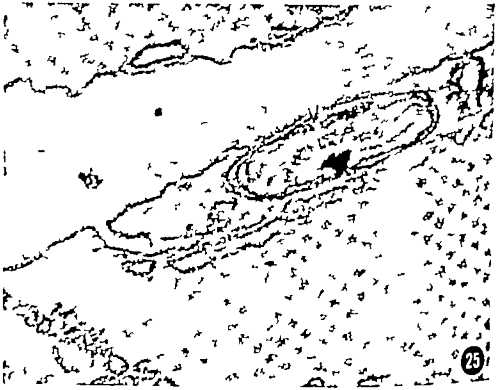

22



23



24



25 This micrograph shows, at higher magnification, the area indicated in figure 10. The sarcoplasmic reticulum may be seen coming in from the plasma membrane for a considerable distance. Also it may be seen that there is no apparent morphological difference between the membranes of the sarcolemma and the sarcoplasmic reticulum. 114,000 ×

Quantitative Analysis of Spermatogenesis of the Rat

A REVISED MODEL FOR THE RENEWAL OF SPERMATOGONIA

YVES CLERMONT
Department of Anatomy McGill University Montreal, Canada

The production of generation after generation of spermatocytes requires that spermatogonia continuously renew themselves. Comparison of the numbers of spermatogonia at the successive stages of the cycle of the seminiferous epithelium of the rat led to the elaboration of a model depicting the periodic renewal of spermatogonia (Clermont and Leblond, '53) This model (fig. 1) referred to as the "Stem Cell Renewal" pattern, was found to be a useful tool for various investigations on rat spermatogenesis (Clermont and Morgentaler '55 Clermont and Perey '57)

A similar approach was adopted by others in investigating the renewal of spermatogonia of various species. Ortavant investigated the ram ('54 '58) and bull ('59) Oakberg, the mouse ('56) Kramer the bull ('60) Our own group applied this method of study to the hamster (Clermont, '54) and the monkey (Clermont and Leblond, '59) While there were variations from species to species, a pattern emerged which was common to all, in that spermatogonia divided at several stages of the cycle and thus gave rise to more and more differentiated cell types. However a minority of so-called dormant cells (A_o, in fig. 1) which arose during the proliferation of spermatogonia delayed their division until the following cycle and thus acted as the stem cells for a subsequent generation of spermatocytes.

In the Stem Cell Renewal model of the rat, there was however an irregularity which was not observed in other species Although the dormant type A stem cell (fig 1 A_o) gave rise to two morphologically similar type A cells these daughter cells did not subsequently divide at the same time (arrows in fig. 1) We wondered if such an irregularity in the model was the reflection of some anomaly in the development of spermatogonia of the rat. Roosen-Runge ('55) had described degenerating cells in the rat seminiferous epithelium, at just about the time in the cycle when the irregularity occurred in the model (i.e. at stage XII) Although this author had identified the cells as disintegrating spermatocytes, it was admittedly difficult to determine their nature, and the problem was re-examined using several approaches Meanwhile the various types of germ cells composing the seminiferous epithelium were recounted using a more refined technique than in our first quantitative study to find out if the new counts were in agreement with those leading to the initial model.

A different criticism of the type of model proposed for the rat was that it was based on averages of cell counts. Such data did not necessarily give a true picture of the behavior of individual spermatogonia. Although it is rather difficult to obtain such information from histological sections an attempt had already been made in this direction by preparing maps of spermatogonia at various stages of the cycle in the monkey From these data an accurate Stem Cell Renewal model could be designed for this species (Clermont and Leblond, '59) The experience gained from this study suggested that at least the following problem could be solved for the rat. As indicated in the model (fig 1 arrow on the right) the mitosis giving rise to the dormant type A cell (A_o) also gives rise to a type A cell which soon has a different fate so that this mitosis would appear to

The cycle of the seminiferous epithelium is the sequence of events by which complete series of cellular associations follow one another in time, in any given area of the seminiferous epithelium. In the rat, the cycle was subdivided into 14 stages, numbered I–XIV each one of them being identified by a given step in the development of the spermatids (Leblond and Clermont, '52a,b). The cellular composition of the stages of the cycle is given in figure 2.

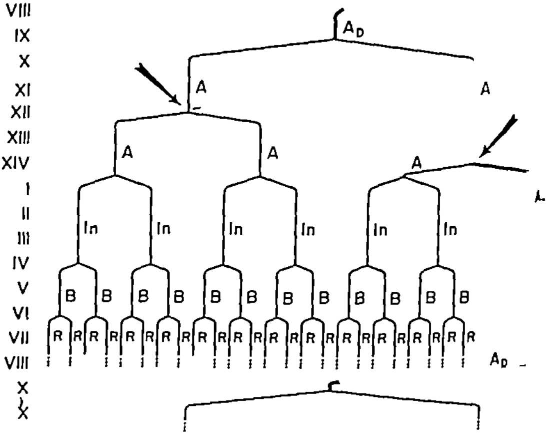


Fig. 1 Diagram showing the initial model proposed for the development and renewal of spermatogonia in the rat (from Clermont and Leblond '53) The Roman numerals on the left side of the diagram indicate the stages of the cycle of the seminiferous epithelium. Lettering A_D, type A rest spermatogonia (also referred to as "dormant" type A spermatogonia); A type A spermatogonia; In intermediate type spermatogonia; B type B spermatogonia; R, resting primary spermatocytes. Each mitosis is indicated by the junction of vertical and two horizontal lines.

According to this model type A stem cell starts dividing at stage IX of the cycle. Of its two daughter cells, one divides at stage XII of the cycle (arrow on the left) the other divides at stage XIV–I of the cycle (arrow on the right) One of the four type A cells produced becomes a dormant type A stem cell insuring the renewal of the spermatogonial population at the next cycle. The other type A cells divide at stage XIV I of the cycle to produce intermediate type cells which in turn produce type B cells which in turn produce primary spermatocytes.

be differential In the monkey testis the existence of such differential mitoses was rejected when it was found that the newly formed stem cells were arranged in pairs and retained this arrangement throughout their life span. Consequently the mitoses which gave rise to pairs of stem cells instead of being differential were equivalent and the spermatogonial renewal model was built accordingly Then do "differential" mitoses occur in the rat testis? And if not how should the model be modified? To answer these questions maps of the spermatogonial population were prepared and analyzed

As a result of these two approaches an improved model will be proposed for the renewal of spermatogonia in the rat testis

---

A differential mitosis consists of the unequal distribution of [illegible] nuclear or cytoplasmic [illegible] and is responsible for the different development of the daughter cells (Ris, '55 [illegible] In this [illegible] the definition implies not only that the two daughter cells are different, but that the difference is detectable by the histological techniques used. Non-differential mitoses are referred to as "equivalent".

MATERIAL AND METHODS

Testes from 16 adult albino Sherman rats were fixed in Zenker formol for 16–24 hours, washed dehydrated through dioxane and impregnated with paraffin. Five micra sections were cut transversely from the mid-portion of the testes and stained with the periodic acid-Schiff hematoxylin technique. Hematoxylin stained the nuclei of the cells of the seminiferous epithelium and the PA Schiff technique outlined the acrosomic systems of the spermatids thus permitting identification of the steps of spermiogenesis (fig. 2)

In our initial quantitative study on the rat (Clermont and Leblond '53) only spermatogonia and resting primary spermatocytes were counted and counts were made of only those nuclei the greatest part of which was within the tissue sections. This method of counting avoided a correction of the counts of cells showing differences of nuclear diameter (Abercrombie 46) In the present investigation all identifiable pieces of nuclei were enumerated and corrected by Abercrombie s formula. This permitted a safe comparison between counts of spermatogonia primary and secondary spermatocytes and spermatids in spite of the considerable differences in their nuclear volume.

Three different series of cell counts were made in cross sections of tubules In the first series type A intermediate type, and type B spermatogonia were counted at stages of the cycle during which few or no mitoses were usually encountered. (The counted cells are those labelled with a cross in table of fig 2) In this series resting and pachytene spermatocytes were also counted at stage VII of the cycle In a second series, primary spermatocytes at various steps of meiotic prophase resting secondary spermatocytes and step 1 and 7 spermatids were enumerated (cells labeled with dots in fig. 2) In a third and last series normal type A spermatogonia and degenerating nuclei at stages XI and XII of the cycle were counted (cells labeled with triangles in fig. 2)

Some observations pertinent t[illegible] the p[illegible]ent investigation were made on [illegible]dioautographs of testes from anim[illegible]l[illegible] injected with a single dose (1 μc p[illegible] g[illegible] of body weight) of thymidine-H[illegible] Th[illegible] l were sacrificed three hours and three days after injection the testes were fixed in Bouin s fluid, the sections were stained with PA Schiff hematoxylin and radioautographed according to the technique of Messier and Leblond (57)

Finally information was collected on the topographical distribution of resting, dividing and even degenerating type A spermatogonia along the basement membrane of tubules. The mapping method used, was essentially the same as the one devised to study the distribution of spermatogonia in the monkey (Clermont and Leblond '59) This method can be briefly described as follows: 50–300 serial sections from a transversely cut tubule were photographed at a low magnification. Each one of these tubular cross sections was examined under the microscope the cells to be mapped were identified and their position along the basement membrane was carefully noted on the corresponding photograph of the section Care was taken to record each cell only once, even if pieces of a given cell were found in two successive sections. Then the spermatogonia from each photograph or drawing were transferred to horizontal strips 5 mm wide a distance made to correspond to the thickness of the magnified sections. To maintain the relative distances between cells a point of reference parallel to the long axis of the tubule was selected and the distances from the cells to that point as well as the distances from cell to cell were measured and used to redistribute the cells along the horizontal strips. This was repeated consecutively for every serial section. If one considers the tubule as a cylinder the method consisted simply of cutting the cylinder wall along a line parallel to the long axis of the cylinder and then unrolling this wall, on which the spermatogonia were mapped, onto a flat surface

RESULTS

Quantitative data on spermatogonia spermatocytes and spermatids

In th[illegible] *first series of counts* spermatogonia [illegible]ere enumerated at stages of the

---

T [illegible] C [illegible]ed T true count, C crude count [illegible] of the section d nuclear diameter

TABLE 1

Number of cells (spermatogonia and primary spermatocytes) per cross section of seminiferous tubule at the stages of the cycle t which no mitoses were observed

Type of cells counted	Stages of the cycle	Mean number of cells ± S.E.
Type A spermatogonia	II, III, V VII, VIII	1.13 ± 0.01
Type A spermatogonia	X–XI	2.38 ± 0.17
Type A spermatogonia	XIII	3.08 ± 0.20
Intermediate type spermatogonia	II–III	7.34 ± 0.20
Type B spermatogonia	V	13.60 ± 1.21
Resting spermatocytes	VII	29.70 ± 0.19
Pachytene spermatocytes	VII	30.01 ± 1.30
Total number of tubules investigated		409

Means and standard errors were calculated from the verage cell counts obtained in four animals approximately one hundred tubular cross sections were surveyed per animal Counts were corrected by Abercrombie's formula.

cycle during which few or no spermatogonial divisions occurred. (Spermatogonia were known to divide five times during one cycle i.e. at stages IX, XII XIV I, IV and VI of the cycle, Clermont and Leblond '53 these stages were thus eliminated from the counts)

The results (table 1) showed that the number of type A stem spermatogonia ... per tubular cross section averaged ..3 from stage II VIII with little variation ... number had approximately doubled ... stage X and XI that is after the mitosis taking place at stage IX. By stage XIII the number of type A spermatogonia had only reached 3.08 that is 1.5 times the number at stages X and XI although the occurrence of mitosis at stage XII of the cycle had led us to expect a doubling of the number again At stages II III, at stage V and again at stage VII the number of cells (In B and R consecutively) approximately doubled each time due to the mitoses observed at stages XIV I IV and VI respectively (table 1)

The number of pachytene spermatocytes per tubular cross section at stage VII of the cycle was closely similar to the number of resting spermatocytes counted at the same stage (table 1) This indicated that there was no change in the number of primary spermatocytes from the time of their formation until the mid pachytene step of the meiotic prophase

The *second series of count* table 2) included a period of spermatogene is going from the leptotene step of the meiotic prophase up to step 7 of sperm iogenesis. During the long meiotic prop se the

TABLE 2

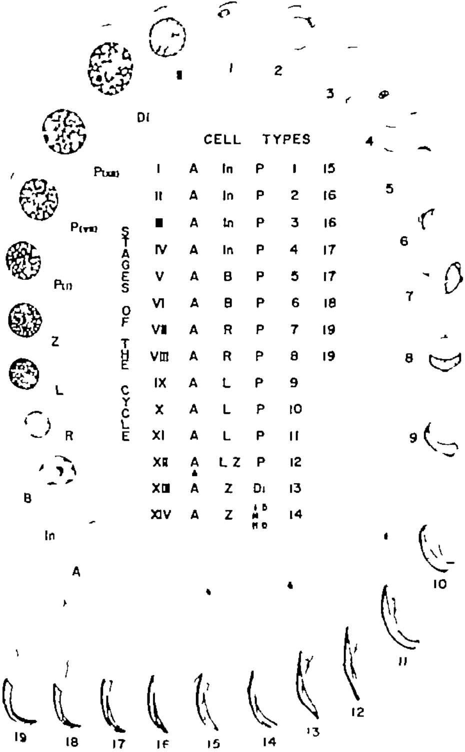
Number of primary and secondary spermatocytes, step 1 and step 7 spermatids per cross section of seminiferous tubule in adult albino rat

Type of cell counted	Stage of the cycle	Mean number of cells ± S.E.
Late leptotene	XI	34.7 ± 2.3
Zygotene	XIV	34.8 ± 2.0
Early pachytene	I	33.3 ± 1.7
Mid pachytene	VII	35.0 ± 1.7
Late pachytene	XII	34.9 ± 1.8
Secondary spermatocytes	XIV	61.3 ± 2.6
Step 1 spermatids	I	101.4 ± 3.3
Step 7 spermatids	VII	101.3 ± 4.9
Total number of tubular cross sections investigated		868

Means and standard errors were calculated from the erage cell counts obtained in five animals, 1.. to 310 tubular cross sections were surveyed per animal. Counts were corrected by Abercrombie formula.

FIG. 2 Starting from the lower left hand corner of the figure and encircling the table drawings illustrate the steps of spermatogenesis in the rat. Lettering A, type A spermatogonium; In, intermediate type spermatogonium B type B spermatogonium; R, resting primary spermatocyte L, leptotene spermatocyte Z, zygotene spermatocyte; P Pm P ... arly mid and late pachytene spermatocytes the Roman numerals in brackets indicate the stages of the cycle at which they are found Di diplotene II, secondary sperm tocyte 1 19 teps of spermiogenesis (reproduced from Leblond and Clermont, '52)

The table in the center of the figure gives the cellular composition of the stages of the cycle of the seminiferous epithelium (Roman numerals, I–XIV) Lettering same as abov In addition, at stage XIV of the cycle I° and II° indicate the first and second matur tion di isions of spermatocytes. The cells labeled with cross (+), dot (●) or triangle (▲) were counted in the first, second or third series of counts respectively



STAGES OF THE CYCLE	CELL TYPES				
I	A	In	P	1	15
II	A	In	P	2	16
III	A	In	P	3	16
IV	A	In	P	4	17
V	A	B	P	5	17
VI	A	B	P	6	18
VII	A	R	P	7	19
VIII	A	R	P	8	19
IX	A	L	P	9	
X	A	L	P	10	
XI	A	L	P	11	
XII	A	L Z	P	12	
XIII	A	Z	Di	13	
XIV	A	Z	I D M II D	14	

Figure 2

number of primary spermatocytes per tubular cross section remained remarkably constant (average = 34 9)

The number of interphase nuclei of secondary spermatocytes found at stage XIV of the cycle 61.3 was slightly less than twice the average number of primary spermatocytes, 69 8 the difference being statistically significant. Finally the numbers of step 1 and step 7 spermatids were identical (101 4 and 101.3 respectively) but significantly less than twice the number of secondary (61.3 × 2 = 122.6) or four times the number of primary spermatocytes (34.9 × 4 = 139 6) indicating that a considerable loss of cells took place during the two maturation divisions. Since each primary spermatocyte theoretically gives rise to four spermatids the number of spermatids actually counted was only 72.6% of the expected yield

Identification and enumeration of the degenerating cells

Degenerating nuclei were occasionally seen along the basement membrane of the tubules of the rat by Roosen Runge ('55) considered them as arising from leptotene spermatocytes. Oakberg ('56) working with the mouse identified similar figures as degenerating type A spermatogonia. These degenerating nuclei, found to occur mostly at stage XII of the cycle in the rat had the following characteristic appearance the chromatin formed several hemispherical globules along the nuclear membrane which eventually coalesced into a dense irregular mass (figs. 10a 10b D) No transition could be seen between the surrounding normal resting germ cells and the degenerating nuclei so that the identification of the latter was difficult. However since the degenerating nuclei were found mostly at stage XII of the cycle the possibilities were limited to four types of cells type A spermatogonia which incidentally underwent division during this stage of the cycle leptotene or zygotene primary spermatocytes pachytene spermatocytes and finally close to the lumen of the tubule step 12 spermatids (figs 10a 10b)

The nature of the degenerating cells was clarified by examination of radioautographs of testes from animals injected with thymidine-H³ and sacrificed either three hours or three days after injection. At three hours many type A cells but no spermatocytes nor spermatids were labeled in cross sections of tubules at stage XII. Many degenerating nuclei were also labeled (figs. 11a, 11b) In contrast, at three days after injection most type A spermatogonia and similarly most degenerating figures were not radioactive whereas all leptotene primary spermatocytes were labeled (fig 12) The more advanced pachytene spermatocytes and step 12 spermatids were not. Since the radioactive degenerating nuclei, seen at three hours after thymidine-H³ injection could only arise from the radioactive cells seen at the same time interval after injection, it was concluded that the type A spermatogonia were the cells which degenerated at stage XII of the cycle

An attempt was made to assess the percentage of type A cells affected by the degenerative process. Counts of normal and degenerating type A spermatogonia were made in a number of tubular cross sections at stage XII of the cycle and, for control at stage XI From the data given in table 3 it was clear that very few or no degenerating cells existed at stage XI but 8 1% of the type A cells found at stage XII were in various stages of degeneration It should be noted that degenerating nuclei were found at stage XII in every one of the six animals investigated although their percentage varied from animal to animal (table 3)

Mapping of type A spermatogonia

I Type A spermatogonia at stage VII of the cycle Information was first collected from maps showing type A stem spermatogonia on the basement membrane of tubules at stage VII of the cycle Of the four maps reconstructed from serial sections one is illustrated in figure 3 On such a map the type A stem cells had a tendency to gather in groups of variable sizes (two are outlined in fig 3 a) which merged into one another lea ing free several rather large areas of basement membrane (such as the shaded area b in fig 3). The density of the population of type A cells precluded their arrangement into groups of 2 4 8 cells as done in the mouse

TABLE 3

Frequency of degenerating type A spermatogonia

Animal number	Stage XI: Number of tubular cross-sections	Stage XI: Number of type A spermatogonia	Stage XII: Number of tubular cross-sections	Stage XII: Number of type A spermatogonia normal plus degenerating	Stage XII: Number of degenerating nuclei	Stage XII: Percentage of degenerating type A spermatogonia
1	27	81	668	2576	203	7.9
2	17	53	677	3805	289	7.5
3	21	60	104	420	58	13.8
4	19	53	137	586	37	6.3
5	17	56	63	256	17	6.6
6	18	55	67	298	38	12.7
Totals	119	358	2016	7941	642	—
Average number of cells per tubular cross-section		3.00		3.93	0.32	Average 8.1(%)

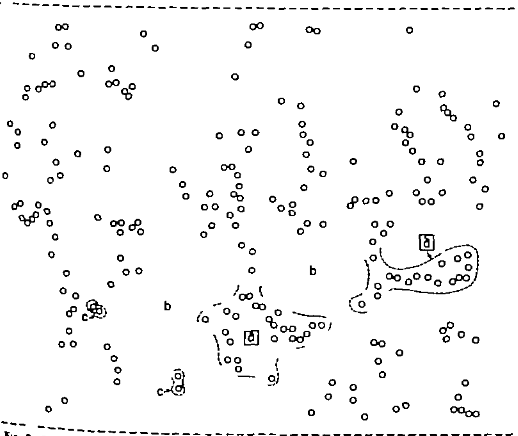


Fig. 3 Map depicting resting type A stem cells at stage VII of the cycle. The stem cells are arranged in irregular groups which merge with each other (two groups are outlined and labeled) Some large areas of basement membrane are free from stem cells (such as the shaded areas labeled b) Pairs of stem cells are seen (labeled) but the large number of these cells arranged in dense groups prevented demonstration of their arrangement in pairs quartets, etc.

(Clermont and Leblond '59). Suggestion of arrangement in pairs were frequent (fig. 3 c). However a comparison by the Student method of the mean distance between the two cells forming a pair to the mean distance from any cells in a pair to the nearest cell outside the pair revealed that this arrangement may be fortuitous and result from a random distribution of the cells (p values above .4).

II. Maps of dividing type A cells at stage IX of the cycle. A second series of maps were reconstructed using only mitotic figures of type A stem cells from tubular cross sections at stage IX of the cycle, i.e. during the first peak of spermatogonial mitosis (fig. 4). It was found that the dividing cells were arranged into groups or islands. The boundaries of such groups of cells could be delimited easily and were therefore indicated on the maps (fig. 4). If two groups of cells were so close that their separation into two distinct islands could be questioned by any [illegible]er, then the two islands were con[illegible]red as one. The results (table 4) [illegible]owed that all islands of dividing spermatogonia were composed of even num[illegible]rs of cells. The size of the islands was extremely variable but those composed of six dividing cells were the most numerous (20.8%).

Now considering the cells within the islands, it appeared that the type A spermatogonia divided in pairs, each member being at exactly the same phase of mitosis

TABLE 4

Number of cells per island of dividing type A stem cells

Number of cells per island	Number of islands	Percentage
2	5	6.5
4	9	11.7
6	16	20.8
8	14	18.9
10	6	7.1
12	[illegible]	[illegible]
14	8	10.4
16	2	[illegible]
18	3	[illegible]
20	0	
22	2	[illegible]
24	1	[illegible]
26–58	4	[illegible]
Total	[illegible]7	

(fig. 4). To test the pair arrangement the mean distance between the two cells of an assumed pair was compared (by the t test) to the mean distance from either paired cell to the nearest dividing cell outside the pair. These measurements were made in the maps containing more than 20 assumed pairs and no consideration was given to the phase of mitosis. In several maps but not in all the difference between the distances was significant (table 5). Even when the arrangement of mitotic figures in pairs was not confirmed by this method — perhaps because of the close packing of the cells — the examination of the maps clearly suggested the existence of such pairs. This was particularly true when the phases of mitosis were taken into account as shown for example in map 4 (fig. 4) for which the p value was 0.04. The fact that the pairs could be demonstrated statistically in several maps and morphologically in all was considered to be sufficient proof of their existence.

III. Mapping of degenerating type A spermatogonia. It was previously noted that degenerating type A spermatogonia were usually found at stage XII of the cycle, that is during the second mitotic peak. Maps of degenerating as well as of dividing type A cells were also reconstructed. It was found that the degenerating type A spermatogonia were arranged in groups sometimes of considerable size (fig. 6). On many occasions counts of degenerating nuclei within these islands showed even numbers. Their arrangement in pairs was not infrequent. Groups of degenerating, normally dividing and normal resting type A spermatogonia were usually clearly separated from each other (fig. 7). In some instances groups of early degenerating nuclei more closely a[illegible]

Fig. 4. Map showing the distribution of dividing type A stem cells at stage IX of the cycle (tubule no. 19 in table [illegible]). The phases of mitosis are indicated. The dividing cells are arranged in groups of various sizes outlined by a solid line. Within these groups the dividing cells are arranged in pairs outlined by dotted lines. In the shaded area the two cells forming a pair being at the same phase of mitosis. The distance between the two cells forming a pair was found to be significantly smaller than the distance from either paired cell to the nearest dividing cell outside the pair ($p < 0.01$).



Figure 4

and irradiated mouse concluded that they belonged to type A spermatogonia. Radioautographs of testes from animals injected with thymidine-H showed that radioactive degenerating nuclei were associated with normal radioactive type A spermatogonia indicating clearly that the former must arise from the latter. Furthermore a close examination of nuclei in areas of basement membrane where degenerating cells as well as mitotic figures were numerous indicated that the degeneration of the type A cells takes place mainly during early prophase.

Eight per cent of the type A cells at stage XII of the cycle underwent degeneration (table 3). Since the type A cells degenerate in prophase or before division a better estimate of the percentage of type A cell affected may be obtained by using respectively the number of degenerating nuclei per tubular cross section at stage XII of the cycle (0.32) and the number of type A spermatogonia per cross section of tubule at stage XI (3.0) i.e. prior to the mitotic peak. The value thus obtained 10.6% is lower than the 25% of degenerating type A cells found in the mouse by Oakberg ('56).

Although no degeneration of primary spermatocytes was observed during the long meiotic prophase (table 2) some of the germ cells degenerated during the subsequent maturation divisions. Such an abnormality in the development of spermatocytes was mentioned for the rat (Roosen-Runge '55) and for other mammals (Oakberg, '55; Ortavant '56; Kramer '60). However it remained to be seen for the rat whether the first and or the second maturation division was affected and to what extent. The present data showed that on the basis of the number of primary spermatocytes the number of step 1 spermatids per tubular cross section is 27.4% lower than expected. Of this percentage approximately 12% of the cells are affected during the first and 15% during the second maturation division. These results differ from those of Roosen-Runge ('55) who reported that 2% of the spermatocytes degenerated during the first maturation division and none during the second division. The percentage of cells lost during the maturation divisions of the rat is greater than that (13%) found in the mouse by Oakberg ('55).

Spermatids also degenerate at some critical steps of their development. Roosen-Runge ('55) estimated that approximately 10% of the spermatids disintegrated during spermiogenesis. Our data established that from step 1 to step 7 of spermiogenesis no spermatid was lost. Difficulties in obtaining corrected counts from older spermatids prevented an accurate estimate of cell death during the later steps of spermiogenesis. However as already pointed out by Roosen-Runge ('55) cytological examination clearly indicates that step 10 and 11 spermatids are the ones which are the most frequently seen to undergo disintegration. This is the time during which chromatin reorganizes in the nuclei, which then change from a sphere to a point sickle (fig. 2).

The spontaneous degeneration of germ cells seems to be closely associated with the chromosomal behavior since in the case of the type A spermatogonia it occurred during prophase of the stage XII divisions, in the case of spermatocytes during the maturation divisions, and in the case of spermatids during the rearrangement and condensation of chromatin. Such an observation was already made by Oakberg ('56) who suggested that the nuclei containing aberrant chromosomes were eliminated at these critical steps of spermatogenesis. The cause(s) of chromosome damage remains obscure however.

At any event considering our data on the degeneration of spermatogonia (10.6%) and spermatocytes (27.4%) and the 10% degeneration of spermatids proposed by Roosen-Runge ('55) *the number of spermatozoa produced per type A stem cell would be in the rat only 52% of theoretical yield.*

Spermatogonial renewal. Analysis of cell counts

First, it was appropriate to see if the initially proposed Stem Cell Renewal model (fig. 1) was supported by the corrected counts obtained in the present investigation. This could be done by calculating with the data of table 1 the ratios of the number of type A stem cells to the num-

TABLE 6

Ratios of the various types of germ cells

Cell type in ratio[1]	Calculated from counts corrected by Abercrombie's formula (table 1)	Calculated from Clermont and Leblond ('53)	Calculated from data of table 1 corrected for the 10.6% cell loss by degeneration at stage XII
$A_0 : A_{(IX–XII)}$	1 2.1	1 1.8	1 2.1
$A_0 : A_{(XII)}$	1 2.7	1 2.7	1 3.0
A_0 : In	1 6.4	1 6.1	1 7.0
A_0 : B	1 12.2	1 11.4	1 13.5
A_0 : R	1 26.3	1 24.0	1 29.0
In : B	1 1.9	1 1.9	1 1.9
B : R	1 2.1	1 2.1	1 2.1

[1] Lettering A_0 dormant type A stem cell; A type A spermatogonia; In intermediate type spermatogonia; B type B spermatogonia; R resting primary spermatocytes.

ber of the other cell types counted (table 6 second column) and to compare them with similar ratios calculated from the published data used to construct the initial model (table 6, third column) These two series of ratios are closely similar (table 6) therefore the initial model need not be modified on the basis of the new series of counts.

But, it was obvious that the degeneration of type A spermatogonia, which was unnoticed in the course of our initial study had to be considered to interpret cell counts correctly and thereby revise the initial Stem Cell Renewal model. We have estimated that 10 6% of the type A spermatogonia degenerated as they entered mitosis at stage XII of the cycle. Consequently the counts of all cells normally arising from these type A spermatogonia (A, In B R) must be at least 10 6% lower than expected. The counts of these cells were thus corrected accordingly and the ratios of type A stem cells to the other more mature elements were recalculated (table 6, last column) As expected these new ratios were higher than those previously obtained. While the ratios obtained from counts uncorrected for cell degeneration fit well with the original model of spermatogonial renewal (fig. 8A) the new ratios calculated after correction for cell loss fit best with a second model illustrated in figure 8B (This figure 8B actually corresponded to the third possibility illustrated and discussed in our first article Clermont and Leblond, '53 fig 2 p 489)

The pattern in this second model was that the type A stem cell (A_0) divided at stage IX giving two type A cells which multiplied simultaneously at stage XII to give four type A cells. These in turn divided at stages XIV I of the cycle into seven intermediate type cells (In) and one new stem cell (A_0) Thereafter as the stem spermatogonium remained dormant, each intermediate type spermatogonium produced two type B spermatogonia which in turn produced four primary spermatocytes.

Pairing of type A spermatogonia Its effect on the model of spermatogonial renewal

According to the model in figure 8B which is based on statistical data, there would be a differential mitosis at stage XIV I of the cycle, since one of the third generation type A cells would give rise to a new type A stem cell and an intermediate type spermatogonium (seen on the right hand side of the diagram) If this were so then maps of spermatogonia reconstructed from tubules at stage II of the cycle that is immediately after this mitosis had taken place should show side by side the two daughter cells which arose from the same type A cell. Hence there would be some pairs (one in four) composed of a dormant type A cell and an intermediate cell. Unfortunately cell crowding was such along the basement membrane that the problem could not be solved by investigating such maps.

The problem may be approached however in an indirect way It may be reasoned

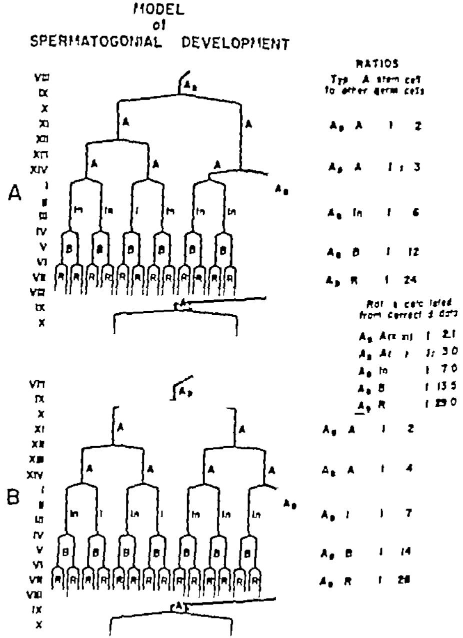


Fig 8 Di grammatic represent tion of two models for the development of spermatogonia. The Roman numeral on the left of the diagrams indicate the stages of the cycle. Lettering A_s, dormant type A spermatogonia (stem cells); A type A spermatogonia; R resting permatocytes. The ratios of type A stem cells to the other germ cells calculated for each model are given on the right of the diagrams. Model A represents the initial scheme proposed by Clermont and Leblond ('53) Model B represents second possibility for the development of spermatogonia (corresponds to third possibility of figure 8 in Clermont and Leblond '53) According to this model, the daughter cell arising t stage IX from the type A stem cell divide simultaneously t tages XII and XIV I of the cycle. Then new stem cell appears which enters long period of dormancy while the other germ cells give rise consecutively to intermediate and type B spermatogonia and finally to resting spermatocytes.

The ratios enclosed in frame on the right, were calculated from cell counts corrected firstly by Abercrombie formula and secondly for the 10.6% cell loss due to degeneration of type A spermatogonia t st ge XII of the cycle These ratios compare better to those calculated for model B than to those f model A.

that if all type A stem cells were paired then the existence of pairs composed of one dormant type A cell and one intermediate type spermatogonium would have to be excluded. Maps of dormant type A stem cells (fig. 3) could not be used profitably to test this possibility but the problem was solved by investigating maps of dividing type A stem cells at stage IX of the cycle. In such maps on which the phases of mitosis were shown (figs. 4 5) it became obvious that these cells although arranged in groups of various sizes divided in pairs, the two members of such pairs being at exactly the same phase of mitosis. In several maps comparison by the "t" test of the mean distance between two cells forming the postulated pairs with the mean distance of any one of the two paired cells to the nearest dividing cell outside the pair confirmed this morphological finding (table 6) If two cells, such as type A_s spermatogonia in proximity to each other, divided in perfect synchronism, it could be safely assumed that these two type A cells had the same mother cell. In other words, the two type A_s cells dividing synchronously at stage IX of the cycle may be assumed to originate from the same type A spermatogonium which has divided at stage XIV I of the previous cycle (fig 8B) It should be mentioned that the duration of interphase of the type A stem cells is approximately eight days (calculated on the basis of a 12-day cycle duration Clermont, Leblond and Messier '59) The synchronism of the paired A_s mitoses after such a long period of dormancy is striking and strengthens the possibility that paired stem cells arise from the same mother cell. Consequently due to the pair arrangement of the type A stem cells, the possibility of a differential mitosis at stages XIV I of the cycle, as indicated in fig 8B should be rejected. Instead we must have an equivalent mitosis the two daughter cells being identical.

To account, therefore for the arrangement in pairs of the type A stem cells the statistical model of spermatogonial renewal illustrated in figure 8B should be replaced by a new one (fig 9) In this new model, two type A stem spermatogonia were used to start with instead of one as in figure 8B The type A spermatogonia divide at stages IX, XII and XIV I of the cycle as their numbers increase in geometrical progression. Following the third mitotic peak, two spermatogonia arising from the same type A cell would return to a dormant state and form a pair of new stem cells (A_s) The other spermatogonia would become intermediate type cells which all divide at stage IV to give type B spermatogonia and these in turn divide at stage VI of the cycle to yield a generation of primary spermatocytes

It should be remembered that some 10 6% of the population of type A spermatogonia found at stage XII of the cycle, degenerate. Thus the theoretical number of spermatocytes produced by the spermatogonia is in actual fact, reduced by the same percentage.

Do all type A stem cells and their progeny behave in perfect agreement with the rigid model just proposed? The following data indicate that variations may exist. Of the type A cells present at stage XII of the cycle some were found to degenerate in groups, sometimes of considerable size (figs. 6 7) Such degeneration obviously affects the progeny of these type A cells, that is the new stem cells as well as the more differentiated cell types (In, B R) As a consequence, the stock of stem cells would have a tendency to diminish over certain areas of the basement membrane To compensate for such a depletion and to maintain the population of stem spermatogonia in a steady state as indicated by the counts one has to postulate that the type A spermatogonia from adjacent areas or else type A cells during forthcoming cycles would have to produce a greater number of stem cells than proposed by the model.

Thus the model proposed here although it fits in with the data collected should still be considered as a statistical representation of the behavior of spermatogonia. This model however is the correct expression of well established facts such as the doubling in the number of all stem cells at stage IX of the cycle the production of pairs of stem cells, the production of four resting spermatocytes per intermediate type spermatogonium. This model also supports the concept proposed earlier

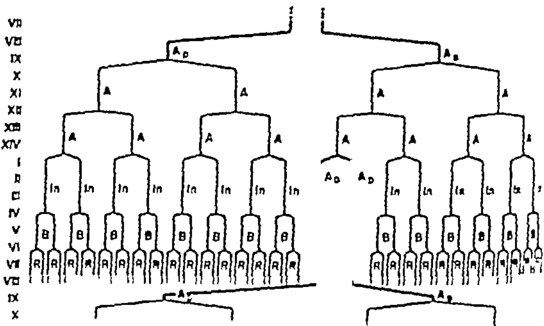


Fig. 9 Diagram representing the most probable model for the development and renewal of spermatogonia in the rat. The Roman numerals on the left of the diagram indicate the stages of the cycle. Lettering: Ap, dormant type A stem spermatogonia; A, type A spermatogonia; In, intermediate type spermatogonia; B, type B spermatogonia; R, resting primary spermatocytes. This model (which is a modification of figure 8B) takes into account the arrangement in pairs of the type A stem cells. Thus a pair of type A spermatogonia starts proliferating at stage IX of the cycle and the daughter cells divide successively at stage XII and XIV, I of the cycle. During this divisions sequence of spermatogonial divisions one type A spermatogonium gives rise to a pair of new type A stem cells which after a period of dormancy insure the renewal of the spermatogonial population during the forthcoming cycle. The other type A spermatogonia give rise to intermediate type spermatogonia which in turn produce type B cells which finally give rise to primary spermatocytes. It should be recalled that due to the degeneration of some type A spermatogonia at stage XII of the cycle the theoretical yield of spermatocytes proposed by the present scheme is reduced by 10.6%.

(Clermont and Leblond '53) that at each cycle of the seminiferous epithelium the spermatogonia renew themselves by producing new stem cells while they simultaneously yield spermatocytes which later give rise to the mature germ cells the spermatozoa.

SUMMARY

The mode of development and renewal of spermatogonia in the adult rat was reinvestigated by analyzing counts of germ cells (type A, In and B spermatogonia, spermatocytes) at the various stages of the cycle of the seminiferous epithelium and by investigating maps of resting and dividing type A stem-spermatogonia. Degeneration of germ cells taking place at critical steps of spermatogenesis was also investigated quantitatively and by means of radioautography in animals injected with thymidine-H³.

The ratios of the average number of type A stem cells to the average number of other germ cells calculated from counts corrected by Abercrombie's formula are not different from the similar ratios calculated from the uncorrected counts already published (Clermont and Leblond '53). Thus the previously published model for the renewal of spermatogonia (fig. 1) would not need modification on the basis of cell counts.

However some 10.6% of the type A spermatogonia degenerate during the prophase of the second spermatogonial mitosis at stage XII of the cycle. The numbers of cells arising from these type A spermatogonia (A, In, B and R) was considered to be below the expected yield

by a similar percentage and the cell counts were corrected accordingly. New ratios of type A stem cells to the other more mature germ cells were calculated from these corrected counts.

Maps of dividing type A stem cells reconstructed from serial sections of tubules at stage IX of the cycle reveal that these cells divide in groups or islands. The numbers of cells per island of dividing cells are variable but are always multiples of two. Furthermore within these islands the dividing type A stem cells are arranged in pairs, the members of each pair located close to each other are at exactly the same phase of mitosis.

Taking into consideration the arrangement in pair of the type A stem cells and the new ratios of type A stem cells to the more differentiated germ cells a new model for the development of spermatogonia was built. According to this model (fig. 9) a pair of type A stem cells starts proliferating at stage IX of the cycle, thereafter the daughter cells divide successively at stage XII and XIV-I of the cycle their number increasing in geometrical progression. Following the third spermatogonial mitosis a pair of cells becomes dormant and form new type A stem cells which will later provide for new generations of spermatogonia. The other spermatogonial elements arising from the third spermatogonial divisions differentiate into intermediate type spermatogonia which give rise to type B spermatogonia during stage IV of the cycle. The type B cells divide at stage VI to produce a generation of primary spermatocytes. This revised "Stem Cell Renewal" model, still considered as statistical, gives an accurate but theoretical representation of the maintenance of the stock of spermatogonial stem cells and of the periodic formation of generations of spermatocytes in the rat. The number of spermatocytes produced per stem cell is in actual fact lower than the theoretical number proposed by th model due to the degeneration of some (10.6%) type A spermatogonia at stage XII of the cycle. Finally the number of spermatids produced by the spermatocytes is only 72.6% of the expected yield due o degeneration taking place during the first and second maturation divisions of permatocytes.

ACKNOWLEDGMENTS

This work was supported by a grant from Population Council Inc. The technical assistance of Mrs. T Troitsky is acknowledged. The illustrations were prepared by Mrs. M Oeltzschner

LITERATURE CITED

Abercrombie, M. 1946 Estimation of nuclear population from microtome sections. Anat. Rec., 94 239–242

Clermont, Y 1954 Cycle de l'épithélium séminal et mode de renouvellement des spermatogonies chez le hamster. Rev Canad. Biol., 13 208–245.

Clermont, Y., and C. P Leblond 1953 Renewal of spermatogonia in the rat. Am. J Anat., 93 475–502.

——— 1959 Differentiation and renewal of spermatogonia in the monkey *Macacus rhesus* Ibid., *104* 237–274.

Clermont, Y C. P Leblond and B. Messier 1959 Durée du cycle de l'épithélium séminal du rat. Arch. Anat. Micro. Morph. Exp., *48 bis* 37–56.

Clermont, Y and B. Perey 1957 Quantitative study of the cell population of the seminiferous tubules in immature rats. Am. J Anat., *100:* 241–268.

Kramer M. F 1960 Spermatogenesis bij de stier Thesis Rijksuniversiteit, Utrecht.

Leblond, C. P and Y Clermont 1952a Spermatogenesis of rat, mouse, hamster and guinea pig as revealed by the "Periodic acid-Fuchsin Sulfurous Acid" technique Am. J Anat., 90: 167–216.

——— 1952b Definition of the stages of the cycle of the seminiferous epithelium in the rat. Ann N Y Acad. Sci 55 548–573.

Messier B and C P Leblond 1957 Preparation of coated radioautographs by dipping sections in fluid emulsion. Proc. Soc. exp. Biol. Med., 96 7–10.

Oakberg, E. F 1956 A description of spermiogenesis in the mouse and its use in analysis of the cycle of the seminiferous epithelium and germ cell renewal. Am. J Anat 99 391–414

Ortavant, R 1954 Etude des générations spermatogoniales chez le bélier C R Soc. Biol., *148* 1958–1961

——— 1958 Le cycle spermatogénétique chez le belier Thesis, Université de Paris

——— 1959 Spermatogenesis and morphology of the spermatozoon In Reproduction in Domestic Animals, Vol. II Ed Cole, H H and P T Cupps Academic Press, New York.

Ris, H. 1955 Cell division. In Analysis f Development. Ed Willier B H., P A. W ss and V Hamburger W B Saunders, Philadelphia

Roosen-Runge E C 1955 Untersuchun über die Degeneration samenbildender Zellen in der normalen Spermatogenese der Ratte Z. Zellforsch mikroskop. Anat *41* 221–235

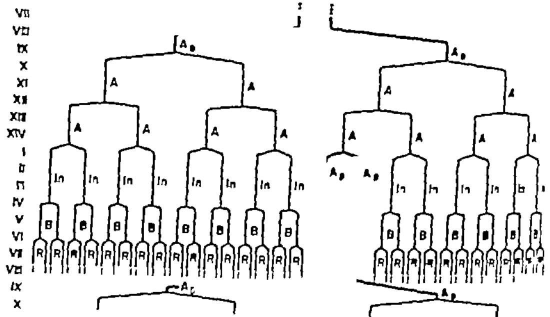


Fig. 9 Diagram representing the most probable model for the development and renewal of spermatogonia in the rat. The Roman numerals on the left of the diagram indicate the stages of the cycle. Lettering: A_0, dormant type A stem spermatogonia; A, type A spermatogonia; In, intermediate type spermatogonia; B, type B spermatogonia; R, resting primary spermatocytes. The model (which is a modification of figure 8B) takes into account the arrangement in pairs of the A stem cells. Thus a pair of type A spermatogonia start proliferating at stage IX of the cycle and the daughter cells divide successively at stage XII and XIV, I of the cycle. During this first wave of spermatogonial division one type A spermatogonium gives rise to a pair of new type A stem cells which after a period of dormancy insure the renewal of the spermatogonial population during the forthcoming cycle. The other type A spermatogonia give rise to intermediate type spermatogonia, which in turn produce type B cells which finally give rise to primary spermatocytes. It should be recalled that due to the degeneration of some type A spermatogonia at stage XII of the cycle the theoretical yield of spermatocytes proposed by the present scheme is reduced by 10.6%.

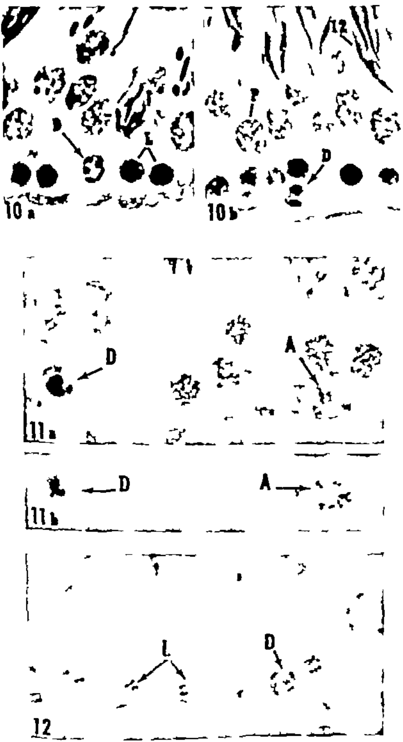
(Clermont and Leblond '53) that at each cycle of the seminiferous epithelium the spermatogonia renew themselves by producing new stem cells while they simultaneously yield spermatocytes which later give rise to the mature germ cells the spermatozoa.

SUMMARY

The mode of development and renewal of spermatogonia in the adult rat was reinvestigated by analyzing counts of germ cells (type A, In and B spermatogonia, spermatocytes) at the various stages of the cycle of the seminiferous epithelium and by investigating maps of resting and dividing type A stem-spermatogonia. Degeneration of germ cells taking place at critical steps of spermatogenesis was also investigated quantitatively and by means of radioautography in animals injected with thymidine-H³.

The ratios of the average number of type A stem cells to the average number of other germ cells calculated from counts corrected by Abercrombie's formula are not different from the similar ratios calculated from the uncorrected counts already published (Clermont and Leblond '53). Thus the previously published model for the renewal of spermatogonia (fig. 1) would not need modification on the basis of cell counts.

However some 10.6% of the type A spermatogonia degenerate during the prophase of the second spermatogonial mitosis at stage XII of the cycle. The numbers of cells arising from these type A spermatogonia (A, In, B and R) was considered to be below the expected yield


D
L
10 a
12
P
D
10 b
D
A
11 a
D
A
11 b
L
D
12

The Structure of Fine Splenic Arterial Vessels in Relation to Hemoconcentration and Red Cell Destruction[1]

LEON WEISS
Department of Anatomy The Johns Hopkins University School of Medicine Baltimore Maryland

Fine arterial vessels arise from the central artery of mammalian spleens and form a rich plexus of slender vessels in the white pulp. In the rabbit most of these run to the periphery of the white pulp and terminate in the marginal zone and in the contiguous red pulp. A smaller number run some distance into the red pulp and there communicate with cordal or perhaps in a few cases, with sinal vessels (MacNeal, Otani, and Patterson, '27; Björkman 47; Snook, '50 58) In the dog the terminating arterial vessels typically bear a collar of phagocytic cells shortly before they end (Mills '26 Solnitzky '37) and constitute sheathed arteries. Sheathed arteries are absent in the spleen of rabbits.

This paper presents observations, made primarily by electron microscopy of this system of arterial vessels in the rabbit and the dog. The material includes normal spleens and spleens after the injection of Thorotrast. New information is presented on arterioles and arterial capillaries in the rabbit and on sheathed arteries in the dog. A limited number of observations have been made on the connections of arterial capillaries with cordal vessels of the red pulp

Splenic arterial vessels are distinguished by distribution, high endothelium, abluminal endothelial projections, and stained openings into the cords. It seems likely that they play a role in separating plasma from the corpuscular elements of blood and that they subject the red cells to mechanical trauma. These points are elaborated in the discussion. Since it seems probable that these vessels may also prepare red cells for destruction in the spleen, a review of the spleen's role in normal red cell destruction has been prepared and is offered as an appendix.

MATERIALS AND METHODS

Animals Spleens were obtained from 14 normal New Zealand albino rabbits, each about 2 to 3 kg in weight and about eight months of age and from four normal mongrel dogs about 10 to 12 kg in weight. Additionally two similar dogs and four similar rabbits were studied after the administration of Thorotrast.

Anesthesia. Rabbits were placed under surgical anesthesia by means of 2 to 3 ml. Nembutal (Veterinary Nembutal 60 mgm/ml Abbott Co. Chicago) administered intraperitoneally in 0 5 to 1.0 ml doses over a period of two hours. Dogs were anesthetized with 6 to 8 ml. Nembutal intraperitoneally and then 4 to 7 ml intravenously

Thorotrast. This preparation of thorium dioxide was administered intravenously in animals under surgical anesthesia. In two dogs the spleen was taken out 45 minutes after the administration of 7 ml of Thorotrast; in two dogs, five minutes after 7 ml Thorotrast. Two rabbits were given 5 ml Thorotrast and the spleen removed after 45 minutes. In another pair given 5 ml Thorotrast, five minutes elapsed before splenectomy The Thorotrast was obtained from Heyden Chemical Corp. N Y

Methods of obtaining tissue In most instances the spleen was removed from an anesthetized animal by cutting the vascular pedicle without attempting to retain the blood in the organ. In three rabbits the

[1] This work supported by Grant Hema C-3373 Hema 1 of the United States Public Health Service. Senior Investigator — Public Health Service.

vascular pedicle was clamped tied off cut and the whole spleen with contained blood put in fixative In two additional rabbits this procedure followed two minutes of passive congestion induced by clamping the splenic vein at its entrance into the portal vein In three rabbits the spleen was removed after fixation in situ by perfusion

Fixation The fixative used was 1% osmium tetroxide buffered to pH 7.45 by veronal — HCl and containing 5% sucrose Except in perfusion the fixative was chilled in ice water Portions of fresh spleen from central and peripheral portions of the organ were cut into blocks approximately 2 mm and fixed for about one hour Whole spleens stayed in fixative 45 minutes to one hour and then the superficial blackened areas were cut into blocks about 2 mm and left in fixative 30 to 45 minutes more

In three rabbits the spleen was perfused by 150 ml fixative preceded by 25 ml saline under a pressure of 100 mm Hg The perfusion required about five minutes The solutions were warmed to [illegible] and perfused cephalad through the abdominal aorta just above the renal arteries after the thoracic aorta hepatic artery and mesenteric arteries were clamped and the splenic vein cut The spleen was left in situ about ten minutes and then large portions 20 to 30 mm in length were placed in 95% ethanol and allowed to harden overnight. Then the blackened areas were dissected free and further dehydrated.

Embedding sectioning and staining Blocks were dehydrated in ethanol and embedded in methacrylate (20% methyl — 80% butyl) or in a few cases in araldite. The methacrylate was polymerized with ultra violet light. It was not prepolymerized. The araldite was obtained as a kit from the New York Society of Electron Microscopists and used according to the directions of Richardson (60)

The blocks were sectioned in a Porter Blum microtome with a diamond knife obtained from the Instituto Venezolano de Investigaciones Científicas Caracas Venezuela.

Thin sections on carbon-coated formvar grids were stained by flotation upon a solution of 2% uranyl acetate two hours at room temperature (Watson, '58). Those studied in the Siemens Elmskop I methacrylate sections were well stained after this procedure while those embedded in araldite were not. Increased contrast was sometimes obtained in the latter material by employing 40 KV rather than 60.

The blocks were also sectioned at 1 and 3 μ and stained for light microscopy with the periodic acid Schiff (PAS) method and hematoxylin (Weiss '57 '59). The perfused spleens were sectioned only for light microscopy

OBSERVATIONS

In the rabbit, arterial vessels ranging in diameter from about 100 μ, the caliber of arterioles to approximately 10 μ, the diameter of capillaries were studied in detail. Snook's work ('38) on the distribution of these vessels in the white pulp and the red pulp was confirmed in preparations examined under the light microscope stained with the PAS method. I however encountered a somewhat greater incidence of connections between arterial terminations and sinuses. Of the limited number of connections seen under the electron microscope all were of the artery-cord variety The proximal arterial vessels were studied primarily in the rabbit: those observed in the dog were similar to those of the rabbit. The sheathed artery of the dog was studied in detail

Rabbit A striking characteristic of the arteriolar vessels in all preparations is a high endothelium. In the smaller arterioles and extending into the capillaries it is often so high that the lumen is considerably diminished or absent (figs. 2, 4 5 6 10) In perfused animals the endothelium is flattened in moderate degree in most but not all vessels and the inside diameter of many of the smaller arterioles and capillaries is somewhat increased. In spleens fixed after passive congestion compressed red cells are present in the arteriolar lumen and the endothelium conforms to the compressed shape of the luminal corpuscle as in figure 15 Seldom is more than one blood cell present in cross section even in vessels as large as 75 μ in diameter In spleens fixed with-

out care to retain blood, red cells are usually absent from arterial vessels. The endothelium is highest over the nucleus (figs. 4 8 and 10) and can be flat elsewhere, so that the luminal endothelial surface presents nodosities in nuclear locations.

The endothelium is rich in mitochondria and RNA particles and, especially in the smaller vessels of this study possesses granules vacuoles, membranes, and, occasionally filaments of a cytoskeletal system (figs. 5 6 7 11 and 12) Cytoplasmic vesicles, many near the cell surface, are inconstantly present. The endothelium of many capillaries possesses slender abluminal extensions into the basement membrane and adventitial extracellular connective tissue. These extensions may be continuous with similar processes derived from adventitial cells, and tend to enwrap the vessel (figs. 5 and 7)

Until vessels narrow to a diameter of about 25 µ the basement membrane is complete. As a rule in smaller vessels the basement membrane is interrupted and may even be absent. In well-fixed preparations the basement membrane is amorphous and finely granular In specimens in which ground substance is washed out, collagenous fibers are revealed. The density of fibers tends to diminish as the caliber and stoutness of the vessel diminishes. Elastic fibers, whose presence may be demonstrated by light microscopy in these arterioles, were not definitively recognized in this material, by electron microscopy The basement membrane is strongly reactive in the PAS technique (figs. 8 and 9) and comprises part of the reticulum, as described by Snook ('58)

A layer of smooth muscle one or two cells thick is characteristic of the largest vessels in this study (figs. 1 2 and 4) In vessels of about 50 to 35 µ in diameter the muscle is represented by slender cytoplasmic processes applied upon the basement membrane and surrounded by relatively abundant ground material variably rich in fibers. In slightly smaller vessels smooth muscle is absent.

Adventitial cells are a constant feature even in vessels of 10 to 15 µ in diameter (figs. 1 2, 4–7) They form a complete layer only in the larger vessels. They may have long processes sometimes continuous with the abluminal endothelial projections mentioned above. Adventitial cells contain considerable concentrations of RNP particles but seldom any filamentous structure.

The extracellular connective tissue contributing to the adventitia is usually a ground material containing few and variable concentrations of fibers. It forms a complete layer around the vessel continuous with endothelial basement membrane and endomysium.

Dog Comparable vessels in the dog resemble those in the rabbit. My observations on the sheathed vessels (figs. 17 to 21) are in agreement with Sonlitzky's. Under the electron microscope the endothelium may be high, containing numerous mitochondria, RNA particles vesicles, filaments or granules — or it may be low the apical and basal surfaces separated by a thin layer of hyaloplasm. The basement membrane is usually incomplete, sometimes absent, or unusually complete. The endothelium is surrounded by a concentration of cells and extracellular connective tissue. This extracellular connective tissue, clearly continuous with the basement membrane and part of the same complex, typically consists of a granular ground substance of variable density but occasionally contains typical collagenous fibers as well. The sheath cells contain a variety of inclusions, some suggesting broken-down red cells They are often rich in RNA particles. Most remarkably they display highly convoluted cytoplasmic junctions with other sheath cells Occasionally abluminal projections mark the endothelium, or adventitial cells of these vessels as in the fine terminating vessels of the rabbit (see especially fig 20).

Spleens after Thorotrast Rabbits and dogs differ markedly in localization of Thorotrast depending upon the presence or absence of the sheathed artery (figs. 11 16 and 17) In the rabbit the Thorotrast is concentrated at the orifice of the terminating capillaries. It is present free in the cordal lumen, within unattached macrophages in the cords, and, to a slightly lesser degree within the lining

cells of the cords. There is some Thorotrast within the walls of the arterial vessels and only a moderate amount within the lining cells and lumen of sinuses. In the dog on the other hand there is little Thorotrast beyond the arterial endings. It is concentrated in the sheaths. This difference in pattern of concentration of particulate material between rabbit and dog spleens was demonstrated by Mills (20) with India ink. Within the sheaths of dogs Thorotrast is present extracellularly and within intracytoplasmic vacuoles. There is a great deal of Thorotrast in the extracellular ground material. It is present moreover in the endothelium of the sheath capillary disposed in ways suggesting transport across the wall (fig. 18).

The distributions of Thorotrast 5 and 45 minutes after injection are similar the principal differences being that after the longer time the vacuoles containing Thorotrast are larger and the distribution more extensive.

It seems possible by electron microscopy to distinguish the thorium dioxide and the dextrins which constitute Thorotrast. The former are dense particles the latter a much less dense and somewhat flocculent material (see especially fig. 11). The distribution of these materials appeared to coincide suggesting that the brilliant PAS reaction of Thorotrast due to the dextrins may be correlated with the dense thorium dioxide visualized by electron microscopy.

PLATES

Figures 2, 4, 8, 9, 10, 13 and 14 are presented with accompanying tracings reduced one-half. Figures 1 through 15 are of rabbit spleen, figures 16 through 21 are of dog spleen. Plates 10 and 11 and figure 15 are of araldite-embedded material. The rest are of methacrylate.

PLATE 1

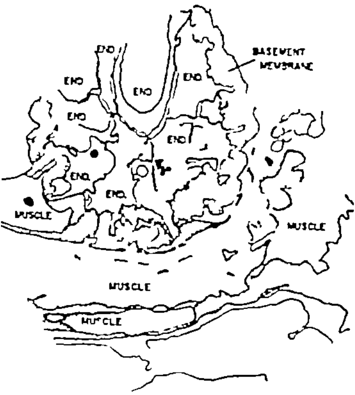
EXPLANATION OF FIGURE

1 *Rabbit.* This arteriole approximately 100 µ in diameter is present *in the outer third of a nodule of white pulp.* Endothelial cells are high, particularly in the region of the nucleus. Cell junctions (C. J.) are relatively simple approximations, typically involving only the infranuclear part of cell. The higher portion of the cell are club-shaped in these undistended vessels. A well developed basement membrane ("ACCU MANT") lies beneath the endothelium. It contains no evident fibers. A single layer of smooth muscle cells, cut almost transversely, lies outside the basement membrane. An adventitial cell extends into the surrounding lymphatic tissue. It is enveloped in a layer of extracellular connective tissue which is continuous with that (marked A.) bounding the muscle layer. × 20,000.


LUMEN

PLATE 2

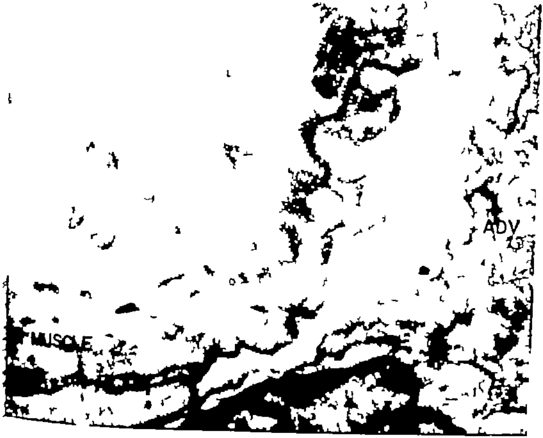
EXPLANATION OF FIGURE



2 Rabbit This arteriole approximately 50 in diameter is present in the outer third of white pulp. The tracing includes field larger than the electron micrograph. The vessel is cut in cross section and its lumen is conspicuously narrower than the preceding vessel. Note the endothelial cell marked END. Endothelial junctions are more complexly plicated than in figure 1. The basement membrane is markedly convoluted, indicating arteriolar constriction. The width and folded course of the basement membrane are indicated in the accompanying tracing. The smooth muscle displays myofilaments and characteristic small dense bodies. X *0,000.

3 Rabbit. This unmyelinated nerve is presumably a post ganglionic sympathetic vasomotor fiber (Kleinpeter '35). It was present in the outer third of a nodule of white pulp in rabbit spleen near the branching of several arterioles. The axons are rich in small mitochondria and contain many small vesicles. A scanty cytoplasmic matrix incompletely surrounds the axons and likely represents Schwann-cell cytoplasm. The nerve is invested by an incomplete but conspicuous fibrous sheath and peripheral to that, slender cellular layers comprising the perineurium. Note the bulge in the fibrous layer (F). In the wall of arterioles slender cytoplasmic strands are often present which resemble the axons present here. But lacking this histological picture it has not been possible to establish neural ...

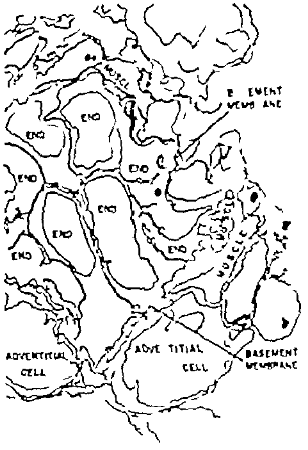
The concentration of mitochondria and vesicles in these axons suggests this may be preterminal segment of ... 20,000.


ADV
MUSCLE


F

PLATE 3

EXPLAN TION OF FIG. 8



A Rabbit. Th arter approximate 30 in di meter w present in the outer portion of Malpi hian capsule It w taken from the same block figures and 3 Thi essel differs from th t in figure primarily i th t the smooth mus l layer is reduced to nder processes of mooth muscle cell sepa ted by gre t deal of ground material. Area i at te of the endothe li l basement membrane (see accomp ying trac i g) indicates some con t ction. The endothe l m i high percent f l endothelial cell re present (END). The cell re in junction lo (ely ly but free les The lumen is an irregular complex slit. The basement membrane f the endothelium merging with the base me l membrane or ex t acellular connective tis ue urrounding the mooth muscle remains prominent. Several peri endothelial cytoplasmic processes are present. They may constitute cytoplasmic extensions of endothelium, of peri cytes or dventitial cells f mooth muscle or even of neurons. Portion of three adventitial lls a pres here × 23,000.



PLATE 4

EXPLANATION OF FIGURES

5 *Rabbit* Thi arteriole cut obliquely displays characteristic endothelium, particularly noteworthy here for the membranous and vesicular components of the cytoplasm (M.C.) The endothelial basement membrane is slender and, in places is made irregular by abluminal endothelial protrusion (E.P.). The adventitial layer includes many slender cytoplasmic processes lying within the complex of ground substance (See figures 4 and 7 for the rabbit and compare with figure 20 for the dog.) Again some of these appear to be smooth muscle; others possibly abluminal extension of the endothelium or extensions of adventitial cell cytoplasm. Possibly some of the cytoplasm is axonal. × 23,000

6 *Rabbit* Thi slender arterial vessel lies within the white pulp. It consist of endothelial cells, two of which have portion of nuclei included in this section, surrounded by basement membrane which is in turn enclosed by layer of adventitial cells. The endothelial cell meet and completely efface the lumen. The endothelial cytoplasm contain moderate number of mitochondria, RNA particles, vesicles, and membranes. Note at the arrow densities in relation to the cell membranes at cell junctions, resembling desmosomes. There are very slender cytoplasmic extension (C.E.) lying in the basement membrane. A portion of the basement membrane is thick and noticeably rich in fibers (F). Several adventitial cell (Ad.) surround the structure; they are surrounded by lymphocytes. × 25,000


F
CE
Ad

PLATF 5

XPLAN ION OF FIGUR

R bbit This section includes tw essels in white pulp pos ibly ne the bifurc tion The endothelium l low le ing rel tiv ly oluminou lumen The endothelial cell re ich in RNA p rticles and contain dense mitochondria A noteworthy h racteri tic of thi endothelium is it blum inal projections i to the rroundi g extracellula connec tiv tis ue (rrow) These projection become continuou with thi irregul lamellae alternati g with l yers f th extracell lar connectiv ti ue These layers follow ci cumf rential pattern round the blood essel nd around the l rge ce tral cell which probably i ad entitial cell The l mellae ha junction with similar extensions derived from d entiti l cells. Compare especially w th fig re 20 f dog spleen

Th preparation w not stained fter fi tion. × 23,000

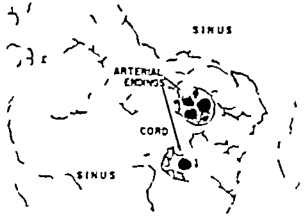
SPLENIC ARTERIAL VESSELS

Leon Weiss



PLATE 6

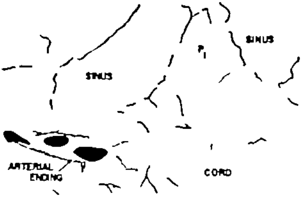
EXPLAN TION OF FIGURES



8 *Rabbit* Most of this light microscopic field of red pulp i occupied by cord. It is complex tructure containi g tw terminal arterial vessels, sequestered cells (predominantly erythrobla t) and ph gocytic cells. The nuclei of the terminal essel are blacked in the accompanyi g tracing in which the distribution of reticulum i shown.

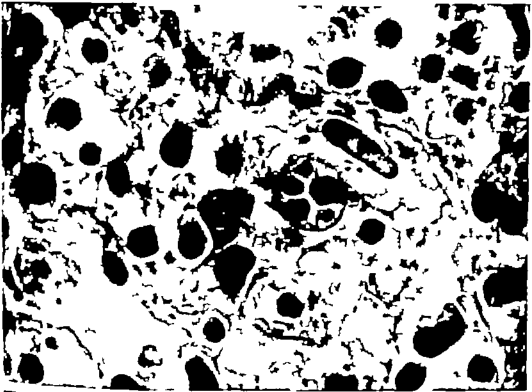
Note the ari tion in the number of nuclei present in the two rterial essel and the ari tion in the height of the endothelium. A red cell i in the lumen of the upper vessel. The di tribution of reticulum is richest around the essels. The reticulum compartmentalizes the cord These formations of reticul m seen in this and the ne t figure are clothed by thi cytoplasmic membranes as m y be seen in the lectron micrographs, figures 13 and 14 Many of the macrophages in the cord appear unattached to the reticulum. Note the free macrophage in the lumen of lower sinus.

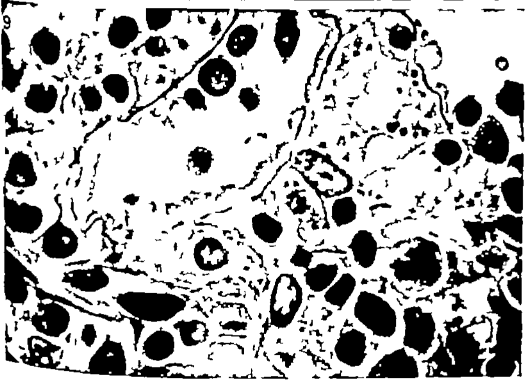
A portion of this field is reproduced a figure 7 in an arlier paper (W iss, '59) The tissue wa taken from animal with an acute hemolytic anemia. Thi preparation is sectioned t 3 tained with PAS nd hematoxylin and photographed 1,500.



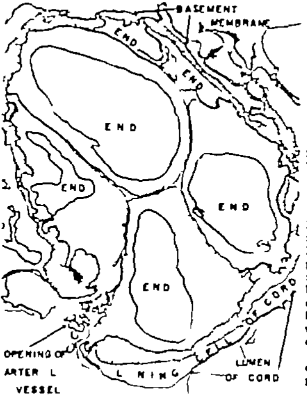
9 Here terminating arterial vessel opens into cord Note the continuation of the basement membrane of the rteriole with the pattern of reticulum in the cord. This cordal reticulum represents the continuation of the arterial terminal, one surface covered with cytoplasm continuous with the endothelial layer the other with cytoplasm continuous with the adventitial layer Compare w th electron micrographs figures 13 and 14 Note the macrophage labeled P in be tracing. This cell is free and contains several red cells T its left it is possible recognize thin cytoplasmic covering of the cordal reticulum. In this preparation such lining cells of the cords, except in the region of the cell center, are ttenuated and closely pplied upon the extracellular connective tissue (= reticulum)

This section was cut from the same block and prepared in the same w y as figure 8 × 1,500.




9

EXPLAN TION OF FIGURE



10 *Rabbit.* This is terminal arterial vessel, pproxim tely 25 μ in diameter It lies within the red pulp protruding and opening into or dal essel (see accompanying tracing). The endothelium is high and displays minimal cell junctions. The endothelial cell are attached, for the most part, only t the b sement membrane Si cell constitute the endothelium here four of them hav ing nucl in section. Not the density along portion f the pproximated pla ma membranes Thi is an occasional finding and may be seen in figure 6 as well. The endothelium contains few mitochondria, moderate concentra ion of RNA particles and consider ble numl er of vesicles, many of the latter sociated with the plasma membrane and suggesting pinocytosis Note the ery fine membranous components of cytopl sm in several endothelial cells The substance of the basement membrane is milar to that in the preceding vessels, although this membrane is very lik ly much poorer in elastic fibers than that in the larger preceding vessels. The membrane here is prominent and shows far less convol tion than in the arlier figures. Smooth m scle ppears bsent although some of the cytoplasmic proces es in the right upper portion of the plat may extend from smooth muscle cells. The lower portion of the essel is an example of the relationship between terminal vessel and the cord into which it empties Here arterial endothelium lies on the obverse surface of basement membrane and the lining cell of the cord lies on its reverse urface The lining cell of the cord actually lies in adventitial relationship to the arterial vessel Not sually where the basement membrane is parted by the opening of an arterial vessel int cord the arterial endothelium may curv round the end of the basement membrane and come to line part of the cordal lumen. This i illustrated on the left side of the arterial opening in thi plate The opening here is slende channel which widens at the cord Note the microvilli. The cord into which this essel empties is filled with cells and only small part of its lumen, t the microvilli, is empty of cells. This structure ppears suited to efficiently control blood flow into the cord

This animal was given Thorotrast five minutes before the spleen was removed. There is little Thorotrast in the cordal lumen t the orifice of the arterial vessel. These details may be better seen in the following plate

In material of the sort Thorotrast is often seen in moderate amount within the arterial endothelium, bounded by membrane This suggests Thorotrast may leave arterial terminal vessel both through the wall and t the orifice. × 30,000.

PLATE 7



PLATE 8

EXPLAN TION OF FIGUR

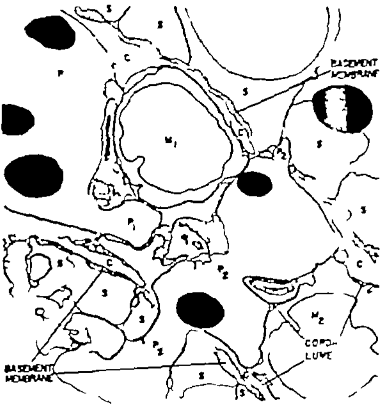
11 *R bbit* Thi section is successive to that in figure 5 perhaps one half micron di tant. Thorium dioxide (marked "T") is present in the arterial lumen and in the passage y between essel A macrophag lies in the cordal vessel t the mouth of the opening and it contains concentration of thorium dioxide possibly captured s the material p ssed through the orifice Most f the thorium dioxide in the macrophage lies within vacuoles some of it is free in the cytoplasm unbounded by membrane Except for that in the macrophag almost all of the thorium dioxide is extracellular RNA ("R") of the arterial endothelium is deeply stained in thi preparation and, on first glance may be onfused with the denser more irregularly sized, shaped and organized thorium dioxide

Again, note the presence of the cordal lining cell d the arterial endothelium separated by common basement membrane A portion of a red cell i also present in the cordal lumen × 52,000.


T
R
M
M
R
T
T

PLATE 10

EXPLANATION OF FIGURE

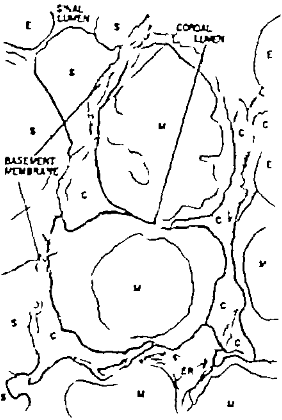


13 *Rabbit* In this section f red pulp a cord occupies mos of the field On another plane of section an arterial ermination has ened into this cord and here the cordal lumen contain several prolong tions of the arterial ending Sinuses are present at right upper and lef lower corners of the field In the accompanying tracing which includes greater are than thi plate the sinal lining cells are A the cordal lining cells "C" A macrophage on the left, P is present in the cordal lumen The macrophage on the right, P_2, presents on the lumen of the lower sinus, passes through the cord undergoing a deep constriction by arterial prolong tions and protrudes ery slightly through the basement membrane of the upper sinus coming to lie between sinal lining cells The arterial prolongations are surrounded by cells P M P M Virtually all of the cordal lumen is filled with cell Small open areas of lumen are indic ted in the tracing. The lining cells of the cord are flat and inconspicuous 32,000


13

PLATE 11

EXPLAN TION OF FIGURE



11 *Rabbit* Thi field contain portion of red pulp ne arterial termin ion and includes portion of sinus The tracing labeled in he same manner figure 13. Note the lining cell of the sinus are higher th those of the cords. The cordal l men is almos compl tely occupied by mononuclear cell The lining cell of the cord re rs flat in places in thickness. Note how the contours of cordal lin g cells and mononuclear cell conform to one another The lowermost mononuclear cell only portion of which included ha a pronounced development of the endoplasmic reticulum in one portion f t cytoplasm ER) Note the compartmentalization of the cordal lume nd compare to figures 8 9 and 13. × 36,000.


14

PLATE 12

EXPLANATION OF FIGURES

15 *Rabbit* This arteriole is just within the white pulp of rabbit spleen The basement membrane is largely trimmed away; it is visible in each of the corners (arrows) The vessel presents two noteworthy features 1 a red cell present in the lumen moderately deformed and close against endothelial cytoplasm and 2 slender elongate luminal cytoplasmic extensions of the endothelium (C P) Compare the latter with the slender luminal processes present in figure 2, and with the abluminal endothelial projections present in figures 4 7 and 20 Although luminal erythrocyte is present no effort was made to retain blood when this spleen was removed 36,000

16 *Dog* This light micrograph was prepared as figures 8 and 9. Thorotrast has been administered 45 minutes before splenectomy The field is of red pulp of dog spleen and includes the sheathed artery Note that the vessel within the sheath bifurcates and is provided with an interrupted basement membrane deeply stained with the PAS reaction. The endothelium is high completely effacing the lumen, although the meeting of endothelial cell luminal surfaces can be made out. The sheath is cellular and deeply marked by PAS reactive material. This material consists of extracellular connective tissue and accumulations of Thorotrast. Most of the large irregular granular material is Thorotrast Note the relation of the sheath to the surrounding red pulp Compare with the remaining figures especially figures 17 18 and 19 750.


CPP

PLATE 13

EXPLANATION OF FIGUR

17 *Dog* This sheathed artery was sectioned from the ame block that in figure 16. The essel consists of an endothelium lying upon basement membrane and ensheathed by a concentration f phagocytic cell The endothel um here i high, the lumen slit. The basement membrane i continuous except for gap between 1 and 2 lock. The crescentic cell containing a nucleus in section lying bove the labeled endothell l cell ("END") may also be endothelium prow ting in this manner beca se of ch ge i direction or bifurc tion of the essel. Along the lower right margin of the plate the endothelium and basement membrane of what i probably a branch of this essel may be seen.

Peripheral to the basement membrane is a complex f ph gocytic cells mixed with irregular sw ths of ground material containing ariable concentrations of fibers. Not the highly folded lengthy cell interdigitations of the she th cells.

Most of the thorium dioxide i present within large cytoplasmic vac noles Many of these acuoles moreover contain other in ested mate rial. A great deal of thorium i lso present between cells and in the extracellular connective tissues.

No smooth m scle ppears present here

The area bounded by the rectangle is presented at higher m gnification in the next plate 4,000

PLATE 13



PLATE 15

EXPLAN TION OF FIGU

19 Dog Thi is portion of another beathed artery of the animal from which figures 17 and 18 were drawn. Again, note the Thorotrast in masses in the reticulum, and between cells. Two kind f cytoplasm ppear present here 1 les dense cytopl sm containing scanty to moderate mount f RNA particles, some rel tively large mitochondria, but lacking granules or endoplasmic reticul m. There is little or no Thorotrast in this cytoplasm nd it probably represent the more gelated ectoplasmic portion of macroph ges. 2 dense cytoplasm containing vacuoles mitochondria granules, and inclusions of Thorotrast. Several granles resemble the small mitochondria present here in size contour and the presence of an external membrane

In figures 18 and 19 distinction must be made between RNA particles and Thorotrast, as in figure 11 Again not that some f the larger aggregates in figures 18 nd 19 made up of Thorotrast, and dense almost spherical bodies probably derived from red cells, may actually be extracellula × 27,000.



PLATE 17

EXPLANATION OF FIGURE

21 *Dog* Thi is sheathed artery from a dog who had gotten no Thorotra t. Note the endothelium i quite low being particul rly ttenuated on the right, and the lumen, containing coagulated pl sma, is large The endothelium, in the sheathed arteries examined almost always formed com- plete layer although the endothelium m y be littl thicker than two cell membranes There is no basement membrane present here The she th cell are rich in RNA and contain many a d diverse inclusions and vacuoles. Broad irregular bands of ground bstance run throughout the fi ld. Highly folded cell junctions re also evident. I places the cyto- plasm contains amorphous, granular ariably dense ground material identical with that present extracellularly Dense masses re present in the reticulum.


LUMEN
END
GS
GS
GS
121

DISCUSSION

Arterial endothelium

The arteries in this material were characterized by a high endothelium and a reduced lumen although this was not an invariable finding in the terminal vessels.

A high endothelium in the terminal segments of arterial vessels in the spleen has been reported by Bannwarth (1891) Weidenreich ('01) Solnitzky ('37) Snook ('50) and especially MacNeal Otani and Patterson ('27) A cuboidal or columnar endothelium has been noted in the capillaries of some perineural connective tissues and in the uterus (Renaut, 1881; Zimmerman, '23 Altschul '54) Interestingly Renaut stresses the value of osmium tetroxide as a fixative in preserving the height of the endothelium A high endothelium is also characteristic of the post-capillary venules in lymphatic tissue (Hummel, '35 Smith and Hénon, '59) The height of this endothelium fluctuates being high when the surrounding lymphatic tissue is active and low when involuted (Pirro quoted by Smith and Hénon, '59) In lymphatic tissue in the intestine of the rat, moreover the endothelium of a given vessel running subcapsularly was high on the side with lymphocytes and low on the subcapsular side (Hummel, '35) The endothelium of post capillary venules displays a marked reaction for esterase as determined by Padykula s modification of Pearse s method (Smith and Hénon, '59) The endothelium of the splenic arterial system in rabbits in material prepared for me in Dr Padykula s laboratory by the method used by Smith and Hénon, was very faintly positive or negative.

A high endothelium extending through the arteriolar and arterial capillary system may be distinctive for the spleen, and absent in the rest of the reticuloendothelial system. Zamboni and Pease ('61) do not report a high endothelium in the arterioles or capillaries of the marrow of the guinea pig and the electron micrograph of an arteriole they provide displayed an unremarkable endothelium. Nor to my knowledge has the finding of an unusually high arterial endothelium been reported for liver I have reviewed by light microscopy preparations of marrow and liver of rabbit embedded in methacrylate after fixation in osmium tetroxide and stained by the PAS method, and have found only a few arterioles in bone marrow with a high endothelium.

Some of the terminal arterial vessels in the dog resembled some of those in the rabbit in the presence of slender abluminal endothelial projections or plates continuous with similar cytoplasmic projections derived from adventitial cells These processes wind irregularly around the vessel. Separating them are layers of extracellular connective tissue These formations account for the dense closely woven reticular fibers noted by Snook ('58) in the rabbit. Abluminal endothelial projections or basal fringes have been observed in other endothelial notably in the kidney and cerebrum (Zimmermann '23 Altschul '54) The structures seen here appear well laid out to modify directly the state of gelation and other characteristics of the extracellular connective tissue over a widespread perivascular area in relation to endothelial activities. Changes in gelation of the connective tissue would affect transport and the capacity of smooth muscle or other elements to change the caliber of the vessel. A lesion characteristic of the collagen disease diffuse lupus erythematosus is the onion-skin artery in the spleen (Klemperer Pollack and Baehr '41) It seems likely that this lesion is an exaggeration of connective tissue lamellations similar to those described here

Sheathed capillaries

The spleen of the rabbit and the spleen of the dog are different after Thorotrast In the dog the Thorotrast was concentrated in the sheath. In the rabbit it was concentrated around the terminations of the arterial capillaries.

A major function of the sheath therefore is the clearance of plasma. This conclusion was drawn by Schweigger Seidel (1862) Hueck ('29) and Mills ('26)

The sheath bears comparison with the centrolobular region of the renal glomerulus. Within five to ten minutes after intravenous administration, Thorotrast en-

ters the centrolobular region in high concentration, penetrating the intercellular substance between intercapillary cells (Latta Mairnsbach and Madden, '60)

It is likely that the primary pathway of materials into the sheath is through the arterial endothelium rather than from the surrounding red pulp The reaction of the endothelium to Thorotrast suggests this transfer since reticular cells subjacent to the endothelium have vacuoles rich in Thorotrast before the more peripheral reticular cells and the pulp around the sheath gives no consistent evidence of Thorotrast retention However material can reach the sheath from the periphery *to a more restricted degree* (Mills '28)

Knisely's ('36) observations on the contraction in the sheath is stimulating in light of Mills and Solnitzky's ('37) observations which I can confirm, that smooth muscle is lacking in the sheath. Their cytoplasmic fibers may indicate a contractile capacity for the endothelium Varying degrees of hydration and swelling in the sheath or in the endothelium may close or open its vessel. As mononuclear blood cells become phagocytic they increase in volume and their cytoplasmic basophilia (= dye binding by RNP) diminishes (Weiss and Fawcett, '53) Gersh and Bodian ('43) observed a parallel situation in anterior horn cells *undergoing* Wallerian degeneration wherein nerve cells increased in volume with *decrease* in Nissl substance They hypothesized that the large RNP molecules broke down into smaller osmotically more active compounds with the result that the *cells* imbibed water and swelled. They demonstrated that these swollen cells *contained* a greater than normal concentration of water by the presence of larger ice crystals on freeze-drying Cells of the sheath, and, indeed, the endothelium, are rich in RNA the former are phagocytic and these considerations may apply Whatever the mechanism, the capacity of macrophages to vary size shape and volume quickly and significantly is evident from their behavior in tissue culture (M Lewis '25 Weiss and Fawcett, '53) It is probable, moreover that Knisely's observation of the abrupt cessation of flow in the sheath depended upon a high endothelium effacing the lumen.

Connection of arterial vessels and cords

The type of connection between arterial ending and cord observed in this study was of the following sort A vessel, perhaps 25 to 30 μ in diameter protrudes into a cordal lumen. Its first opening into the cord is through a slender slitted opening in its side running from the arterial lumen, between arterial endothelial cells, piercing the basement membrane, passing between adventitial cells, and finally communicating with the cordal lumen. At this point of entrance the arterial wall consists of three elements endothelium, basement membrane and adventitial cell which in fact, constitutes a lining cell of the cord since its free surface presents on the lumen of the cord. As the vessel passes further into the cord the arterial endothelium becomes less high, the rest of the wall becomes thinner and more openings into the cord appear as radii from the lumen. As a result the wall becomes quite incomplete and may be represented as pronged or fingerlike extensions of the arterial wall fanning out into the cords, continuous with the partitions compartmentalizing the cords (*vide infra*) In the periphery of the splenic lobule (Mall, '02) away from the entrance of the arterial capillary the cords of the rabbit are somewhat wider poorer in these partitions and come closest to resembling sinuses The channel between arterial vessel and cord as observed here, is clearly dependent for its diameter on the height and volume of the arterial endothelium The arterial endothelium as MacNeal Otani and Patterson ('27) stated is well disposed to control corpuscular and plasma flow into the cords.

Relations of cords and sinuses

I believe that the interpretation of cords as blood vessels gains additional support from these observations. The cords are lined by cells similar to the lining cells of other reticuloendothelial blood vessels and they have direct connections with arterial blood vessels. The cords and sinuses form a dynamic system of vessels capable of profound reorganization and

change in form (Weiss '59). It is clear however, from my continued study of this material under experimental conditions (Weiss, '59) and in the present work, that the cords may not be considered, as I suggested earlier (Weiss '57) simply as collapsed sinuses. They differ from sinuses primarily in that they are partitioned by strands or plates of extracellular connective tissue clothed by reticular cells. This connective tissue, impregnable by silver and reactive to the periodic acid-Schiff procedure has classically been recognized as a component of the reticulum of the spleen (Mall, '00 '02 Snook, '50 '58). If one recognizes the cords as blood vessels it seems appropriate and in accordance with modern usage supported by electron microscopy to designate this connective tissue as a basement membrane since it underlies the lining cells of the vessels. The relationship of cords to sinuses in human beings has been defined by Koboth ('39) on the basis of reconstructions made from sections stained for reticulum. She characterized the cords as consisting of space compartmentalized by regularly spaced fibers of reticulum, forming a mantle around a sinus. A given cord, separating two sinuses, formed two such mantles, one for one sinus the other for the other. Rather heavy strands of reticulum, moreover ran down the middle of the cord, separating it into halves and forming the peripheral margin to each of the two mantles. Earlier ('38) Blechschmidt had suggested cords might be part of the vascular system. Koboth states that this mantle is not extravascular but a vessel. It communicates with the sinus, and constitutes with its sinus the unit of structure of the red pulp. She pointed out, moreover that sinus and mantle had the same type of lining cell. Thus priority in establishing the vascular nature of all of the red pulp belongs to Koboth and Blechschmidt.

A further point of difference between cords and sinuses is that cordal lining cells tend to be much flatter in regions away from the cell center than do sinal lining cells. The cordal lining cells in the unstimulated spleens comprising the material of this study may be so attenuated that their presence would go unrecognized in the light microscope. A free macrophage pressed against such a lining cell would be interpreted as attached to the basement membrane (see fig. 13). Except in those cases where the lining cells have been stimulated to leave their basement membrane they are present over the whole surface of the basement membrane and thus help establish the fundamental pattern of the red pulp viz.: lining cell, lumen lining cell, basement membrane lining cell, lumen.

Separation of plasma and corpuscles

As inferred from a highly corrugated basement membrane and deep complex endothelial infoldings the diminution of the lumen in the arterial vessels studied here was due to vascular constriction consequent to cessation of distending blood pressure agonal or fixation-induced constriction of blood vessels and collapse of the organ. Knisely ('36) apparently found blood flow through these vessels unremarkable except during contraction of the sheath. With fixed under pressure equal to normal blood pressure the vessels underwent only moderate distension and the endothelium though flattened, maintained a cuboidal form. The well known difficulty in obtaining perfusate through splenic arteries when introduced through the splenic vein (Stieda, 1862 Mall, '02 Tait and Cashin, '25 and, especially Mills '26) may be in part laid to this obstrusive arterial endothelium. In life there must therefore be considerably more luminal volume in many arterial vessels than seen here. But slight arteriolar constriction or increase in volume of the endothelium may considerably diminish or efface the lumen. Four possibilities suggest themselves depending upon the extent of vascular constriction 1 blood flow in an arteriole or arterial capillary completely blocked 2. plasma passed and cells thereby concentrated in a proximal segment 3 erythrocytes forced through a narrow irregular channel beset with nodosities and 4 blood flow unimpeded.

In addition to any hemoconcentration in a proximal arterial segment following arteriolar or capillary constriction, the applicability of *plasma skimming* to this

splenic system of arterial vessels must be considered. This phenomenon depends upon the marked tendency of plasma to flow in the peripheral and not the axial blood stream and is enhanced by branches leaving the main stem at large angles approaching 90 Thus Pappenheimer and Kinter ('56) hypothesized that the afferent arterioles of the juxtamedullary glomeruli would skim most of the plasma from the blood of the interlobular artery leaving the subcapsular afferent arterioles blood with a relatively high hematocrit. The layout of the arterial vessels in the white pulp and marginal zone would appear adapted to this sort of partition with some branches having higher hematocrits than others. I have found a great number of right-angled branches in the splenic arterial bed and it is evident from the figures of Jäger ('29) MacNeal, Otani and Patterson ('27) and Snook ('50 '58) that they have. Interestingly Hueck ('29) observed that the narrow radiating follicular capillaries carry mainly blood plasma.

The arteries are morphologically suited to active transport. They are rich in mitochondria, contain vesicles in the cytoplasm and at the cell surface and display moderate to marked surface activity After Thorotrast, moreover this material is present within vesicles in the arterial wall and in the basement membrane. One may postulate therefore the passage of fluid across the arterial wall, further concentrating the luminal corpuscles.

Beyond the arterial system, other mechanisms for hemoconcentration are present. Knisely ('36) observed a red cell mass sequestered in a sinus progressively concentrated as its plasma leaked out into the surrounding pulp. Björkman ('47) found that starch grains roughly of blood cell size stayed in sinuses while smaller ones went into cords. Barcroft and Poole ('27) and Barcroft and Florey ('28) showed that blood in the red pulp of dogs and cats has a higher hematocrit than in the peripheral blood because splenic lymphatics carried plasma away Interestingly Barcroft and Florey rejected plasma skimming as the basis of hemoconcentration of the whole pulp because shutting down venous return did not bring the process to a standstill but enhanced it. This does not, however rule out plasma skimming within the white pulp.

Trauma to red cells

In their passage through the arterial vessels of the spleen therefore, red cells may be subjected to mechanical trauma and to concentration not imposed in other arterial beds.

Splenic arterial vessels may compress red cells subjecting them to mechanical assault. It is true that red cells are distorted as they squeeze through common capillaries. But these are easily distendible tubes whereas the arterial sels are thick walled muscular structures capable perhaps of an action that of the crop of a bird. Red cells become mechanically more fragile as they age, as determined in the dog by Stewart, Stewart, Izzo and Young ('50) mechanical fragility appears significant in *vivo* since reticulocytosis (Brown, '23) increased bilirubin excretion (McMaster, Brown and Roux, '23) have been observed in dogs vigorously exercised after rest. Concentration of red cells would likely enhance their susceptibility to mechanical trauma, particularly if they have suffered a drop in zeta potential which normally accounts for their mutual repulsion. Red cells would be forced against other cells and not cushioned by plasma. Such concentration and a dense population macrophages as occur distal to the arterial vessels moreover, provide red cells with hazards in addition to mechanical trauma (Ham and Castle, '50- Whitby '35 and Crosby '59) This vascular passage may influence the life span of red cells and constitute one factor in establishing the spleen's action in taking certain red cells out of the circulation which other organs let by The site of destruction of normally aged red cells is discussed in the appended review

SUMMARY

Arterial vessels in rabbit spleens form a rich vascular network in the white pulp and terminate in the white pulp marginal zone cords and in small number sinuses This system of vessels possesses a high endothelium. In terminal vessels thelium is frequently high effacing the

lumen, but it may be low. The endothelium forms a complete layer. The endothelium of terminal vessels may be rich in mitochondria, RNA, vacuoles, granules and presents an irregular luminal surface. A basement membrane is present in arterioles and present, as well, even in terminating arterial capillaries. Muscle and adventitial layers are present in arterioles.

The muscle and adventitial cells are enveloped in a ground material containing variable concentrations of fibers continuous with the basement membrane of the endothelium. This complex of extracellular connective tissue is brilliantly stained in the periodic acid-Schiff reaction and constitutes a portion of the classically defined reticulum as revealed by methods of silver impregnation. The adventitial layer contains cells of varied conformation, often rich in RNA, mitochondria, granules and vesicles. The endothelium and the adventitial cells display long slender processes which tend to wind about the vessels in irregular lammellations alternating with layers of extracellular connective tissue.

The limited number of arterial endings observed under the electron microscope connected with cordal vessels not sinuses. The arterial lumen communicates with the cordal lumen by narrow clefts through the arterial wall. As the arterial vessel runs further into the cord, additional clefts develop in its wall, and its wall became reduced to finger-like or pronged extensions which continued further into the cord and compartmentalize it. Cordal lining cells are often very attenuated in regions away from the cell center. Sinuses lacked the compartmentalized character of the cords and their lining cells tend to be higher.

In the dog, unlike the rabbit, the terminal arterial capillaries bear a sheath of phagocytic cells embedded in swaths of ground substance. Typically an incomplete basement membrane ensheaths the endothelial tube — although it is sometimes complete and sometimes absent. It is continuous with the ground substance of the sheath and with it forms the reticulum of the sheath. The endothelium was similar in appearance to that of terminal arterial vessels in the rabbit. The sheath cells display complex convoluted cell junctions and also slender cytoplasmic extensions which may be continuous with the basal cytoplasmic extensions of the endothelium.

After the administration of Thorotrast in the rabbit most of the colloid was present intra- and extra-cellularly in the cordal vessels around the arterial endings. Most of the intracellular material was in free macrophages and not in lining cells. The walls of the terminal arterial vessels and the lining cells of sinuses contained a slight amount of Thorotrast. In the dog the Thorotrast was concentrated in the cells and in the ground substance of the sheath. It was present in the endothelium and basement membrane of the sheathed capillary. With the doses employed only small to moderate amounts were present elsewhere in the red pulp.

It appears that in life, depending upon the degree of constriction, or upon the height of the endothelium in these arterial vessels, four possibilities are present in regard to the flow through them. 1 Blood flow is unimpeded. 2. Erythrocytes are drubbed through narrow nodose irregular channels. 3. Plasma is passed and erythrocytes retained and thereby concentrated. 4 Blood flow is stopped. The possibilities of further corpuscular concentration due to plasma skimming and active transport of plasma across the arterial wall are presented. It is thought likely moreover that these arterial vessels impose mechanical trauma on red cells and therefore contribute to the spleen's capacity to remove selectively red cells which escape disposal elsewhere.

LITERATURE CITED

Altschul, R. 1954 Endothelium. Its development, morphology function and pathology. The MacMillan Co., New York.

Bannwarth, J 1891 Untersuchungen über die Milz. Arch. f. mikr Anato., 38 345–446.

Barcroft, J and H. W Florey 1928 Some factors involved in the concentration of blood by the spleen. J Physiol 66 231–234.

Barcroft, J and L. T Poole 1927 The blood in the spleen pulp. Ibid., 64 23–29

Björkman, S E. 1947 The splenic circulation. With special reference to the function of the spleen sinus wall. Acta Med. Scand. 128 Suppl., 191 1–89

Blechschmidt, E. 1938 Vorweisungen von Mikrokorrosionen Zur Frage der Architektur der

roten Milzpula. Verh. anat. Ges. 35 G Fischer Jena.

Broun, G. O 1923 Blood destruction during excercise. III. Exercise is a bone marrow stimulus. J Exp. Med., 37 187–206.

Crosby W H. 1959 Normal functions of the spleen relative to red blood cells A review Blood, 14 399–408.

Gerth, L, and D Bodian 1943 Some chemical mechanisms in chromatolysis. J Cell. and Comp Physiol., 21 253–280.

Ham, T H., and W B. Castle 1940 Relation of increased hypotonic fragility and of erythrostasis to the mechanism of hemolysis in certain anemias. Trans. Assoc. Am. Phys., 55 127–132.

Hayboe, F G. J and L. Whitby 1955 Splenic function A study of the rationale and results of splenectomy in blood disorders. Quart. J Med., 48 N S. 24 365–391

Hueck, W 1929 Ueber das Mesenchym II. Betr Z. path Anat., 83 152.

Hummel, K. P 1935 The structure and development of the lymphatic tissue in the intestine of the albino rat. Amer. J Anat. 57 351–383.

Jäger E. 1929 Die Gefässversorgung der malpigischen korperchen in der milz. Zeitschr Z. Zellforsch u. mikr An t., 8 578–601.

Klemperer P 1938 The spleen. In Downey's handbook of hematology 3 1591–1754. Paul B. Hoeber Inc., N Y

emperer P A. D Pollack and G. Baehr 1941 Pathology of disseminated lupus erythematosus. Arch. of Path., 32. 569–631.

nisely M. H. 1936 Spleen studies. I. Microscopic observations of the circulatory system f living unstimulated mammalian spleens. Anat. Rec 65 23.

Koboth I. 1939 Über das Gitterfasergerüst der roten Milzpulpa mit einem Bertrag Zu Ihrer Gefasstruktur und Blutdurchströmung. Beitr Z. Path. Anat. u.f. allg. P th., 103 11–29

Latta, H., A. B. Maunsbach and S C. Madden 1960 The centrolobular region of the renal glomerulus studied by electron microscopy J Ultrastructure Research, 4 455–472.

Lewis, M. R. 1925 The formation of macrophages epithelioid cells and giant cells from leucocytes of incubated blood. Amer J Path., 1 91–100

MacNeal, W J S. Otani and M. B Patterson 1937 The finer vascular channels of the spleen Ibid., 3 111–122.

Mall, F P 1900 The architecture and blood vessels of the dog' spleen Zeitschr F Morphol. Bd. 2 S 1–42.

——— 1902 On the circulation through the pulp of the dog' spleen. Am. J Anat., 2: 315–332.

McMaster P D G. O Brown and P Rous 1923 Studies on the total bile. I. The effects of operation, exercise hot weather relief of obstruction, intercurrent disease and other normal and pathological influences. J Exp Med., 37 395–420.

Mills, E. S. 1926 The vascular arrangements of the mammalian spleen. Quarterly J Exp Physiol., 16 301–319

Pappenheimer J R., and W B. Kinter 1956 Hematocrit Ratio of blood within mammalian kidney and its significance for renal hemodynamics. The Amer. J Physiol., 185 377–390

Renaut, J 1881 Note sur la forme de l'endothelium des arterioles, des venules, et des capillaires sanguins. Arch. Physiol. Norm. et Path., 8 191–193.

Richardson, K. C., L. Jarett and E. H. Finke 1960 Embedding in epoxy resins for ultrathin sectioning in electron microscopy Stain Technology 35 313–323.

Schweigger-Seidel, F 1963 Untersuchungen über die Milz. Arch. F path. Anat. u. Physiol., 27 460–504.

Smith, C., and B K. Henon 1959 Histological and Histochemical study of high endothelium of post-capillary veins of the lymph node. Anat. Rec., 135: 207–211

Snook, T 1950 A comparative study of the vascular arrangements in mammalian spleens Amer. J Anat., 87 31–78.

——— 1958 The histology of vascular terminations in the rabbit' spleen. Anat. Rec 130 711–730.

Solnitzky O 1937 The Schweigger Seidel sheath (ellipsoid) of the spleen. Ibid., 69 55–70.

Stewart W B., J M. Stewart, M. J Izzo and L. E. Young 1950 Age as affecting the osmotic and mechanical fragility of dog erythrocytes tagged with radioactive iron. J Exp. Med. 91 147–159

Stieda, L. 1862 Zur Histologie der Milz Virch. Arch., 24 540–550.

Tait, J and M. Cashin 1925 Some points concerning the structure and function of the spleen. Quart. J Exp. Physiol., 15: 421–445

W tson, M. L. 1958 Staining of tissue sections for electron microscopy with heavy metals. J Biochem. and Biophys. Cytology 4 475–478.

Weidenreich, F 1901 Das Gefässsystem der menschlichen milz. Arch. G. mikr. Anat., 58 247–378.

Weiss, L. 1957 A study of the structure of splenic sinuses in man and in the albino rat with the light microscope and the electron microscope. J Biophys. and Biochem. Cytol., 3 599–610.

——— 1959 An experimental study of the organization of the reticuloendothelial system in the red pulp of the spleen. Journal of Anatomy 93 465–477

Weiss, L., and D. W F wcett 1953 Cytochemical observations on chicken monocytes, macrophages and giant cell in tissue culture. J Histochem. and Cytochem., 1 47–65.

Wilson J W 1958 Hepatic structure in relation to function in liver function. Ed. Ralph Brauer Public no. 4 Amer. Inst. Biol. Sciences. Washington, D C. pp. 175–192, 193–197 Discussion P 187 P 193 and ff.

Zamboni, L., and D C. Pease 1961 The vascular bed of red bone marrow Journal of Ultrastructure Research, 5 65–85.

Zimmermann, K. W 1923 Der feinere Bau der Blutcapillaren, Ztschr Anat., 68: 29–110

APPENDIX

THE ROLE OF THE SPLEEN IN THE REMOVAL OF NORMALLY AGED RED CELLS

The reticuloendothelial system, and in particular the spleen, has been recognized as the site of destruction of senescent and pathologic erythrocytes. In such conditions as congenital hemolytic anemia and Thalassemia, characterized by a population of defective red cells the spleen may exercise so selective an action in taking red cells out of the circulation that splenectomy is followed by prolonged red cell survival and marked clinical improvement. However in other cases characterized by abnormal red cells as for example, acquired hemolytic anemia, accelerated red cell destruction may occur in the reticuloendothelial system as a whole the spleen having no special part, and splenectomy being of no value (Wintrobe, '56) It has become possible relatively recently to define experimentally the site of red cell destruction with the use of red cells labeled with radioactive isotopes and to determine the site of their sequestration in the body by externally placed counters or by removal and analysis of tissues.

Jandl ('58a, '58b '60) has defined conditions under which red cells damaged by antibodies were removed by the spleen or by the reticuloendothelial system as a whole. Where the red cells were only moderately damaged, as, for example coating them with metal-protein complexes or by reaction with the incomplete agglutinins of the anti-D system, they were sequestered in the spleen. On the other hand, when severely damaged by complete agglutinins of the anti-A B or O systems, or by lysins they were sequestered diffusely throughout the reticuloendothelial system with the liver as the chief site. Cutbush and Mollison ('58) reported similar findings. Wagner and his associates ('61) too have had similar findings, but they damaged red cells by heating rather than by agglutinins. When red cells were heated at 50 C for one hour they were taken up by the spleen; when heated for two hours they were taken up primarily by the liver The localization of red cells in the foregoing experiments was determined by externally placed counters in human beings. The red cells had been tagged with radioactive chromium.

With regard to the site of removal and degradation of normally aged red cells the conclusion has been drawn that the spleen has no special place (Singer and Weisz, 45 Miescher '56 Ehrenstein and Lockner '58) Singer and Weisz found no significant difference in red cell survival in dogs after splenectomy They estimated the life span of red cells by noting, in dogs prepared with biliary fistulae the time elapsed between massive bleeding and augmented flow of bile Miescher and Allgower quoted by Miescher ('57) report a case in which red cell life as determined by labeling with Cr^{51} fell within the normal range after splenectomy due to trauma in a human being.

However evidence comparing life span in normal and splenectomized individuals must remain uncertain because removal of the spleen may remove influences on hematopoiesis in addition to erythroclasia. End points in the determination of red cell life span by recognition of peaks of augmented bile flow moreover are notably imprecise and even with radioactive tagging a period of indeterminancy of several days must be accepted. In addition, it is likely that red cells produced after massive hemorrhage in the dog are not normal. In rabbits, life span after hemorrhage was 38 to 48 days instead of the normal span of 61 to 65 days (Neuberger and Niven, '51)

Additional information on the fate of normally aged red cells in intact subjects has been provided by labeling red cells with radio-Cr or radio-Fe by Miescher ('56) Ehrenstein and Lockner ('58) C.

A. Finch, Hegsted Kinney Thomas Rath Haskins S Finch and Fluharty ('50) and Hughes Jones and Szur ('57) Miescher reinjected 18 ml of a rabbit's blood after tagging the red cells with Cr^{51} After 25 to 30 days the bone marrow contained 30 to 75% of the radioactivity; the liver 23 to 49% the spleen 6 to 40% From these data and the results of his experiments on red cell life span after splenectomy cited above Miescher concluded that in physiological erythroclasia the spleen had no special part. However this material examined about one month after administration of Cr^{51} appears to neglect possible movement of the tag by elution from the cells or after degradation of the tagged red cells. Gray and Sterling ('50) who introduced the use of radio-Cr for labeling red cells suggested that hexavalent Cr is taken up by erythrocytes and trivalent Cr combines with plasma protein. After red cells are labeled with the hexavalent $Na_2Cr^{51}O_4$, however the Cr is reduced to the trivalent form within the cells. Kraintz and Talmage ('52) followed the fate of intravenously administered trivalent Cr and found in both rabbit and rats although there were significant differences in the manner in which these species handled the material, a considerable amount of radioactivity went to bone. By radioautographs of tibia moreover it was learned that the radioactivity was harbored in marrow diffusely — not in erythroblasts or other cells.

Miescher's conclusions on the role of bone marrow and the lack of selective activity by the spleen in normal red cell destruction have been supported by Ehrenstein and Lockner Twenty milliliters rabbit blood were replaced with a corresponding amount of washed red cells from a sister animal, all labeled with Fe^{59} After a few hours labeled iron was located in the depot Fe fraction (in ferritin or hemosiderin) of various organs and from this data it was concluded that red cells had been broken down in these organs Ehrenstein and Lockner found the depot Fe concentration in the spleen higher than that of any other organ studied but calculated that 74% of the radioactivity was present in marrow and 2.0% in spleen. They state that the spleen is 1/35 the volume of red marrow arriving at this figure, presumably by multiplying the marrow/spleen ratio of radioactive depot iron by the marrow/spleen ratio of the concentration of radioactive depot iron. Despite the relatively small size of the spleen in the rabbit a volume of red marrow 35 times that of the spleen seems excessive. Richet (1894) gives the ratio of spleen/body weight in the rabbit as 0.545 gm/kilo. This is roughly 1/2 000 body weight. If the assumption of red marrow as 1.1% of body weight given by Ehrenstein and Lockner is accepted the red marrow would be only 20 times the volume of the spleen. For this reason it would be of great interest to learn the distribution of depot iron radioactivity in this material at longer time intervals than a few hours after the transfusion of radioactive cells. The bone marrow may reach saturation more quickly than the spleen. Even after so short a period moreover it would be of value to know if there had been any appreciable transfer of ferritin from spleen to marrow Iron in the body is efficiently reutilized for hemoglobin production and the marrow of course is the erythropoietic organ. It is important, moreover considering studies on rabbit red cells to note that, different from human red cells, a significant number are destroyed early in their career Neuberger and Niven ('51) determined that few red cells in man died before reaching an age corresponding to about three-fourths or four-fifths of the mean life span. In some rabbits on the other hand, at least a significant proportion of cells are destroyed within one or two weeks of their appearance in the circulation. Such cells may be handled as those red cells badly damaged in the experimental studies of Jandl ('58a, '58b '60) Finch et al. ('50) Miescher ('56) and Cutbush and Mollison ('58)

In their study of iron metabolism, Finch and his associates provide data on the site of red cell destruction in dogs. After the circulating red cells in two dogs had been labeled with Fe^{59} the animals were loaded down with non-radioactive iron to block reutilization of Fe^{59} and thereby prevent its dispersion from sites where

its red cells had been destroyed. At death 15 months later the concentration of radioactivity in the spleen exceeded that found in liver by a factor of roughly four in one animal and two in the other. An analysis of bone marrow was not presented. It would appear that the interpretation of red cell destruction as applies to normal red cell destruction is complicated by the extensive deposits even in non-reticuloendothelial organs, of nonradioactive hemosiderin. This was the price paid to prevent radio-Fe reutilization. These deposits may have accumulated to a degree affecting the normal circulation in the spleen, liver and bone marrow before most of the labeled cells were ready for removal.

Hughes Jones and Szur ('57) followed the course of radioactivity by surface counting at one to seven day intervals in each of five patients with localized carcinoma in whom 3 to 6 ml of blood had been reinjected after labeling with radio-Cr. By the twenty-fifth day half of the Cr^{51} had left the blood and the greatest excess count relative to the heart was 150/min. for liver and 300/min. for spleen. After considering the errors inherent in surface counting and elution, Jones and Szur conclude, because of the excess counts over the spleen, that the spleen likely destroys normally aged red cells.

Noting Jones and Szur's and Miescher's results the question arises as to the effectiveness with which marrow may be evaluated by surface counting. It is of interest here that in Winkelman, Wagner McAfee and Mozley's results ('60) in which a scanner traveling over the thorax and abdomen of a supine subject records radioactivity on an x ray plate which is then also exposed for a conventional x ray of the upper abdomen and thorax, no activity is registered from the sternum, ribs or vertebrae under conditions where registration from spleen and/or liver is marked. While it is likely that radioactivity from marrow may be recorded by surface counting, it is possible that this technique gives deceptively high values for the spleen. This possibility arises from the work discussed above on the concentration of red cells in the splenic pulp. Such concentration may occur in the course of normal blood flow unassociated either with sequestration or blood destruction.

None of the studies cited on red cell destruction have been supported by comprehensive histological examination. The value of histological observations in experiments in which radioactivity alone is estimated is apparent since it is not the red cell which is tagged that is followed but the tag itself. The tag may be present in intact cells in fragments of red cells, remain adherent to hemoglobin or be eluted from the red cells. It may be transferred to macrophages phagocytizing whole or fragmented red cells or if the tagged entity is reduced to sufficiently small size it may be accepted by virtually any pinocytotic cell. Littoral macrophages in the red pulp may remain as part of the system of lining cells. Other macrophages, derived from the lymphocytes and monocytes of the cords or detached from their littoral fastenings are free and may move within the spleen and be swept through the splenic vein into the liver. They may remain there giving deceptively high values to liver radioactivity if they carry the tag, or flow out into the pulmonary bed. They may thence enter the alveolar space or possibly pass through the capillary bed. The former may be expectorated or swallowed, the latter are destined for the systemic circulation. Along their course the macrophages may be disrupted and their contents, along with the radioactive label, handled by other elements in the reticuloendothelial system. Or if the tag is eluted or reduced to a sufficiently small complex, that portion not excreted would be handled by kidney bone marrow liver or spleen in the manner described by Kraintz and Talmage ('52) and Visek, Whitney Kuhn III, and Comar ('53). Reconsidering the intact labeled erythrocyte, it is clearly important to distinguish transient sequestion as described for example by Knisely ('36) and the movement of normally concentrated streams of formed elements as may occur in the spleen, from that terminal trapping antecedent to destruction. The reader is referred to Wilson's paper ('58) and discussion that follows by Knisely others, for further discussi d

ences to the movement of macrophages Miescher ('57) moreover reviews and contributes new data on the manner in which red cells are broken up and phagocytized

It is clear that under experimental and pathological conditions moderately damaged red cells are removed by the spleen and severely damaged red cells by the reticuloendothelial system as a whole The role of the spleen in the physiological destruction of red cells probably turns on how rapidly a red cell declines from a viable to a non viable state Should red cells normally decline abruptly to the counterpart of severely damaged experimental or pathological cells they may be removed diffusely through the reticuloendothelial system. Or should they be harbored in marrow or elsewhere during a period of more gradual deterioration and released to the blood in a markedly degraded state the same fate would await them. However if red cells deteriorate gradually while circulating they may pass through a stage of moderate damage during which time the spleen might exercise its special power in removing red cells There is evidence that red cells do gradually deteriorate as they age (Crosby '59) This stage may be long enough to expose the red cells to the spleen yet short enough to lie within the period of indeterminancy of available methods for determining life span Jandl's estimate of splenic blood flow in human beings based upon the hemoglobin concentrating in the spleen and splenic blood mixing time as 4% of the circulating blood each minute provides more than 500 passes every 24 hours for the spleen. As mentioned above, the period of indeterminancy in isotopic method of determining red cell life must be put at least several days I proffer the possibility that those cells living the greater part of their statistical life span may decline sufficiently slowly to pass through a phase in which they are vulnerable to the spleen Only if they elude the spleen by languishing elsewhere during their decline are they removed throughout the reticuloendothelial system. In the rabbit where a significant portion of red cells may be defective at the outset, the spleen may be less active in physiological blood destruction than in man.

ACKNOWLEDGMENTS

I wish to thank Mrs. Marie O'Brien for her invaluable technical help.

I am indebted to Dr David Bodian for his advice throughout the preparation of this work and to Col. William H Crosby for a discussion of the problem of the destruction of red cells.

LITERATURE CITED

Crosby W H 1959 Normal functions of the spleen relative to red blood cells A review. Blood, 14: 390–408.

Cutbush, M., and P L. Mollison 1958 [illegible] tions between characteristics of blood group antibodies in vitro and associated patterns of red-cell destruction in vivo. Brit. J. Haemat., 4 115–137

Ehrenstein G V and D. Lockner 1958 [illegible] of the physiological breakdown of the red blood corpuscles. Nature, 181: 911.

Finch, C. A., M. Hegsted T D. Kinney [illegible] Thomas, C. E. Rath, D Haskins, S. Finch and R. G. Fluharty 1950 Iron metabolism, the pathophysiology of iron storage. Blood, 5: 983–1008.

Gray S. J and K. Sterling 1950 The tagging of red cells and plasma proteins with radioactive chromium. J Clin. Invest., 29: 1604–1613.

Jandl, J H. 1955 Sequestration of [illegible] cytes and of abnormal red cells by [illegible] t low pressures. Ibid., 37 904

Jandl, J H and A. S. Tomlinson 1958 The destruction of red cells by antibodies in man. II. Pyrogenic leukocytic and dermal responses to immune hemolysis. Ibid., 37 1202–1228

Jandl, J H and M. E. Kaplan 1960 The destruction of red cells by antibodies in man. III. Quantitative factors influencing the patterns of hemolysis in vivo. Ibid 39: 1145–1156.

Jones, N C. H., and L. Szur 1957 Determination of the sites of red cell destruction using ^{51}Cr-labeled cells. Brit. J Haemat., 3 320–331.

Kraintz, L., and R. V Talmage 1952 Distribution of radioactivity following intravenous administration of trivalent chromium 51 in the rat and rabbit. Proc. Soc. Exp. Biol. and Med. 81 490–492.

Miescher P 1956 Le Mécanisme de L'Erythroclasie a L'Etat Normal. Revue D'Hematologie 11 248–259.

——— 1957 The role of the reticulo-endothelial system in haematoclasis pp. 147–[illegible] Physiopathology of the reticuloendothelial system. Ed. by B N H Iperno, B. Benacerraf and J F Delafresnaye. Blackwell Scientific Publications. Oxford.

Neuberger A., and J F S. Niven 1951 Haemoglobin formation in rabbits. J. Physiol 112 292–310.

Richet, C. 1894 II Poids du cerveau, du foie et de la rate des mammifères. Arch. de physiol. norm. et path., 6 232–245.

Robinson, W. L. 1926 The vascular mechanism of the spleen. Amer. J Path., 2: 341–356.

Singer, K., and L. Weisz 1945 The Life cycle of the erythrocyte after splenectomy and the problems of splenic hemolysis and target cell formation. Amer. J. Med. Sciences, 210 301–323

Yuck, W J L. B. Whitney V S. G. Kuhn, III and C. L. Comar 1953 Metabolism of Cr^{51} by animals as influenced by chemical state. Proc. Soc. Exp. Biol. and Med., 84 610–615.

[1]Wagner H. N Jr. 1961 Personal Communication.

Winkelman, J W H. N Wagner J J G. McAfee and J M. Mozley 1960 Visualization of the spleen in man by radioisotope scanning. Radiology 75 465–466.

Wintrobe, M 1956 Clinical Hematology 4 Ed. Lea and Febiger Philadelphia.

Parts of this work were presented at Annual Sessions of the American Association of Anatomists (Anat. Rec., 1961, 139 286 and 1962, 142 290).

Cytogenesis of the Human Fetal Pancreas[1]

JAMES L. CONKLIN
Department of Anatomy University of Michigan, Ann Arbor Michigan

The initial survey of pancreatic islet formation in the human fetus was re by Pearce ('03) who described the of the islets from the primi the pancreatic tubules. The islets were first identifiable in a 54 mm fetus as clusters of small eosinophilic cells at tached to the tubule but following vascu larization, as observed in a 90 mm fetus they became separated from the tubules by an encroachment of connective tissue. by Seyfarth ('20) and Nakamura ('24) confirmed the origin of the islets but differed from Pearce in that they found the first islets in 50 and 80 mm fetuses respectively

The occurrence of two cell types in the fetal islet was initially reported by Weichselbaum and Kryle ('09) while Kardasewitch ('27) described two cell types within the duct system of a 45 mm fetus. The first indication of islet development was noted by Kardasewitch in a 60 mm fetus when small darkly stained cells, the "In-selcytes, began to proliferate but "typi cal" islets were not observed until the 90 mm stage.

Neubert ('27) also described the de velopment of islet cells from ductule epithelium and, in addition, from cells located at the terminal ends of the ducts. These cells contained intensely stained granules and exhibited a "muddy" appear ance which was typical of all young islet cells. Furthermore, such scattered islet potential cells were always found on the outer surface of groups of cells arranged around adjacent blood vessels a grouping referred to by Neubert as an "Inselfeld."

In a more recent study of the fetal pancreas, Ferner and Stoeckenius ('51) divided islet development into three stages (a) single cells, (b) "Inselfeld," and (c) "Mantelinsel." The first stage observed in a 130 mm fetus consisted of alpha cells within the walls and terminal processes of the duct system and beta cells within the walls of the intercalated ducts and terminal processes. These alpha cells were considered to be the "muddy" cells previously described by Neubert ('27) Beta cells were not as numerous as alpha cells and always appeared in close proximity to the blood capillaries.

In the "Inselfeld" stage, single or small groups of cells had accumulated to form islet processes These islet processes contained alpha and beta cells and also a rose colored cell with ungranulated cytoplasm. In the "Mantelinsel" stage, the beta cells were present as a core within the islet and were surrounded by the rose-colored cells which were, in turn, enclosed within a shell of peripherally located alpha cells The intermediate zone of the islet was considered by Ferner and Stoeckenius to be an area of transformation in which the alpha cells lost granules and acquired the characteristics of the beta cells, since some of the rose-colored cells contained a few alpha granules and others contained a few beta granules.

In contrast to the numerous reports of islet development in the human fetus there have been few studies concerned with the development of the pancreatic acini. The first account is that of Neubert ('27) who described the geometrical development of the acini but did not, how ever describe the staining characteristics of the acinar epithelium. Several investigators have made cursory observations on the time of appearance of the acinar cells. These include the presence of acini in a 25 mm embryo (Kardasewitch, '27) a 42 mm fetus (Lewis '12) and in a fetus of nine weeks (Leigner '32)

Although there is general agreement regarding the mode of development of the

[1] This research was supported, in part, by Predoctoral Fellowship CF 7813-C2, National Cancer Institute, and grant RG-6909 United States Public Health Service.

pancreatic parenchyma there is obvious lack of agreement as to the stages at which the developmental events occur In addition the description of Ferner and Stoeckenius ('51) of the conversion of one cell type into another differs from the reports of other investigators. One of the reasons for these discrepancies may be the variety of staining methods employed many of which were nonspecific or only partially selective. These techniques included picric acid and eosin or safranin (Pearce '03) differential solubility (Lane '07) neutral gentian and acid fuchsin (Bensley 15) Mallory-azan (Bloom '31) and chrom alum hematoxylin and phloxine (Gomori 41 Ferner and Stoeckenius '51) The most selective staining method thus far developed for the demonstration of all islet cell types i.e., aldehyde fuchsin (Gomori '50) and Masson trichrome (Masson '29) has not been previously employed in a study of the development of the pancreatic islets of the human fetus.

The present study was undertaken in an attempt to describe the sequential development of the parenchyma of the human pancreas employing the aldehyde fuchsin and Masson trichrome techniques and other contemporary histochemical methods. Particular attention was directed toward the histochemical differentiation of both islet and acinar tissues in order to (a) describe the process of cellular maturation and (b) to determine the time of development of the several cell types.

MATERIALS AND METHODS

The tissues employed in this study consisted of samples of pancreata from 54 human fetuses ranging in size from 29 mm to approximately 360 mm crown-rump length This size range corresponds to the eighth week through the thirty ninth week of fetal development (Patten '53) The specimens were fixed in either 10% neutral buffered formalin, Bouin's fluid or Zenker formol. After paraffin or celloidin-paraffin embedding the tissue sections were subjected to the following staining procedures hematoxylin and eosin or the Masson trichrome method, (Masson '29) for routine histology aldehyde fuchsin (Gomori, '50) Masson A and light green as a distinguishing stain[1] for the beta, alpha and delta cells of the pancreatic islets; periodic acid Schiff and colloidal iron (Mowry '58) controlled by digestion with diastase, for identifying glycogen, neutral and acid mucopolysaccharides methylene blue buffered to pH 5 6 controlled by digestion with ribonuclease, for the demonstration of ribonucleic acid Bodian's protargol procedure (Lillie, '54) for revealing argyrophilic cells; the dimethylaminobenzaldehyde technique (Adams '57) for the staining of tryptophan containing proteins; the Altmann-Masson procedure (Severinghaus and Thompson, '39) for demonstrating mitochondria; incubation in naphthol-AS-acetate and garnet GBC (Gomori, '52) for exhibiting nonspecific esterase activity.

In the description which follows the specimens have been arbitrarily divided into several selected age groups which are expressed in terms of crown-rump length. This grouping was done in order to facilitate description and has no developmental significance.

RESULTS

The dorsal and ventral anlagen of the pancreas have fused prior to the onset of the fetal period. However the tissues derived from each of the anlagen can be distinguished by their relationship to the portal vein. There are no apparent differences between the parenchymal derivatives of the dual primordia at any stage of development.

At the beginning of the fetal period (circa 30 mm CR) the pancreatic parenchyma consists of a system of multibranched epithelial tubules which terminate distally either as solid cords or as small clumps of cells (fig. 1) The latter will be referred to as cell buds since, as will be described, they ultimately give rise to both acinar and islet epithelium. Mitotic figures are numerous in the cell buds and in the terminal cell cords and less numerous throughout the remainder of the tubule system. The tubules (fig. 2)

---

[1] Generously made available from the Embryological Research Collection of the Department of Anatomy, The University of Michigan Medical School, and from the Wenner-Gren Cardiovascular Research Institute, Stockholm, Sweden, through the courtesy of Doctors Alexander Barry, Jonathan T Lanman, and John Lind, respectively

are composed of moderately eosinophilic cuboidal cells which contain small, intensely basophilic nuclei. Acidophilic connective tissue fibers enclose the tubules while the sparse intertubular stromal fibers are argyrophilic.

30–65 mm CR (8–11 weeks). Throughout this phase of the fetal period, there is an increase in the number of epithelial buds at many sites along the duct system. Early in the period, certain of the cell buds along the course of the tubule system (paratubular cell buds) and also some of the terminal cell buds gradually acquire a basophilic cytoplasm. In addition, the nuclei of these cells are less intensely stained and consequently nucleoli are distinguishable. Nucleoli are not visible in the duct epithelium at this stage and the nuclei are darkly stained. Also at this time distinctive cell types become apparent with the appearance of argyrophilic cells in the pancreata of fetuses of about 30 mm CR length. These argyrophilic cells are located in the paratubular cell buds (fig. 3) but are not present in the terminal cell buds or within the walls of the tubules. Later in this period, about 55 mm CR, an occasional cell of the paratubular cell buds contains a few small Masson A positive granules sparsely scattered throughout its cytoplasm. These cells, which are considered to be alpha cells, are most numerous in those cell buds located within the head of the pancreas and less frequent in other parts of the organ.

65–90 mm CR (11–12.5 weeks). The tubules of the pancreas have an arborous type of origin but in their distal course attain a parallel arrangement. The interval between adjacent tubules is filled by a loose stroma of argyrophilic fibers and an extensive capillary network whose primary branches form plexuses around the tubules. The cell buds increase in size by cellular proliferation and by the end of the period, paratubular cell buds from adjacent tubules begin to merge with each other. Many of these expanding cell buds grow toward capillaries within the stroma and as the buds undergo fusion, as observed in an 65 mm fetus, the capillaries become enveloped within a mass of cells. This gives rise to the configuration of a cordlike cluster of cells penetrated by a capillary bed and corresponds to the "Inselfeld" stage of Neubert ('27).

Argyrophilic cells are now present in some of the terminal cell buds although still most abundant in the paratubular cell buds. Alpha cells are much more numerous and are present in the walls of the tubules and the terminal cell buds, in addition to the paratubular cell buds. These alpha cells are ovoid, about 20 μ in diameter, with light gray cytoplasm that contains numerous red staining granules. The nuclei are large and contain prominent particles of chromatin and several large nucleoli. The alpha cell granules also stain positively after the dimethylaminobenzaldehyde (DMAB) technique (fig. 4).

Another distinctive cell type appears in the cell buds during the early part of this period. This cell, ranging in size from 15 to 22 μ in diameter, has a large nucleus, an occasional nucleolus and finely granular cytoplasm. Since the cytoplasm demonstrates affinity for light green, this is considered to be the delta cell. The remaining cells of the cell buds are the smaller basophilic cells which were previously described. Near the end of the period, about 85 mm CR, many of the small cells of the cell buds stain simultaneously with aldehyde fuchsin and light green with the result that the cytoplasm is colored a pale gray and has a muddy appearance (fig. 5).

90–110 mm CR (12.5–14.5 weeks). The parenchyma has become organized into lobes and lobules (fig. 6) and the various parts of the duct system can be distinguished. The lobar ducts (fig. 7) consist of tall columnar cells while the intralobular ducts (fig. 8) are composed of a low columnar or cuboidal epithelium. The epithelium of the intercalated ducts (fig. 9) is either low cuboidal or simple squamous. The cytoplasm of all the duct cells is lightly eosinophilic while the nuclei are large and variably contain nucleoli.

During this period many of the terminal duct cells assume the acinar arrangement typical of the adult pancreas. The cells enlarge, become pyramidal in shape, and are grouped around a central

lumen. In a few of the acini intercalated duct cells become partially enclosed by acinar cells thus giving rise to centro-acinar cells The nuclei of the acinar cells are large vesicular and contain prominent nucleoli while the cytoplasm has a muddy appearance after staining with aldehyde fuchsin and light green.

Glycogen is present in moderate amounts in the large duct cells (figs. 10 and 11) It increases in the smaller duct cells and is present in large amounts in the acinar cell buds (fig. 12) Islet cell buds are prominent by the absence of glycogen (fig. 13)

Initially the islets contain four cell types i.e. argyrophilic alpha, delta and nongranular (presumably immature) cells while later in the period the most prevalent islet cell types are alpha and delta cells. However while the alpha cells continue to increase the delta cells are observed to gradually decline and simultaneously cells appear which have a dark green cytoplasm that contains very fine aldehyde fuchsin positive granules. A short time later some of the largest islets contain cells, approximately 25 μ in diameter which possess coarse cytoplasmic granules that are stained by aldehyde fuchsin or colloidal iron (fig. 14) These cells have distinctive large vesicular nuclei and large nucleoli and are considered to be beta cells. By the end of the period, many beta cells are evident and some of the islets demonstrate the "Mantelinsel configuration (fig. 15) described by Ferner and Stoeckenius ('51) Typically the beta cells lie in the center of the islet surrounded by other cell types. The argyrophilic and alpha cells lie in the peripheral area of the islet while the delta and immature beta cells lie either within the beta cell core or at the junction with the alpha cell layer A small number of ungranulated immature cells are scattered throughout the islet. Scattered beta cells are also present in the walls of the intralobular and intercalated ducts (fig. 16)

The basement membranes of the tubules and the connective tissue capsules of the islets are acidophilic and PAS and colloidal iron positive The fibers of the intertubular stroma are no longer argyrophilic, stain lightly with acid dyes and exhibit a slight affinity for either aldehyde fuchsin or colloidal iron.

110–150 mm CR (14.5–17 weeks) During this stage the acinar epithelium demonstrate the greatest change. The entire cytoplasm of these cells becomes intensely basophilic but gradually the basophilia becomes most prominent in the basal areas of cell (fig. 17) Shortly thereafter small granules appear in the basal cytoplasm which are DMAB positive (fig 18) and exhibit nonspecific esterase activity (fig 19) similar to the zymogen granules of the adult. As the zymogen granules become more numerous and increase in size the largest granules accumulate in the apical cytoplasm. Although most of the acini contain zymogen granules by the end of this stage, few of the cells exhibit the density of granulation characteristic of the adult acinar cell Despite the accumulation of zymogen granules the acinar cells still contain large quantity of glycogen which is concentrated in the apical cytoplasm. Long filamentous mitochondria are evenly distributed throughout the cytoplasm of these cells.

The mitochondria of the islet cells are more variable in number and size. The beta cells usually contain many fine granular mitochondria (fig. 20) while those of the alpha cells are similar but not as numerous. The delta cells differ conspicuously since they contain few very small mitochondria (fig. 21)

Midway through the period the granules of some beta cells become aggregated in the cytoplasm adjacent to blood capillaries and an occasional cell is observed which appears to be degranulated. Later in the period, the alpha cells are observed to undergo similar morphological changes

The intertubular connective tissue fibers no longer stain with aldehyde fuchsin but are acidophilic and PAS and colloidal iron positive similar to the peritubular basement membranes.

150–210 mm CR (17–22 weeks) In addition to their localization in the islets alpha beta and delta cells are still present in a few of the intralobular and intercalated ducts. Their presence in the latter sites is thought to indicate continued

formation of islet cell buds since these cells occasionally are in mitosis.

Glycogen begins to disappear from the interlobular duct epithelium early in the period and is completely absent from 190 mm specimens. In addition, the glycogen of the intercalated ducts and acini slowly decreases and, except for a few scattered droplets, is absent in the 200 mm fetus. The acinar zymogen granules continue to increase and by the 210 mm stage many of the acini are filled with esterase positive granules (fig. 22)

Early in the period, the islets begin to lose the "Mantelinsel" configuration. This occurs by fusion of adjacent islets with the result that the various cell types become randomly dispersed throughout the islet. In fetuses of 160 mm CR, many of the alpha cells are degranulated and there is a concomitant increase in the number of argyrophilic cells. The argyrophils remain elevated until midway through the period when they decline and alpha cells are again more numerous. After this the number of argyrophils remains low and only an occasional such cell is present in the islets.

There is a continued increase in both the number of degranulated beta cells and in the number of beta cells which exhibit polarization of cytoplasmic granules around the islet capillaries. This appears to occur in a cyclic manner with the result that one islet will contain a preponderance of degranulated cells (fig. 23) while in an adjacent islet all of the beta cells well be either partially or completely filled with granules (fig. 24) Immature epithelial cells continue to be present in the islets. The islet cells are only lightly basophilic (fig. 25) with the beta cell exhibiting the most intensely basophilic cytoplasm.

Thin connective tissue septa separate the various lobules and the sparse intralobular connective tissue consists mainly of fibers which surround the acini, islets and ducts.

350 mm CR (39 weeks) The acinar tissue has increased and the intercalated ducts are much less prominent than before. The islets are larger and more prominent than in the adult organ, and very few of them are of the "Mantelinsel" type None of the earlier stages of islet formation are observed, i.e. the "Inselfeld" stage or single cell stage and although a few immature cells are present within the islets no mature islet cell types are found in any part of the duct system However many of the islets are still attached to the duct system by a cord of small, nongranular epithelial cells. The morphology of the various cell types is as previously described.

DISCUSSION

As noted by previous investigators both the acinar and islet epithelia develop from the primitive pancreatic tubules These tubules branch repeatedly and give rise to an arborescent duct system from which small groups of cells proliferate to form islet and acinar cell buds.

The tubular epithelium exhibits the least alteration of any of the parenchyma. The cytoplasm of these cells remains lightly acidophilic and except for changes in the nuclei, the primary change is in the size and shape of the cells This involves an enlargement of the cells of the lobar ducts and an apparent decrease in size in the cells which form the intercalated ducts. The nuclear changes which occur near the end of the third month consist of a decrease in nuclear basophilia and an enlargement of the nucleoli.

The most striking characteristic of the tubular epithelium of the fetal period is the glycogen which is present from late in the third month to the end of the fifth month (circa 70–200 mm CR) The exact time of appearance of glycogen was not determined with certainty because of the lack of mercuric-fixed tissues prior to the third month. Glycogen could not be demonstrated in formalin or Bouin's fixed material prior to this stage, however but could be demonstrated in such material at subsequent stages. It is doubtful therefore that it was present in any quantity prior to the period indicated. Disappearance of glycogen was observed to occur in a progressive fashion so that it was lost from the lobar ducts then from the intralobular and intercalated ducts and last of all from the terminal cell buds. The same type of progression was noted by Sorokin Padykula and Herman ('59) in

the fetal lung and was considered to be a reflection of the maturity of the cells i.e. the more primitive epithelium contained the most glycogen. This probably accounts for the early disappearance of glycogen from the presumptive islet cells and indicates the later maturation of the tubule and acinar epithelium. This does not explain completely however the persistence of glycogen in the acinar epithelium after the appearance of mature zymogen granules although more subtle metabolic changes may be more closely related to the maturation of these cells

The cells which will produce islet tissue are recognizable late in the second month by the accumulation of cytoplasmic ribonucleic acid and the prominence of nucleoli and probably correspond to the "Insulocytes of Kardasewitch ('27) They are located in cell buds which are derived directly from the primitive tubules in contrast to cell buds which later originate from intralobular and intercalated ducts. While some authors (Simard '37 Bencosme '55 Mori and Haga, '60) have designated the difference in derivation of cell buds as primary and secondary islet ..., this seems to be an unnecessary ...tion. The mature islets appear to be the same regardless of origin and the difference in derivation is probably only another indication of the progressive maturation of the tubule epithelium.

As the islet cell buds increase in size they grow into the intertubular stroma and the cells become intimately associated with blood capillaries. This stage of development was referred to as the Inselfeld" by Neubert ('27) and Ferner and Stoeckenius ('51) Seyfarth ('20) suggested that the islets exerted an inductive effect on acinar development. Although this could not be determined in the present study it is true that the islets do appear before the acini and always lie near the center of the lobule surrounded by acinar tissue

The "Mantelinsel stage described by Ferner and Stoeckenius was said to persist until the fourth postnatal year In the present study this stage was predominant only during the fifth fetal month and the adult type was most common thereafter While Pearce ('03) reported that the islets lost their attachment to the tubule epithelium. it was observed that many of the islets were still attached to the intercalated ducts at the end of the fetal period.

All of the cells of the immature islet cell buds are intensely basophilic but after the appearance of specific cell types, only the beta cells continue to be moderately basophilic.

The first distinctive islet cell to appear is the argyrophilic cell. This cell is probably an intermediate in the formation of the alpha cell as suggested by Ferner and Stoeckenius ('51) Hultquist and Thorell ('53) and Bencosme ('55) The argyrophilic cell appears just before the alpha cell, is found in the same location as the alpha cell, and there is a reciprocal relationship between the numbers of these cells, i.e., as the alpha cells become more numerous the argyrophilic cells decrease. Also the staining characteristics of these two cells are suggestive of such a relationship The argyrophilic cells which are also argentaffinic, are DMAB negative while the alpha cells are DMAB positive. Since the argentaffin reaction is demonstrated by aminophenols, among other phenolic compounds (Pearse '60) the argentaffin granules may consist of tryptophan precursors such as hydroxyanthranilate or hydroxykynurenine. These substances would be expected to exhibit an affinity for silver while the tryptophan of the alpha cell granules would not. The acidophilia of the alpha cell granules is probably due to the many free amino groups of glucagon.

Although Ferner and Stoeckenius ('51) suggested that the delta cell was a degenerative type, evidence has been obtained in the present study which suggest that this cell is intermediate in the formation of the beta cell First, the delta cells appear slightly before the beta cells are apparent. Secondly prior to the appearance of the latter acidophilic cells are observed which contain small aldehyde fuchsin-positive cytoplasmic granules. It is thought, in agreement with Munger ('58) that these are the muddy cells described by Neubert ('27) and Bencosme ('55) and not alpha cells as suggested by Ferner and Stoeckenius ('51). Finally the distribution of the delta cells

within the "Mantelinsel" is similar to the distribution of the beta cells.

Although Ferner and Stoeckenius ('51) reported the transformation of alpha into beta cells, no evidence for such a transformation was observed in the present study. The transformation zone which they described in the "Mantelinsel" consists primarily of immature epithelial cells which develop into either alpha or beta cells. Mature islet cells are also produced by mitotic division of existing alpha, delta and beta cells.

The order of appearance of the pancreatic islet cells of the human fetus differs from that observed in other species. In the rat (Hard, '44), rabbit (Bencosme, '55) and mouse (Munger, '58; Mori and Hegre, '60) the beta cells appear before the alpha cells. In the present study the argyrophilic cell was present at the end of the second month (30 mm CR) followed by the alpha cell in the middle of the third month (60 mm CR), the delta cell slightly later and the beta cell early in the fourth month (85 mm CR) of the fetal period. Although Kardasewitch ('27) and Pearce ('03) placed the development of islets after acinar formation, the islets begin to develop in the second month while acinar cells do not appear before the end of the third month. This difference in observation is probably due to the difficulty in distinguishing between islets and acinar cell buds when specific stains are not employed.

The first indications of maturation of the acinar epithelium are the affinity of the cytoplasm for aldehyde fuchsin, the enlargement of the nucleoli and a decrease in nuclear basophilia. The latter events undoubtedly reflect an alteration in nucleic acid metabolism since it is shortly after this that the cytoplasm becomes intensely basophilic. Following the accumulation of cytoplasmic ribonucleic acid, cytoplasmic granules appear which exhibit nonspecific esterase activity and contain demonstrable tryptophan, both of which are characteristic of the mature acinar zymogen granules.

No evidence of secretory activity by the acinar epithelium was observed although the cells seem fully capable of secretion from the fifth month onward. Of the islet cells only the beta cell appears to secrete during the fetal period. From the end of the fourth month (130 mm CR) to term beta cells were observed which offered morphological evidence suggestive of secretory activity. The alpha cells offered transitory evidence of secretion during the early part of the fifth month but did not appear to be active after this time. In studies of other species (Hard, '44; Bencosme, '55; Munger, '58) it was observed that the alpha cells did not function during the fetal period; in fact, did not develop until several days after birth.

There does not seem to be any correlation between the onset of secretory activity of the islet cells in the human fetus and the beginning of secretory activity of other endocrine glands. According to Gillman ('48) the follicles of the thyroid gland contain colloid by the eighth week while chromophil cells are present in the pars distalis by the ninth week. Also according to Gillman, the adrenal cortex offers evidence of hormone production in the ninth week and has the capacity for cortisol biosynthesis by the twelfth week (Bloch and Benirschke, '59). This capacity for secretion by the other glands does correspond to the beginning of islet cell maturation.

Several changes were noted in the stroma of the pancreas which provide information about the maturation of the stromal fibers. Reticular fibers are the predominant type until about the eighth week of development when the fibers which enclose the parenchymal elements acquire the staining characteristics of collagenous fibers. The intertubular fibers remain reticular-like until the end of the third month when they cease to be argyrophilic and stain very lightly with aldehyde fuchsin and colloidal iron. By the end of the fourth month they no longer stain with aldehyde fuchsin, are acidophilic and PAS and colloidal iron positive. These changes probably reflect changes in the ground substance during the maturation of the precollagenous fibers.

The merging of islets with ganglia was described by Neubert ('27) and confirmed by Simard ('37) who suggested the term, neuroinsular complex, to describe ganglia which contained beta cells. Bencosme

('55) also reported having observed these structures but their existence has been questioned by Coupland ('58) and Munger ('58) Neuroinsular complexes were not observed in the present study and although many of the ganglia are in close proximity to both islets and acini, there seemed to be a well defined connective tissue capsule separating the parenchyma from the ganglia.

SUMMARY

The sequential development of the human fetal pancreas has been investigated by histochemical methods.

The pancreatic islets are initially derived from the primitive pancreatic tubules and secondarily from the intralobular and intercalated ducts. In addition, islet growth is supplemented by mitotic division of mature islet cell types

The islet cells develop sequentially with the argyrophilic cell appearing during the eighth week of development, followed by the alpha, delta and beta cells during the tenth eleventh and thirteenth weeks respectively The argyrophilic cell is considered to be an intermediate in the for ...n of the alpha cell while the delta cell is thought to be a precursor or intermediate of the beta cell. The alpha and beta cells are fixed cell types and transformation of one type to the other was not observed.

From the end of the fourth month until term, the beta cells exhibit morphological evidence of secretory activity The alpha cells offer only transitory indications of secretory activity early in the fifth month

Glycogen is present in the duct epithelium and acini during a part of their development but is absent from the islets at all stages.

The pancreatic acini differentiate from the cells at the terminal ends of the intercalated ducts. The first indication of acinar differentiation is an apparent alteration in nucleic acid metabolism. This is followed by the appearance of zymogen granules which possess the characteristics of those observed in the adult pancreas.

Although zymogen granules are present, the acini offer no evidence of secretory activity during the fetal period

ACKNOWLEDGMENTS

The author is indebted to Doctors Alexander Barry and Burton L. Baker for advice and encouragement and to Miss Mary Silvester for technical assistance.

LITERATURE CITED

Adams, C. W M. 1957 A p-dimethylaminobenzaldehyde-nitrite method for the histochemical demonstration of tryptophane and related compounds. J Clin. Path., *10* 56–62.

Bencosme, S A. 1955 The histogenesis and cytology of the pancreatic islets in the rabbit. Am. J Anat., *96* 103–151

Bensley R. R. 1915 Structures and relationships of the islets of Langerhans. Harvey Lect., *10* 250–289

Bloch, E., and K. Benirschke 1959 Synthesis in vitro of steroids by human fetal adrenal gland slices. J Biol. Chem., *234* 1085–1089.

Bloom, W 1931 A new type of granular cell in the islets of Langerhans of man. Anat Rec., *49* 363–371

Coupland, R. E. 1958 The innervation of pancreas of rat, cat and rabbit as revealed by cholinesterase technique. J Anat., *92*: 143–149.

Ferner H., and W Stoeckenius, Jr. 1951 Die Cytogenese des Inselsystems beim Menschen. Ztschr f. Zellforsch. u. mikr. Anat., *35*: 147–175.

Gillman, J 1948 The development of the gonads in man, with consideration of the role of fetal endocrines and the histogenesis of ovarian tumors. Contrib. Embryol., *32* 81–133. (Carnegie Inst. Wash. Pub. No. 210.)

Gomori, G. 1941 Observations with differential stains on human islets of Langerhans. Am. J Path., *17* 395–406.

——— 1950 Aldehyde-fuchsin A new stain for elastic tissue. Am. J Clin. Path., *20* 665–666.

——— 1952 Microscopic Histochemistry University of Chicago Press, Chicago.

Hard, W L. 1944 The origin and differentiation of the alpha and beta cells in the pancreatic islet of the rat. Am. J Anat *75*: 369–403.

Hultquist, G. T and B Thorell 1953 Cytological changes during the embryonal formation of Langerhans islands as revealed by ultraviolet microscopy Acta path. et microbiol. Scandina 32 245–250.

Kardasewitch, B L 1927 Embryologie der Langerhansschen Inseln des menschlichen Pankreas. Ztschr. f. d. ges. Anat *83*: 793–803.

Lane, M. A. 1907 The cytological characters of the areas of Langerhans. Am. J Anat *7*: 409–422.

Leigner B 1932 Studien zur Entwicklung des Pankreas, besonders der Langerhansschen Inseln. Ztschr f. mikr.-anat. Forsch *30*: 494–529

Lewis, F T 1912 The early development of the entodermal tract and the formation of its subdivisions. In Keibel, F and F P Mall.

eds., Manual of Human Embryology J. B. Lippincott Co vol., 2, Pp 295–334
Lillie, R. D. 1954 Histopathologic Technic and Practical Histochemistry 2nd ed. The Blakiston Company Inc., New York.
Masson, P 1929 Some histological methods Trichrome stainings and their preliminary technique. J. Techn. Methods *12* 75–90.
Mori, T., and A. Haga 1960 Histological and histochemical observations on the developing pancreas of fetal mouse. Tohoku J Exper Med., 72: 45–58.
Mowry R. W 1958 Improved procedure for the staining of acidic polysaccharides by Müller's colloidal (hydrous) ferric oxide and its combination with the Feulgen and the periodic acid-Schiff reactions. Lab. Invest., 7 566–576.
Munger, B. L. 1958 A light and electron microscopic study of cellular differentiation in the pancreatic islets of the mouse. Am. J Anat., 103 275–311.
Nakamura, N. 1924 Untersuchungen über das Pankreas bei Föten, Neugeborenen, Kindern und im Pubertätsalter. Arch. path. Anat., 253: 286–349.
Neubert, K. 1927 Bau und Entwicklung des menschlichen Pankreas. Arch f. Entwicklungsmech. d. Organ., *111* 29–118.
Patten, B. M. 1953 Human Embryology 2nd ed. The Blakiston Company Inc., New York.
Pearce, R. M. 1903 The development of the islands of Langerhans in the human embryo. Am. J Anat., 2: 445–455.
Pearse, A. G. E. 1960 Histochemistry 2nd ed. Little, Brown and Co., Boston.
Severinghaus, A. E., and K. W Thompson 1939 Cytological changes induced in the hypophysis by the prolonged administration of pituitary extract. Am. J Path., *15* 391–412.
Seyfarth, C. 1920 Neue Beiträge zur Kenntnis der Langerhansschen Inseln im menschlichen Pankreas und ihre Beziehung zum Diabetes mellitus. Gustav Fischer Jena.
Simard, L. C. 1937 Les complexes neuro-insulaires du pancreas humain (Neurocrinie et fonction paraganglionnaire) Arch. anat. micr., 33 49–84.
Sorokin, S., H. A. Padykula and E. Herman 1959 Comparative histochemical patterns in developing mammalian lungs. Develop. Biol., *1* 125–151.
Weichselbaum, A., and J Kyrle 1909 Über das Verhalten der Langerhansschen Inseln des menschlichen Pankreas im fötalen und postfötalen Leben Arch. f. Mikr Anat., 74: 223–258.

PLATE 1

EXPLANATION OF FIGURES

1 Parenchymal cell buds (B) in the pancreas of 30 mm CR fetus. Hematoxylin and eosin. × 75.

2 The pancreatic tubules of 30 mm CR fetus. The nuclei of the tubular cells are small and intensely basophilic. Hematoxylin and eosin. × 125.

3 Argyrophilic cells within paratubular cell buds of a 30 mm CR fetus. Protargol. × 250.

4 Alpha cells (A) within an islet as demonstrated by the dimethylaminobenzaldehyde technique. × 400.

5 "Muddy" cells (M) in the parenchyma of an 85 mm CR fetus. Aldehyde fuchsin, Masson A and light green. × 250.

6 A pancreatic lobule. The intralobular duct (D) is centrally located while islets (I) are encircled by developing acini. Aldehyde fuchsin, Masson A and light green. × 75.

7 A pancreatic lobar duct. The duct epithelial cells are lightly stained and enclosed within an aggregation of acidophilic connective tissue fibers. Aldehyde fuchsin, Masson A and light green. × 400.

8 A pancreatic intralobular duct. Aldehyde fuchsin, Masson A and light green. × 400.

9 A pancreatic intercalated duct. The outer perimeter of the duct has been outlined in ink. This duct and the intralobular duct are enclosed by thin basement membrane. Aldehyde fuchsin, Masson A and light green. × 400.

10 Glycogen in an intralobular and intercalated duct of a 100 mm CR fetus. Colloidal iron and periodic acid-Schiff (PAS) × 250.

11 Diastase control. Colloidal iron and PAS. × 250.

12 Glycogen in the acini of a 110 mm CR fetus. Only the connective tissue fibers are PAS positive in the adjacent islet (I) Colloidal iron and PAS. × 250.

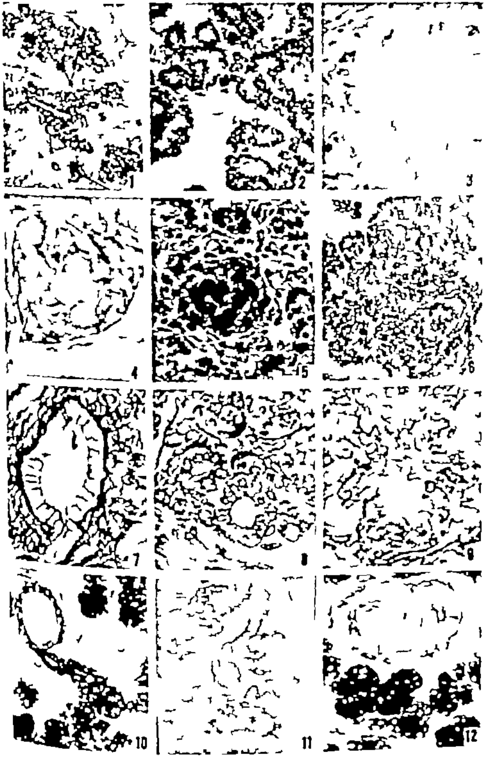

1
2
3
4
5
6
7
8
9
10
11
12

PLATE 2

EXPLANATION OF FIGURES

13 An islet (I) nd islet cell bud (B) of 110 mm CR fetus. Note the bsence f glycogen in these structures. Colloidal iron and PAS × 250.

14 Beta cells in an islet of a 100 mm CR fetus. Aldehyde fuchsin, Masson A and light green. × 630

15 A "Mantelinsel" in the pancreas of a 110 mm fetus. The beta cells (darkly stained) are centrally located and surrounded by other islet cell types. Aldehyde fuchsin Masson A and light green × 250.

16 A beta cell (B) in the wall f an intralobular duct. Beta cells are also visible in an islet cell bud (lower left) Aldehyde fuchsin, Masson A and light green. × 250

17 Basophilia in the basal region of the acinar cells. The nucleoli are also prominently stained. Methylene blue. × 400

18 The demonstration f tryptophane in the acinar zymogen granules. Demethylaminobenzaldehyde technique. × 2.0

19 Nonspecific esterase activity in the acinar epithelia. Small granules first appear in the basal area (G) and then ggregate in the pical cytoplasm. N phthol-AS-acetat and garnet GBC. × 650.

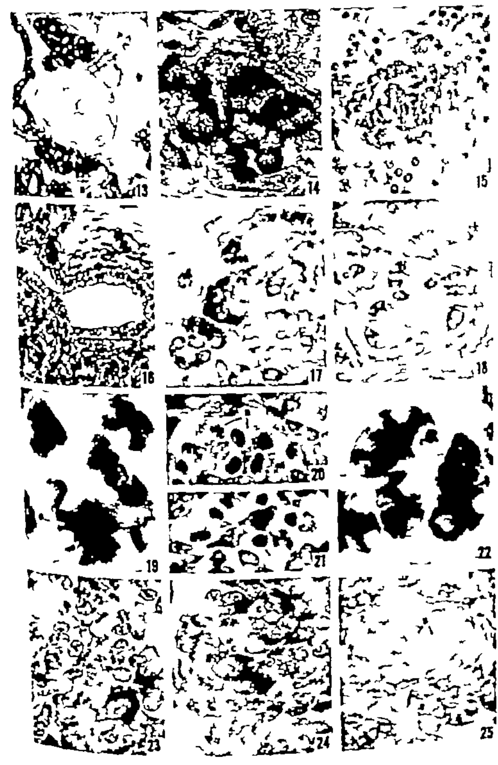
20–21 Mitochondria in the beta cell (B) and delta cell (D) Altmann acid fuchsin and light green. × 650.

22 Nonspecific esterase activity in the acini of 210 mm fetus. N phol-AS acetate and garnet GBC × 650

23 Degranulated beta cell (B) in fetal islet. Granule-containing beta cell are present t the lower right. The photograph is taken through the area of contact of two merging islets (dashed line) Aldehyde fuchsin Masson A and light green. × 650

24 Partially degranulated beta cells. Note the accumulation of cytoplasmic granules adjacent to the capillaries (C) Aldehyde fuchsin Masson A and light green × 650.

25 Lightly basophilic beta cells (B) in fetal islet. Only the nucleoli are prominently stained. Methylene blue. × 400



Initiation of Cell Proliferation in the Vaginal and Uterine Epithelia of the Mouse[1]

CARMIE A. PERROTTA
Biology Department, Brookhaven National Laboratory Upton New York and Department of Anatomy Yale University New Haven, Connecticut

The vaginal and uterine epithelia in the castrate mouse are in a resting state. After appropriate estrogen stimulation, these epithelia proliferate at a high rate. This proliferation has been studied in terms of mitotic indices by Allen, Smith and Gardner ('37) Biggers and Claringbold ('55) and Tice ('61). Allen, Smith and Gardner found maximal mitotic activity at 37 hours after the administration of estrogen. Forty-eight hours after estrogen the mitotic activity had slightly declined. In the vagina of the mouse, Biggers and Claringbold found a latent period of 12 hours after the administration of estrogen and a maximum mitotic rate at 20 to 36 hours.

Recent developments in high resolution autoradiography have made it possible to study another aspect of proliferation, namely DNA synthesis. If labeled DNA precursors are injected into animals, they are incorporated into those cells in the process of doubling their DNA. These cells may be visualized in autoradiographs. Tritiated thymidine has proved an efficient label for this purpose (Hughes et al., '58).

Tritiated thymidine with autoradiography has been used to survey cell proliferation and migration in the reproductive tract of the normally cycling mouse ([illegible] and [illegible], '60). Multiple injections of tritiated thymidine at four hour intervals during 24 hours of proestrus showed that a cell, originally laid down in the basal layer of the vaginal epithelium, was displaced by cell migration toward the lumen at a rate which brought it to the surface by the end of the estrus cycle. [illegible] such a multiple injection technique in the normally cycling mouse gives [illegible] information on epithelial proliferation, it does not allow for a detailed analysis of the proliferative cycle.

Using a single injection of tritiated thymidine on castrate rats under conditions of constant estrogen stimulation the following details of the proliferative cycle of the vaginal epithelium have been worked out (Peckham, '61) the approximate length of the generative cycle was found to be thirteen and one-fourth hours the duration of the S phase about six hours the minimum combined G_2 and mitosis time about one and three-fourths hours and the G_1 time about five and one-fourth hours. It was observed that cells begin their movement from the basal layer only several hours after reaching a mitosis. The turnover time of the non dividing cells was between 30 and 45 hours.

Peckham studied the vaginal epithelium in a steady state. The present investigation is a study of the initiation and subsequent cessation of proliferation which occurs in the castrate mouse after a single injection of estrogen. By this method, it is possible to gain additional information on the mechanism of estrogen action.

Before a cell can enter mitosis it must undergo at least two metabolic events one is DNA synthesis and the other a further process which takes place in G_2. So far in most steady state populations studied, a cell which has completed DNA syn-

---

[1] Research carried out in part at Brookhaven National Laboratory under the auspices of the U. S. Atomic Energy Commission and in part at Yale U., supported by an Institutional Grant from the Am. Cancer Soc. upon recommendation of the Univ. Committee on Atypical Growth and grant from the Am. Cancer Soc. (E no. 181).
The author held Special F [illegible] from the Public Health Service (no. GF 12,766) during the work carried out at BNL.

The generative cycle is divided into mitosis (M), presynthetic or postmitotic interphase (G_1), synthesis phase (S), and postsynthetic or premitotic interphase (G_2).

thesis passes through a brief G_2 into mitosis. In the liver the proliferative stimulus of partial hepatectomy will produce DNA synthesis before mitosis (Holmes and Mee, '55). This may not necessarily be a general phenomenon for in the mouse ear epidermis Gelfant ('61) believes that there is a population of cells that holds up in the G_2 phase for long periods of time. These cells can be specifically stimulated to undergo mitosis by cutting the ear. It is therefore possible that a proliferative stimulus may act in at least one of two ways: one is to give the signal for a cell to enter DNA synthesis, and the other to give the signal for a cell to enter mitosis which has undergone DNA synthesis prior to the application of the proliferative stimulus. In the light of this one specific question which the present experiments were designed to answer is whether estrogen triggers interphase cells to enter the S phase or whether it triggers cells to undergo mitosis which had synthesized DNA before the administration of estrogen.

MATERIALS AND METHODS

The mice used were an inbred strain derived from a pathogen free stock of Swiss mice developed at Walter Reed Medical Research Center. Twenty-nine young adult, virgin, ovariectomized mice were each given 0.125 µg estradiol benzoate in one subcutaneous injection of 0.05 ml sesame oil to stimulate proliferation. At various intervals during 50 hours after the administration of estrogen 70 µc of tritiated thymidine was given in a single subcutaneous injection to label cells synthesizing DNA. Both estradiol and tritiated thymidine were injected simultaneously into each of two animals, which served as controls. Mice were killed 45 minutes after the administration of tritiated thymidine. By that time the tracer is taken up and few if any labeled cells have divided. Genital tracts were removed, vaginas were slit longitudinally along the dorsal surface and fixed in Bouin's fluid. Mid-portions of the vaginas and uterine horns were embedded in paraffin and sectioned at 6 µ. Deparaffinized sections were dipped into NTB nuclear track emulsion, exposed for four days developed in D/19 and stained with a modification of Groat's four color stai[n]. In one group of animals, estradiol injec[tions] were so timed that all were harveste[d] at 3:00 P.M. In a second group the tim[e] of injection with estradiol was always [at] 12 noon.

The following three types of quantit[a]tive observations were made on the va[gi]nal epithelium: (1) labeling index, (2) mitotic index and (3) rate of cell produc[tion]. The labeling index is the percentag[e] of basal epithelial cells labeled with tr[i]tiated thymidine: a sufficient number o[f] cells was counted until 50 to 100 label[ed] cells were obtained. To estimate the ep[i]thelial mitotic index, the number of mit[o]tic and interphase cells was counted unt[il] a sample of 2,000 cells or a sufficien[t] number of cells to contain six mitoses wa[s] accumulated. Samples of this size gi[ve] rough estimates of mitotic indices. T[o] estimate the rate of cell production, coun[ts] were made of the number of non-bas[al] cells above 50 consecutive basal cell[s]. Non-basal cells are those cells in the up[per] layers of the epithelium. In genera[l] non-basal cells do not proliferate. An in[crease] in the ratio of non-basal to bas[al] cells is proportional to the rate of ce[ll] production as long as there is no gro[ss] loss of epithelial cells i.e. before corn[ifi]cation of the epithelium.

The percentage of tritium labeled ce[lls] was determined from samples of abo[ut] 300–900 cells in the surface epitheliu[m] (non-glandular) of the uterine horn, a[nd] mitotic indices from samples of abo[ut] 300 cells.

RESULTS

Vaginal epithelium. The tritium lab[el] was found mainly in the cells in the bas[al] layer of the epithelium (figs. 5–9). Lab[el]ing indices are shown in figure 1a. Abo[ut] 3% of the basal epithelial cells were la[]beled in the epithelium of control animal[s] and in the epithelium of animals injecte[d] with tritiated thymidine three and s[ix] hours after the administration of estr[a]diol. Three animals at 12 hours show[ed] labeling indices of about 40% and [a] fourth animal showed a labeling index [of] 8%. This suggests that there is a variab[le] interval of time near 12 hours after estr[o]gen administration when the vaginal e[p]i[thelium]

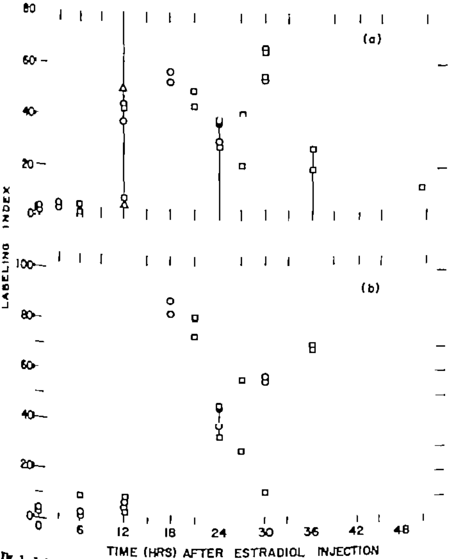


FIG. 1 Labeling indices in the basal layer of vaginal epithelium ( ) and uterine epithelium (b) 45 minutes after tritiated thymidine injection. Each symbol represents one animal. Squares are labeling indices obtained in experiments where all animals were killed at 3 00 P.M. Circles from experiments where all animals were injected with estradiol at noon. Triangles are labeling indices from different regions in one 12 hour animal.

...um undergoes the initial wave of ... synthesis. A fifth animal at 12 ..., showed a labeling index of 5% in ...ventral region and 50% in the lateral ...ns. This suggests that in the early ...s after estrogen administration there ...regional differences in the time of ...ation of waves of DNA synthesis. The ...ing index rose to 55% at 18 hours, ...ned to approximately 35% at 24 hours, rose again at 30 hours to about 60% and was again low at 36 hours. The epithelium at 50 hours after the injection of estradiol had a labeling index of about 12%

Mitotic indices are shown in figure 2a. The mitotic index was approximately 0 01% at 6 and 12 hours. It was about 3.5% at 18 hours. It ranged from 1 to 5% with a mean of 2.4% at 24 hours.

The mitotic indices were about 0 9 and 2% at 26 hours. Thus, the mitotic index rises after the increase in labeling index.

Ratios of non-basal to basal cells are shown in figure 3 The ratio in the epithelium of control animals was about 0.9 1 It increases to approximately 2.3 1 by 36 hours after the administration of estrogen, which implies a production of about 1 4 cells per basal cell within that time. There is little additional cell production after this time.

Uterine epithelium. Labeling indices are shown in figure 1b. About 2% of the epithelial cells were labeled in the uteri of control animals. About 5% of the cells were labeled in animals injected with tritiated thymidine at 6 and 12 hours after the administration of estrogen. The labeling index rose to about 85% at 18 hours, declined to about 40% at 24 hours, and rose again at 30 and 36 hours. The low labeling index of 12% of one animal at 30 hours may be the result of occasional

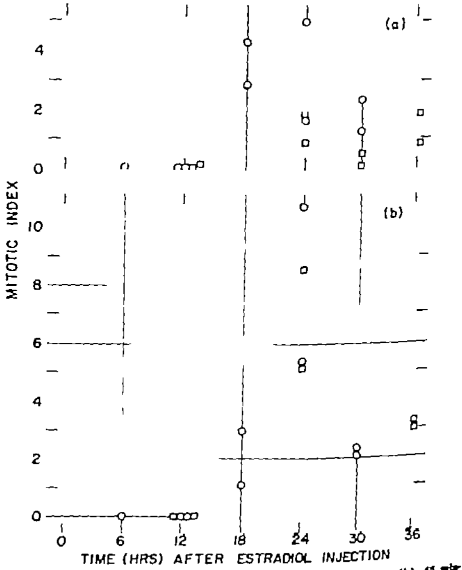


Fig. 2 Mitotic indices in vaginal epithelium ( ), and uterine epithelium (b), 45 minutes after the injection of tritiated thymidine. Symbols refer to legend of figure 1

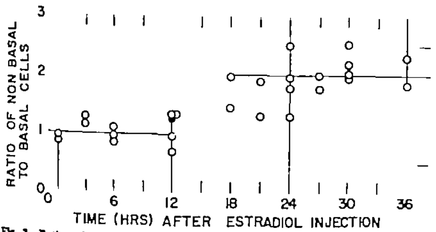


Fig. 3 Ratios of non-basal to basal cells. Each symbol represents one animal.

individual quantitative variations in sensitivity to estrogen.

Mitotic indices are shown in figure 2a. No mitoses were found in samples of 300 epithelial cells from animals at 6 and 12 hours. The mitotic index was approximately 2% at 16 hours. Higher mitotic indices of about 5 to 11% were found at 24 hours. The mitotic index was about 2% at 30 hours and about 3.1% at 36 hours. The rise in mitotic index succeeds the rise in labeling index, as in the vagina.

The vaginal epithelia of three out of four animals at 12 hours showed high labeling percentages while the uterine epithelium of these same animals showed low labeling percentages (fig. 1) This indicates that the initial wave of DNA synthesis in the uterus may lag that in the vagina. However this is not always the case, for in other experiments (to be published latter) it was found that the initial wave of DNA synthesis in the uterus may occur at the same time as in the vagina, or may actually precede it by a few hours. The high labeling index at 18 hours in the uterine epithelium suggests that the cells of the uterine epithelium enter the S phase more synchronously than the cells of the vaginal epithelium.

DISCUSSION

In fast growing tissues of the mouse the duration of the S phase is about six eight hours (Quastler '61) Peckham ('61) has shown that in the estrogenically stimulated rat vagina, the S phase is about six hours, and the total generation time about thirteen and one-fourth hours. The results of the present study suggest, therefore that following a latent period of about 12 hours after the administration of estrogen vaginal epithelial cells start synthesizing DNA over a few hours and then undergo cell division for the first time Some of these same cells enter DNA synthesis and undergo division for a second time.

Ratios of the non-basal to basal cells give a better estimate of cell production than the number of cell layers since the cells in the upper layers tend to become spinous shaped and flattened out. For example the epithelium of animals 36 hours after the administration of estrogen is six-seven layers thick (fig 9) However the ratio of non-basal to basal cells was not 5 1 or 6 1 but about 2.3 1 The estimate of the production of 1 4 cells per basal cell by 36 hours after the administration of estrogen may be somewhat low since some superficial cells have been exfoliated within that time However cell loss through exfoliation is not a major factor until cells become cornified and are sloughed off in great amounts. This occurs later than 36 hours after the administration of estrogen. Hence about 1 4 cells per basal cell at least, have been produced by 36 hours after the administration of estrogen This seems a reasonable estimate when correlated with labeling indices which imply that all or most of the basal cells have

divided once and some of these have divided twice within 36 hours following the administration of estrogen.

Jensen ('60) reported that there is *maximum radioactivity* in the uterus and vagina of the rat at the same time after the administration of estrogen. This suggests that any differences in the time of *initiation of DNA synthesis* between the uterus and vagina is not because the estrogen reaches these two organs at different times, but is the results of differences in *response of the uterus and vagina.* Walker ('60) stated that sufficient DNA synthesis occurs just before proestrus in the uterine epithelium to provide complete renewal, and this DNA synthesis occurs earlier in the uterus than the vagina. This statement rests largely on the labeling in only one animal injected during late diestrus. The results of the present investigation show that the conclusion that DNA synthesis always occurs in the uterine epithelium before the vaginal epithelium is not generally valid.

The present investigation has shown that in the vaginal and uterine epithelium, following the administration of estrogen, the increased rate of DNA synthesis precedes *the increased rate of mitosis. This* is the same sequence as in the liver after partial hepatectomy (Holmes and Mee '55) There is no evidence that estrogen stimulates mitosis directly

The low labeling index in the vaginal and uterine epithelium during the first 6–12 hours after the administration of estrogen shows that the effect of estrogen to stimulate DNA synthesis is not immediate. There is evidence that estrogen is present in the vagina and uterus as soon as one hour after the administration of estrogen Jensen ('60) *found that there* was maximum radioactivity in the vagina and uterus of the rat one to two hours after the injection of tritiated estradiol.

One is, therefore confronted with the problem of what the action of estrogen is between the time it reaches the genital tissue (probably one hour after the administration of estrogen) and the time DNA synthesis is initiated in the epithelium of the uterus and vagina. To resolve this problem, possibly one should study what the action of estrogen is on the enzymes concerned with DNA synthesis This is suggested in the light of the study of regenerating liver which showed striking increases in DNA polymerase and thymidine kinase coincident with the initiation of DNA synthesis (Bollum and Potter '59) It could be important to determine if estrogen is a factor which controls the emergence of enzymes involved in the synthesis of DNA.

SUMMARY AND CONCLUSIONS

Proliferation in the epithelia of the uterus and vagina of the castrate mouse following a single injection of estradiol benzoate was studied by pulse labeling with tritiated thymidine and autoradiography Following a latent period of 12 hours after the administration of estrogen, the vaginal epithelial cells start synthesizing DNA over a few hours and then undergo *mitosis for a first* time. Some of these same cells enter DNA synthesis and undergo mitosis for a second time. The cell production in the vaginal epithelium by 36 hours after the administration of estrogen is about 1 4 cells per basal cell The increased rate of DNA synthesis is followed by an increased rate of mitosis in the epithelium of both the uterus and vagina. There is no evidence *that mitosis* is directly stimulated by estrogen. The mechanism of the proliferative action of estrogen is discussed.

ACKNOWLEDGMENT

I wish to thank Dr H Quastler for his advice and continued interest during the experimental work and preparation of the manuscript.

LITERATURE CITED

Allen, E G. M. Smith and W V Gardner 1937 *Accentuation of the growth effect of theelin* on genital tissues. Am. J Anat., 61 321–341.

Biggers J D and P J Claringbold 1955 Mitotic activity in the vaginal epithelium of the mouse following local oestrogenic stimulation. J Anat., 89: 124–130.

Bollum, F S., and V R. *Potter* 1959 Nucleic acid metabolism in regenerating rat liver VI. Soluble enzymes which converts thymidine to thymidine phosphate and DNA. Cancer Research, 19 561–565.

Gelfant, S. 1961 Initiation of mitosis in relation to the cell division cycle. Exptl. Cell Research (in press)

Holmes, B. E., and L. K. Mee 1955 Radiobiology Symposium. *Ed.* by Z. M. Bacq and

P Alexander Butterworths Scientific Publications, London, 220–234.

Hughes, W L., V P Bond, G Brecher E. P Cronkite, R. B. Painter H. Quastler and F G. Sherman 1958 Cellular proliferation in the mouse as revealed by autoradiography with tritiated thymidine. Proc. Natl. Acad. Sci., 44 476–483.

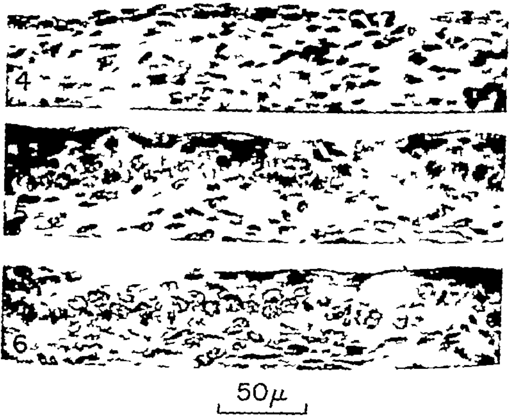
Jensen, E. V 1960 Fate of steroid estrogens in target tissues. Advanced abstracts of First International Congress of Endocrinology Copenhagen, Abstract no. 368

Peckham, B 1961 Cellular behavior in the *vaginal epithelium of estrogen-treated rats.* (In press.)

Quastler H 1961 Effects of irradiation on *synthesis and loss of DNA.* (In press.)

Tice L. W 1961 Some effects of estrogen on uterine epithelial mitosis in the mouse. Anat. Rec., *139* 515–522.

Walker B E. 1960 Renewal of cell populations in the female mouse. Am. J Anat., *107* 95–105.

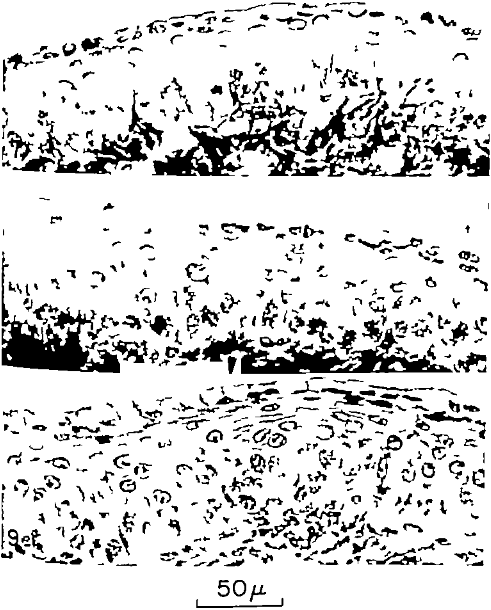


Autoradiographs of vaginal epithelium

4 From an animal injected with tritiated thymidine six hours after estradiol injection. The epithelium is two layers thick. Few cells are labeled (none in the portion shown). × 500

5 From an animal injected with tritiated thymidine 12 hours after estradiol injection. Label is present in many cells of the basal layer of the epithelium. The epithelium is two to three layers thick. × 500.

6 From an animal injected with tritiated thymidine 18 hours after estradiol injection. Over half of the cells in the basal layer show label. The epithelium is three layers thick. × 500

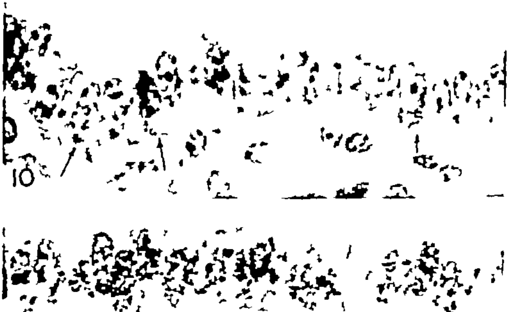


Aut adiographs of vaginal epithelium.

7 From an animal jected with tritiated thymidine 24 hours after estradiol injection. The number of labeled cell in the basal layer are fewer than t 18 hours compare with figure 6. The ep thel um is four fiv layers hick × 500.

8 From an animal injec ed with tritia ed thymidine 30 hours fter estradiol i jection. Over half of the cell in the basal layer show label The ep helium is fi to si layers thick. 500

9 From an animal injected with tritiated thymidine 36 hours ft estradiol injection. The number of cells in the basal layer showing label is les han 30 hours compare with figure 8 The epithelium is six t seven la ers h 00



Autoradiograph of uterine epithelium.

10 From an animal injected with tritiated thymidine 12 hours after estradiol injection. Three cells show label (arrows). Small dark dots are tritium grain; larger dots are nuclear elements which have taken up stain. × 1,250.

11 From an animal injected with tritiated thymidine 18 hours after estradiol injection. Most of the epithelial [illegible] show label. × 1,250.

12 From an animal injected with tritiated thymidine 36 hours after estradiol injection. A large number of the epithelial cells show label. Two mitotic figures [illegible] present. × 1,250.

Teratogenic Effects of Tolbutamide on the Early Development of the Fish *Oryzias latipes*[1]

MORRIS SMITHBERG[2]
Department of Anatomy University of Florida, College of Medicine Gainesville Florida

The developing fish embryo has proved to be very sensitive to environmental change. Malformations have been produced under the influence of both physical and chemical agents, including low temperature (Lereboullet, 1864; Loeb '15; Stockard, '21; Briggs and Wilson, '59) ultraviolet radiations (Hinrichs, '25); X irradiation (Solberg, '38a) and changes in the ionic content and strength of the medium (Loeb, 1893; Stockard, '06) An azo dye trypan blue has been reported to be teratogenic in the developing Zebra fish (Battle and Laale, '60) but was ineffective in embryos of the Medaka (Oryzias latipes) (Briggs and Wilson '59) Abnormalities in embryos of Fundulus (Oppenheimer '50) and in Oryzias (Waterman, '39; Ishida, '51) have also been reported after exposure to various drugs.

The present studies involved the effects of an antidiabetic drug, tolbutamide (sodium), on the development of the Medaka fish. The embryos of this fresh water fish were chosen not only for their ease of recovery but also because of the considerable quantity of morphological and physiological data that have been accumulated (for bibliographic review see Briggs and Egami, '59)

The main purpose of the present experiments was to determine what relationships exist among stage of development concentration of the agent and length of exposure of the embryo to the drug To this end, Medaka embryos in various developmental stages were exposed to several concentrations of tolbutamide for varying lengths of time Altogether there were four stages of embryos four concentrations of the drug, and four lengths of exposure.

Two other series of experiments were performed. 1 Attempts were made to reverse the effects of the drug by the addition of glucose to the experimental medium. 2 Preliminary studies were made to test the permeability of the developing normal and drug-treated embryo to radioactive sodium.

MATERIALS AND METHODS

Medaka fish were obtained commercially and maintained by conventional methods (c.f. Rugh, 48) in aquaria containing aerated tap water at room temperature. Lighting conditions were controlled with an automatic timing device. Each morning clusters of fertilized eggs were removed from the anal fins of several females and placed in glass vessels containing either sterile distilled water or a recommended salt solution (Rugh 48) Phosphate buffer was added to the salt solution to maintain a pH of about 7 6–7.8.

The embryos were separated from their clusters and randomly mixed. After being washed several times, the embryos were placed in salt solutions containing tolbutamide in four concentrations 0.25, 0.50 0 75 or 1 0% Embryos in four stages of development were selected for treatment: 2–4 cell stage 8–16 cell stage blastulae, and embryos 24 hours old (optical vesicle stage) Embryos were treated for one two three or four days and at the end of treatment they were transferred to a buffered medium. Several changes of fresh fluid were made until the untreated embryos serving as experimental controls hatched Control solutions contained salts of approximately equivalent ionic strengths as those used in the experimental

[1] This investigation was supported by research grant (RG-611) from the National Institutes of Health, Public Health Service U. S. Department of Health, Education and Welfare.

[2] Present address Department of Anatomy University of Minnesota, Minneapolis, Minnesota.

series. Hatching usually occurred between 12 and 20 days after egg laying. No less than 3 cm of fluid per embryo was maintained in all dishes. Observations for malformations were made before during, and after treatment.

Both treated and untreated embryos were fixed in Bouin's or Stockard's medium and after the usual preparation procedures were examined histologically It was advantageous to cut away the chorion of unhatched embryos after fixation.

For statistical analysis the embryos were classified according to whether they had developed normally or abnormally or had died. The final analysis was based on the percentage of abnormalities observed in embryos surviving until the end of the experiment.

Glucose studies

The effects of the addition of glucose to the solution containing the drug tested. Glucose in concentrations of 0.25 0.50 or 1.0% was added to similar concentrations of tolbutamide in a factorial experiment. This series of experiments was performed on embryos in the blastula stage treated for three days. Embryos in glucose solutions without drug served as control animals

Experiments with radioactive sodium. The turnover of Na^{24} was tested in fish embryos with or without the addition of 1 0% tolbutamide. The experimental group of embryos were placed in 1% tolbutamide plus the isotope while control embryos were exposed to the medium containing only the istope ten embryos per group were used. After a period of two to four days, the embryos were washed quickly in several changes of distilled water in order to remove excess isotope radioactivity was then counted in a deep well counter Counts were taken initially at 15-minute intervals between countings, the embryos were returned to vessels containing large volumes of distilled water Further counts were ascertained at convenient intervals until the background radiation level was reached

RESULTS

Observations Perhaps the most remarkable finding of these experiments was that every abnormal embryo showed stasis or absence of extra- and intraembryonic circulations, and an associated heart defect. The "hearts" of many of these abnormal embryos were little more than pulsating threads of tissue (fig. 1B) Yet in spite of circulatory failure differentiation of the other tissues ensued, i.e., the neural system, somites, notochord, etc., were apparently well differentiated. Development was not suspended during the exposure of the embryos to the drug.

Approximately 50% of the abnormal embryos, in addition to having vascular malformations also showed abnormal eyes (figs 1B, C) and abnormal body curvature. The eye malformations were confined mainly to the derivatives of the eye cup (retina and iris) Degeneration of the eye cup followed after the circulation was disrupted. The lens was always present even after the remainder of the eye had degenerated (fig. 1B) The malformed embryos also showed abnormal curvatures of the trunk and tail (fig. 1C) Embryos with circulatory failure did not hatch except in rare instances and eventually died whether or not they were mechanically removed from their chorions. Less than 1 of the untreated control animals were abnormal. In general, more of the 2-4 cell stage embryos succumbed to the treatment than any of the other embryos treated. Drug concentrations of less than 0.25% produced no significant increase in abnormalities, while concentrations of 2.0% were lethal.

Statistical analysis Basically this is a three factor experiment with four levels of each of the factors. Altogether there were a total of 84 tabular cells within the analysis tables. The number of embryos in each of the treatment cells ranged from 35 to 100 with 86 % of the cell (65 of 84) containing 35 to 50 embryos each. A total of 3 621 embryos was used in the experiment.

Figure 2 shows the percentage of abnormal embryos for each of the three factors of the experiment, developmental stage concentration of the drug, and duration of exposure. It is apparent that the earlier in development the embryo is exposed to

The author gratefully acknowledges the aid of Dr. Robert G. Hoffmann of the College of Medicine, University of Florida for his aid in the statistical analysis of the data.

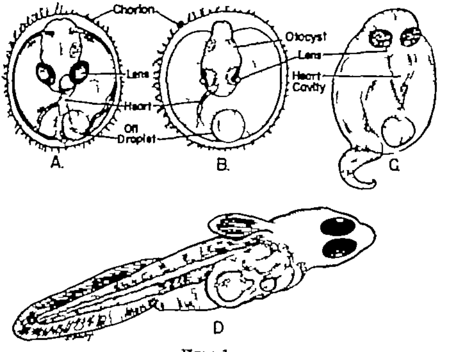


Figure 1

A. Semidiagrammatic representation of an unhatched normal early Medaka embryo showing characteristic features.
B. Medaka embryo of same age as 1A showing absence of extra-embryonic circulation and completely degenerated derivatives of the eye cup; the lens is externalized. The heart is reduced to pulsating thread of tissue.
C. Abnormal Medaka embryo with chorion removed. Eye abnormality is less severe than in IB. Heart cavity is outlined and trunk and tail are abnormally curved.
D. Normal embryo recently hatched of the same age as embryos depicted in IB and 1C. Note small size of yolk sac as compared to abnormal embryos.

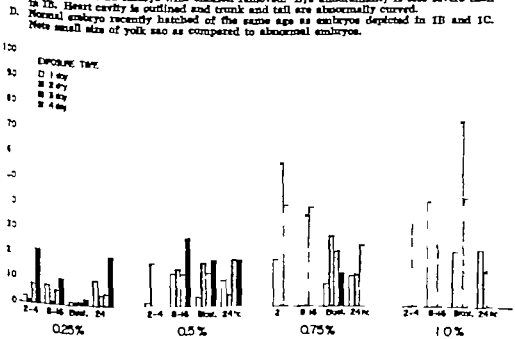


Figure 2

the drug, the greater is the likelihood that it will be abnormal. For example treatment of the 2–4 8–16 blastula and 24-hour embryos resulted in 36 30 21 and 19% abnormalities respectively These values may be obtained by averaging over the other two factors of concentration and exposure time. By employing similar calculations a drug concentration of 1% produced 51% malformations while a concentration of 0.25% resulted in only 6% abnormalities Intervening stages showed intermediate frequencies. The same general result was obtained with regard to duration of exposure. Treatments for 4 3 2, and 1 day(s) produced 40 32 18 and 6% malformations respectively The longer the developing embryos are exposed to the drug the greater is the likelihood that they will be malformed

Figure 3 shows the relationship between drug concentration and the percentage of abnormal embryos for each of the developmental stages. The straight lines for each of the age groups have been fitted by the usual least-squares statistical method. The similarity of the slopes of the lines for the three youngest developmental stages is remarkable For the 24-hour stage how ever the slope differs considerably and its point of interception of the concentration axis is also quite different. Thus the exposure of 24-hour embryos to low concentrations of tolbutamide produced an unusually high proportion of abnormal embryos. This may be due to chance. Had this not occurred, the line for the 24-hour embryos still would have sloped much less than the other three lines though its departure from the other three would not have been as great. The main point is that the percentage of abnormal embryos observed increases at about the same rate from one concentration to the next. This increasing percentage is almost identical for stages 2–4 and 8–16. It is only slightly less for the blastula stage. The 24-hour stage may or may not be exceptional (see discussion)

A similar plot of the data was made which related the percentage of abnormal embryos for each of the drug concentrations against the days of exposure. There were no differences between days two and three but there were large differences at each concentration between days one and four For example a drug concentration increase from 0 50 to 0 75% produced about the same percentage increase with

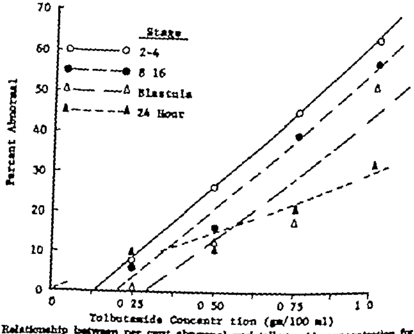


Fig. 3 Relationship between per cent abnormal and tolbutamide concentration for four developmental stages.

each developmental stage group. A possible exception to this may be the 24-hour stage group. In summary we may say that developmental stage, drug concentration, and exposure time operate relatively independently of one another

Tests of statistical significance of these data were handled in the following fashion. As a preliminary analysis an ordinary three-factor analysis of variance was done using as the error term the three-factor interaction. With this analysis all of the main effects — that is, the factors of stage time and concentration — were statistically significant at far less than the 1% level. One of the interactions was significant the one for stage and drug concentration. This, however was barely statistically significant at the 5% level. As can be seen from figure 3 this was no doubt due to the slightly different behavior of the 24-hour stage in comparison with the other stages.

Studies with glucose The effects of glucose alone and the effects of glucose added to the medium with drug were tested. It was reasoned that the addition of glucose might (1) reverse the action of the drug (2) produce a more radical anomaly but not change the proportion of anomalous embryos, (3) produce a larger percentage of anomalies or (4) have no effect at all. The results of these experiments are shown in table 1

TABLE 1

The effects of the addition of glucose and tolbutamide on production of malformations. Summary of data in which embryo of stages previously used were treated for three days

Glucose (%)	1.0		0.5		0.25	
Tolbutamide (%)	N	No. abnormal	N	No. abnormal	N	No. abnormal
1.0–0.5	43	43	30	30[a]	31	31
0.25	14	2[b]	10	0	13	1
0.0	62	0	48	0	34	0

All embryos showed both defective circulation and defective eyes.
One embryo showed both defects, the other only vascular defect.
Showed only vascular defect.

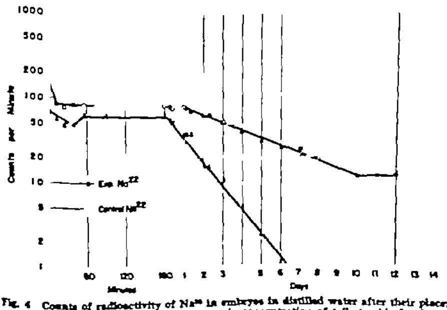


Fig. 4 Counts of radioactivity of Na²² in embryos in distilled water after their placement in medium containing N ²² and teratogenic concentration of tolbutamide for four days. Control embryos were placed in solutions containing N ²² without drug.

The embryos in which glucose alone was added to the solution showed no abnormalities. On the other hand, 100% of the embryos grown in media containing both glucose and the drug showed abnormalities when the concentration of tolbutamide used was greater than 0.25%. All of the malformed embryos showed cardiovascular defects, eye defects and abnormal body curvature.

Isotope studies. In order to study any permeability changes resulting from the action of the drug, embryos were placed in a salt solution containing Na^{24} to which a teratogenic concentration of the drug was added. Embryos placed in salt solution containing Na^{24} without drug served as controls. The results of these experiments are shown in figure 4.

The curves obtained by both groups of animals following their placement in distilled water showed three distinct phases. There was an initial steep drop in both the experimental and control groups with the experimental curve somewhat steeper. Both groups of embryos then paralleled each other in a gradual phase in which the turnover of Na^{24} slowed considerably. Fl[illegible] the turnover of Na^{24} was again more [illegible]id in the experimental group with counts reaching the background level 6 days earlier than the controls.

DISCUSSION

The sodium salt of tolbutamide in the range of dosages tested produced a high percentage of malformations in the early embryonic stages of the Medaka. The malformations invariably consisted of a drastically interrupted extra- and intraembryonic circulation, associated heart anomalies, and abnormal body curvature. The rudimentary hearts of most of the anomalous embryos continued to pulsate but no blood was observed to pass into or out of the heart. The embryo in effect was heartless, a situation which may have resulted in the coincidental finding of defective eyes. Under the influence of the drug alone about 50% of the malformed embryos, especially those exhibiting the greatest degree of heart involvement, showed coincident eye malformation. When glucose was added to the medium also containing the drug, all the embryos showed cardiovascular involvement and all showed eye defects provided the concentration of drug used was greater than 0.25%. The probability that the eye anomalies are secondary to the circulatory failure gains support from experiments with heartless amphibian embryos (Knower, '07; Kemp, '53). Kemp ('53) has suggested that many anomalies resulting from various teratogenic agents may be secondary to circulatory failure. In the present experiments and those with heartless amphibian embryos, differentiation of many other organs continued regardless of the vascular failure.

The curvature of the trunk and tail of some of the abnormal embryos may have been mechanically produced, that is, the result of the confinement of the enlarging embryo within the narrow limits of the rigid chorion. This compartment is less confining in normal development due to the diminishing size of the yolk sac as it is absorbed into the body of the embryo. Marked retardation of the absorption of the yolk sac was characteristic of abnormal embryos (fig. 1C). However, this argument is weakened by the fact that not all embryos which are otherwise abnormal and which have large yolk sacs have abnormal body curvature. It is still possible that abnormal trunk and tail curvature occurred because of other reasons.

It seems evident that the primary site of action of the drug is on the circulatory system of the Medaka embryo. Similar defects have been produced in this species by 2,4-dinitrophenol (Waterman, '39; Ishida, '51). The circulatory system responded similarly in Fundulus following treatment with various organic solvents (Stockard, '15).

Statistical analysis of the experimental data summarized in figure 2 showed that the three factors, namely developmental stage, concentration of the drug, and length of exposure to the drug, all played independent roles in the production of the defects. In short, it may be stated that the *earlier* the stage treated, the *higher* the concentration used, and the *longer* the treatment period, the *greater* is the likelihood of producing a defective embryo.

The question arises as to the most critically susceptible period in the developing

system. The species used in the experiments did not lend itself to a study aimed at sharp discrimination of susceptibility among the earlier stages treated owing to the rapid development from the fertilized egg to the blastula stage. For example no clear differential susceptibility could be discerned between the 8–16 cell stage and the blastula stage (fig. 3) However it is evident that a clear difference existed between the 2–4 cell stage and the 24 hour stage. The 2–4 cell stage embryo succumbed in greatest numbers in the higher concentrations of drug irrespective of length of treatment. It seems clear then that the earliest stages are the most susceptible to environmental change.

On plotting figure 3 we noted that the 24-hour embryo did not respond in a similar fashion as did the other stages used, as indicated by the slopes of the lines obtained. It is tempting to dismiss this difference as biological variability however it is quite possible that this stage of development, characterized by near completion of gastrulation, represents a crucial period in the developing system This period is marked by important changes in the fish embryo. For example higher doses of irradiation were required to induce anomalous embryos at this stage of development as compared to earlier stages (Solberg, '38b) Ishida, ('51) found that 2 4-dinitrophenol had little effect at this time and the early embryo appeared to be impermeable to heavy water until overgrowth of the yolk sac was completed (Krogh and Ussing, '37) Hishida and Nankano ('50) showed that the respiratory quotient changes at the time of gastrulation in Medaka. In light of this evidence, the erratic response of the 24-hour stage embryo to the drug may be partially explained.

Mode of action of the teratogen. One hypothesis to explain the action of the drug would presume a change in permeability of the plasma membrane. Information concerning the properties of the various membranes surrounding the fish embryo stems from physiological studies on various fish embryos (for review see Smith '57). It has been revealed that the outer chorion presented a little more than a physical barrier (Svetlov '29 Gray '32; Shanklin '59) and that the plasma membrane was relatively impermeable to most substances (Gray '32) Vital dyes, al though freely permeable to the outer chorion, did not penetrate the inner cellular membrane (Hayes, '30 Adler '32) The permeability of the egg membrane to water is diminished shortly after fertilization (Manery and Irving, '35) and also to heavy water (Krogh and Ussing, '37) Embryos seemed to be permeable to high concentrations of potassium, as evidenced by retardation of the heart beat of Medaka embryos (Ikeda, '34 '37) Malformations have also been produced by exposure to high concentrations of potassium (Loeb 1893) High concentrations of sodium have been reported to accelerate the development of the Medaka embryo (Ikeda, '37) Shanklin ('56 '59) using radioactive sodium and other salts in permeability studies on Fundulus has shown that various cations pass in and out of the cells under the apparent control of glycolytic mechanisms.

Changes in permeability are also implicated in the present study by the following observations (1) the percentage and severity of the abnormalities induced by tolbutamide alone were strikingly increased by the addition of glucose to the medium while glucose alone was not teratogenic. (2) Pilot experiments with Na[22] in the medium showed a different turnover pattern when the drug was added to the medium (fig. 6)

Stockard ('10 '21) was able to produce cyclopia and cardiovascular abnormalities in embryos of Fundulus by the action of diversified agents, including chloroform, acetone, ether and alcohol. He advanced the notion that there was no specificity in the effect of the diverse agents and that the stage of development affected was the underlying factor In addition he proposed that suspended development also plays an important role in teratogenesis of fish. The anomalies produced by tolbutamide strikingly resemble those produced in Stockard's experiments however no suspension of development was noted in the treated embryos. The present experiments implicate not only the developmental stage but also the concentrations used and the length of treatment. It is believed by the present

author that the action of the drug effects a change in permeability of the plasma membrane which in turn upsets the internal environment, resulting in abnormal development. The organic solvents may have also induced permeability changes in Fundulus, perhaps by the dissolution of the lipid components of the cellular membrane

An alternate hypothesis would propose that the drug entered the cell and acted as a poison or metabolic inhibitor Although the importance of the indirect effect of surface phenomena has been emphasized above direct action of the drug has not been excluded. Further experimentation is in progress which may decide which of these hypothesis is more realistic.

SUMMARY

1 Tolbutamide (sodium) when introduced into the medium of the developing Medaka fish caused various consistent abnormalities. The abnormalities produced were (1) absence of extra- and intraembryonic circulation with associated heart anomalies (2) degeneration of eye cup derivative and (3) abnormal curvature the trunk and tail.

2. The experiment was designed to determine whether any interrelationships exist among three factors: stage of development, concentration of the drug and length of exposure of the embryo to the drug Four stages of embryos were treated ranging from the 2-cell stage to the 24-hour stage. Four concentrations of the drug (0 25 to 1 0%) and 4 exposure periods (one to four days) were used

3 It was established that each of the three factors asserted its effect independently the earlier the stage treated, the higher the concentration used, and the longer the treatment period the greater is the likelihood of defect. No suspension of development during treatment was observed

4 The mode of teratogenic action of the drug is discussed in light of altered permeability of the cellular membrane

LITERATURE CITED

Adler P 1932 Versuche über Vitalfarbung am Forellen-Ei. Protoplasma 15 15–23

B ttle H. L, and H. W Lasle 1960 Trypan blue-induced anomalies in embryos of the zebrafish (Brachydanio rerio) Anat. Rec. 138 333.

Briggs, J C., and N Egami 1959 The Medaka (Oryzias latipes) A commentary and a bibliography J Fish. Res. Bd. Canada, 16 363–380.

Briggs J C., and J G. Wilson 1959 Comparison of the teratogenic effects of trypan blue and low temperature in the Medaka fish (Oryzias latipes) Quart. J Fla. Acad. Sci 22 64–68.

Gray J 1932 The osmotic properties of the eggs of the trout (Salmo fario) J. Exp. Biol 9 277–299

Hayes, F R. 1930 The metabolism of developing salmon eggs. I. The significance of hatching and the role of water development. Biochem. J 24 723–734.

Hinrichs M. A. 1925 Modification of development on the basis of differential susceptibility to radiation. I. Fundulus heteroclitus and ultraviolet radiation. J Morph. and Physiol., 41 239–265.

Hishida, T and E. Nankano 1954 Respiratory metabolism during fish development. Embryologia, 2: 67–79

Ikeda, Y 1934 Permeability of the egg membrane of Oryzias latipes. Fac. Sci. Tokyo Imp. Univ 3 499–504.

——— 1937 Effect of sodium and potassium salts on the rate of development in Oryzias latipes. Ibid., 4 307–312.

Ishida, J 1951 Effects of 2,4-dinitrophenol on oxygen consumption during early development of the teleost, Oryzias latipes. Annot. Zool. Japon., 24 181–186.

Kemp N E. 1953 Morphogenesis and metabolism of amphibian larvae after excision of heart. I. Morphogenesis of heartless tadpoles of Rana pipiens. Anat. Rec., 117 405–425.

Knower, H. McE. 1907 Effects of early removal of the heart and arrest of the circulation on the development of frog embryos. Ibid 1 161–165.

Krogh, A., and H. H. Ussing 1937 A note on the permeability of trout eggs to D_2O and H_2O J Exp. Biol., 14 35–37

Lereboullet, M. 1864 Recerches sur les monstruosités d Brochet observées dans l'oeuf et sur leur mode de production. Résumé des expériences précédentes. Ann. Sci. Nat. (Zool. et Paleo.) Ser 5, 1 257–320.

Loeb J 1893 Über die Entwicklung von Fisch embryonen ohne Kreislauf. Pflüg. Arch., 54 525–531

——— 1915 The blindness of the cave fauna and the artificial production of blind fish embryos by heterogeneous hybridization and by low temperatures. Biol. Bull., 29 50–67

Manery J F and L. Irving 1935 Water changes in trout eggs at the time of laying J Cell. and Comp. Physiol., 5 457–464.

Oppenheimer J 1950 The development of Fundulus heteroclitus embryos in solutions of metrazol J Exp. Zool., 113 65–86.

R gh, R. 1948 Experimental Embryology Burgess. Minneapolis.

Shanklin, D R. 1956 Factors influencing the transport of sea water across the ectoderm of Fundulus heteroclitus N ture 177 431–432.

——— 1959 Studies on the Fundulus chorion. J Cell. and Comp. Physiol., 53 1 12.

Smith, S. 1957 Early development and hatching. The Physiology of Fishes, 1: 323–359. Chap. 7 Brown, ed. Academic Press, N. Y.

Solberg, A. 1938a The susceptibility of the germ cells of Oryzias latipes to X-radiation and recovery after treatment. J. Exp. Zool., 78: 417–440.

——— 1938b The susceptibility of Fundulus heteroclitus embryos to X-radiation. Ibid., 78: 441–465.

Stockard, C. R. 1906 The development of Fundulus heteroclitus in solutions of lithium chlorid, with appendix on its development in fresh water. Ibid., 3: 99–120.

——— 1910 The influence of alcohol and other anaesthetics on embryonic development. Am. J. Anat., 10: 369–392.

——— 1915 Experimental blood and vascular endothelium in embryos without circulation of the blood and in the normal embryo. Ibid., 18: 227–327.

——— 1921 Developmental rate and structural expression: an experimental study of twins, double monsters, and single deformities, and the interaction among embryonic organs during their origin and development. Ibid., 28: 115–277.

Svetlov, P. 1929 Entwicklungsphysiologische Beobachtungen an Forelleneiern. Roux. Arch., 114: 771–785.

Waterman, A. J. 1939 Effects of 2,4-dinitrophenol on the early development of the teleost, Oryzias latipes. Biol. Bull., 76: 162–170.

Histo-Physiological Analysis of the Preganglionic Connections of the Superior Cervical Sympathetic Ganglion

JAMES L. HALL [1,2]
Department of Anatomy Ohio State University Columbus Ohio

Branches of the cervical sympathetic ganglia innervate many important structures in the head and neck. They supply sympathetic innervation to the blood vessels, the smooth muscles of the eye, the arrector pili muscles and to salivary and other glandular structures. They control the blood supply of the thyroid gland and thus indirectly regulate its hormonal secretion (Billingsley and Ranson, '18a) Cervical sympathetic filaments also supply the carotid glomus. Knowledge concerning the factors regulating the activity of these ganglia is obviously important.

Richins and Hall ('58) demonstrated that electrical stimulation of the cervical sympathetic trunk affects metabolic activity in cervical sympathetic ganglia. At the present time however the relationships of the segments of the spinal cord to the preganglionic fibers passing into the cervical sympathetic ganglia are not well understood. The purpose of this study is to further investigate the segmental origins of these components.

The cervical symapthetic ganglia have been studied by the use of the gallocyanin method (Einarson, '32) and the toluidine blue procedure as employed by Richins and Hall ('58) The two methods were used for checking each other The tissues were observed for indications of metabolic activity within the cervical sympathetic ganglia before and after selective stimulation of nerve roots attached to surgically isolated spinal cord segments.

REVIEW OF LITERATURE

An analysis of the preganglionic nerve fibers passing to the superior cervical ganglia of the cat was made by Billingsley and Ranson ('18b) Using the Marchi technique for degenerated nerve fibers they counted a total of 3 851 myelinated preganglionic fibers in the cervical sympathetic trunk. One-hundred-twenty-three thousand, six hundred and three neurons were counted in the superior cervical ganglion. This indicated a ratio of one preganglionic fiber for every 32 neurones. They concluded that the preganglionic fibers originate from the first to seventh thoracic segments of the spinal cord The first thoracic segment gave origin to the greatest number of fibers and fewest came from the seventh segment. There seemed to be a decreasing progression from upper to lower thoracic segments. Billingsley and Ranson ('18a) also made an exhaustive study of the branches of the superior cervical ganglion. These course along the external and internal carotid plexuses and supply sympathetic innervation to many structures in the cranial region.

Foley and Schnitzlein ('57) using degenerative estimation techniques, found some preganglionic fibers in the upper cervical sympathetic trunks after sectioning dorsal and ventral roots of thoracic nerves one to eight. They reported the most prominent changes after sectioning roots T 1 through T-5 with T-5 contributing either the most fibers or a large portion of the total fibers. T-6 through T-8 according to their findings contributed approximately less than 7% to the total number of fibers. These authors point out, however that T-5 does not always contribute a significantly greater number of fibers than do the roots of T 2 T-3, T-4

The results of electrical stimulation of preganglionic nerve fibers were reported

[1] Supported by U.S.P.H.S. Predoctoral Fellowship PF-4347

[2] Dissertation presented to the faculty of the Graduate School of St. Louis University in partial fulfillment of the requirements for the degree of Doctor of Philosophy

by Langley (1892) He noted dilation of the pupil of the cat's eye in response to stimulation of the first to third thoracic spinal nerves He failed to elicit this response when stimulating the eighth cervical or fourth thoracic nerve and concluded that the preganglionic outflow from the first three thoracic segments of the spinal cord is mainly concerned with the mechanism of the eye.

The results of stimulation of nerve cells have been reported by various authors Hodge (1888 1889 1892, 1894) noted an increase in the size of the nucleus an irregular shape and darker staining capacities after electrical stimulation. He also reported shrinkage of the cytoplasm and a lessened power to reduce osmic acid. Vas (1892) and Lambert (1893) observed enlargement of the cells and peripheral displacement of chromidial substance following brief electrical stimulation. Mann (1894) Nissl (1898) and Pick (1898) saw changes in cellular size and distribution of chromatin. Spitzka and Radasch ('12) noted production of lesions particularly along blood vessels in the brain after electrocution. Kocher ('16), however could no structural differences between normal and fatigued nerve cells.

More recently Heinbecker and O'Leary ('30) have shown that prolonged stimulation of autonomic ganglion cells results in granulation of the nuclear chromatin and clumping about the nucleolus. Ingersoll ('34) saw a decrease in the size of the celiac ganglion cells and nuclei. Winkelman and Moore ('44) observed no morphological changes in the cerebrum of the cat following electric shock treatment, but Ferraro Roizin and Helfand ('46) saw some vacuolization and pyknosis of nerve cells in the monkey brain. These seemed to be related to circulatory disturbances.

While Penfield ('20) had observed no changes in the Golgi apparatus following variations in nerve cell activity Kuntz and Sulkin ('47) and Sulkin and Kuntz ('48) used prolonged faradic stimulation to induce a breakdown of the Golgi network in the autonomic ganglion cells of cats. They also reported hyperplasia of interstitial tissue and capsule cells.

Einarson ('32, '33 '51) and Einarson and Krogh ('55) utilized gallocyanin-chrome alum staining for estimation of basophilia in nerve cells. They found that ganglion cells of *Aplysia*, a mollusc, almost emptied of cytoplasmic basophilic substance following electrical stimulation. It was suggested that the chromophobe cells are in a state of excitation and the chromophil cells in a state of inhibition. Hartelius ('52) also employed gallocyanin-chrome alum staining for study of the cerebral nerve cells of cats following electrically induced convulsions. The decrease in basophilia was not so striking as that reported in *Aplysia* but it was considsignificant. Liu, Baily and Windle ('50) using the buffered thionin technique did not observe changes in the chromidial pattern of the nerve cells of the spinal cord or spinal ganglia after electrical stimulation and they stressed the importance precautions against post mortem and fixation artifacts. Prolonged antidromic stimulation with 20 volts or more did cause some changes in the cat's hypoglossal nucleus. Hamaty and Truex ('54) saw a decrease of chromatin in the ganglion of the SA and AV areas of the adult dog's heart following vagal stimulation. Richins and Hall ('58) reported altered toluidine blue staining reactions in the superior cervical ganglion following trans-synaptic stimulation.

Changes in the appearance of neurons can thus be demonstrated following electrical stimulation. Using such stimulation and the gallocyanin-chrome alum (Einarson, '32) and the toluidine blue (Richins and Hall, '58) staining techniques the author has studied the segmental origins from the spinal cord of the preganglionic sympathetic nerve fibers which synapse in the cervical sympathetic ganglia.

MATERIALS AND METHODS

Twenty-nine healthy adult cats were used as experimental animals. Sodium Nembutal anesthesia was administered intraperitoneally (3 mg per kg of body weight) In each animal the adrenal glands were ligated bilaterally to minimize the effects of adrenalin. The incisions were sutured and covered with toweling soaked in physiological saline solution.

In ten of the animals a midline incision was made in the neck, and the left vago

sympathetic trunk was exposed. The trunk was separated from the common carotid artery and severed caudal to the superior cervical and nodose ganglia. The distal end of the severed trunk was stimulated with an Electrodyne stimulator at ten volts and a frequency of 20 per second for a period of three hours. After stimulation the superior cervical sympathetic and nodose ganglia were removed together and treated identically throughout the preparation of the tissue sections. Experimental and control sections were mounted on the same slide for staining.

In some experiments drugs known to act on the autonomic system were injected intravenously previous to stimulation. Ergotamine ethanesulphonate (0.5 mg per kg of body weight) was employed to depress the adrenergic components. Atropine sulphate (0.5 mg per kg of body) was used for paralysis of cholinergic post ganglionic components and hexamethonium bromide (1 mg per kg of body weight) was injected to block the ganglionic synapses.

In 18 animals the spinal cord was exposed and completely transected cranial and caudal to the spinal nerve roots of the selected cervical or thoracic segment. The spinal nerve roots on one side were severed but left intact on the opposite side. The ventral root of the intact side was stimulated with an electrodyne stimulator at ten volts and a frequency of 20 per second for a period of three hours. This procedure was followed isolating individually the eighth cervical to the eighth thoracic segments of the spinal cord inclusive.

The cervical sympathetic ganglia and the adjacent nodose ganglion were removed from the stimulated and control sides. They were identically fixed and sectioned and mounted together on the same slides for staining.

The toluidine blue method as employed by Richins and Hall ('58) and the gallocyanin-chrome alum method of Einarson ('32) were used in this investigation. The toluidine blue method for chromaffin tissue was developed by Wiesel ('02) and modified by Hess and Hollander ('47) and Pearse ('53). It was used to demonstrate metachromasia and was employed for study of glandular tissue by Kramer and Windrum ('55). They observed no differences in staining reactions after fixation in 10% formalin and after 4% lead acetate in 10% formalin. It is significant that Tandler ('58) considered the lead acetate reaction specific for phosphate groups and that Landsmeer and Giel ('56) considered post-chromation necessary for successful staining of phosphates for Richins and Hall ('58) found lead subacetate fixation and post-chromation necessary for successful demonstration of their toluidine blue reaction.

The gallocyanin-chrome alum method demonstrates basophilia (Einarson, '33, '51, '55). Since dispersion of the basophilic chromidial substance is observed in neurones after electrical stimulation this method was chosen to supplement the toluidine blue method.

OBSERVATIONS

A. The control superior cervical ganglion

The unstimulated superior cervical ganglion stained with toluidine blue contains neurones in which the nuclei and cytoplasm are blue in color. A moderate amount of granularity can be seen in the cytoplasm with homogeneous dispersion of the chromidial substance. The nuclei of the glial elements are blue and the cytoplasmic processes are yellow-green.

With the gallocyanin-chrome alum technique the neurones appear dark blue. The cytoplasm is granular with evenly dispersed chromidial substance. The nucleus is light staining with a darker basophilic nucleolus. The glial cells have blue nuclei and light blue cytoplasmic processes.

B. The effects of sympathetic trunk stimulation

After electrical stimulation of the cervical sympathetic trunk and staining with toluidine blue the neurones in the superior cervical ganglion are somewhat enlarged and green in color. The cytoplasm is green but clusters of dark staining chromidial substance may be seen at the periphery. The nucleus is light staining and eccentric in position. A nuclear cap of darker staining chromatin material may be located near a small portion of its

periphery The nuclei of the glial cells are blue and their cytoplasmic processes are yellow-green.

Depletion of the chromidial substance is demonstrated by the gallocyanin-chrome alum method. There is almost complete disappearance of this material except at the extreme peripheries of the cells. The cells are somewhat enlarged, with eccentric nuclei. There is no change in the staining reaction of the glial tissue.

C *The effects of autonomic drugs (See Table 1)*

1 *Ergotoxine ethanesulphonate* This drug blocks the effects of stimulation demonstrable with toluidine blue. The neurones in both control and experimental tissues appear blue and granular Glial cell nuclei are blue and the cytoplasmic processes are yellow-green.

2. *Atropine sulphate* With toluidine blue the neurones stain lavender-blue after intravenous injection of atropine sulphate. The cytoplasm and nuclei show this metachromatic reaction both before and after stimulation Nuclei of the glial cells are blue and the cytoplasmic processes are pale blue.

3 *Hexamethonium bromide* Both the nuclei and cytoplasm of the neurons stain lavender with toluidine blue. Stimulated and control tissues show similar staining reactions. Glial cell nuclei and cytoplasmic processes are pale blue.

D *Stimulation of spinal nerve roots*

Color changes and chromidial depletions in the neurones identical to those resulting from stimulation of the cervical sympathetic trunk are produced in the cervical ganglion after stimulation of ventral roots of the first three thoracic segments. Stimulation of the ventral roots of the eighth cervical and fourth to eighth thoracic segments inclusive, however to elicit these changes.

DISCUSSION

A. *The preganglionic connections of the superior cervical sympathetic ganglion*

Stimulation of the cervical sympathetic trunk provoked demonstrable changes in the morphology and staining characteristics of the neurones in the superior cervical ganglion. Enlargement of neurones, increase of the cytoplasmic-nuclear ratio dispersion of chromidial substance, and peripheral displacement of the nucleus, as variously reported in the literature (Hodge 1888 1889 1892, 1894) (Vas 1892) (Lambert 1893) (Nissl 1896) and (Ped 1898) etc. have been confirmed.

The morphological changes previously reported have been produced mainly however by direct stimulation of the neurones or by retrograde stimulation of axons. Trans-synaptic stimulation, as employed by Richins and Hall ('58) has seldom been used. The toluidine blue method, as used by these workers, has been successfully used to demonstrate changes in the superior cervical ganglia following stimulation of the preganglionic fibers located in single isolated spinal nerve roots This has made possible a study of the preganglionic components of the various spinal nerve roots with reference to their

TABLE 1

Toluidine blue staining reactions after intravenous injection of autonomic drugs Superior cervical ganglia

		N drug		Ergotoxine		Atropine		Hexamethonium	
		Control	Stimulated	Control	Stimulated	Control	Stimulated	Control	Stimulated
Nerve Cells	Nucleus and Cytoplasm	Blue	Green	Blue	Blue	Lavender Blue	Lavender Blue	Purple to Lavender	Purple to Lavender
Glial Cells	Nucleus	Blue	Blue	Blue	Blue	Blue	Blue	Blue	Blue
	Cytoplasm	Yellow Green	Bright Yellow Green	Yellow Green	Yellow	Pale Blue	Pale Blue	Pale Blue	Pale Blue

possible connections with the cervical sympathetic ganglia. Stimulation of the isolated ventral nerve roots of thoracic spinal cord segments one two and three resulted in changes in the morphology and staining reactions of the superior cervical ganglion on the side stimulated, but not in the contralateral ganglion. These spinal nerves, therefore appear to carry the preganglionic components terminating in the superior cervical ganglion. Stimulation of spinal roots more caudal in position produced no observable changes in the ganglia. A widespread reaction was observed in the superior cervical ganglion after stimulation of any one of the three thoracic nerve roots. No differences in degree or distribution of the reactions in the ganglion were seen. This could indicate that the techniques employed were not highly selective and subject to diffusion, or that the synaptic connections of any one of the spinal nerve roots are widespread to all parts of the ganglia. The segmental relationships established are in agreement with the findings of Langley (1892) who could not elicit the pupillary response by stimulation at the level of the fourth thoracic segment, but who succeeded in doing so when stimulation was applied to ventral roots T 1 to T 3 inclusive. Billingsley and Ranson ('18a) using the Marchi technique, also reported that the principle preganglionic outflow to the superior cervical ganglion originates from the first three thoracic segments.

Our findings do not support the findings of Foley and Schnitzlein, that T-4 or T-5 contribute significantly to the superior cervical ganglion. However this apparent disparity could be due to several factors inherent in the two different approaches with the more logical conclusions being that they do not synapse with adequate numbers of ganglion cells to effect changes demonstrable by our method. It might be speculated that some of these fibers pass through the superior cervical ganglion and synapse with aberrant ganglia along the course of intracranial arteries.

B The toluidine blue reaction

The exact nature of the toluidine blue staining reaction used in this investigation is difficult to establish Tandler ('56) suggested that lead fixation is specific for phosphate groups and Landsmeer and Giel ('56) believed that phosphate groups in brain tissue act as substrates for staining with toluidine blue These observations plus the fact that post-chromation is necessary for the success of the toluidine blue reactions, suggest that it acts upon phosphates.

Phosphate groups are the most abundant of the assayed components of nerve tissue Elliott ('55) lists more than 30 phosphorous compounds in such tissues. Since histological methods for investigating them are scarce further investigation of the toluidine blue reaction should prove significant

C The effects of autonomic drugs

Hexamethonium bromide blocks the synapses in the superior cervical ganglion, and ergotoxine depresses the adrenergic neurones which comprise most, if not all of the ganglionic neurone population. The activity in the ganglion which normally results from preganglionic stimulation is thus inhibited by intravenous injection of these drugs. The absence of the altered staining effects seen in animals not treated with drugs is thus readily understood

Atropine depresses cholinergic postganglionic neurones. These are presumably not present in the superior cervical ganglion. The reason for the pronounced metachromasia following intravenous injection of this drug, therefore, is not clear but the drug might interfere with the processes involved in the development of the staining effects. Metachromasia is also observed in the neurones of the superior cervical ganglion following administration of hexamethonium. Richins and Hall ('58) suggested that it might be due to an accumulation of basic metabolites.

The results are summarized in table 1 of the Appendix.

CONCLUSIONS

Stimulation of the ventral nerve roots of isolated spinal cord segments T 1 to T 3 inclusive results in changes in the morphology of the neurones of the superior cervical sympathetic ganglion and in alteration of their staining reactions. The responses indicate that these segments ar

the chief source of preganglionic outflow to the ganglion.

The altered toluidine blue staining reactions seen after trans-synaptic stimulation (Richins and Hall, 58) are confirmed. Changes may also be demonstrated by use of the gallocyanin-chrome alum technique of Einarson ('32) The fact that these responses to stimulation may be nullified by pharmacologic blocking of the autonomic components indicates that they have real significance in the study of the functional activity within the ganglion.

SUMMARY

Electrical stimulation of preganglionic fibers of the severed cervical sympathetic trunk produces demonstrable changes in the superior cervical ganglion of the cat. Altered staining reactions and morphological changes are manifested with the toluidine blue method as employed by Richins and Hall ('58) and the gallocyanin-chrome alum method of Einarson ('32)

Stimulation of the ventral nerve roots of isolated thoracic spinal cord segments one to three inclusive also produced the effects in the ganglion. The preganglionic autonomic components therefore pass to the superior cervical ganglion from these segmental levels Stimulation of the ventral roots of the eighth cervical segment of the spinal cord or of the fourth through the eighth thoracic segments showed no such effects.

Autonomic drugs may be used to nullify the observed effects of stimulation. This supports the concept that the responses are produced by nervous activity resulting from the stimulation employed.

ACKNOWLEDGMENT

The author wishes to acknowledge the valuable counsel and assistance of Dr Calvin A. Richins of the Anatomy Department, St. Louis University School of Medicine in the preparation of this material.

LITERATURE CITED

Billingsley P R., and S. W Ranson 1918a On the number of nerve cells in the ganglion cervicale superius and of nerve fibers in the cephalic end of the truncus sympathicus in the cat, and on the numerical relations of preganglionic and post ganglionic neurones. J Comp. Neur 29 359–366.

——— 1918b Branches of the ganglion cervicale superius. Ibid., 29 367–384.

Einarson, L. 1932 A method for progressive selective staining of Nissl and nuclear substance in nerve cells. Am. J Pathol [illegible] 295–308.

——— 1933 Notes on the morphology of the chromophil material of nerve cells and its relation to nuclear substances. Am. J Anat., [illegible] 141–1[illegible].

——— 1951 On the theory of gallocyanin chrome alum staining and its application for quantitative estimation of basophilia. A selective staining of exquisite progressivity Acta Pat. et Microbiol. Scandinav 28 82.

Einarson, L., and E. Krogh 1955 Variations in the basophilia of nerve cells associated with increased cell activity and functional stress. J Neurol. Neurosurg. Psychiat 18 1 12.

Elliott, K. A. C., I. H. Page and J. H. Quastel 1955 Neurochemistry Charles C Thomas, Springfield, Illinois.

Ferraro, A., L. Roizin and M. Helfand 19[illegible] Morphologic changes in the brain of monkeys following convulsions electrically induced. J Neuropath. and Exper. Neurol 5: 285–308.

Foley J O., and Schnitzlein 1957 The contribution of individual thoracic spinal nerves to the upper cervical sympathetic trunk. J Comp. Neur 108 109–120.

Hamaty D., and R. C. Truex 1954 Effects of vagal stimulation on the distribution of chromatin in the cells of the intracardiac ganglia. Ibid., 101 495–514.

Hamburger C. A., and H. Hyden 1949 Transneuronal chemical changes in Deiter's nucleus. Acta Oto-Laryng. (Suppl.) 75: 82.

Hartelius, H. 1952 Cerebral changes following electrically induced convulsions. Acta Psychiat. et Neurol. Scandinav (Suppl.), 77, 128 pp.

Heinbecker P and J L. O'Leary 193[illegible] A method for the correlation of cell types with fiber types in the autonomic and somatic nervous systems. Anat. Rec., 46: 219.

Hess, M., and F Hollander 1947 Permanent metachromatic staining of mucus in tissue sections and smears. J Lab. and Clin. Med. 32 905–909

Hodge C. F 1888 Some effects of stimulating ganglion cells. Am. J Psychol., 1 479.

——— 1889 Some effects of electrically stimulating ganglion cells. Ibid., 2: 376.

——— 1892 A microscopical study of changes due to functional activity in nerve cells. J Morph., 7 95–168.

——— 1894 A microscopical study of the nerve cells during electrical stimulation. Ibid. 9 449–463.

Ingersoll, E. H. 1934 The effect of stimulation upon the coeliac ganglion cells of the albino rat. J Comp. Neur 59 267–284.

Kocher R. A. 1916 The effect of activity on the histological structure of nerve cells. Ibid. 26 341–357

Kramer H., and G. M. Windrum 195[illegible] The metachromatic staining reaction. J. Histochemistry and Cytochem., 4 227 237

Kuntz, A. 1953 The Autonomic Nervous System. Lea and Febiger Philadelphia, 4th ed.

Lambert, M. 1893 Note sur les modifications produites par l'excitations électrique dans les cellules nerveuses des ganglions sympathiques. Compt. rend. Soc. de Biol., 5 879–881.

Langley, J. N. 1892 On the origin from the spinal cord of the cervical and upper thoracic sympathetic fibers with some observations on white and grey rami communicantes. Phil. Transact. Roy Soc. Lond., 183 Series B, p. 85.

——— 1896 On the union of cranial autonomic (visceral) fibers with the nerve cells in the superior cervical ganglion. Jour Physiol., 20, 140–470.

Lindemann, J. H. F and R. Gial 1956 Staining properties of brain tissue before and after treatment with potassium dichromate. J Histochem. & Cytochem., 4 69–78.

Lu, C. N., H. L. Bailey and W F Windle 1956 An attempt to produce structural changes in nerve cells by intense functional excitation induced electrically. J Comp Neur 92; 169–

Mann, C. 1894 Histological changes induced in sympathetic, motor and sensory nerve cells by functional activity. J Anat. & Physiol., 29 100–108.

Nissl, F 1896 Die Beziehungen der Nervenzellensubstanzen zu den thätigen, ruhenden und ermüdeten Zellzuständen. Neur. Centralbl., 15 30–40.

Pearse, A. G. E. 1953 Histochemistry Theoretical and Applied. Little, Brown & Co., Boston.

Penfield, W G. 1920 Alterations of the Golgi apparatus in nerve cells. Brain, 43; 290–305.

Pick, F 1898 Über morphologische Differenzen zwischen ruhenden und erregten Ganglienzellen. Deutsche med. Wchnschr., 24; 341–342.

Robins, C. A., and J L. Hall 1958 Toluidine blue staining reactions in superior cervical and nodose ganglia following stimulation and drug administration. J Neuropathology and Exp Neurology 17 333–337

Shetnin, J J 1932 On the changes in the size, shape and distribution of the basophil substance in the neurocytosome after fixation in different fluids. Anat. Rec 52 83–96.

Spitzka, E. A., and H. E. Radasch 1912 The brain lesions produced by electricity as observed after legal electrocution. Am. J M. Sci., 144 341–347

Stewram, N. 1954 A specific staining for nucleic acids with toluidine blue. Acta. Anat., 20 36–39.

Sulkin, N M., and A. Kuntz 1950 A histochemical study of the autonomic ganglia following prolonged preganglionic stimulation. Anat. Rec., 108 285–2?8.

——— 1953 Histochemical alteration in autonomic ganglion cells associated with ageing. J Gerontology 7 533–543.

——— 1948 The Golgi apparatus in autonomic ganglion cells and peripheral neuroglia and its modification following stimulation and induced hypertension. J Neuropath. and Exp Neurol., 7 154–161.

Tandler D. J 1958 An acid component of the nucleolus; the cytochemical specificity of the lead acetate reaction. J Histochem. and Cytochem., 4 331–340.

Vas, F 1892 Studien über den Bau des Chromatins in der sympathischen Ganglienzelle. Arch. f. mikr Anat., 40; 375–389

Wiesel, J 1902 A chromaffin stain. Anatomische Hefte, Abteilung 1, Wiesbaden., 19 481–522.

Winkleman, N W and M. T Moore 1944 Neurohistologic findings in experimental electric shock treatment. J Neuropath. and Exper Neurol., 3 199–209.

Tubule Cells of the Rectal Salt-Gland of *Urolophus*[1]

WILLIAM L. DOYLE
Department of Anatomy The University of Chicago Chicago Illinois

Burger and Hess ('60) demonstrated a salt-excreting function for the rectal gland of the dogfish, *Squalus* thus furnishing a second example of a major extra-renal salt-regulating organ recently discovered in vertebrates. K. Schmidt Nielsen et al. ('58) (K. Schmidt Nielsen, '60) previously discovered this function of the nasal gland in marine birds. In teleost fishes, although the role of the gill in salt regulation has been recognized for over 30 years, the cellular localization of the function is not yet clarified (Doyle and Gorecki, '61)

The anatomy and histology of the elasmobranch rectal gland has been known for several decades and was described for *Squalus* by Hoskins ('17) Bernard and Hartmann ('60) and Bulger (unpublished '61) have made preliminary observations on the cytochemistry of these glands The present work is concerned with electron microscopic observations on the structure of the cells of the tubules in the rectal gland of the round sting-ray *Urolophus jamaicensis* (Cuvier 1817) (= *Urobatis sloani*) with a few notes on the dogfish, *Squalus*.

MATERIALS AND METHODS

Specimens of adult male and female *Urolophus* were collected by skin divers and held for a few days in live-boxes at Fort Lauderdale Florida, prior to shipment by air to the laboratory in Chicago. Of 16 specimens studied, four were discarded as being in poor condition.

Specimens held in the aerated sea-water in which they were received are termed normal specimens. To ensure activity of the rectal gland some specimens were treated by injection of 3 ml of 5% sodium chloride into the stomach. This caused marked dilation of the gastric and rectal gland blood vessels within a few minutes Treated specimens were fixed 20 minutes after injection and are designated salted.

Glands of normal and salted specimens were quickly excised sliced transversely and fixed for 40 minutes in 1% osmic acid buffered according to Palade at pH 7 4 with the addition of 0.2 M sodium chloride for some specimens. This mixture was replaced with 10% formalin similarly buffered and adjusted in salinity After 15 minutes in formalin the specimens were placed in 50% alcohol, quickly dehydrated and embedded in methacrylate or epoxy resin (Shell Epon 812) For certain specimens the Michaelis buffer (barbital-acetate HCl) in Palade's fluid was adjusted to pH 6.9 7 4 and 7 7 The usual Palade fluid has an osmolarity of 0.20 and this was varied by addition of sodium chloride or urea to give total osmolar values of 0 56 to 1 0 The addition of urea equivalent to blood concentrations had no beneficial effects on the fixation. In general the variations in pH and salt content of the osmic acid fixatives gave minor differences in results.

Figures 2, 4 10 11 are selected from a normal specimen fixed in a 0 56 osmolar solution at pH 7 7 Figures 3, 5 6 7 8 9 are selected from a salted specimen fixed in a 0.20 osmolar solution at pH 6.9 Figures 4 to 11 inclusive are from specimens stained with lead after sectioning All of the illustrations are taken from material embedded in methacrylate

RESULTS HISTOLOGY

The simple tapered cylindrical shape of the digitiform gland of *Squalus* other dog fishes, sharks, and skates is somewhat

[1] Supported in part by grant (RG-C-3973) from the United States Public Health Service and in part by grant from the Wallace C. and Clara A. Abbott Memorial Fund of the University of Chicago.
The technical assistance of Katharine Doyle and Sonia Michaelson is acknowledged.

modified in *Urolophus* In *Squalus* (see also Hoskins 17) primary and secondary simple tubular glands radiate from a large straight central duct via short lobular ducts. There is a peripheral arterial supply to a capillary network which courses centrally to a venous drainage via sinusoidal vessels bordering the lumen of the central duct. The capillary blood flow is concurrent in direction with the flow of secretion in the tubules. In *Urolophus* the gland is somewhat S-shaped and lobulated; the central duct branches and there is an increased number of lobular ducts The overall pattern of vascular supply is similar to that in *Squalus* but the central sinusoidal veins are disposed in the connective tissue layer surrounding the central ducts. The central ducts have a multilayered cuboidal epithelium in which there are a few scattered intra-epithelial mucous glands. The lobular ducts immediately adjacent to the central ducts usually have two layers of epithelial cells, and at the next branching the ducts have a simple columnar epithelium A thin layer of connective tissue surrounds the ducts. Nerves are prominent between the lobular ducts The secretory tubules show some simple bifurcations near the periphery but are for the most part unbranched

Whereas adult *Squalus* are approximately one meter long and weigh a few kilograms the *Urolophus* are small sting rays about the size and shape of a dinner plate (16–18 cm in diameter) excluding the tail, and 30–34 cm overall, weighing only 300–400 gm. The rectal glands are correspondingly reduced in size and its tubules are only 1–2 mm long In cross sections however the tubules of *Squalus* and *Urolophus* are very similar

The tubular lumen averages 6 μ in diameter but varies from 3.2 to 30 μ It is surrounded by six to nine columnar cells which vary in height from 18 to 8 μ depending upon the distention of the lumen Mucous cells are found rarely scattered singly in the tubular epithelium. The secretory cells have subspherical nuclei with one or more deep infoldings of the basal aspect of the nuclear membrane (fig 2) Nucleoli are prominent.

Cell membranes

In the light microscope cross sectior of the tubules show indistinct cell boundaries which appear as broad, bright regions in phase microscopy In the electron micrographs (figs. 2, 3 7 8) this effec is seen to be the result of considerabl interdigitation of lateral cell boundaries In *Urolophus* these interdigitations are neither as deep nor as numerous as they are in *Squalus* There is a distinct basement membrane (M fig 11) which tend to extend upward a short distance betwee adjacent cells. In most cells the basal cel membranes are infolded primarily at th boundaries of adjacent cells so that mo of the base of the cell is relatively smooth At the apical boundaries of the cells ther are distinct, heavy plasmodesms betwee cell boundaries at lumen (figs. 3 10) an a short distance behind the heavy struc tures there are shorter ones with later striations. At the surface of the lumen th adjacent cell boundaries are approximatel 100 A apart.

Cytoplasmic particulates

In paraffin sections of formalin-fixed tis sues there is a weak basophilia and a mod erately strong PAS reaction. Small granu les which stain with Sudan Black B ar readily seen with phase-contrast micros copy These inclusions are insoluble in al cohol after formalin fixation, and they ar readily identified in the electron micro scope as dense lamellated (myeloid) phos pholipid bodies. In the electron m granules typical of glycogen and RNA par ticles appear in figures 4 5 6, 8, 10. Th RNA particles help to delineate the inco spicuous endoplasmic reticulum.

Mitochondria

The tubule cells contain large number of long rod-shaped mitochondria with dis tinct transverse cristae. The average di ameter of the mitochondria is 0.3 μ. Th cristae are moderately closely spaced, th distance between adjacent cristae betw about twice the thickness of the cristae In contrast, in *Squalus* the mitochondria are somewhat larger in diameter and th cristae are more closely arranged, bein about the same distance apart as th thickness of the cristae. The closer pack

ing of cristae in *Squalus* may reflect a higher rate of metabolism correlated either with the differences in habits of the two genera or possibly related to the temperature differences in habitat between the Gulf of Mexico and the Gulf of Maine

Golgi material

Membranes typical of the Golgi material are characteristically present in the supranuclear region (figs. 4 8 9) In figure 4 8 there are also shown parts of two large vesicles containing what appear to be residua of Golgi membranes a similar smaller structure is seen immediately to the right of the lamellar array Vesicles of this type similar to figures of lysosomes are to be found in great variety including ones which present multilayered but irregularly concentric membranes. Some of the latter have a superficial resemblance to the much more regularly lamellated myelin figures of the dense lipid bodies (figs 4,5). Despite a wide range of shapes and sizes and heterogeneity of content, these membranous residua are clearly distinct from the phospholipid bodies in this material and do not make a continuous series with them.

Lipid inclusions

Between the nucleus and the apex of the cell there are three cytoplasmic components which are rarely seen in the periphery or basal portions of the cell. These are the Golgi membranes the compound vacuoles to be described below and the lipid inclusions. In the electron microscope the dense lipid inclusions show a variety of internal structures (figs. 3 (arrow) 4 6 8), notably myeloid" lamellations characteristic of phospholipids (cf Stoeckenius, '59) They range in size from 1 0 μ down to 0.25 μ in diameter with most being larger than 0.5 μ. Surrounding most, but not all, of the dense bodies a thin bounding membrane can be distinguished These lipid bodies are obviously heterogeneous, but they are always distinguishable from the vesicular elements of similar size containing membranous residua (fig. 4,8).

Endoplasmic reticulum

A fine tubular form of the endoplasmic reticulum is found sparsely distributed in our preparations of the gland. The gland shows slight basophilia in the light microscope and we find relatively little rough surfaced endoplasmic reticulum. In preparations stained with lead the small 150 A RNA particles which are relatively abundant (fig 10) are less immediately obvious because of the prominence of numerous larger 300 A glycogen granules (fig 8) The accumulations of these larger lead staining granules are consistent with light microscope observations on the distribution of PAS staining for glycogen

Vesicular elements of the cytoplasm

In addition to or possibly existing as modifications of the endoplasmic reticulum, there are numerous vacuoles in the cytoplasm which seem to fall into certain natural size classes

The interdigitating cell membranes are lamelliform but give rise to tubular extensions in some regions. These tubular extensions contain intercellular substance and they give rise to rows of vacuoles (V figs. 9 11) At the lateral borders of the cell the vacuoles are quite uniform in size and average 400 A in diameter with sharply defined boundaries.

Scattered throughout the cytoplasm but most numerous in the supranuclear region are vacuoles with an average diameter of 350 A and well defined membranes. They are diagrammed in text figure 1 B C D E, F and appear in figures 4 6 8 Vacuoles of this size are found (1) free and randomly distributed in the cytoplasm (2) grouped in closely packed but evenly spaced clusters (text figure 1 B) and (3) enclosed in outer vacuoles about 0 4 μ in diameter (text figure 1 C D) The last two categories are almost exclusively confined to the supra-nuclear region of the cell along with the Golgi membranes and lipid bodies. For discussion the 350 A vacuoles are designated unit vacuoles.

Close to the lumen of the tubule are found many vacuoles which are larger (average diameter 550 A) and which have a wider range of sizes than those just described (figs. 7 10) Their walls appear to be thinner than either of the previously described (400 A and 350 A) classes of vacuoles and they appear to fuse with the apical cell membrane (or possibly to arise

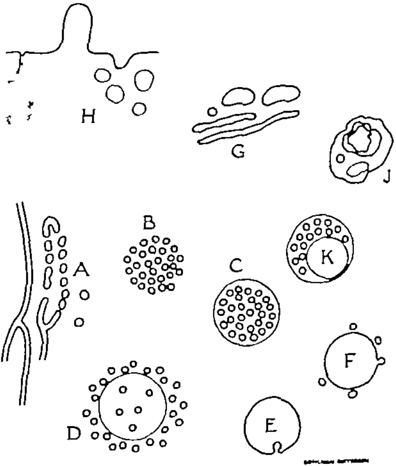


Fig. 1 A. Diagram of rows of vacuoles near lateral cell boundary Compare with figures 9 and 11 Vacuoles of the 400 Å class.
B. Dense aggregates of 350 Å "unit" vacuoles free in the cytoplasm.
C, D Multivesiculate bodies as in figures 4 6, 8.
E. Re-entrant figure of possible mode of origin of enclosed unit vacuoles.
F Figure illustrating fusion of free "unit" vacuole with outer vacuole. There is a suggestion of this in figure 4.
G. Golgi membranes.
H. Vacuoles with thin walls and varying diameters averaging 850 Å and found near the lumen. Compare figures 7 and 10.
J Membranous residua (see text) Compare B, figure 4.
K. Compound form of multivesiculate body with dense material around the unit vacuoles.

from it) These vacuoles are difficult to distinguish from those bordering the Golgi membranes (figs. 4 8 9)

We are unable to distinguish whether the unit vacuoles have a so-called unit membrane as opposed to a single membrane on the apical vesicles.

DISCUSSION

No tests were made on the rate of secretion by the rectal gland, but we have assumed that the gland is functionally comparable to that in *Squalus*. No striking structural differences were observed between glands in the "normal" specimens and those salted by injection of sodium chloride. Burger ('62) has observed continuous secretion at varying rates from the rectal gland in most cannulated specimens of *Squalus* even when in diluted sea water Accordingly it is probable that all of the specimens examined in this work

had actively secreting rectal glands. As yet, no physiological control mechanism has been demonstrated.

Burger and Hess ('59) showed that the secretion of the rectal gland in *Squalus* is approximately half-molar sodium chloride and contains very little urea. The blood is approximately one-third molar with respect to both sodium chloride and urea. Thus the gland concentrates sodium chloride a little less than twofold over the blood value, and this is done isosmotically by virtue of retention of urea. Assuming a similar situation for *Urolophus* and assuming that the primary secretion in the tubule is the same as that in the excretory duct, these gradients of urea and sodium chlorides are developed across a simple columnar epithelium.

Ignoring the morphology it might also be assumed that a uniformly increasing salt gradient exists from the base to the apex of the cell. But the fine structure of these cells is dominated by vesicular components to such a degree that these elements must be considered with respect to their possible role in salt concentrating mechanisms.

In the cytoplasm there are a variety of vesicular components (text figure 1) which can be arranged in series. It is observed that vacuoles occur in rows near the lateral interdigitations of the cell membranes (figs. 8 11 V and text-figure 1A). The individual vacuoles are somewhat larger (400–450 Å in diameter) than those prevalent in the supra-nuclear region of the cytoplasm which are quite uniformly 350 Å in diameter. The 350 Å vesicles will be called unit vacuoles. Along with Golgi membranes and lipid granules, they are most prominent in the supra-nuclear cytoplasm. They occur free in the cytoplasm singly or occasionally as groups (text figure 1B) which are densely packed and evenly spaced. Similar vacuoles are found enclosed (figs. 4 6; text-figure 1C D) in outer vacuoles of 40 ± 07 μ diameter. The enclosed unit vacuoles are identical in appearance with those free in the cytoplasm but are surrounded by vacuolar fluid in place of cytoplasmic ground substance. Sections of the larger outer vacuoles may contain 30–50 unit vacuoles rather evenly spaced. Occasionally quite complex forms (text-figure 1K) have been found in specimens kept for 24 hours in poorly aerated sea water.

All of these configurations have a striking resemblance to the outlines of coacervates shown by Bungenberg de Jong (in Kruyt, 49) for a variety of model systems. His observations made with the light microscope referred primarily to much larger systems often 300 μ in diameter. Foams and polyphase liquid systems in general and coacervate systems in particular invite hypotheses for salt concentrating mechanisms since they characteristically involve local changes in ionic composition. At the same time, Bungenberg de Jong's demonstrations of inverse relationships in gels containing nucleic acids, of conditions for charge reversal, and the discrepant character of phosphatid coacervates require that we have much more information about the interior of cells before the analogies between the different systems can be very usefully applied. It should also be noted that the dimensions involved in the multivesiculate bodies of these cells are such that the forces significant to mesomorphic states may be more reasonably expected to apply here than in some of the previous analogies drawn from light microscopy. Lawrence's observations (in Kleinzeller and Kotyk, '61) on a new type of interfacial interaction seem more pertinent here. His phase diagrams for ternary systems of soap amphiphil and water offer interesting possibilities in salt transport mechanisms. Since the multivesiculate bodies are apparently equally well preserved after initial fixation in either formalin or osmic acid over an appreciable range of osmolarity and pH values of 6.9–7 7 they appear to be much more stable than Bungenberg de Jong's systems.

Sections of outer vacuoles as large as 0 5 μ in diameter have been found containing only one unit vacuole but empty circular vacuoles of that diameter are rare

Rhodin (personal communication) has noted a specialized apical layer in the epithelial cells of the gills of *Squalus* which we have confirmed for [illegible] and *Urolophus*. Rows of elongate vacuoles, reminiscent of the cortical cytoplasm of some marine eggs, are present at the surface. This specialized layer is absent from the gills of the marine and fresh water teleosts examined to date. In the excretory duct of the rectal gland, in [illegible] similar fashion but on a larger scale, the apical cytoplasm of the surface epithelial cells of the ducts is filled with moderately dense vesicles. The relation (if any) of this surface specialization to retention of urea has not been studied.

There appears to be a limited range in di ameter of the outer vacuoles from 0.29 to 0 66 μ with an average diameter of 0 40 μ ± 07 μ A.D Since not all of the sections were meridional, the upper range of sizes found seems most probable. In 40 examples measured, two were found below 0.3 μ and two above 0 5 μ in diameter The rarity of smaller sizes suggests a sudden formation of these outer vacuoles. Of the forms shown in text figure 1 groups B C and D are common, whereas E and F are rare. We have never seen what might be considered fusion of the unit vacuoles in group B Whether free in the cytoplasm or enclosed in outer vacuoles one character istic of the groups of the 350 A vacuoles is the uniformity of spacing between them. The absence of smaller sizes of the outer vacuoles may be a result of extremely rapid fusion of groups of unit vacuoles followed by an almost simultaneous appear ance of enclosed unit vacuoles. Alternatively a sudden phase reversal might give rise simultaneously to both the outer vacu oles and to the enclosed unit vacuoles whose membranes would be reversed in symmetry in comparison with free unit acuoles.

Although a few U-shaped outlines of sec- ons of incomplete outer vacuoles partially surrounding groups of unit vacuoles are to be found in this material, they are rare. Such formations might be sections of newly forming outer vacuoles or of collapsing ones. The remnants of such outer vacuoles might account for structures like J in text figure 1 On such an hypothesis the enclosed unit vacuoles would disappear by complete fusion with cytoplasmic mat rix, and the fluid of the outer vacuole would be discharged in the cytoplasm to give rise to the thin-walled vacuoles H (text-figure 1) The latter appear to fuse with the apical cell membrane

Compound vacuoles (multivesiculate bodies) of the sort described here are not rare in secretory epithelia, but they are seldom so prominent as in the *Urolophus* rectal gland (They are a regular feature of the cytoplasm in *Squalus* but appear to be somewhat less abundant.) The simul taneous occurrence of prominent complex phospholipid bodies in this cell invites a search for interrelationships between them and the vacuoles. In the present work no sequential relationship has been demonstrated. Consistent experimental production of lipid inclusions has been demonstrated by Spargo, Straus and Fitch ('60) in the renal papilla of potassium deficient rats. It may be significant that these bodies develop in the region of maximal sodium concentration

Physiological and biochemical evidence has established the presence of lipids in vacuolar and other cytomembranes. In some more recent work the relation cific lipids to ion (especially sodium) port has been presented. Hokin and Hokin ('60) and Hokin (in Kleinzeller and Kotyk, '61) have stressed the significance of phosphatidic acid turnover to sodium transport. They have demonstrated high activities in the salt-gland of marine birds. The biochemistry of phosphatides has been explored by Kennedy ('61) and Borkenhagen, Kennedy and Fielding ('61) and others. The pertinence of these and findings to morphological aspects of phagocytosis and pinocytosis has been reviewed by Karnofsky ('62) Karnofsky notes the absence of net synthesis of phospholipid in given situations which have high turnover rates and he discusses the phospholipid fractions which are most probably concerned in membrane phenomena.

The situation in the salt-gland of marine birds is quite different from that in the elasmobranch rectal gland The morphological pattern of elaborately infolded cytomembranes found in the marine birds is replaced by the prominent vacuolar mechanism described above. In the birds there are well defined nervous pharmacological and osmotic mechanisms regulating the activity of the gland In the elasmobranchs these mechanisms are yet to be determined. Studies on the phosphatidic acid metabolism of the elasmobranch gland have not been completed. It may well be that the striking morphological differences between the bird and elasmobranch glands reflect insignificant differences at the biochemical level. On the other hand, one might expect significant cytochemical differences in localization which might serve to test hypotheses such as Hokin s ('60)

SUMMARY AND CONCLUSIONS

In contrast to the morphology of the principal cells of the salt-gland in marine birds where the cytoplasm is deeply divided into thin leaflets formed by extensive basal infoldings of cell membranes (Doyle '60) the most striking feature of the cytoplasm of the principal cells of the rectal salt gland in *Urolophus* is the large number of compound vacuoles (multivesiculate bodies) in the apical half of the cell. Basal infoldings are not extensive, but lateral interdigitations are very numerous and run deeply into adjacent cells so that in the light microscope or in phase contrast, the lateral cell borders appear deeply indented. Also in contrast to the tubule in the birds, the terminal bars appear to be quite rigid so that even after the use of strongly hypertonic fixatives and reagents which shrink the cytoplasm enough to open up wide intercellular spaces the apical regions of the cell boundaries remain closely apposed. It seems likely that the salt transporting mechanism in the rectal gland of the sting-ray *Urolophus* is characterized by a series of vesicular components of some complexity and there is reasonably good evidence for the discharge of large numbers of small vacuoles into the lumen of the gland by fushion with the apical cell membrane. Possibilities that phase reversal occurs among vesicular components and some considerations of recent biochemical mechanisms relating specific lipids to salt transport are discussed.

LITERATURE CITED

Bernard, G. R., and J. F. Hartmann 1960 Cytological and histochemical observations on the elasmobranch rectal gland Anat. Rec., *137* 340.

Burger J W 1962 Further studies of the rectal gland in the spiny dogfish. Physiol. Zool., *35* 205–217

Burger J W., and W N Hess 1960 Function of the rectal gland in the spiny dogfish. Science, *131* 670–71

Bockenhagen, L. F E. P Kennedy and L. Fielding 1961 Enzymatic formation and decarboxylation of phosphatidylserine J Biol. Chem., *236* PC 28.

Doyle, W L. 1960a The principal cells of the salt gland of marine birds. Exper Cell Res., *21* 386–393.

——— 1960b Fine structure of salt regulating epithelia. Anat. Rec., *136* 184

Doyle, W L., and D Gorecki 1961 The so-called chloride-cell of the fish gill. Physiol. Zool., *34* 81–85.

Hokin, L. E., and M. R. Hokin 1960 The turnover of phosphatidic acid and phosphoinositide in the avian salt salnd. J Gen. Physiol., *44* 61–68.

Hoskins, E. R. 1917 On the development of the digitiform gland of the intestine in *Squalus acanthias*. J Morph *28* 329–367

Karnofsky M. L. 1962 Metabolic basis of phagocytic activity Physiol Rev *42* 143–168.

Kennedy E. P 1961 Biosynthesis of complex lipids. Federation Proc *20* 934–940.

Kleinzeller A., and A. Kotyk 1961 Membrane Transport and Metabolism. Academic Press, New York.

Kruyt, H R 1949 Colloid Science *2* Morphology of Coacervates by Bungenberg de Jong. Elsevier Amsterdam.

Schmidt-Nielsen, K. 1960 The salt-secreting gland of marine birds. Circulation, *21* 955–967

Schmidt Nielsen, K., C. B Jorgensen and H. Osaki 1958 Extra-renal salt excretion in birds. Amer J Physiol., *193* 101 107

Spargo, B F Straus and F Fitch 1960 Zonal renal papillary droplet change with potassium depletion. Arch. Pathol., *70* 599–612

Stoeckenius, W 1958 Fixierung von Myelinfiguren aus Phosphatiden und Eiweiss mit OsO_4 und $KMnO_4$. Fourth Int Cong Electron Micr *2* Springer Berlin.

PLATE 1

EXPLANATION OF FIGURES

1 Cross section of secretory tubule × 2,250. Typically infolded nuclei. The cell boundaries appear to be broad as a result of interdigitations shown in figures 2 and 8 This lumen is 8.5 × 2.0 μ.

2 Central portion of tubule in cross section × 7,500. Portions of acini at lower left and upper right. At the lumen there are prominent plasmodesms. In the cell at lower left there is a group of three dense phospholipid droplets among the mitochondria (arrow) Lumen approximately 3 μ in diameter Salted specimen.


2


3

PLATE 2

EXPLANATION OF FIGURES

4 Typical supra-nuclear cytoplasm × 36,000. Segment of nucleus at lower right. Golgi membranes at left center. Multivesiculate body in center corresponding to F in text figure and at lower right like D. Lamellated dense bodies near Golgi array should be compared with those in figures 5 and 6. Membranous residua, R. Salted specimen.

5 Phospholipid droplet with four areas of myeloid lamellation. × 35,500. Normal specimen.

6 Three dense lipid agglomerates and two multivesiculate bodies. The long axis of the large ovoid conglomerates approximately 1 μ. Glycogen particles in the cytoplasm. × 35,250. Salted specimen.

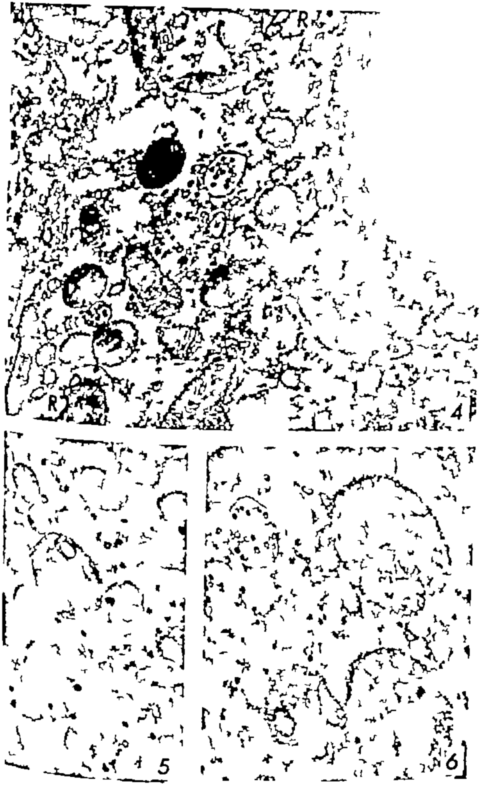

R
R
4
5
6

PLATE 3

EXPLANATION OF FIGURES

7 Lumen of tubule in normal specimen. × 35,250. Numerous vacuoles of 550 Å class in the apical cytoplasm. Compare figure 10. Note constriction of intercellular space at lumen.

8 Supra-nuclear cytoplasm near cell border with three multivesiculate bodies containing unit vacuoles averaging 350 Å in diameter. Compare C in text figure 1. Glycogen granules and smaller RNA particles stained with lead. Salted specimen × 32,250.

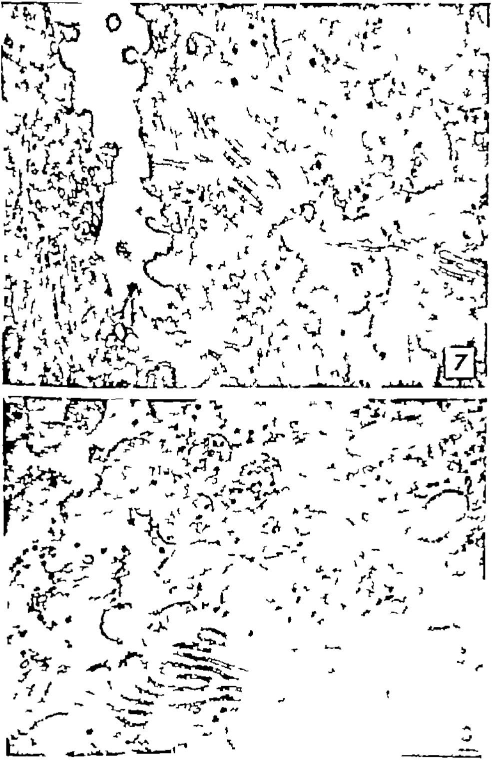

7

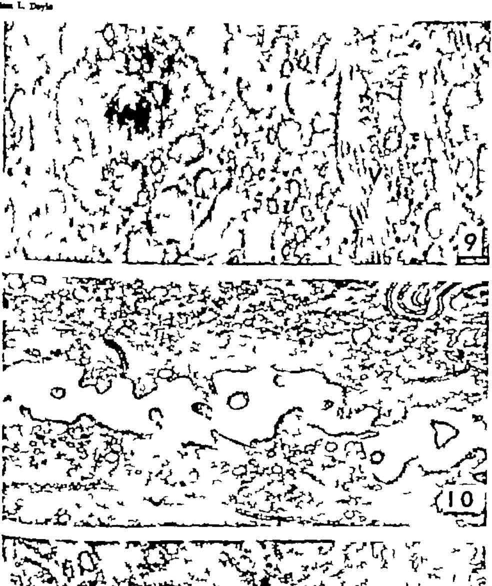
PLATE 4

EXPLANATION OF FIGURES

9 Salted specimen × 25,200 Cell boundaries and associated rows of 400 Å vesicles, V at right. Golgi region upper left. RNA particles lower center

10 Normal specimen × 36,000 Longitudinal section of lumen. Apical vacuoles of the 550 Å class. Some fine tubular endoplasmic reticulum with RNA particles in upper portion.

11 Basal portion of cell in normal specimen × 36,000 Connective tissue along lower border and basement membrane, M, above it, V vacuoles approximately 400 Å in diameter


9
10
11

Morphogenetic Studies of the Rabbit

XXIX. ACCESSORY OSSIFICATION CENTERS AT THE OCCIPITO-VERTEBRAL ARTICULATION OF THE DACHS (CHONDRODYSTROPHY) RABBIT[1]

P. B. SAWIN, MARY RANLETT AND DORCAS D. CRARY
Roscoe B. Jackson Memorial Laboratory
Bar Harbor, Maine

Reports by independent investigators of the manifestations and inheritance of disproportionate dwarfism in a number of species agree in showing evidence of generalized retardation of growth common to all and monogenic origin. They differ with reference to genetic dominance (some dwarf genes being dominant and others recessive) and in the pattern of localization of the greatest retardation effect. Usually the endochondral bones of the skull and the limbs are more severely affected, but the pattern varies and is species specific. When more than a single such gene is known per species the localization is found to be gene specific. Whether or not it is in part mediated by endogenous normal growth processes which may vary both between and within species depending upon the assembled genome is a question which merits careful examination. The critical test of species or gene specificity should be revealed by transfer of specific genes between genomes (genetic backgrounds). In such tests, a gene producing a qualitative or quantitative change in a region of ordinarily high stability would be particularly useful, especially so if that region had been of substantial evolutionary significance. The dachs gene (*Da*) with its pronounced effects in the posterior skull and atlanto-axial region of the rabbit appears to be just such a case and, although the entire cervical region in mammals is considered by most morphologists to have become singularly stabilized in number of elements and in their shape development and function, it nevertheless is one which has passed through a certain precise evolutionary change accompanying the development of the tetrapod skeleton (Evans '39, Williams, '59). Abnormalities of this region compared with the thoracic and lumbar regions, are relatively few. Yet the *Da* gene, arising as a single semidominant mutant, has induced extremely bizarre changes in the morphological pattern of this region, changes which fit into present ontogenetic and phylogenetic knowledge and which may help to elucidate some of the genetic processes involved in mammalian phylogenetic development. In a previous communication (Sawin, Ranlett, and Crary '59) the effect of the *Da* gene upon the spheno-occipital complex was described. In this paper we shall describe variations induced in the occipito-vertebral articulation and discuss them in relation to present knowledge of the dynamics of bone development. Both are preliminary steps in a study of these regions as influenced by the gene when transferred to new genetic backgrounds.

MATERIALS AND METHODS

The material on which this study is based is the same collection of 114 dried skeletons and 132 alizarin stained early postpartum specimens previously studied with reference to the skull sutures (Sawin, Ranlett, and Crary '59). The range in age is from birth to twenty-one and one half months (the greatest age so far achieved by any dachs *DaDa* rabbit).

[1] This investigation was supported (in part) by PHS research grant C[illegible]C from the National Cancer Institute, Public Health Service, and aided by a grant from the American Cancer Society. The authors wish to express their appreciation to the assistants, Eugene Farris and Adelaide Cameron, who aided in [illegible]ration of specimens and illustrations.

OBSERVATIONS

In the earlier study of the more mature skeletons of the dachs (Sawin and Crary '57a) variation in position of what was considered to be the dens and a bilateral duplication of parts particularly of the atlas ventral arch or hypocentrum, were noted. In fact, a generalized tendency for refinement of vertebrae and for expression of accessory elements such as independent traction epiphyses at the tips of many of the dorsal vertebral processes was noted throughout the skeleton. Such epiphyses were not associated with the ventral spinous processes on vertebrae 20–23 although these processes appeared longer than normal. Because of the bizarre alteration in shape of the epistropheus, the full significance of the accessory elements was not recognized at the time of collecting data for the earlier paper It was not until Rafferty ('56) examined a group of new born dachs that the real nature and relationship of these elements began to be suspected In attempting to describe and interpret the variation in these relationships we shall consider (1) the variations normal elements (2) identification of y elements by their position and elationship to their neighbors, and (3) the spacing, whether fusion or articulation of neighboring elements.

Variations in normal elements

The relative position of the elements of the last two rings of bones of a normal (non-dachs) skull (excluding the elements associated with the sense organs of the ear) and of the atlas and axis are shown in figure 1 with the accessory elements induced by the dachs gene shown in broken lines.

The arrangement in the dachs is essentially the same as in the normal. The differences consist of displacement or abnormal spacing of functional parts accompanied by inclusion of accessory elements and subsequently by irregularities of fusion of adjacent normal and/or accessory parts resulting in malformation and malocclusion. The atlas centrum and neural arches are essentially normal except for occasional irregularities of fusion The well-known normal union of the atlantal neural arches with the ventral arch (anterior arch in man) rather than with its centrum, and the union of atlas and axis centra to form the major portion of the epistropheus typical of most mammals is rarely disturbed, but the normal fusion of the proatlas with the epistropheus is rare.

The *atlas hypocentrum* of the dachs is in its normal position, ventral to the dens, to the plane of the other vertebral centra, and to that of the endochondral basal elements of the skull (figs. 2 and 4 of plate 1). It is less stable than in normal animals, being found in some individuals as two bilaterally symmetrical or asymmetrical parts, particularly in newborns (see fig. 6). In eight cases, it was found as a distinctly Y-shaped element as if formed by the fusion of two such elements (fig. 5)

Two cases were found in which the *atlas centrum* had likewise arisen as two separate centers of ossification.

The proatlas centrum

In the normal rabbit, the proatlas appears as a single ossifying unit (centrum only) lying anterior to the atlas centrum, to which it fuses. (The typical position is dorsal to the ventral arch as shown in plate 1 fig. 2) In our studies it never appears earlier than five days postpartum In the dachs this unit is found in the same position (fig 5) but is more variable in size shape, the time at which it appears and in the direction of its fusion as will be seen below It was found at birth in two cases and by five days in all cases It may arise as two centers and at all ages varies considerably in size and shape, not infrequently being found as two bilaterally symmetrical or asymmetrical centers in early postnatal development (figs 6, 7 9 and 10) and even in well advanced skeletons (fig 13) It is often found to arise simultaneously with an accessory element, referred to below as the proatlas ventral arch. Frequently it fuses later either anteriorly to basioccipital (fig. 11), or ventrally to an accessory proatlas ventral arch (fig. 12, plate 1) rather than posteriorly to the epistropheus. Sometimes it is found to ossify as two centers which ultimately may (or may not) fuse as shown in figure 12.

SCHEMATIC DIAGRAM OF POSTERIOR SKULL AND VERTEBRAL ELEMENTS

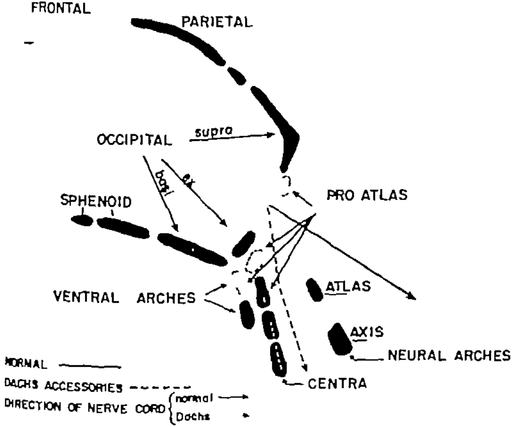


Fig. 1 The occipito-atlanto-axial complex of the rabbit and the direction of the nerve cord are indicated by *solid lines*. The accessory centers of ossification and the modified position of the cord with reference to the skull occurring in the dachs (DaDa) rabbit are shown by broken lines.

Accessory ossification centers

A total of eight accessory elements ha e been observed in the dachs

Proatlas ventral arch The most common of these is one which arises at about the same time as the atlas ventral arch and lies anterior to it and at the same dorsoventral level (figs. 10 and 12 plate 1) It varies considerably in size and shape and very often arises as two bilaterally symmetrical or asymmetrical elements (figs. 6 7 and 10) which at later ages are found in various degrees of fusion with each other (fig. 10) Frequently they seem to encroach upon and at later ages fuse with the basioccipital The distinction as to whether the element is proatlas centrum or hypocentrum is determined by its dorsoventral level with respect to atlas centrum and basioccipital The proatlas centrum distinguished by its more dorsal position may also arise as a paired element.

Proatlas neural arches. Two other accessory elements are prominently associated with the exoccipitals. They are most easily seen in early postnatal specimens as posteromedial extensions already fused with the exoccipital. They *tend to* be partially separated by indentations, marked (3) in figures 5 and 21 (1) in figures 8 15 and (2) in 30 Occasionally they are found attached to the *neural* arches of the atlas in all three genotypes

(fig. 11). In several of the older specimens they have been found as relatively flat discs fused into the occipital condyles where they provide the entire articulating surface of the condyle. In other specimens the only suggestion of their presence is the increased width of the exoccipitals themselves, examples of which are to be seen in figures 6, 14, 19, 26 and 27 (compare with figs. 4 and 18 with narrow exoccipitals). Figure 15 shows an asymmetrical basioccipital and pair of exoccipitals. The left member is broad and bears the condyle; the right is narrow and has a projecting element which, due to its position, is assumed to be an accessory proatlas neural arch. It is fused to the exoccipital and bears the articulating condyle separated from the exoccipital proper by the obvious indentation. In some degree this variation can be misleading since in photographing the manner of orientation may result in exaggeration of width. However, these differences as examined in most specimens are very real and will be referred to again in discussion of spacial significances. These accessory elements of the exoccipital are not peculiar to the alone since, as shown in table 1, may occur in normals also (fig. 11), nough with less frequency ($p = < .05$).

It is particularly noteworthy that in the dachs the cases in which these accessory elements attach to the atlas neural arches are relatively rare. Since in species other than man, the proatlantal arch rudiment is considered to fuse either with the atlantal neural arch or with the occipital bone and in man it assists in the formation of the occipital condyles (Senseniq '57), these extensions separated in many cases by indentations appear to be evidence of the proatlas neural arches. In the dachs, as in man, they are more often associated with the occipital bone than with the atlas neural arch.

Dorsal accessories. The last pair of accessory elements in the complex is located at a relatively high dorsoventral level. They occur as ossifications projecting medially into the foramen magnum which in normal rabbits is nearly round. Figures 22 and 23 show their most usual expression as simple outgrowths (4) from the exoccipitals. However, as in figures 24 and 25 they may occur as small independent elements, in part articulating with the supra-occipital as well as the exoccipital.

Thus a complex of accessory ossified elements has been described as occurring with a varied degree of expression in all homozygous dachs. Their position, degree of organization, and functional adaptation for articulation of the skull and vertebral units indicates that they are not fortuitous inclusions but compensations or adjustments to changes in basic developmental processes.

Spatial relations. The nature of these processes is at least partially revealed by study of these relationships between normal and accessory elements longitudinally in time and as they become developmentally modified. In early postnatal animals with the more complete expression of the accessory complex, there is visible evidence of crowding. In older animals, as in figures 32 and 33, this crowding becomes accentuated, leading to fusion and misshaping of adjacent elements, as in the flattened scale-like proatlas neural arches

TABLE 1

Shows the incidence of posteromedial extensions of exoccipital separated by indentations which are believed to be proatlas neural arches as observed in normal and dachs rabbits

		Indentation	
dada and Dada	38	11(22.5)	49
DaDa	53	36(40.5)	89
	91	47(34.1)	138

$\chi^2 = 4.56$ df = 1 $p = 0.05$

TABLE 2

Spacing of normal and/or accessory elements

Age	Number	% Open
Birth	31	35.5
1 Month	10	20
1 Month +	76	41.8
Total	*117*	38.3

$\chi^2 = 2.36$ n.s.

Open relationship includes all dachs, both with or without the accessory elements (proatlas centrum and ventral arch, whether single or bipartite, and proatlas neural arches) in which the space for the normal and accessory elements was larger than in normal rabbits of the same age. Close relationship is that in which all space is occupied except for [illegible] uniform minimal space surrounding all elements, which is typical of the non-dachs (*dada*).

in figure 33. At the other extreme in a few cases such as those portrayed in figures 30 and 31 accessory elements may be present without manifesting obvious crowding. In occasional cases (at least at birth) wide spacing occurs without the presence of accessory ossification centers.

Ossification of the proatlas centrum in both normal and dachs tends to occur at around 35 days postcopulation (pc) and in a small per cent of individuals it is found at birth. In a similar small per cent it does not appear until well into the second month postpartum. A plot of the present data shows a distinct trend for the ossification of this centrum in the dachs to be more precocious than in the normal but on the other hand there may be individuals in which it fails to occur at all. In this population it is always more closely associated, and frequently fused, with the accessory proventral arch (when such is present) than with the atlas centrum. Table 3 shows that the proatlas ventral arch is in two bilaterally placed parts in 53% of individuals at birth, but in only 36.3% of 33 individuals observed some time after one month of age could two parts be identified. This may indicate a tendency to fuse as portrayed, for example, in figures 9 and 10.

These relationships of size and spacing of normal and accessory elements in many respects are very similar to those between sphenoid and occipital complexes, as described by Sawin, Ranlett, and Crary ('59). In the latter where fusions occur in sutures not normally closed, or remain partially open where normally they do close there also occurs a distortion of elements due to abnormal interrelationships or crowding. Further evidence bearing on the significance of these interrelations is revealed by examination of symmetry of the paired ossification centers of this region.

Asymmetry of normal and accessory elements. As described above, all of the atlas and proatlas (normal or accessory) elements, both the normally paired and those which are bipartite accessories, can be asymmetrical. These asymmetries may involve only one pair of elements but frequently two or more are involved. The most common of these relationships have been shown photographically (figs. 15 and 20 referred to above, and figs. 26–29). The last four are perhaps more revealing of the actual growth processes involved than is the mere presence of accessory elements themselves because almost invariably differentials in size within one pair are reflected in some way in one or the other element of the next adjacent pair. Most striking of these are the relations between asymmetrical proatlas ventral arches (or in some cases a bipartite dens) and the basioccipitals (figs. 26 and 27). They are clearly shown also in figures 28 and 29 where, in both cases three pairs of elements are actualy affected. In figure 28 these include basioccipital, proatlas ventral arch, and atlas ventral arch and in figure 29 the basioccipital exoccipital, and proatlas ventral arch. Thus there is a tendency for deficiencies in one element to be compensated or replaced later by greater growth of adjacent elements or by the inclusion of an accessory element.

Tabulation of the dachs data on the basis of asymmetry of the proatlas centrum and ventral arch reveals a decrease in the two older age groups bordering on statistical significance. Asymmetries also are found involving the exoccipitals and atlas

TABLE 3

Distribution of dachs rabbits with respect to the presence or absence of accessory elements of the proatlas including centrum (C) and proatlas ventral arch (P.V.A.)

	Total	No accessories	P.V.A.	P.V.A. C	Bipartite P.V.A.
Birth	49	1	32	16(32.0)	26(53.0)
1 Month	17	3	3	11(64.7)	8(47.0)
1 Month +	33	1	8	24(72.7)	12(36.3)
Total	99	5	43	51(51.5)	46(46.4)

Figures in parentheses are per cent.

neural arches of both dachs, heterozygotes and normals in 17 cases. These are characterized by notches either medially in the exoccipital (fig. 8 to right) or laterally on the atlas neural arch (fig 11) They are most striking in the dachs where their *shape and extension* medially is such as to indicate their compensatory tendencies. The fact that this abnormality occurs in normals as well as dachs indicates that this region is susceptible to variation *which was neither observed nor suspected* prior to its discovery in the dachs. It may or may not be a matter of coincidence that such abnormalities have been controversial in studies of human anatomy of the region (Sensenig '57)

DISCUSSION

At least four explanations have been proposed for the effects of genes which induce such localized retardations as are found in the dachs. Briefly they can be stated as (1) retardation at a critical time (Landauer '31) (2) failure of mesenchymal condensations to attain a *critical size* at proper time (Grüneberg, '52) (3) failure of such condensations to reach a *critical stage* with respect to cell differentiation or biochemical change (Grüneberg, '55) and (4) growth depression of regions where an allometric ratio already normally exists (Curry '59) Based on present information, none of these theories can be completely excluded, yet none fully accounts for the effects of the dachs gene in this region as described above. Landauer's interpretation of the creeper fowl would apply to the dachs insofar as a nonspecific reduction of growth rate is concerned If one particular time, stage or biochemical activity is more critical than another it would seem that the period of mesenchymal condensation as reported by Curry for droopy ear is the most likely in view of the growth pattern similarities induced by the two genes. However the association of growth depression within a region involving an existing allometric ratio as the critical influence which Curry suggests, *seems to apply more specifically* at least to the occipitovertebral portion of the dachs pattern because it takes into account the interrelation between neighboring tissues. The first three theories which refer to only one time size or stage, appear be based on assumption of a relative ti sue autonomy Judged by present edge of the etiology of bone and direction of growth, this may be garded as the exception rather than rule. As a generalized abnormality of region the ultimate adult pattern traceable to one tissue, seems to be pendent upon at least three relationships taking place at *times as the animal develops. These are* (a) reduction in size of normal elements in cluding minimal luxation and displacement, and maximal spacing, (b) of accessory elements, and (c) atypi fusion.

The first of these is obviously a change in the rate of growth of tissues which, though first observed in the *in the case* of a number of such could occur much earlier However *exact* point at which a defective allele gins to function is not easy to Demerec ('34) refers to certain ducing major effects in the wings eyes of *Drosophila*. Although otherwise visibly normal, these flies were later *to manifest cell lethality in the hypoderm* region of the thorax. He concluded the presence of all major genes of a gene complex are essential for vital function of a cell from one cell generation to another Thus any retardation effect in the initial stages might be very small though the early embryology has not been examined, it is obvious in dachs specimens at birth that size is reduced or spacing of the usual occipito- ossification centers is irregular and more apparent in some individuals than in others. It appears to be the first step leading to induction of accessory fication centers. Understanding of the nificance of the dachs accessory can be better understood by considering where and under what circumstances such accessory skeletal units are known In the axial skeleton they arise in at four ways three of which are associated with growth processes directionwise with the vertebra itself; (1) as inclusions the primary anteroposterior of the axial skeleton by splitting ( ) bilateral pairs of ossification centers

stead of the normal single and (3) as one or more duplications in a dorsoventral orientation, the last a result of the functional relationship between vertebra and muscle. Elements of the first occur as homoeotic complete single vertebrae or parts thereof at any one of the regional borders. Such elements have been described and extensively studied descriptively and experimentally in many species and their possible origin speculated upon. In domestic and laboratory animals many of these variations are recognized as "normal" for breeds, strains, and sublines. Others are more sporadic in occurrence and asymmetries of such elements, such as hemivertebrae, may lead to scoliosis and other abnormalities. In this category fall the accessory proatlas of droopy ear (*de*) and Danforth's short tail (*Sd*) which is acquired by the splitting of the dens into an anterior and a posterior part, the anterior in some cases being incorporated by fusion into the occiput. The proatlas neural arches of the dachs likewise appear to arise in this way. Such accessories are essentially duplications within the longitudinal arrangement of the axial skeleton and could arise from abnormality in the primary cephalocaudal growth gradient. They may however be localized in the activity of some one of the secondary gradients oriented in the same direction, the activities of which are responsible for the differential lengths of the parts of the several vertebral regions.

The second type of accessory element, arising by bilateral duplication or paired ossification centers in place of one is typical of many normal elements notably those of the skull vault and the vertebral neural arches which are paired, whereas the basal bones (basisphenoid, basioccipital, for example) vertebral centra, and sternebrae are single. Some of these always arise singly; others, such as the vertebral centra and sternebrae, are usually single but quite subject to duplication. In many cases bipartite centers later fuse into one in such manner that their double origin is never suspected. In the mouse bipartite vertebral centra were considered to occur as a part of generalized mesodermal growth retardation initiated around the twelfth day (MacDowell, et al '42) In the rabbit bipartite centra have been described by Sawin and Crary ('57a) as occurring in the thoracic and lumbar regions of two races III and X, at around 21–22 days gestation. More recent observations of later fetal ages lead us to belive that they are normally manifest for a short time only and disappear by coalescence. Cases which persist are abnormal probably due to prolonged retardation of growth. It is interesting to note that this biparted condition in the axial skeleton seems to fall in regions where there is quantitative evidences of increased breadth, as is frequently the case with the proatlas and atlas hypocentrum.

A third type of accessory is illustrated by the duplication of centers in the third dimension. Evidence for this type is not as abundant as for the other two and the variation is not as easily recognized. This is due to the relative degeneration of the segmental arrangement of somite derivatives in mammals. Its most extensive expression in the rabbit has been seen in individuals homozygous for the achondroplasia gene (*ac*) (Crary and Sawin, '62) Here multipartite centra may arise as a single dorsal center and one or more ventral centers. This is most frequently seen in the thoracic region. Better known evidence is found in the well-known ventral arch of the atlas and the chevron bones of the tail, which are considered remnants of the ventral arches of the vertebrae in lower vertebrates.

All three types of accessory are manifest in the variation at the occipitovertebral border of the dachs. Possibly some types of dens variation in the dachs may arise by anteroposterior splitting but our present observations show the duplication to be only in the other two dimensions. Frequently the dens itself is bipartite and the accessories are developed dorsally ventrally and laterally They include (1) the proatlas hypocentrum or ventral arch, which may develop singly or biparted (type 2) (2) a pair of centers whose relation to the occipitals is comparable to the elements which other investigators have found fusing either to the atlas neural arches or to the exoccipitals and which have been designated proatlas neural arches (Sensenig, '57); and (3) a rela-

tively new pair of accessory elements articulating with or attached to the supraoccipitals and extending into the foramen magnum. Insofar as we can find, these latter elements have not been previously described in other species. Their position on either side of the brain or cord and extending posteromedially suggests that they also are a part of the proatlas complex of elements which together comprise a unit which is transitional between the occipital skull complex and the first vertebra. Specifically it probably represents a more complete form of the half vertebral segment which in the normal animal is the dens epistropheus. The dens (when present either singly or biparted, or even its locale when absent) seems to be the center around which the complex is oriented. Both the atlas and proatlas hypocentra and the proatlas neural arches are of significance historically, the one being considered homologous with the chevron bones of the tail vertebrae (Evans, '39) and the other sometimes recognized as variants fused into the exoccipital or the atlas neural arches (Sensenig, '57).

That initiation of new centers or reestablishment of historically lost centers of ossification can in most cases adjust for deficient or retarded growth in some ways may appear paradoxical. However, the fact that all of the accessory centers of the proatlas region are organized in the same relative positions as those of adjacent normal atlas, axis, or skull elements indicates that they are not fortuitous, but arise from a single modification of the inherent growth forces responsible for differentiation of this region. Furthermore, once established, the accessory units resulting from this compensatory mechanism together with the normal units have a combined growth capacity sufficiently greater than the available space so that some degree of fusion is inevitable. Establishment of new centers in some way increases the growth potential of the region.

The fourth type of accessory center has been reported as occurring in the dachs rabbit at the tips of many of the vertebral processes (spinous, mammillary and particularly the transverse) (Sawin and Crary, '57b). These were interpretated as traction epiphyses because they occurred in tendons or at the muscle insertions rather than being performed in cartilage. Like the accessory elements of the occipitovertebral border, they were found at points where generalized retardation was interfering with the normal attachment and function of interrelated parts.

Traction epiphyses were first described by Parsons ('04). Their origin and evolution in birds and mammals and their relation to sesamoid bones have been described and discussed by Barnett and Lewis ('58). Their origin is related to the functional activity between muscle and bone, but they are not a component part of that bone. Further examination of dachs and normal vertebrae at various ages reveals the fact that, like the bipartite centra, these epiphyses at the tips of the spinous, mammillary, and transverse processes are not peculiar to the dachs, but may be found in other races of rabbits at various ages and under relatively normal circumstances. They appear to occur particularly in individuals which show other evidences of skeletal retardation, especially as the animal approaches adolescence. Thus these elements appear as compensatory adjustments to retarded development of the specific bony processes involved and are apparently under the tension influences of muscle and tendons normally associated with these processes.

Tension and compression appear to be prime factors in the establishment, differentiation, and shaping of all mesodermal tissues. Response of connective tissue to such forces has been demonstrated by Weiss ('29), Glücksman ('39, '42) and Weiss and Amprino ('40) in precloral mesenchyme and young scleral cartilage *in vitro*. These authors have shown that the thickness of cartilage apparently is varied inversely according to the amount of tension prevailing during formation. Strong tensions tend to suppress the differentiation of chondrogenic tissue. Moderate tensions affect the differentiating cartilaginous plate, the stronger the tension the thinner the plate. Further, a definite relation was indicated between stretch, size of proliferating surface, and growth rate.

In an intensive study of normal and screwtail mice Bryson ('45) has shown

that the influence of rapidly developing costal cartilage delays and inhibits ossification of the sternum at the region of contact in both screwtail and normal, resulting in a segmented sternum, whereas retarded development of approaching costal cartilage sufficient to prevent contact permits the ossification of the entire sternum as a single unit. The same sort of situation was found by Stein and Mackensen ('57) in the loop tailed mouse. The opposite effect, coalescence of several ribs into one cartilaginous continuum, apparently occurring by overgrowth of the ribs can also take place in the congenital hydrocephalic mouse as shown by Grüneberg ('53) The relationship between bone and cartilage in the sternum has been beautifully confirmed experimentally by Chen ('52, '53) who favored a mechanical explanation rather than a chemical one. Thus, some sort of effect upon the chondrification-ossification process by the mere interrelation of developing tissues is indicated. Such interrelations have been studied intensively by numerous investigators (notably Watanabe, Laskin, and Brodie '37 and Washburn, 47) with respect to association of the developing skull bones and the sutures by which they are separated, or by fusion, joined together These have been reviewed by Young ('59) who has shown further that experimental alteration of the cranial contents adapts the skull to fit and modifies the time sequence of maturation in sutural areas. The trabeculae of new bone are laid down according to arrangement of sutural tissue i.e parallel to sutural cells and fibers He concludes that the skull is a complex of relatively independent functional components which are intimately related to particular soft tissue and that borderline regions are susceptible to forces arising in more than one group of neighboring soft tissues, depending on *direction* and *extent* of these forces. Such interrelation of tissues, however is not limited to the skeletal tissue but may arise much earlier Zwilling ('56) has evidence of reciprocal dependence of embryonic limb bud ectoderm and mesoderm.

These same influences arising from the interrelationship of tissues are clearly shown by Fitch ('57) in the study of cleft palate and other anomalies associated with the mutants urogenital (*ur*) and phocomelia (*pc*) of the mouse where the change in spatial relationships of the head is accompanied by alteration of length and width dimensions of parts by accessory ossification centers between the frontal bones of the skull; and by duplication of ossification centers (bipartite) accessory elements and fusions in the vertebrae.

The third manifestation of retardation, *fusion of skeletal units* has been mentioned in passing several times above. Fusion, as in the case of the epiphyses of the vertebrae and long bones, is an event of maturation, which terminates the capacity for growth. However there are other cases of elements in many species which fuse prematurely under *normal* circumstances, for example in the frontal bones of the human skull, certain of the skull sutures of the rabbit (Sawin, Ranlett, and Crary '59) the pelvis and sacrum etc. The pattern of such fusions is varied from species to species and at least some lines within species (Grüneberg '50 Searle, '54; Deol, '55) Premature and abnormal localization of fusion particularly of the sphenoid and occipital bones, is also found in at least certain of the achondroplasias. In man (Stein '55) and in dwarf cattle (Tyler et al. '57) it is considered pathognomonic. In the dachs rabbit the amount of fusion in this region is varied and is accompanied by diminution of fusion in the occipital complex (Sawin Ranlett, and Crary '59) Now having also found in the same population of dachs a diminution of fusion in the epistropheus accompanied by a tendency for fusion of the proatlas accessory elements to the occipital complex, it appears that there is a forward shift of the fusion process at both the occipital and proatlas borders

Apparently the situation is closely similar to that described by Curry for droopy ear in that re-establishment of the proatlas hypocentrum either as a single or bipartite element in some manner inhibits normal fusion of the proatlas and atlas centra. Either the proatlas centrum alone or with its own hypocentrum joins with the basioccipital or the proatlas hypocentrum usurps the position of the proatlas centrum and fuses with the basioccipi

In either case the atlas centrum is forced to form a two way articulating surface or single condyle for articulation of the skull as shown by Sawin and Crary (57b) Both are reminiscent of the situation found in birds crocodiles monotremes and other earlier vertebrate forms. Hence fusion cannot be considered exclusively as a maturation phenomenon The manifestations of crowding with fusion occurring at the more closely approximated borders reveals the pattern to be dependent upon the relative intimacy and growth capacity of neighboring ossification centers generated by establishment of accessory centers under the early influences of retardation.

Fusion and induction of accessory elements both seem to be dependent upon interrelations of adjacent elements, in a manner paralleling the length to width pattern of growth observed in the *ur/ur* mice by Fitch ('57) Genetic differences in the directional pattern of vertebral growth (length and width) have also been described by Sawin and Crary ('56) in unrelated and closed racial populations of normal rabbits and in normal and dwarf cattle (Tyler Julian and Gregory '57) The concept of orientation and directional growth patterns is by no means new The law variously referred to as of developmental direction, anteroposterior development, and cephalocaudal growth is well known. It is based on the finding that development (including growth and differentiation) in the long axis of the body appears first in the head region and progresses towards the tail, with secondarily a similar progression in the transverse plane beginning in the mid-dorsal region, and progressing lateroventrally in body and proximodistally in limbs (Kingsbury '24) In plants Sinnott and Dunn ('35) developed the concept of genetic control of relative rates of growth in specific directions or dimensions by study of size and shape of plant organs. Although in animals the suggested physiological gradient mechanism by which it operates is extremely difficult to establish the patterns of differential growth arising from and centering around it have been empirically recognizable particularly in the skeleton and in most of the soft tissues for more than 00 years as described by numerous investigators. In laboratory animals the primary anteroposterior gradient is perhaps more clearly portrayed in the work of Butcher ('29) on the developing somites of the rat. Retardation of this gradient was found by Hubbs ('26) to result in production of extra somites whereas acceleration acts in a contrary manner This was confirmed by Danforth ('32) and by Roonsefell and Dahlgren ('35) in studies of the effect of temperature on the vertebrae of the fowl and fish The nature or extent of the secondary gradients is not clear but Ibsen ('47) on the basis of genetic studies in the rabbit, considered the ribs to be influenced by at least one subsidiary gradient of high intensity Danforth ('30) in a study of human vertebrae concluded that there is no such thing as a "particular vertebrae but that each vertebra is the result of numerous influences acting as individual gradients. This overlapping of gradients is apparent in the figures of fetal rabbit vertebral centra (Sawin and Crary '56) where interaction of both anteroposterior and transverse subsidiary gradients are portrayed in photographs both of bipartite centra and by measurements. This overlapping of gradients was recognized not only by Danforth but also by Huxley ('32) who pointed out that "the localized growth change is not in reality fully localized, but must operate within the framework of the main growth gradient of the body obviously an interaction effect.

Still another large mass of experimental evidence is available which although not directly bearing upon this particular problem illustrates the importance of knowledge of the interrelation of growth influences. This consists of the numerous studies of growth processes by heteroplastic organ transplantation in amphibia, which are summarized and documented by Twitty and Elliott ('34) These studies have been instrumental in demonstrating (1) the stability of the specific growth rate of a species; (2) the manner in which both intrinsic and extrinsic regulatory influences may operate in modifying it; (3) the manner in which they can regulate and compensate for disharmonic size and (4) the influence of functional and me-

chanical factors on size and on localized growth.

Thus, in view of our present knowledge of the etiology of bone differentiation discussed above, failure of normal coordination of the successive growth processes of mesenchymal condensation, chondrification, and ossification initially induced by early generalized retardation could account for both the morphological aberrations at the occipitovertebral border and also through genetic mechanisms the historical changes through which the mammalian occipitovertebral articulation has been evolved. The processes involved seem to be in no way unique since they have been demonstrated to be operative elsewhere both experimentally and genetically. The value of the dachs gene resides in the number of processes which are portrayed by it in its expression in this specific region. The intrinsic growth of the region, which normally is relatively stable (not only within the species but in mammals generally) is retarded. This is compensated by induction of accessory ossification centers which portray the effects of growth gradients in three directions (anteroposterior, transverse, and dorsoventral) and by their functional interrelations which in turn lead to abnormality in articulation and fusion. In the light of this chain of events the primary defect of growth retardation may not have any one specific critical time stage of development, or biochemical state but might well arise at conception (as suggested by Demerec (34) on the basis of experiments in *Drosophila*) and repeatedly create critically unbalanced relations, minor and unnoticeable at first, but which increase making it more difficult for adjacent tissues to compensate and fulfill their normal obligations.

Study of the changes in pattern of growth determined by the interaction of the processes in this region when the *Da* gene is transferred to new genomes should afford unique opportunity to evaluate the ontogenetic and evolutionary processes involved, and these are now in progress.

SUMMARY AND CONCLUSIONS

1. Study of the variation in morphology and localization of retardation in the occipito-atlanto-axial region of 246 rabbits (dachs and normal controls) ranging in age from birth to 21 months compared with normal controls of the same race shows abnormality of spacing, induction of from one to eight accessory ossification centers and fusion of normal and accessory parts. By their relations to normal centers of the region these are considered to represent the component parts of a complete extra unit of the axial skeleton comparable either to a vertebra with centrum neural arches and hypocentrum, or to the last or occipital ring of skull bones. Having as it does components of both vertebra and skull, it may be considered as a transitional unit inserted between the two.

2. The proatlas centrum, which in normal rabbits first appears by the thirty fifth day (postcopulation) is much more variable being found in some cases at birth (31) and in others not until after 60 days. Its fusion tends to be anteriorly to the occiput or ventrally to the hypocentrum.

3. The syndrome of dachs abnormality in this region is compared with that of similar variants in other animals and discussed in relation to retardation, induction of accessory ossification centers, and abnormal spacing the role of intrinsic and extrinsic factors of tension and compression, the interrelations of adjacent tissues and the orientation of cells and directional growth as produced experimentally by tissue transfer and by other mutations and in relation to the phylogenetic history of this region.

4. The syndrome can be interpreted on the basis of present experimental knowledge of skeletal development. It has its origin at least as early as mesenchymal condensation, and at a time when the primary cephalocaudal gradient is still active and the secondary or transverse gradient is being established (at least in this region). From this point on, the range of effect, the number and size of ossification centers and their degree of ultimate fusion, are largely determined by the initial rate of growth of each center and its relationship (proximity and position) with respect to normal and accessory neighbors.

LITERATURE CITED

Barnett, C. H., and O J Lewis 1958 The evolution of some traction epiphyses in birds and mammals. J Anat., 92 593–600.

Bryson, V 1945 Development of the sternum in screwtail mice Anat. Rec., 91 119–148.

Chen, J M. 1953 Studies on the morphogenesis of the mouse sternum. II. Experiments on the origin of the sternum and its capacity for self-differentiation in vitro. J Anat., 86: 387–401.

——— 1953 Studies on the morphogenesis of the mouse sternum. III. Experiments on the closure and segmentation of the sternal bands. J Anat., 87 130–149

Crary Dorcas D., and P B. Sawin 1957 Morphogenetic studies of the rabbit. XVIII. Growth of ossification centers of the vertebral centra during the 21st day Anat. Rec., 127 131–150.

Curry G. A. 1959 Genetical and developmental studies in Droopy-eared mice J emb. and exp. Morphol., 7 39–65.

de Beer, G. R. 1937 The development of the vertebrate skull. 552 pp. Clarendon Press, Oxford.

Demerec, M. 1934 The gene and its role in ontogeny Cold Spring Harbor Symp. Quant. Biol., 2 110–117

Deol, M. S. 1955 Genetical studies on the skeleton of the mouse XIV Minor variations of the skull. J Genet., 53 498–514

Evans, F G. 1939 The morphology and functional evolution of the atlas-axis complex from fish to mammals. Ann. N. Y Acad. Sci., Vol. XXXIX, pp 29–104.

Fitch, Naomi 1957 An embryological analysis of two mutant in the house mouse, both producing cleft palate J Exp. Zool., 136 329–357

Glücksman, A. 1939 Studies on bone mechanics in vitro II. The role of tension and pressure on chondrogenesis. Anat. Rec 73 39–55.

——— 1942 The role of mechanical stresses in bone formation in vitro J Anat., 76 231–238

Grüneberg, H 1950 Genetical studies on the skeleton of the mouse. I. Minor variations of the vertebral column. J Genet., 50 112–141

——— 1953 Genetical studies on the skeleton of the mouse. XII. Congenital hydrocephalus. Ibid 51 317–326.

——— 1955 Genetical tudies on the skeleton of the mouse XVI. Tail kinks Ibid., 53 536–550.

Julian, L. M., W S Tyler T S Hare nd P W Gregory 1957 Prem ture losure of the spheno-occipital synchondrosis in the horned Hereford dwarf of the short-headed" ariety Am. J Anat., 100 253–281.

Landauer W 1931 Untersuchungen über das Kriiperhuhn. II. Morphologie und Histologie des skelets in besondere des skelets der langen extremitäten knochen Zeit. mikro. anat. Forsch. 25 115–180.

MacDowell E. C J S Potter T Laanes and E. N Ward 1942 The manifold effects of the screwtail mouse mutation. J Hered., 33: 439–449.

Nievergelt, K. 1948 Übersicht über das auftreten der Luxatio atlanto-epistrophica beim Menschen. Schweiz. Med. Wochenschr., 78 8052.

Noback, C. R. 1944 The developmental anatomy of the human osseus skeleton during the embryonic fetal and circumnatal periods Anat. Rec., 88 91–117

Parsons, F G 1904 Observations on traction epiphyses. J Anat., 38 248–258.

Pearce, Louise, and W A. Brown 1945 Hereditary achondroplasia in the rabbit. J. exp. Med., 82: 261–280.

Rafferty S. 1956 The effect of the dachs gene on the skeleton of the rabbit newborn. Unpublished student thesis.

Sawin, P B and D. D. Crary 1957a Reporte centra t onset of ossification in two races of rabbits. Abst. Anat. Rec., 127 362.

——— 1957b Morphogenetic studies of the rabbit. XVII. Disproportionate adult size induced by the Da gene Genetics, 42: 72–91.

Sawin, P B Mary Ranlett and D. D. Crary 19[illegible] Morphogenetic tudies of the rabbit. XXV The spheno-occipital synchondrosis of the Dachs (chondrodystrophy) rabbit. Am. J Anat., 10[illegible] 237–260.

Searle, A. G. 1954 Genetical studies on the skeleton of the mouse. IX. Causes of skeletal variations within pure lines. J Genet., 52 68–102.

Sensenig, E. C. 1957 The development of the occipital and cervical segments and their associated structures in human embryos. Carnegie Inst. of Wash. Pub. 611 Contributions to Embryology 36 141–152.

Stein, I., R. O. Stein and M. L. Beller 1955 Living bone in health and disease First Ed. Lippincott, Philadelphia, 134

Stein K. F., and J A. Mackensen 1957 Abnormal development of the thoracic skeleton in mice homozygous for the gene for looped tail. Am. J Anat., 100: 205–224.

Theiler K. 1951 Die Entstehung der Densluxation bei der short Danforth-Maus. Arch. der Julius Kl s. Stiftung für Vererbungsforschung, Social Anthropologie und Rassenhygiene Band XXVI 450–454

Twitty V C nd H. A. Elliott 1934 The relative growth of the amphibian eye studied by means of transplantation. J Exp. Zool 68 247 291

Tyler W S., L. M. Julian and P W Gregory 1957 The nature of the process responsible for the short headed Hereford dwarf as revealed by gros examination of the appendicular skeleton Am J Anat., 101 477–496.

Washburn, S L. 1947 The relation of the temporal muscle to the form of the skull. Anat Rec 97 239–248.

W tanabe M D M. Laskin and A. C Brodie 1957 The effect of muscle xplantation on growth of the zygomaticomaxillary suture Am J Anat 100 319–329

Weiss, P. 1929 Erzwingung elementarer structurverschiedenheiten am in vitro wachsenden Gewebe. Roux Arch., *116*: 438.

Weiss, P. and R. Amprino 1940 The effect of mechanical stress on the differentiation of scleral cartilage in vitro and in the embryo. Growth, *4*: 245–258.

Williams, E. E. 1959 Gadow's arcualia and the development of tetrapod vertebrae. Quart. Rev. Biol., *34*: 1–32.

Young, R. W. 1959 The influence of cranial contents on postnatal growth of the skull in the rat. Am. J. Anat., *105*: 383–415.

PLATE 1

XPLANATION OF IGURES

1 ept where otherwise t ted ll figures re ventral view f dach (*DaDa*) occipito-ert bral region of the k ll. Not the shape f b oc ipit l i kulls figures 2, 3 4 nd 11 (normal nd heterozygotes) as on p red with dach fig res 5 6 and 7

2 Norm l (*bada*) t birth Show in mid line (t p to bott m) re ba i phenoid basioc ipit l tl tl ent l rch tl en t um, nd xis trum l ter ll in same order re otic bones exoc ipital nd th nd xis neu l rches Proatl entrum i bsent t this g Normally it is found fl d y fter birth b tuplaci g the tral rch

3 Het or gou (*Dad*) dachs kull l 24 hours postp t m howing tl t bottom ith norm l vent l rch (2) between t broad ex ipitals (1 nd 3)

4 Show (*Dada*) w th t rd tion f exoccip it ls, nd tl rches but no accessory os ific tion ent rs (newborn)

5 Sho newborn xi entrum nd neu l rches t bottom tl trum nd rches (1) with y h peri tl ent l rch (2) nd ry m ll pres ious proatl centrum i k lon N w the lt red hape of t k i l t he exoc ipit l t which pro t w l rche t i sed d from h h h i l medi ll

6 Show tl ent l rch f f sed bil t l enters (1) nd t v ry m ll os ific tion ter (proatl h procentrum (se 3 d ys) The tlas entrum (very sm ll) lies below the en l rch

7 Newbor show f sed h no ipital yn hondrosis, h ea l h ped basioc i i l bip th proatla rei l rch nd se to

fuse dorsally with the proatla centrum r dens. Ventral arch has been displaced t right.

8 Shown with norm l ventral arch bip rtite proatlas centrum (2) nd l rge proatlas neural arches fused t exoccipital (1) Not the crowded relationship f parts.

9 Animal (tillborn) how a simil r pattern with unusually l rge asymm trical bipartit proatlas centrum.

10) xtremely l rge bipartit proatla ventral rch tending t fuse with ba ioccipital and ex eption lly wide exoccipital with accessory neural arch lso fu ing (28 days postnatal)

11 At birth (*Dada*) how proatl neural arches fu ing t atl neural rches Not spacing f pa t nd relative size f tla neural rches. Atlas ventral arch is removed i order t show the still rtil ginous tip f the den des l ping on the tl centrum. See lso figure 15.

12 Show posterio view of tla with much red iced tral rch (1) fused t bipartit procentral rch (2) (note t top) nd t proatlas centrum (3) lyi g between (se 31 d y)

13 Vent l view of posterior of 3 months k ll bowi g occipit l condyles t bottom edge (1) an ymmetrical two parted proatl entrum (2) wi h both pa fused to the basioc ipi l nd open sphenooccipit l ynchondrosis and ba isphenoid jus bov



PLATE 2

EXPLAN TION OF FIGURES

14 Shows extreme width of exoccipitals and no accessory units. Compare relative refinement of tlas neural arches with figures 10 and 11 (age 1 day)

15 Shows asymmetry in length of basioccipital nd in width of exoccipitals. The cleft in the exoccipital on the right, it is believed separates proatlas neural arch (1) which has united with the exoccipital (age 4 days)

16 Shows extreme breadth of exoccipitals asso-ci ted with bipartit tlas and proatlas ven-tral rches partially fused to ea h other butterfly shape (age 34 days)

17 Show relatively broad exoccipitals, with very small proatlas centrum (2) in liberal space (ge 20 days) Atlas ventral rch removed.

18 Shows very narrow exoccipitals (1) with proatlas neural arches occurring as small fl t scales (2) fused anteriorly to the con-dyles of the exoccipitals. Compare with figure 23. Note the telescoped relationship of basisphenoid nd basioccipital nd fused synchondrosi (see fig 23)

19 Ventral iew kull which likewise has very narrow exoccipitals (1) and bipartite pro-tlas ventral arch (2) and with part par tially independently fused to the basioccipital between the condyles (3) (Age 3 mon hs.) (See fig. 24)

20 Shows ventral view of axis (below) and tlas of same specimen as in figure 19 with retarded asymmetrical ventral arch (1) and proatlas neural arches (3) partially fused to tlas neural arches (5) A bipartite proatlas centrum partially protrudes anteriorly (2)

21 In this specimen the normal ventral arch (1) and proatlas ventral arch (2) are fused. *Proatlas neural arches (3) lying anterolater* ally to the proatlas centrum and ventral arch are large nd fused with very narrow exoc-cipitals (4) Although difficult *to show* photographically they are quite clear in the specimen itself.

22-25 Show posterior views of skulls (22, 24 and 25 inverted) with bnormally sh ped for amina magna with two dorsolateral ossifica-tions (4) projecting int them. Note that in 22 and 23 these ppear solidly fused as parts of the ex or supraoccipitals, whereas in 24 and 25 they are small and separated by distinct sutures indicating *origins as in*-dependent ossific tion centers. Note also in figure 23 *independent centers l* belled one f four which, *in order* are identifiable (1) as protruding normal though narrow exoc-cipital, (2) bipartite proatlas (dens) (3) two scale-like *ossific tion centers partially* fused to the exoccipital (accessory exoccipit al) and (4) the projections in the lumen *of foramen magnum*


14
15
16
17
18
19
20
21
22
23
24
25
2011
CZ39
2I7
9133

PLATE 3

EXPLANATION OF FIGURES

Asymmetries of accessory elements.

26 Newborn with tlas ventral arch displaced shows an asymmetrical proatlas entral arch and basioc cipital. Note extreme breadth f xoccipitals.

27 Shows proatlas ventral arch (1) t which is f sed ingle asymmetrically placed proatlas centrum (2) Not relationship to the asymmetrical basioc cipital. The tlas ventral arch is displaced to right, age four days.

28 Asymmetry of tlas and proatlas ventral rches with rel th ly minor effect upon basioccipital. Age 23 days.

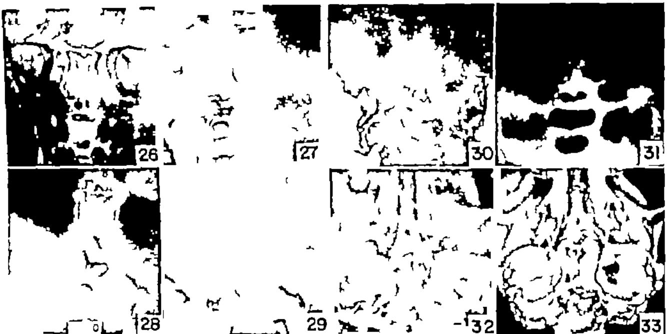
29 Shows slight asymmetry of all units, g 23 days.

30 Shows newborn dachs with ventral arch removed and l beral spacing f normal element i spite f rel tively precocious proatlas centrum (1) and accompanying large proatlas neural arches (2) projecting medially and fused to exoccipitals.

31 Dachs of 28 days with relatively liberal spacing in tlas region in spit of well developed bipartite proatlas ventral arch with parts fused

32 Dry kull of 30-d y dachs with proatlas ventral arch (1) fused to bipartite dens (2) and crowding both basioccipital and narrow exoccipitals.

33 Shows extreme crowding of biparted proatlas (1) nd proatlas ventral arch (2) and almost complete fusion to the basioccipital (3) The roughened surface of the condyles is also indicative of the tlas fusion.


26
27
28
29
30
31
32
33

One hundred and sixty bats were collected at intervals during the spring of 1959 by Dr J N Layne and prepared by the author All animals came from the vicinity of Gainesville Florida.

In order to obtain material at regular intervals several bats were kept in captivity with varying degrees of success. The bats were placed in a small animal cage and kept in the author's office with no attempt made to regulate the temperature and humidity They were fed on a daily diet of 15 to 20 meal worms per individual. Fresh water was made available in a petri dish at all times.

Complete serial sections of the entire female reproductive tract of pregnant specimens were prepared from the preovulatory stage to mid-gestation. After mid-gestation the conceptuses were removed and partial serial sections were made of the uterus containing the placenta and fetal membranes. The ovaries were generally removed and fixed separately

For the morphological and develop- study a chronological series of uteri fixed in Bouin s, Zenker's, Helly's and 10% formalin were embedded in paraffin and cut at 5 to 10 μ. These were stained with Harris' hematoxylin and eosin, Masson s trichrome, Mallory azan and *in toto* in HCl carmine. Histochemical preparations were also used, where appropriate to elucidate the morphology of certain areas.

Alkaline phosphatase activity was examined in a chronological series of pregnant uteri fixed in cold acetone and cold formalin. Paraffin sections of 5 μ were stained according to the method of Gomori (41) Sections were incubated in a buffered substrate of sodium B-glycerophosphate at a pH of 9 6 for from 5 to 60 minutes. Control slides were incubated in the same solution for the same period of time but with the sodium B-glycerophosphate excluded.

Cold acetone-fixed sections were treated for acid phosphatase activity in a substrate of sodium B-glycerophosphate at a pH of 4 7 for 36 hours. Control slides first treated for 15 minutes in 0 01 M sodium fluoride to inhibit the enzyme, were incubated along with the test slides.

The presence of lipids was investi... throughout the gestation period by the ... of material fixed in "formal- (Baker 46) and subsequently chromed. Frozen sections of 10 to 15 were prepared and subjected to tests to determine their lipid ... McManus s Sudan black B method (' '53) was employed to determine the lipid content. Neutral lipids were ...mined by the use of Cain s (47) Nile ... sulphate method. Control slides were tracted with acetone. The ... test (Baker 46) was used to ... phospholipids control slides being tracted with pyridine.

For the study of birefringent lipids ...sues fixed and sectioned as above mounted in glycerin and examined ... the polarizing microscope.

Tissues fixed in 2% osmic acid and ...bedded in methacrylate (Palade '52) subsequently sectioned at 5 μ, mounted glycerin and examined under the li... microscope.

Paraffin sections 8 μ thick, fixed in Zenker s Helly s, Bouin s ... 10% formalin were treated by McM... (46) periodic acid Schiff test to ...strate their glycogen content. ... from all phases of gestation was ... Control slides were first treated with sal... for 30 minutes at 37 C.

Two tests were used to determine presence of iron. Perls method ('53) for ferric iron was applied to 6 paraffin sections of material fixed in acetone, buffered formalin (pH 7) 10% formalin. The Turnbull blue for ferrous iron (Pearse '53) was appl... to similarly prepared tissues.

For demonstration of the Golgi ...tus the DaFano-Cajal method (... '57) was employed. The material was ...tioned at 2 to 5 μ.

Tissues fixed in *Helly s, Zenker s* ... formalin and buffered formalin (pH ... were sectioned at 8 μ and subjected ... Schmorl s thionin and the toluidine ... methods (Pearse '53) to demons... metachromatic substances Solutions 0 25% and 5 × 10 M ... toluidine blue were used The ... were stained *30 seconds* the latter hours. Examinations were made ...

water and immediately upon mounting. Material for the demonstration of RNA was prepared in the same manner. The sections were then incubated in veronal buffer (pH 6.78) for three hours at 50 C. Control slides were incubated in a 10% solution of ribonuclease in veronal buffer for the same length of time. These were then stained together for 24 hours in a 5×10^{-4} M solution of toluidine blue.

Sections of Bouin's and formalin-fixed material were incubated for three hours at 37°C in a 10% solution of hyaluronidase in 0.85% saline. Control slides were incubated for the same length of time in 0.85% saline and were then stained simultaneously in 5×10^{-4} M toluidine blue.

The Feulgen reaction (Stowell, 45) was employed to demonstrate the presence of desoxyribonucleic acid using material fixed in Bouin's and Helly's fluids and sectioned at 8 μ.

To determine the gross circulatory pattern of the placenta, several dissections of the fetus and umbilical cord were performed under the dissecting microscope. For the microscopic study of the placental circulatory pattern, a variation of the milk-injection method (Carleton, '57) was found to be the most satisfactory. While working with the delicate fetal circulation, it was found that washing the blood out of the vessels with sodium sulphate previous to injection was unnecessary. It was also found that light cream (preferably homogenized) proved to be superior to milk as perfusing fluid when followed by the Sudan black B stain for lipid. Injection was most satisfactory when the abdomen of the fetus was opened and the left umbilical vein cut. The injection was then made into the right umbilical artery. After ligature of the umbilical cord, the fetus was removed and the entire uterus and placenta were fixed in the prescribed fixative. After gelatin embedding frozen sections were stained in Sudan black B.

OBSERVATIONS

Many early attempts were made to maintain bats in captivity without a substantial degree of success, probably due to the substitution of unnatural foods. This led to such statements as that of Gates ('36):

> The free-tailed bats, *Tadarida cynocephala* (LeConte) apparently do not thrive in captivity. They will eat nothing, drink little and resent handling, apparently never becoming tame enough to be handled without resentment.

Constantine ('52) and Krutzsch and Sulkin ('58) have presented programs for the maintenance of free-tailed bats in captivity. The author followed the program of Constantine more closely but without any attempt to maintain a constant temperature and humidity. It was also found to be unnecessary to keep the female bats in individual containers, as many as four being kept in the same cage at one time.

Observations made on a group of four bats which were separated from a shipment arriving at Ithaca on April 10, 1959 and maintained in captivity for an extended period are perhaps of special interest. All four learned to feed in captivity with only one forced feeding of meal worms on the day of their arrival. The next day no feeding was attempted and the third day meal worms were put into a Syracuse dish and cut into several pieces to prevent their escape. These were then put on the floor of the cage, along with the water which had been kept in the cage constantly.

Two of these animals were sacrificed within two weeks, and the conceptuses were in perfect condition. One of the remaining bats aborted on May 12, 1959. The posterior portion of the fetus had been resorbed, whereas the head and thorax were still in relatively good condition. This bat was still in captivity during the month of July and was eating well. The fourth one carried her conceptus until June 20, 1959, when she was sacrificed for tissues at term. At this time weights and measurements of the mother and fetus were recorded. Total weight of mother and fetus was 15.2 gm, weight of the mother 11.7 gm, weight of the fetus 2.7 gm, and weight of the placenta and fetal membranes plus fluid 0.8 gm. Crown-rump measurement of the fetus was 24.5

mm. The head of the fetus was toward the cervix of the mother The fetus was in excellent condition and undoubtedly would have been born within a few days.

All observed parturitions of the *Tadarida* have been breech births (Sherman, '37) but this is probably not an invariable situation. In the present study records were kept of the orientation of the fetus during the last third of the gestation period. Out of 23 specimens observed, 19 had their cephalic end directed toward the head of the mother Seventeen of these had the dorsal surface of the embryo against the ventral body wall of the mother the remaining two were orientated with their ventral surface toward the maternal ventral body wall. Four fetuses had their heads toward the cervix and their dorsal aspect toward the ventral body wall of the mother Owing to the extremely cramped condition in the uterus (the fetus weighing about one fourth as much as the mother) it is assumed that a reversal of this position before birth would be very unlikely Therefore although the majority of births e breech births about one fetus out of ery five may be delivered head first.

GROSS MORPHOLOGY

The uterus of *Tadarida brasiliensis* is of the bicornuate type The corpus uteri opens via a single cervical papilla into the vagina. There is no externally visible constriction at the juncture of the vagina and uterus. The corpus uteri is relatively long 2.5 mm, and gives rise to two bilaterally symmetrical cornua, each approximately 1 mm in length The fallopian tubes enter at the apices of each cornu, slightly toward the median aspect via and oviducal papilla. The oviduct is irregularly coiled and about 4 5 mm long. At its distal end it opens onto the inner surface of the ovarial bursa into the periovarial space. An opening also exists between the periovarial space and peritoneal cavity A number of fimbriae surround the opening The right ovary is about 1 mm in diameter but the left is usually not more than 0 5 mm and may be considerably smaller

Out of 35 specimens collected on February 21 1959 about two weeks before normal copulation and ovulation (Sherman, '37) 31 showed a marked dilatation of the right horn of the uterus. The ovarie were prepared and examined histologically but no ovulation had occurred.

It was noted that of the 126 pregnan uteri observed, all implantations occurre in the right horn, and, as revealed b histological examination, all ovulation and resulting corpora lutea occurred i the right ovary No corpora lutea were ob served in the smaller left ovary These observations are in agreement with thos of Sherman ('37) who found that out o 30 specimens examined all ovulations ha occurred in the right ovary

HISTOLOGY

Progravid female reproductive tract

Since these animals were collected onl during the spring a brief discussion wi follow of the histological structure of th reproductive tract prior to ovulation. A complete description of the entire cycle i impossible with the material available

Shortly before ovulation, the stratifie squamous epithelium of the vagina is ex tremely thick, 15 to 20 layers of cells, an on occasion even a greater thickness wa observed. A high degree of cornification i present and many of these cells hav sloughed off into the lumen of the vagina A much reduced layer of stratified squam ous epithelium, eight to ten cells thick lines the cervical papilla and continue into the corpus uteri (fig. 33) In the co pus uteri a further reduction of the strati fied squamous epithelium is observed Near the cervix it is eight to ten cells i thickness but it decreases throughout t length of the corpus and is from three t five cells thick at the fundic end where transition to endometrial tissue occurs (fi 32) No glands are to be found in th cervix or proximal two-thirds of the corpu uteri. Endometrial tissue and uteri glands are limited to the bilateral cornua but in some individuals uterine gland may be found in the outer one-third of th corpus uteri. However when this doe occur they are sparce and shallow Th bilateral cornua are richly endowed wi relatively long, slightly convoluted tubula glands which may be branched and dilat at their fundic end and filled with a secre tion. A simple cuboidal epithelium line the uterine glands and is continuous wi

the epithelial lining of the cornu which is also simple cuboidal in nature; no cilia are present. The dilatation of the right cornu prior to ovulation seems to be a result of a considerable hypertrophy of the endometrium, especially of the cells in the gland-bearing area; deeper in the region of the gland crypts the cells are not hypertrophied, and the stroma here is much denser. Interestingly the endometrium of the left horn is not hypertrophied and the cornu thus remains undilated. Many leucocytes are scattered throughout the endometrium, being most concentrated just beneath the epithelial lining of the uterus. It is difficult to distinguish precisely where the endometrium ends and the muscularis begins.

The epithelial lining of the papillary and intramural portions of the fallopian tube is low cuboidal and non-ciliated in nature. The major portion of the tube however is lined by a columnar epithelium which has ciliated and non-ciliated cells interspersed with one another. The infundibular portion and fimbriae are covered by a tall columnar epithelium with very prominent cilia on all of the cells.

In these progravid animals the right ovary contains many large vesicular follicles but the left contains very few. After ovulation, a corpus luteum is established which persists throughout gestation.

Immediately after ovulation when progesterone is presumably elaborated by the newly formed corpus luteum, the endometrial tissue rapidly increases in thickness until the entire endometrium and epithelium of the right cornu is involved. Concomitantly the diameter and length of the glands increase and they become tortuous (fig. 22). With the subsequent expansion of the blastodermic vesicle the endometrium becomes flattened and differentiation between the muscular and endometrial layers becomes more difficult.

The yolk sac

Cells delaminate from the inner cell mass and proliferate to form a complete lining of the trophoblastic vesicle creating a bilaminar omphalopleure. Mesoderm from the primitive streak area spreads laterally between the trophoblast and the newly established endoderm. The cavity of the yolk sac is at first very large, the omphalopleuric wall coming into contact with the endometrium on all sides except for a relatively small antimesometrial area devoted to the formation of the amnion (figs. 3 and 4). Once the yolk sac has reached a diameter of about 2.5 mm the allantois begins to develop (fig. 7). At this time the neural tube of the embryo has begun to close and a well developed foregut is present, but the hindgut has not yet begun to form. With continuing growth of the embryo and the lateral extension of the exocoelom the embryonic half of the yolk sac begins to infold into the abembryonic half and concurrently the originally squamous endodermal cells hypertrophy becoming cuboidal to columnar in appearance. This hypertrophy of the endoderm accompanies the spread of the mesoderm and vitelline vessels laterally. The previously smooth inner surface of the yolk sac is now irregular and continues to become progressively more so as invagination of the yolk-sac roof progresses. Simultaneously the expansion of the exocoelom causes the lateral walls to collapse. The inner surfaces eventually become approximated and the original cavity is obliterated. It is not until late in the gestation period however that they become intimately fused (figs. 5 14). The vitelline blood vessels eventually completely surround the yolk sac but the exocoelom does not, resulting in a permanent adherence of the yolk sac to the chorionic wall over a small area near the original abembryonic pole. The mesothelium on the outer surface of the free portions of the yolk sac also becomes hypertrophied although somewhat later than the endoderm, and numerous redundant villi or folds develop on this side of the membrane increasing the surface exposed to the exocoelom. This process begins about the early limb bud stage. The vitelline blood vessels lie between these two much interdigitated glandular appearing epithelia.

Numerous granules of variable size are very frequently observed within the cytoplasm of the mesothelial cells of the yolk sac after mid-gestation (fig. 15). They were not present in tissue examined at term. These granules presumably pro-

degenerative (figs 11 12) [These large multinucleated cells may be found at term, although they are relatively scarcer at this time.]

As the discoidal placenta becomes established and functional, further changes become evident in the area of the diffuse placenta. The first extravasation of blood mentioned above occurs about mid-gestation and subsequently the more superficial maternal blood vessels are also eroded until their blood is extravasated into the surrounding tissue. Thus the maternal blood vessels are progressively eliminated from the area, and at term the rich network of *fetal* capillaries has been displaced to the internal surface, although some vessels still penetrate more deeply During the later third of gestation the remaining parietal tissue becomes permeated with lipid material (figs. 29 30)

The decidua basalis is not extensively infiltrated by trophoblastic tissue, and portions of the uterine glands may still be recognized in this area at mid-gestation T" endometrium here eventually plasmo- and at term the entire area is com- -d of large multinucleated cells some ^I which appear pycnotic.

Turning again to the area overlying the opening of the fallopian tube which is destined to become the discoidal placenta a large pad *of* admixed cellular and syncytial trophoblastic tissue is early observed (fig 5) Many mitotic figures are present within it. During the early limb bud stage the allantoic vessels migrate over the inner surface of the chorion and the placental pad" *may be observed to be partly* covered by them. But within a short period the yolk sac is completely displaced and the allantoic vessels overgrow the entire surface of the future placenta. Concomitantly the maternal vessels of the endo*metrium infiltrate the trophoblastic zone.* Shortly allantoic blood vessels begin to infiltrate the area and ramify in close relation to the maternal labyrinth The placental barrier prior to mid-gestation (10–12 mm embryo) is thus composed of the *fetal endothelium a thin layer of fetal* connective tissue a well defined layer of trophoblast, the basement membrane of the maternal capillaries and the maternal endothelium which is not always easily identifiable (fig. 16)

Shortly after mid-gestation, the matern endothelial nuclei disappear and as placenta advances in age the membrane too becomes irregular and distinct. PAS preparations which re the membranes clearly in the early p' centa do not permit a clear cut identification of them in the placenta at term. gestation advances the fetal capillarie extensively invade the trophoblastic tissue and by term the trophoblastic nent is relatively inconspicuous (fig. 17) In consequence the fetal capillaries a network around the maternal l channels and in many cases only ultrathin membrane of indeterminate position can be distinguished the fetal and maternal circulations (s. also Wimsatt '58)

The umbilical cord and fetal circulation

Five vessels are to be found in the definitive umbilical cord (figs. 1 and 2): vitelline artery which comes from the *sal aorta just cephalic to the ren* l a vitelline vein which enters the vena cava just cephalic to the iliac veins, a right and a left umbilical artery and left umbilical vein. At term, two vessel are much larger than the others, the l *umbilical vein and the right* umbilic artery These two vessels are responsi for the entire blood supply to and from t discoidal placenta The right umbil artery vascularizes in a general way central portion of the placenta and *small branches into the adjoining* chorion. Some of these small enter the yolk sac where it lies over smooth chorion other small from the placental disc enter the periphery of the yolk sac where it adjoins *disc.* The left umbilical vein receives eral large branches which *arise* from circumference of the placenta. *It* also ceives smaller branches from the smoot chorion The left umbilical artery is relatively small at term and sends *only to the chorion outside the placental* disc. The vitelline vein and artery comprise the main vascular supply of glandular yolk sac (fig 1) It was t

determined when the other vitelline vessels and the right umbilical vein disappear

HISTOCHEMISTRY

Alkaline phosphatase

Alkaline phosphatase activity in the uterus, prior to implantation, is very prominent in the apical portion of the epithelial cells lining the uterine glands (fig. 22) Activity was also observed in the nuclei of these cells as well as in the secretions found in the lumen of the glands. In specimens examined prior to ovulation, no activity was observed in the epithelial cells lining the lumen of the uterus, but as the time of ovulation approached the phosphatase activity became prominent in these cells also.

In a free uterine blastocyst the trophoblastic cells show a positive reaction. The cellular trophoblast does not continue to react positively but the syncytial trophoblast derived from it gives an intense reaction from the time of its origin throughout gestation. A wide band of activity in the syncytial trophoblast is to be observed over the entire area of the diffuse labyrinthine placenta at any stage after the syncytial trophoblastic tissue has begun to develop (figs. 23 24) In the area of the decidua basalis, however this activity is much reduced. A ring of activity outlines each maternal blood space in the discoidal placenta, being concentrated in the layer closest to the maternal blood, probably the basement membrane of the maternal endothelium, which is inconspicuous or has disappeared (fig. 25)

A positive reaction is detected in the outer layer of the splanchnic mesoderm of the yolk sac, first noticeable at the very early limb bud stage when the mesodermal epithelium is squamous in nature (fig 23) This activity remains after hypertrophy of the mesothelial cells and throughout the remainder of gestation The endothelium of all blood vessels in the yolk sac gives a positive reaction from the early limb bud stage onward (fig 26)

Acid phosphatase

Prior to ovulation, an acute acid phosphatase reaction was observed in the endometrial tissue adjoining the fundic portions of the uterine gland whil a weak reaction was obtained in the endometrial tissue near the lumen of the uterus (fig. 20) At term an intense positive reaction is observed in the deeper portion of the decidua parietalis close to the decidua basalis where the membranous chorion undercuts the discoidal placenta This activity diminishes toward the antimesometrial area and is lost almost completely in the decidua basalis. Areas of acid and alkaline phosphatase activity do not coincide in this marginal region of the disc (figs. 21 24)

Lipids

Treatment with Sudan black B failed to reveal any lipid in the uterus up to the limb bud stage material was not available from the limb bud stage until well beyond mid-gestation (embryos of 15–18 mm) In these later stages large quantities of lipid occur throughout the entire trophoblastic tissue overlying the decidua parietalis (fig. 29) The droplets nearest the fetal side tend to be the largest while those toward the myometrium are very fine Only a small amount of lipid occurring in fine droplets is observed in the decidua basalis. Sudanophilic lipid is also found in the trophoblastic cells surrounding the maternal blood spaces in the discoidal placenta

The endodermal cells of the yolk sac after mid-gestation, contain large droplets of lipids stained by Sudan black B Most of these droplets are near the basilar portion of the cells. A background wash appears in the hypertrophied mesothelium on the external surface of the yolk sac, but discrete droplets are absent.

In the yolk sac the large lipid droplets of the endoderm and lipid wash of the mesothelium stained by the Sudan black B method both stain red with Nile blue sulphate Sudanophilic lipids of the decidua parietalis were also stained red with Nile blue sulphate (fig. 30). These droplets however contained an eccentrically located clear area, which was proportional in size to the size of the droplet. Large droplets contained more than one of these clear areas.

In the decidua parietalis where a strong Nile blue staining was obtained for neutral lipid a positive result was also

in his paper on unilateral progesterone reaction in the uterus of *Pteropus* suggests two possible mechanisms by which the reaction in the fruit bat may be explained. He found an isthmus of tissue joining the ovary to the uterine wall in which small blood vessels were observed he theorized that the progesterone secretion from the corpus luteum could be preferentially distributed to the distal end of the right horn, thus conditioning the implantation site He also suggested that direct diffusion of progesterone might occur through this short isthmus of tissue.

No isthmus was observed in *Tadarida*; however a preferential blood flow carrying estrogen and progesterone to the right horn and causing the threshold to rise sufficiently to effect a reaction there and not in the left cornu, is still a possibility It may be found that an explanation of this peculiar unilateral activity lies in the difference in the relative responsiveness of the endometrium of the two horns to estrogen and progesterone.

Morphogenesis of the yolk sac of *Tadarida* seems very closely related to that of certain members of the Vespertilionidae, e.g. *Myotis lucifugus lucifugus* (Wimsatt, 45 and 49) the Emballonuridae e.g. *Taphozous longimanus* and the Hipposideridae e.g. *Hipposideros bicolor pallidus* (Gopalakrishna, '58) and contrasts greatly with that of the Phyllostomidae (Hamlett, '35) and Desmodontidae (Wimsatt '54) Plates accompanying a paper by Sansom ('32) show that the early stages of the yolk sac of *Molossus rufus* and *Molossus obscurus* are also very close to those found in *Tadarida*. The differences in the morphogenesis of the yolk sac of the Molossidae, as compared with the Phyllostomidae and Desmodontidae seem to be directly related to the types of implantation observed in each. The fact that yolk sac morphogenesis in the Vespertilionidae and Emballonuridae parallels that of *Tadarida* is probably due to the fact that their mode of implantation is similar being partially superficial in the Vespertilionidae and Emballonuridae and completely superficial in the Molossidae This condition allows the yolk sac to expand with the enlarging chorionic sac, which ultimately fills the entire uterine cavity The yolk sac in these families is vascularized very early in advance of the lateral spread of the exocoelom and an important physiological role is undoubtedly performed by the resulting relatively close approximation of the fetal and maternal blood vessels. This phase of the yolk sac is rapidly ended by lateral extension of the exocoelom and invasion of the allantoic splanchnic mesoderm which supplants the vitelline circulation. The yolk sac becomes detached from the trophoblastic tissue in all but one small area, where it remains attached until term. This attachment is close to the developing discoidal placenta and is mesometrial, or at the most abembryonic position of the yolk sac, where the advancing vitelline vessels nearly meet. As the allantoic vessels invade the area of the trophoblast previously occupied by the vitelline circulation, the yolk sac begins to collapse and the endoderm hypertrophies into a tall columnar epithelium. The mesothelium of the yolk sac facing the extra-embryonic cavity also hypertrophies. As the yolk sac continues to collapse, the two epithelia become very interdigitated and are separated only by a thin layer of connective tissue containing the vitelline vessels. This situation is paralleled in the Vespertilionidae (Wimsatt 45) The yolk stalk is obliterated before the limb bud stage

Shortly before mid-gestation the hypertrophied mesothelial cells of the yolk sac begin to accumulate spherical bodies of proteinous material as previously observed in *Myotis lucifugus* by Wimsatt (45, 48, 49) and in two other Vespertilionids by Branca ('23) and Gerard ('28) Great numbers of these acidophilic and PAS-positive globules were to be found in the yolk sac during the period following mid-gestation (fig. 15) but were not found at term In *Tadarida* as in the Vespertilionidae these accumulations are first confined to the infolded segments of the mesothelium which are not directly exposed to the exocoelomic cavity but eventually appear also in mesothelial cells on the exposed surfaces Contrary to the situation in *Myotis lucifugus* in which the inclusions are present at term (Wimsatt 45) they seem not to persist to term in the yolk sac of *Tadarida*

Several attempts have been made to explain these and similar granules in the rodents (Wislocki, Deane and Dempsey '46) and in bats (Wimsatt, 49). It seems possible, in view of the disappearance of these granules in *Tadarida* during the late stages of gestation, that they may provide a source of energy. The granules appear during the height of vascularization while the embryo's requirements are relatively low. Thus, they may be a complicated energy store, which is built up and is later degraded and used by the embryo via the vitelline circulation.

In addition to the cellular inclusions many deposits of relatively acellular material, possibly fibrinoid, are loosely connected to the yolk sac, and possibly to the amnion. It is evident that the material in question arises at least in part in the mesenchymal tissues of the yolk-sac wall, but whether from plasma elements or degenerating connective tissue fibers or ground substances was not determined. The substance is PAS-positive and stains orange in Masson preparations. It persists to term and appears whitish in gross dissections.

The method of formation of the definitive amnion by actual folding is not common in many species of bats thus far described and is therefore of particular interest. Sansom ('32) describes amniogenesis in the Molossidae as being by cavitation. His study however is of very early blastocysts. In his summary he states that the roof of the cavity which he observed eventually thins and disappears. His description could seem to relate to the formation of the early primitive amnion. The true amnion is not formed until much later and is not completed until the neural tube stage. The peculiarity of the prominence of the tail fold of the amnion in amniogenesis has not been described before and is possibly due to the extreme delay of the migration of mesoderm into the proamniotic region. The absence of this mesoderm may be a factor in preventing the head fold of the amnion from migrating in its usual manner. The somatopleure of the proamnion rises slightly quite early but becomes arrested and remains relatively unchanged until the hind fold migrates far forward to effect a junction. This method of amniogenesis contrasts sharply with that of other Chiroptera: amniogenesis in Phyllostomatidae (Hamlett '35) and Desmodontidae (Wimsatt, '54) is wholly by cavitation; in Vespertilionidae the definitive amnion appears to be formed not by an actual folding process, but by an upgrowth of ectodermal elements from the margin of the embryonic disc (Duval, 1895, 1896, 1897; Gerard, '28; Wimsatt, 44).

Allantoic development does not contrast greatly with that found in the families mentioned above. It would seem however that the allantois of *Tadarida* arises somewhat earlier than presumed by Hamlett ('35) for Phyllostomatidae and that the cavity attains a greater diameter than that described for the other bats. The development begins before the formation of the hindgut, and the sac achieves its maximum size during the early limb bud stage, but by the late limb bud stage rapid degeneration and infiltration of mesenchymal tissue obliterates the entire cavity and stalk except for the extreme proximal end. Traces of the stalk may be found in the umbilical cord until mid-gestation (embryo of 10-12 mm).

Since implantation in *Tadarida* is superficial, no decidua capsularis is formed. The trophoblast expands and comes in contact with the uterine [illegible] entire circumference. A rapid and [illegible] sive erosion of the maternal tissues [illegible] sues. None of the previously [illegible] have shown the degree [illegible] in the Molossidae [illegible] zation of the yolk sac [illegible] gree of erosion [illegible] cellular trophoblast [illegible] cytial trophoblast [illegible] cytolizes the epithelium [illegible] and [illegible] of the uterus [illegible] endometrium.

As some inv[illegible] other species [illegible] for changes betw[illegible] physiological ex[illegible] culation [illegible] cir[illegible] vitelline circ[illegible] via the appropriate [illegible] It seems over most of the [illegible] exchange [illegible] surface as be[illegible] placenta. The [illegible] the cords which run deep [illegible] the endometrium are not however [illegible] by the [illegible]

sels. The allantoic vessels supplant the vitelline circulation and allantoic capillaries and connective tissue penetrate the trabeculae of trophoblastic tissue, and in this manner establish a diffuse labyrinthine endothelio-chorial type placenta, the second major physiological exchange device with the maternal circulation. This placental relationship which covers the entire inner wall of the uterus has not been described before in Chiroptera (or any other mammal to my knowledge) and may be contrasted with the diffuse villous syndesmochorial type found in *Myotis lucifugus* as described by Wimsatt (45) It is destined to play a major role in the physiological exchange between mother and fetus throughout the remainder of gestation. These functions will be discussed further in relation to the histochemical findings.

When implantation is completed the embryonic disc is located antimesometrially while the "pad" which is now distinguishable and which is destined to become the discoidal placenta is located [me]sometrially overlying the entrance of [the] fallopian tube This to my knowledge [i]s in distinct contrast to all other Chiroptera studied. In the Phyllostomidae Vespertilionidae and Desmodontidae implantation (and subsequently the discoidal placenta) is antimesometrial, and the embryonic disc is also oriented antimesometrially In the suborder Megachiroptera represented by one family Pteropidae (Moghe, '51 '58) both implantation which is interstitial and orientation of the embryonic disc are mesometrial. Therefore the Molossidae represent the only Chiroptera presently known to have the definitive placenta and embryonic disc orientated at opposite poles of the blastodermic vesicle

The mode of establishment of the discoidal placenta is of particular interest since it appears to differ in several respects from that reported in other Chiroptera. The initial erosion of the superficial endometrium is rapid If typical syncytial trophoblast was originally present here it has disappeared in the earliest formative stage of the discoidal placenta available in this study for the region is occupied by a dense "pad" of trophoblastic elements which seem to consist in the main of cytotrophoblast. The fundic portions of uterine glands and endometrium associated with them remain distinguishable beneath this pad until the limb bud stage. No extravasation of maternal blood is observed in the decidua basalis region such as occurs in the parietalis as described earlier The glands of the parietalis likewise disappear much earlier In other families of bats erosion is apparently maximal in the area of the presumptive decidua basalis.

Wimsatt ('58) in his analysis of the placental barrier in Chiroptera presents a new concept of the relationships between the maternal and fetal circulations. His discussion is mainly concerned with the development and organization of the definitive barrier It includes a brief discussion of the Molossidae. An interpretation of the early stages as found in the present study will now be presented with a brief comment on the definitive morphology Three reasons for the belief that the syncytial trophoblast disappears early in the area of the discoidal placenta are: (1) no extravasation of the maternal blood is observed thus erosion which in the parietal areas is attributable to syncytial trophoblast is arrested prior to rupture of the endothelium (2) only one layer of epithelial cells is observed between the maternal blood space and the fetal connective tissue even at very early stages and (3) with the phase microscope (but not with the light microscope) a plasma membrane can often be detected around the cells in the early placental pad and frequently also in conjunction with the trophoblastic cells surrounding the maternal blood spaces in later stages

The maternal endothelium and basement membrane on which it lies are readily apparent in the earl[y] stages as also observed by Wimsatt ('58) The enclosed maternal vessels during the growth of the discoidal placenta subsequently increase their diameter many fold. This rapid expansion of surface area is probably a contributing factor in the progressive thinning of the endothelial cytoplasm and the apparent disappearance of the endothelial nuclei. By mid gestation and there[illegible] after it is impossible to locate any maternal endothelial nuclei

By mid-gestation also the fetal capillaries have begun to push into the trophoblast surrounding the maternal spaces and this process continues until eventually the fetal vessels comprise a dense and extensive network of capillaries embedded within the walls of the maternal blood spaces thus achieving an extremely close association with the maternal blood passages. The trophoblastic elements are indistinct at term, at which time only an occasional trophoblastic cell nucleus may be located in the wall surrounding the maternal blood space, where previously there had been a continuous layer of trophoblast. The placental barrier is now reduced at many points to an exceedingly thin membrane the definitive constituents of which are impossible to observe with the light microscope However despite the heavy infiltration of the walls of the maternal channels by fetal capillaries it is difficult to imagine how the maternal blood could be contained without some continuous encompassing tissue Therefore it will probably be found that either remnants of a highly attenuated maternal endothelium remain (which seems unlikely) or a no less attenuated trophoblastic membrane is involved

The most striking histochemical features of the decidua parietalis area involve alkaline phosphatase lipids and iron All three are maximally apparent in the area beneath the placental margin but are observed nevertheless elsewhere in the parietalis. Glycogen on the other hand is not found here in significant amounts in later stages but is presert early within the cytotrophoblastic comp onents of the chorion which overlie the parietalis at all stages

Many papers h e been presented linking the enzyme a kaline phosphatase with sites of glycogen deposition Wislocki and Dempsey (45) found that an area of alkaline phosph ase activity invariably intervenes betwee the maternal blood vessels and the g cogen depositions in the placenta of th sow cat rodent and man Wimsatt (48 found thi relationship also present in the placenta of *Myotis lucifugus* In *T darida* similar situation prevails The glycogen deposits observed during the limb bud st ge are separated from the maternal capillaries by an area of intense phosphatase activity The blood spaces of the discoidal placenta are conspicuously ringed by alkaline phosphatase which intervenes between the glycogen deposits located in the trophoblast and the maternal blood spaces.

The hypothesis that lipid metabolism and alkaline phosphatase activity are related (Hard, 46; Wimsatt, 48) is supported by the observations of the present study Neutral fats and phospholipids abound in the trophoblastic tissues overlying the decidua parietalis where phosphatase activity is so prominent. It should be pointed out, however that phosphatase activity is present before lipids are demonstrable by the technique applied. Neutral lipids, as revealed by Nile blue sulphate are also present in the mesothelium of the yolk sac; and as revealed by Sudan black B and Nile blue are present in the trophoblast in close approximation to the phosphatase activity of the parietal area.

It is evident that the embryo must acquire its iron supply from the mother but the means by which it achieves this end apparently differ from one species to another In some mammals, iron is secreted by the uterine glands, in others erythrocytes are destroyed in the uterine lumen and in still others the main source of iron is by direct absorption from the maternal blood (Wislocki Deane and Dempsey 48 Wislocki and Dempsey 46abc Wislocki and Wimsatt 46 Flexner Vosburgh and Cowie 48 Wimsatt 49) Within the Chiroptera alone several methods of obtaining iron have been observed. A specialized placental hematoma may represent the principal source in the Emballonuridae (Wimsatt and Gopalakrishna '58) in *Myotis* it has been concluded t at practically all the embryo s requirem nt are met by pa sage d) from the m tern l blood through ... nou ... f h allant ... (Wim ...)

It h ... l ed ... h ... *T* ... *and* ... n ... chc ... th e ... tn ... dular or ... eq ... um ... dantation ... ted ... since eros ... f ... ndom ... *rida* takes pl ... ry earl ... rial deposits are

absorbed by the advancing trophoblast. The extravasated maternal blood of the decidua parietalis which was described earlier is quickly broken down and absorbed by the trophoblast. Since these deposits of iron are so conspicuous it seems only logical to interpret them as major supplies of fetal iron in *Tadarida*. This does not exclude the possibility of course that later requirements of the fetus may be met by more direct transmission of iron through the barrier of the discoidal placenta.

SUMMARY AND CONCLUSIONS

It was found that *Tadarida cynocephala* can be maintained in captivity during pregnancy with normal development of the fetus

Gross and microscopic structure of the uterus fallopian tubes and ovary prior to ovulation are described. A unique situation is observed in that the cervix and corpus uteri are lined by a thin stratified squamous epithelium

Implantation is central and superficial and the embryonic disc is oriented antimesometrially The discoidal placenta is established mesometrially however a situation which has not been described before in Chiroptera in combination with an antimesometrial orientation of the embryonic disc The yolk sac is large at first but subsequently it collapses forming a glandular appearing body which retains a narrow attachment to the chorionic wall abembryonically

An extensive chorio-vitelline placentation characterizes the early stages of development. The allantoic circulation displaces the vitelline circulation however and establishes an allantoic placental relationship over the entire uterine wall this has been termed a diffuse labyrinthine endotheliochorial placenta This relationship in the parietalis area presumably plays a far more important role in *Tadarida* than in other bats in which a comparable intimacy between fetal and maternal components has not been observed outside the main placental disc

The fine structure of the discoidal placenta is labyrinthine presumably endotheliochorial in the earlier stages but becoming hemochorial during the latter half of pregnancy Peculiarities of its formation and structure in comparison with the discoidal placenta of other bats are emphasized.

The distribution of alkaline and acid phosphatases lipids glycogen and iron within the placenta and adnexa are described and their significance discussed

ACKNOWLEDGMENTS

I wish to express my thanks to Dr William A Wimsatt for his suggestion of the problem and for his interest and guidance during the course of the study to Dr Howard A Schneiderman for suggestions and encouragement to Dr James N. Layne through whose kindness the majority of the bats utilized were obtained, to Mr Anthony Guerriere for technical assistance and to Miss Elizabeth B Wirth for help in preparing the drawings

LITERATURE CITED

Anderson, J W and W A Wimsatt 1953 The fetal membranes and placenta of the tropical American noctilionid bat *Dirias albiventer minor* Anat Rec 117 573-574

Baker J R. 1946 The histochemical recognition of lipine Quart J Micr Sci 87 441-470.

Branca, A 1923 Recherches sur la vésicule ombilicale. II La vésicule ombilicale des chiroptères Arch d Biol 33 517-604

Cain, A. J 1947 The use of Nile blue in the examination of lipoids Quart J Micro Sci 88 383.

Carleton, H M and R A. Drury 1957 Histological Technique Oxford University Press, London.

Constantine D G 1952 A program for maintaining the free-tailed bat in captivity Jour Mamm 33 395-397

Duval, M 1893-97 Études sur l'embryologie des Chéiroptères Jou de l'Anat et de la Physiol 31 93-160 and 427-4 1 32 105-164 and 420-454 33 1 31

Flexner L B G J Vosburgh and D C Cowie 1948 Sources of fetal iron in the guinea pig as determined with radioactive iron Anat Rec 100 661 (Abstract)

Gates William H 1936 Keeping bats in captivity Jou Mamm 17 268-273

Gerard P 1929 Contributions à l'étude morphologique de la vesicule ombilicale chez les Chéiroptères (Vespertilio noctula Schreb) Arch d Biol 39 203-218

——— 1928 Recherches histophysiologiques sur les annexes foetales des Chéiroptères (Vesperugo noctula Schreb) Ibid 38 327-351

Gopalakrishna A 1949b Studies on the embryology of Microchiroptera. Part IV An analysis of implantation and early development in *Scotophilus wroughtoni* (Thomas). Proc. Ind Acad Sci 30 220-212

—— 1950a Studies on the embryology of Microchiroptera. Part V Placentation in *Scotophilus wroughtoni*, (Thomas) Ibid., 31 235–251.

—— 1958 Foetal membranes in some Indian microchiroptera. J Morph., 102: 157–197

Lobel, W L. 1948 A histochemical and quantitative study of phosphatase in the placenta and fetal membranes of the guinea pig. Am. J Anat 78 47 77

Lutsch, P D., and A. E. Sulkin 1958 The laboratory care of the Mexican free-tailed bat. Jour. Mamm., 39 263–265.

McManus, J F A. 1946 Histological demonstration of mucin after periodic acid. Nature, 158 202.

Marshall, A. J 1953 The unilateral endometrial reaction in the giant fruit-bat (*Pteropus giganteus* Brünnich) J of Endocrin 9 42–

Matthews, L. H. 1937 The female sexual cycle in the British horseshoe bats. Trans. Zool Soc London, 23 224–266.

Moghe, M. A. 1951 Development and placentation of the Indian fruit bat, *Pteropus giganteus giganteus*, (Brunnich) Proc. Zool. Soc. London, 121 703–721.

—— 1956 On the development and placentation of the megachiropteran bat — *Cynopterus sphinx gangeticus* Proc. N t. Inst. Sci. India, 22: 48–63

Mossman, H. W 1937 Comparative morphogenesis of fetal membranes and accessory uterine structures. Contrib. Embryl., Carn. Inst. Wash 26 127 246.

Palade, G. E. 1952 A study of fixation for electron microscopy J of Exper Med., 95 285–298.

Pearse, A. G 1953 Histochemistry Theoretical and Applied J & A Churchill, London.

Reeder, E. 1939 Cytology of the reproductive tract of the female bat, *Myotis lucif gus lucifugus*. J Morph., 64 431–453.

Sansom, G. S 1932 Notes on some early blastocysts of the South American bat Molossus. Proc. Zool. Soc. London, Pt 1 pp 113–118.

Sherman, H. B. 1930 Birth of the young of *Myotis austroriparius*. Jour Mamm., 11 495–503.

—— 1937 Breeding habits of .e free tailed bat. Ibid 18 183–184.

Srivastava, S. C. 1952 Ple ... the mouse-tailed bat, *Rhinopom* k... r (Chiroptera) Zool. Soc. Bengal ... 1 5–131

Stowell, R. E. 1945 Feulge ... thymonucleic acid. Stain Tec ... 1

Van Beneden, E. 1888 De l ... n et de la constitution du placen ... murin

(*Vespertilio murinus*) Bull d l'Ac R des Sci. d. Belg., ser 3, 15 351–364

—— 1899 Recherches sur les premie stades du developpment d murir *V spertil murinus*) Anat. Anz 16 305–334

Wimsatt W A. 1944 An analysis of implantation in the bat, *Myotis lucifugus lucifugus* Am. J Anat., 74 355–411

—— 1945 The placentation of vespertilionid bat, *Myotis lucifugus lucifugus* Ibid 77 1–51

—— 1948 The nature and distribution of lipoids in the fetal membranes and placenta of the bat, *Myotis lucifugus lucifugus* with observations on the mitochondria and Golgi pparatus. Ibid 82: 393–468

—— 1949 Cytochemical observations on the fetal membranes and placenta f the bat, *Myotis lucifugus lucifugus*. Ibid 84 63–142.

—— 1954 The fetal membranes nd placentation of the tropical American vampire bat *Desmodus rotundus murinus*. Act Anat 21 285–341

—— 1958 The allantoic placental barrier in Chiroptera A new concept of its organization and histochemistry Ibid 32 141 186.

Wimsatt, W A., and A. Gopalakrishna 1958 Occurrence of placental hematoma in the primitive sheath-tailed bats (Emballonuridae) with observations on its structure development and histochemistry Am J Anat 103 35–68.

Wimsatt, W A., and H. Trapido 1952 Reproduction and the female reproductive cycle in the tropical American ampire bat, *Desmod rotundus murinus*. Ibid., 91 415–445

Wislocki, G. B., H. W Deane and E W Dempsey 1946 The histochemistry of the rodent placenta. Ibid., 78 281–346.

Wislocki, G. B., and E. W Dempsey 1945 Histochemical reactions of the endometrium in pregnancy Ibid., 77 365–403.

—— 1946a Histochemical reactions in the placenta of the cat. Ibid., 78 1–45.

—— 1946b Histochemical reactions of the placenta of the pig. Ibid 78 181 226.

—— 1946c Histochemical age changes in normal and pathological placental illi (Hydatidiform Mole Eclampsia) Endocrinol 38. 90–109

Wislocki, G. B and D W F wcett 1941 The placentation of the Jamaican bat (*Artibeus jamaicensis parvipes*) Anat. Rec., 81 304–317

Wislocki, G. B., and W A. Wimsatt 1947 Chemical cytology of the placenta in two North American shrews (*Blarina brevicauda* and *Sorex fumeus*) Am. J Anat., 81 269–308.

PLATE 1

EXPLANATION OF FIGURES

3 A cross section of the uterus. The arrow on the right indicates the much retarded head fold of the amnion. The arrow at the top shows the precocious development of the tail and lateral folds (hematoxylin and eosin) × 45.

4 A specimen which has been cut so that a cross section of the anterior and posterior portions of the body is shown. The amnion ( ) completely covers the posterior portion of the embryo, while the anterior portion is exposed to the uterine cavity (u). The yolk sac cavity (y) and the extra-embryonic coelom ( ) are shown (hematoxylin and eosin) × 45.

5 A view of the area of the "placental pad" (p) during the early limb bud stage showing the allantoic and vitelline circulation overlying the pad. The arrow indicates the allantoic vessels. Note the hypertrophy of the endoderm of the yolk sac (y) (eosin methylene blue) × 62.

6 Cross section of the caudal portion of the embryo in the limb bud stage. The arrows indicate three portions of the allantoic stalk which is open to the allantoic cavity (hematoxylin and eosin) × 93.

7 Early stage of the allantoic diverticulum (al) showing the initial evagination into the extraembryonic coelom ( ). The posterior portion of the amniotic cavity ( ) is shown (hematoxylin and eosin) × 95.

8 A low power view showing the relationship of the "placental pad" (p) and the oviduct (arrow) during the limb bud stage (hematoxylin and eosin) × 34.

9 A section at limb bud stage showing the allantoic cavity (al) at the height of its development. The arrow indicates the allantoic stalk which is still open at this stage (hematoxylin and eosin) × 45.

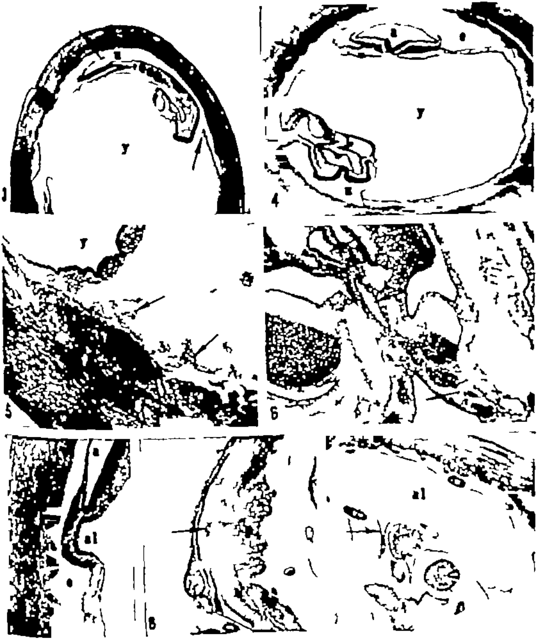

3
y
4
y
5
y
6
al
8
al

PLATE 2

EXPLANATION OF FIGURES

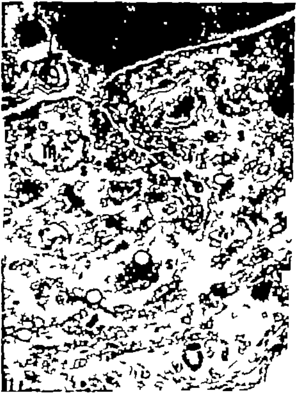
10 A high power view of the trophoblast underlying the yolk sac at the limb bud stage. The cytotrophoblast (t) has separated from the syncytial trophobl st as esult of shrinkage when fixed. The sy-cytial trophoblast is infiltrating and eroding the endometrium. The vitelline blood vessels (v) are closely associated with the tropho-blast t this stage (eosin methylene blue) × 320

11 A section f the uterine wall at mid-gestation showing the infiltra-tion of allantoic blood vessels and connective tissue (rrows) Syn-cytial trophoblast ( ) surrounds the maternal blood essel (m) The layer of large multinucleated cells (d) next to the myometrium at the bottom of the picture is decidua parietalis (Masson trichrome) × 200.

12 A section through the uterine wall bout mid-gestation The necrotic zone (n) is formed from degener ting decidual lls which first plasmolize and form multinucleated cells. The arrows indicate area of extravasated maternal blood (Masson trichrome) × 100.

13 A cross section of the discoidal placenta t term (eosin methylene blue) × 7





11



12



13

PLATE 3

EXPLANATION OF FIGURES

14 A low power view showing the relationship of the placenta (p) and the glandular yolk sac (y) during the later half of the gestation period. The decidua parietalis area is indicated by arrows (eosin methylene blue) × 15.

15 The yolk sac at mid-gestation. The arrow indicates the proteinous granules in the mesodermal cells. The endodermal cells ( ) at the bottom do not contain these granules (Masson's trichrome) × 485.

16 The discoidal placenta at mid-gestation, showing the maternal blood spaces (m) surrounded by a layer of trophoblastic cell. The arrows indicate the position of fetal capillaries (Masson trichrome). × 325.

17 The discoidal placenta near term showing fetal blood vessel (f) and the extensive fetal capillaries surrounding the maternal blood space (m). Arrows indicate the placental barrier (McManus PAS and hematoxylin) × 270

18 A cross section of the uterus during early gestation showing glycogen in the cellular trophoblast which is closely associated with the vitelline vessels (v). The arrow indicates glycogen in maternal blood vessel (McManus PAS) × 90.

19 Glycogen deposits in the endodermal cells of the yolk sac near term. The arrow indicates the mesodermal cells which do not contain glycogen (McManus PAS) × 240

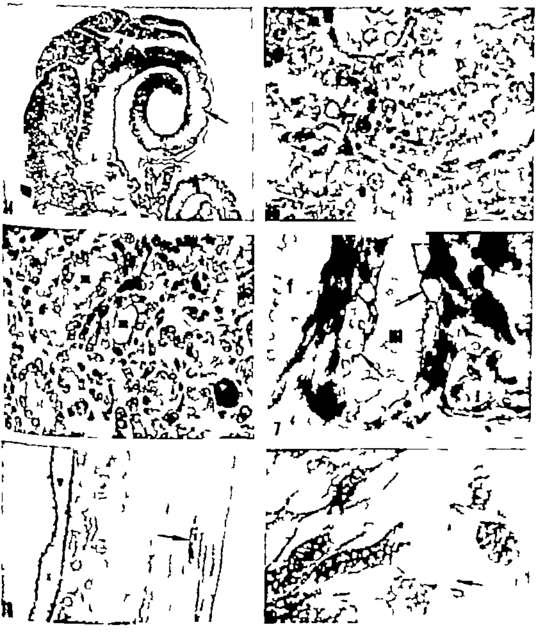


PLATE 4

EXPLANATION OF FIGURES

20 Acid phosphatase in the progravid terus (counterstained with paracarmine) × 82.

21 Acid phosphatase activity near term in area of the decid parietalis where the membranous chorion undercut the discoidal placenta (paracarmine counterstain) × 95.

22 Alkaline phosphatase activity in the uterine gland (arrows) of the progravid uterus. This activity is also evident around blood ssels in the muscular wall of the teru (paracarmine counterstain) × 82.

23 Alkaline phosphatase activity in the re of the decidua parietalis, *d ring the limb bud stage. The main reaction is served i the* maternal endometrium which ha been infiltrated with trophoblast. The mesothelial cells (arrow) of the yolk sac are also positive (paracarmine counterstain) × 45.

24 A section showing alkaline phosphatase activity in the discoidal placenta (p) yolk sac (y) nd decid parietal near term. A ring of activity is seen around each of the mat rnal blood spaces in the discoidal placenta. Activity in the mesothelial ell of the yolk sac i prominent, however the zone f positiv re ction in the parietalis is the most evident (paracarmine counterstain) × 25.

25 Alkaline phosph tase activity (arrows) surrounding the maternal blood spaces (m) in the discoidal placenta near term (paracarmine counterstain) × 245.

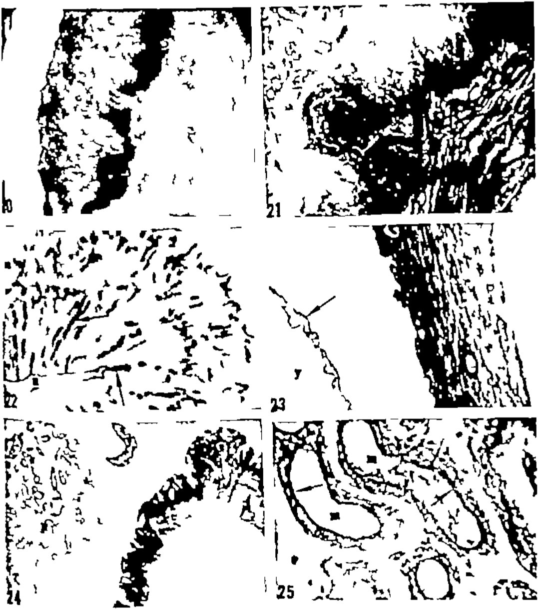

21
22
23
y
24
25

PLATE 5

EXPLAN TION OF FIGURES

26 Alkaline phosphatase activity in the yolk sac, near term. The reaction is confined to the mesothelial cells and endothelium of the blood vessels (arrow) (paracarmine counterstain) × 320.

27 Iron deposits in the endometrium of the erus prior to ovulation. The clear areas (g) are cross sections of the uterine glands (turnbell blue ferrous iron) × 365.

28 The darkly tained material indicates iron deposit in the area of the decidua parietalis about mid-gestation. Note the number of allantoic blood vessels (arrows) (PAS and Perl ferric iron) × 52.

29 Sudan black B preparation showing the total lipid content throughout the trophoblast of the decidua parietalis area, near term (neutral red counterstain) × 52.

30 Neutral lipid droplets in the trophoblast of the decid parietalis area near term (nile blue sulphate) × 365.

31 A section of yolk sac at term showing mesothelial cell without lipid (arrow) and endoderm containing lipid droplets (osmic acid) × 320.

32 A section of the uterus before ovulation showing the tr tified squamous epithelium lining the corpus uteri (arrow) and a portion of the uterine cavity ( ) (hematoxylin and eosin) 325

33 A section through the cervical papilla showing the thick stratified squamou epithelium lining the vagin ( ) as well the cervical canal (c) (hematoxylin and eosin) 93.

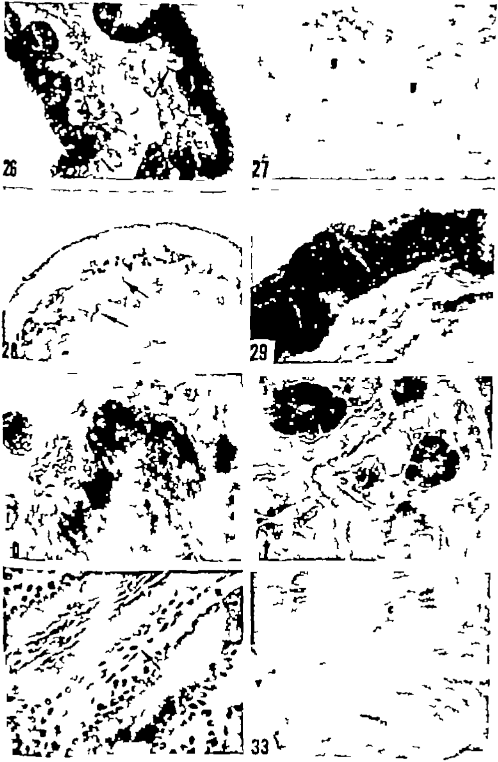

26
27
28
29
33

PLATE 5

EXPLAN TION OF FIGURES

26 Alkaline phosphatase activity in the yolk sac near term. The reaction is confined to the mesothelial cell and endothelium of the blood vessels (arrow) (paracarmine counterstain) × 320

27 Iron deposits in the endometrium of the uterus prior to ovulation. The clear areas (g) are cross sections of the uterine glands (turnbull blue ferrous iron) × 365.

28 The darkly stained material indicates iron deposits in the area of the decidu parietalis about mid-gestation. Note the number of allantoic blood vessels (arrows) (PAS and Perl's ferric iron) × 82.

29 Sudan black B preparation showing the total lipid content throughout the trophoblast of the decidua parietalis area, nea term (neutral red counterstain) × 52.

30 Neutral lipid droplets in the trophoblast of the decidua parietalis area near term (nile blue sulphate) × 365.

31 A section of yolk sac t term showing mesothelial lls without lipid (arrow) and endoderm containing lipid droplets (osmic acid) × 320.

32 A section of the uterus before ovulation showing the st tified squamous epithelium lining the corpus uteri (rrow) and portion of the uterine cavity (u) (hematoxylin and eosin) × 323

33 A section through the cervical papilla showing the thick str tified squamous epithelium lining the gin ( ) well the cervical canal ( ) (hematoxylin and eosin)

Ultrastructure of the Human Submaxillary Gland

I. ARCHITECTURE AND HISTOLOGICAL RELATIONSHIPS OF THE SECRETORY CELLS[1]

BERNARD TANDLER
Division of Pathology, Sloan-Kettering Institute for Cancer Research Sloan-Kettering Division of Cornell University Medical College New York, New York

While mammalian salivary glands have been extensively studied by means of the light microscope (Zimmermann '27 Babkin, '50; Rauch, '59) they have received only scant attention from electron microscopists. The earliest electron microscopical observations were limited to a clarification of the morphological nature of the ergastoplasm of serous cells (Bernhard et al., '52, Gautier and Diomede-Fresa, '52; Palade and Porter '54) More recently the ultrastructure of both rat and mouse salivary glands has been described (Scott and Pease, '59 Leeson and Jacoby '59, Leeson and Booth '61; Rutberg, '61 and Parks, '61) The myoepithelial elements of the human submaxillary gland have been examined by Takahashi ('58) while Ferner and Gansler ('61) have published a study of the human submaxillary and parotid glands.

The present paper is the first of a series describing the complete ultrastructure of the human submaxillary gland. It presents several features of acinar cell architecture not previously reported.

MATERIALS AND METHODS

Specimens of submaxillary gland were obtained in the operating rooms of the Memorial Hospital for Cancer and Allied Diseases in New York City Specimens were secured from 18 patients of both sexes ranging in age from 31 to 76 years undergoing surgery for the removal of primary tumors of the neck region or of cervical nodes containing metastatic deposits. All the submaxillary gland tissue obtained for this study had a normal light microscopical appearance

Prior to operation, varying dosages of Demerol, Seconal, and an antisialogogue atropine or scopolamine, were administered to the patients. Anesthesia was usually induced with sodium pentothal, and was maintained by a mixture of nitrous oxide-oxygen and ether A muscle relaxant, succinylocholine chloride, was administered as required.

Small slivers of tissue were excised with a minimum of handling, and with the blood supply to the gland still intact, and were immediately dropped into a pool of cold fixative. The tissue was finely minced with a razor blade and transferred to a vial containing fresh cold fixative Not more than two minutes elapsed between the removal of the tissue sample from its blood supply and the completion of the mincing process. The fixatives employed were 1 or 2% osmium buffered with veronal-acetate (Palade '52) and containing sucrose (Caulfield, '57) 2% osmium buffered with phosphate (Millonig, '61) or chromate-dichromate (Dalton, '55) or unbuffered 3% potassium permanganate (Mollenhauer and Zebrun, '60) Most of the tissue was embedded in a 6 1 mixture of butyl and methyl methacrylate containing 2% Luperco CDB but at later stages of the investigation, Epon 812 (Finck, '60) or a mixture of Epon 812 and Epon 815 (Kushida, '59) was used. The methacrylate was polymerized by ultraviolet light at room temperature. The epoxy resins

[1] This work was supported in part by grant CRTY 5018 from the National Cancer Institute, U. S. Public Health Service, and by grants from the Lillia Babbitt Hyde Foundation and the Brown-Hazen Fund.

Present address: Department of Anatomy, New York University School of Medicine, New York 16, New York.

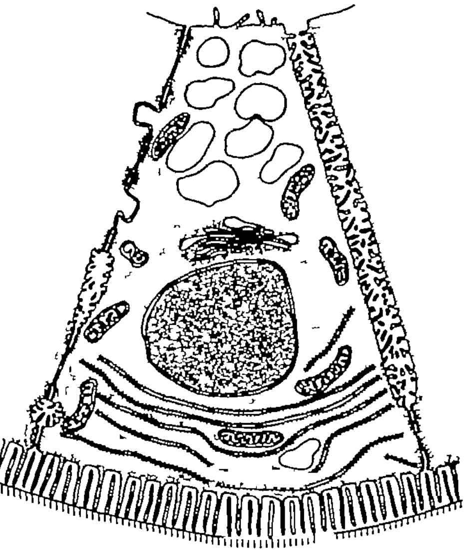


Fig. 3 Diagram summarizing the surface specializations of the secretory cells of the human submaxillary gland. The base of the cell is thrown into slender folds which interdigitate with a series of foot processes emanating from adjacent cells. The foot processes are depicted as the discontinuous folds. The basal folds are resting on the basement membrane The luminal surface is sparsely provided with microvilli. On the right is secretory pillary sectioned longitudinally containing many microvilli. It opens to the lumen, and extends close to the cell base On the left are two secretory capillaries, one sectioned obliquely the other transversely They are sealed off from the extracellular space by terminal bars. The lower capillary is shown in direct relation to the basal folds, being separated from them only by terminal bar The various surface and internal components of the cell are not drawn to scale.

ue preparations. Basal folds of one density and in continuity with a cell of the same density alternate with discontinuous folds of a different density (fig 6) The increased density of some of the secretory cells may be artifactitious arising from mechanical trauma sustained by the tissue prior to fixation (Scharrer '38)

were polymerized by heat (50 to 60 C) Silver-gray sections were cut with a Sorvall thin-sectioning microtome or with an LKB Ultrotome and were stained with either uranyl acetate (Watson '58a) lead hydroxide (Watson, 58b Dalton and Ziegel, '60) or lead subacetate (Dalton and Ziegel '60). The sections were examined in a Siemens Elmiskop I electron microscope using the double condenser and a 50 μ aperture in the objective lens or in an RCA EMU 2B electron microscope. The accelerating potentials were 80 and 50 kv respectively Micrographs were taken at magnifications from approximately 2 700 to 30 000 diameters

For purposes of orientation 1 5 μ thick sections were stained with azure B bromide and examined in a phase-contrast microscope.

OBSERVATIONS

The secretory cells of the serous and mucous acini exhibit an unexpected degree of complexity both in their architecture and in their histological relationships. The most conspicuous specialization of the secretory cells is an elaboration of the basal surface. The basal membrane is thrown into a series of tall, narrow folds which extend from the cell base to the basement membrane (figs. 4 6 7 8) That these are folds and not microvilli as encountered in the intestinal striated border is shown by the complete lack of cross sectional profiles If these folds were finger-like in structure the probability that they would all lie in the same plane of section is negligible The folds are quite slender about 400 to 650A in width and would merit the appellation cytoplasmic lamellae if it were not for the fact that Rhodin ('58) has already used this term in another connection The term "basal folds will therefore be used to denote these structures.

The basal folds are taller at the periphery of the cell than in its center and may extend for some distance along the lateral surfaces. They cover the entire cell base. The basal folds may radiate from a central locus as do the spokes of a wheel, or they may be disposed in a parallel array The former arrangement is more common The folds do not end at the lateral margins of the cell, but extend outward as a series of foot processes (figs. 1 2) Viewed from above the cell has the appearance of a multipointed star The foot processes penetrate deeply into the recesses between the basal folds of adjoining cells.

In sections parallel to the basement membrane and passing through the basal folds the interdigitation of the foot processes is clearly discernible (fig. 5). Alternate longitudinally cut basal folds are continuous with the cytoplasm of the overlying secretory cell. The alternate discontinous folds arise from a neighboring cell. This can be demonstrated by the presence of light and dark cells in the ti-

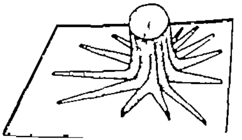


Fig. 1 Three dimensional representation of the secretory cell. The cell is viewed from above and is resting on the basement membrane. The basal folds extend outward in series of foot processes. Two foot processes are shown cut short to demonstrate their appearance in profile

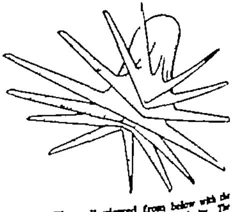


Fig. 2 The cell viewed from below with the basement membrane omitted for clarity The basal folds are continuous across the entire cell base. Between the folds are grooves or furrows whose width slightly exceeds that of the foot processes. Foot processes from neighboring cells extend into these grooves. The basal folds and their processes are arranged in a radial fashion

one of a few infolded membranes (Parks '61), or a few microvilli (Rutberg '61) The basal surface of rat sublingual gland cells is unremarkable (Leeson and Booth '61). In their report on *human submaxillary glands*, Ferner and Gansler ('61) make no mention of specializations on the basal surfaces of the secretory cells

A system of basal folds equal in complexity to that in human submaxillary gland is also found in the human sublingual gland, while less elaborate systems are present in human parotid and lacrimal glands (personal observations) Similar but less conspicuous basal specializations have been reported in the utricle of the guinea pig (Smith '56) the gastric parietal cells of the beaver *stomach* (Ito '61) and the Malpighian tubules of the leaf hopper, *Macrosteles* (Smith and Littau '60).

The basal folds of the secretory cells of the human submaxillary gland greatly increase the surface area of the secretory cell base. It is estimated that the basal folds, together with their extensions in the form of foot processes increase this area by a factor of 60 Interdigitation of the processes is the arrangement most economical of space. The relative ease with which adjacent folds are separated during polymerization of the methacrylate indicates that the foot processes are probably not involved in cell adhesion

The cytoplasm of the basal folds is devoid of the usual cytoplasmic organelles. This observation is in contrast to the arrangement found in the striated ducts of the gland (Tandler '62) where there exists a consistent and intimate association between mitochondria and highly folded plasma membranes. The absence of mitochondria from the basal folds suggests that the transfer of material through the cell membrane is not dependent upon a large concentration of high energy compounds and that the transport is not an active one The increased area of the basal surface enhances the movement of materials into and out of the cells by simple diffusion and may be of value in facilitated diffusion.

Secretory capillaries have been interpreted classically as being involved in the secretory process (Zimmermann '27) Granules or other material of possible secretory origin are however very rarely encountered within the lumina of the secretory capillaries in the human submaxillary glands studied. This may be due to the treatment of the patients with antisialogogues prior to operation. Junqueira, Rothschild and Vugman ('58) have found that the primary effect exerted by atropine on exocrine cells is the inhibition of the discharge of secretory granules.

It is possible that water and dissolved materials gain access to the acinar lumen via the system of channels formed by the basal folds and the secretory capillaries. Rawlinson ('34) found that upon stimulation of the gland secretory material of a granular nature was "washed out from the secretory capillaries evidently by a diluting fluid. It should be pointed out that the secretory capillaries and the basal folds are separated into two compartments by continuous terminal bars. Miller ('61) has presented electron microscopical evidence that terminal bars act as permeability barriers in kidney tubules If the same is true in the submaxillary gland, then the transfer of fluid from the spaces between the folds to the secretory capillaries must be through the secretory cells. The distance over which the fluid must be transported is greatly reduced, however The interposition of selectively permeable plasma membranes probably enables the secretory cells to control the final composition of the fluid in the acinar lumen

While the primary secretion of the acinar cells is thought to be isoosmolar (Burgen and Seeman, '58) the final saliva is characteristically hypoosmolar (Thaysen Thorn and Schwartz, '54) Burgen and Seeman '58) have adduced evidence that the major reabsorption of ions takes place in the duct system of the gland. That the secretory capillaries are also involved, to some extent, in reabsorption of ions is suggested by the great number of microvilli encountered in their lumina, although microvilli have been found in association with several cell types known to be secretory (Florey '60; Hally '58) It is conceivable that an initial isoosmolar secretion is liberated near the terminus of the secretory capillary and that progressive reabsorption of ions occurs as the secre-

Whatever the actual status of the cells of different densities, they constitute convenient morphological markers.

The extremely rare observation of a desmosome-like structure joining two basal folds (fig. 8) tends to support the thesis that adjacent folds arise from different cells.

In methacrylate sections (figs. 4 6) the adjacent folds are widely separated and the area between them is quite electron-lucent. In epon sections (figs 7 8 10) on the other hand adjacent folds are seen to be closely coherent, and the space between confronted plasma membranes is occupied by an amorphous substance of a density similar to that of the basement membrane.

The folds are delimited by a 75A thick plasma membrane which can be resolved into a unit membrane (fig. 10) Round tubular or flask-like invaginations of the plasma membrane are frequently encountered (fig. 6) The membrane surrounding the invaginations retains its characteristic triple-layering with no obvious change in dimensions. The content of the invaginations is of an electron density greater than that of the cytoplasmic matrix.

In sections cut parallel to the basement membrane and lying between the cell base and the nucleus basal folds are disposed in a corona around the lateral margins of the cell (fig 9) The interdigitation of the folds with foot processes from adjacent cells is apparent. At a higher level adjacent cells are closely coherent along their lateral borders and the foot processes at this level rather short are tightly interlocked (fig. 10) Above the level of the nucleus the lateral surfaces of adjacent cells are closely approximated except where a secretory capillary is present. The cell membranes pursue a relatively straight course and exhibit many desmosomes. At their apical margins cells are tightly joined by terminal bars The luminal surface of the secretory cells lacks specialized structures, except for a very few microvilli (fig 11)

The secretory capillaries are continuations of the acinar lumen (fig. 11) Where several adjacent cells form a secretory capillary at their line of junction each cell provides a portion of the wall of the capillary (fig. 13) Longitudinally oriented terminal bars morphologically similar to "tight intercellular junctions in other tissues (Farquhar and Palade '61) insure the cohesion of the capillary walls, and close off the capillary from the space between adjacent cells.

The secretory capillaries may appear round or angular in cross section, and vary from 0 1 to 0.5 μ in diameter They open to the acinar lumen and at their basal end receive several tributaries, some of which may be horizontally oriented. Unlike the apical cell membranes, which are almost devoid of specializations, the membranes of the secretory capillaries are provided with numerous finger-like projections (figs. 11 12, 13) The microvilli protrude into the capillary lumen, where they are most often seen in profile. They may be so abundant that they appear to occlude the lumen. It is obvious, from their morphology that the secretory capillaries are permanent structures, and not merely transient clefts produced by the passage of fluids as Rubashkin ('08) has suggested

In some instances a secretory capillary of fine caliber may lie extremely close to the cell base. The relationship between secretory capillaries and the basal folds is disclosed by the section passing obliquely through the cell base (fig 13). The lumen of the capillary may lie extremely close to the extracellular space between the basal folds. This distance may be as small as 0 4 μ One or two terminal bars are however interposed between the secretory capillary and the extracellular space

DISCUSSION

Previous electron microscope studies on salivary glands of lower forms have given little intimation of the structural complexity of the secretory cell base of the human submaxillary gland. In rat salivary glands, Scott and Pease ('59) have reported the presence of a few microvilli between the base of the secretory cells and the basement membrane While the lateral surfaces of serous cells of mouse parotid gland display a considerable degree of interfoliation the basal surfaces are devoid of specialization, except for the pres-

ence of a few *infolded* membranes (Parks '61) or a few microvilli (Rutberg, '61) The basal surface of rat sublingual gland cells is unremarkable (Leeson and Booth, '61) *In their* report on human submaxillary glands, Ferner and Gansler ('61) make no mention of specializations on the basal surfaces of the secretory cells.

A system of basal folds equal in complexity to that in human submaxillary gland is also found in the human sublingual gland while less elaborate systems are present in human parotid and lacrimal glands (*personal observations*) Similar but less conspicuous basal specializations have been reported in the utricle of the guinea pig (Smith, '58) the gastric parietal cells of the beaver stomach (Ito '61) and the Malpighian tubules of the leaf hopper *Macrosteles* (Smith and Littau '60)

The basal *folds* of the secretory cells of the human submaxillary gland *greatly* increase the surface area of the secretory cell base. It is estimated that the basal folds together *with their* extensions in the form of foot processes increase this area by a factor of 60 Interdigitation of the processes is the arrangement most economical *of space* The relative ease with which adjacent folds are *separated* during polymerization of the methacrylate indicates that the foot processes are probably not *involved in cell adhesion*.

The cytoplasm of the basal folds is devoid of the usual cytoplasmic organelles. This observation is in contrast to the arrangement *found in the striated* ducts of the gland (Tandler '62) where there exists a consistent and intimate association *between mitochondria* and highly folded plasma membranes. *The absence of* mitochondria from the basal folds suggests that the transfer of material through the cell *membrane is* not dependent upon a large concentration of high energy *compounds* and that the transport is not an active one The increased area of the basal surface enhances the *movement of materials* into and out of the cells by simple diffusion and may be of value in facilitated diffusion.

Secretory capillaries *have been inter*preted classically as being involved in the secretory process (Zimmermann '27) Granules or other material of possible secretory origin are however very rarely encountered *within* the lumina of the secretory capillaries in the human submaxillary glands studied. This may be due to the treatment of the patients with antisialogogues *prior to operation*. Junqueira, Rothschild, and Vugman ('58) *have found* that the primary effect exerted by atropine on exocrine cells is the inhibition of the *discharge of* secretory granules.

It is possible that *water and* dissolved materials gain access to the acinar lumen via the system of channels *formed* by the *basal folds* and the secretory capillaries. Rawlinson ('34) *found that upon* stimulation of the gland secretory *material of a* granular nature was "washed out" from the secretory capillaries, evidently by a diluting *fluid*. *It should* be pointed out that the secretory capillaries and the basal folds are separated into two compartments by continuous terminal bars Miller ('61) has *presented electron microscopical* evidence that terminal bars act as permeability barriers in kidney tubules. If the same is true in the submaxillary gland then the *transfer of fluid from* the spaces between the folds to the secretory capillaries must be through the secretory cells. *The distance* over which the fluid must be transported *is greatly reduced*, however The interposition of selectively permeable plasma membranes probably enables the secretory *cells to* control the final composition of the fluid in the acinar lumen.

While the primary secretion of the acinar cells is thought to be isoosmolar (Burgen and Seeman '58) the final saliva is characteristically hypoosmolar (*Thayson* Thorn and Schwartz, '54) Burgen and Seeman '58) have adduced evidence that the *major reabsorption* of ions takes place in the duct system of the *gland* That the secretory capillaries are also involved to some extent, in reabsorption of ions is suggested by the great number of microvilli encountered in their lumina, *although* microvilli have been found in association with several cell types known to be secretory (Florey '60; Hally '59) *It is* conceivable that an initial isoosmolar secretion is liberated near the terminus of the secretory *capillary* and that progressive reabsorption of ions occurs as *the* secre-

tory products move through the capillary towards the *acinar lumen*

SUMMARY

The micromophology of normal human submaxillary glands has been studied with the electron microscope. The bases of the secretory cells display complex specializations. The entire basal plasma membrane is thrown into numerous slender (400 to 650Å wide) folds which extend beyond the lateral margins of the cell as a series of radiating foot processes. These basal folds are devoid of cytoplasmic organelles. Foot processes of adjacent cells interdigitate loosely. It has been calculated that the laciniate configuration of the cell base increases the basal surface area at least 60 fold. This increase facilitates diffusion of materials into the cell. Numerous tubular secretory capillaries formed by adjacent secretory cells open into the acinar lumen. These capillaries possess a great number of microvilli. Secretory capillaries of finer caliber are separated from the basal folds by only one or two terminal bars, a distance as small as 0.4 μ. This arrangement may provide a pathway for and dissolved materials to gain access to the acinar lumen from the extracellular space. The morphology of the secretory capillaries suggests that they may participate in the reabsorption of some constituents of the primary secretion of the acinar cells. This activity may in part, contribute to the characteristic hypoosmolarity of the saliva.

ACKNOWLEDGMENTS

The author is indebted to Dr. Fredrick H. Shipkey for his continued interest and encouragement, to Dr. Frank Gerold for supplying the tissue used in this study and to Dr. A. S. V. Burgen for his valuable advice and suggestions. The technical assistance of Miss Helen Zoccolillo, Miss Cynthia C. Folkers, and Mrs. Mona Brandreth is gratefully acknowledged.

LITERATURE CITED

Babkin, B. P. 1950 Secretory Mechanism of the Digestive Glands. Paul B. Hoeber Inc., New York.

Bernhard, W., F. Haguenau, A. Gautier and C. Oberling 1952 La structure submicroscopique des elements basophiles cytoplasmiques dans le foie, le pancreas, et les glandes salivaires. Z. Zellforsch., 37: 281–300.

Burgen, A. S. V. and P. Seeman 1958 The role of the salivary duct system in the formation of the saliva. Can. J. Biochem. Physiol., 36: 119–143.

Caulfield, J. B. 1957 Effects of varying the vehicle for OsO_4 in tissue fixation. J. Biophys. Biochem. Cytol., 3: 827–830.

Dalton, A. J. 1955 A chrome-osmium fixative for electron microscopy. Anat. Rec., 121: 281.

Dalton, A. J. and R. F. Zeigel 1960 A simplified method of staining thin sections of biological material with lead hydroxide. J. Biophys. Biochem. Cytol., 7: 409–410.

Farquhar, M. G., and G. E. Palade 1961 Tight intercellular junctions. Proceedings of the First Annual Meeting of the American Society for Cell Biology. November 1961, p. 61.

Ferner, H., and H. Gansler 1961 Elektronenmikroskopische Untersuchungen an der Glandula submandibularis und parotis des Menschen. Z. Zellforsch., 55: 148–178.

Finck, H. 1960 Epoxy resins in electron microscopy. J. Biophys. Biochem. Cytol., 7: 27–30.

Florey, H. W. 1960 Electron microscopic observations on goblet cells of the rat's colon. Quart. J. Exp. Physiol., 45: 329–336.

Gautier, A., and B. Diomede-Fresa 1953 Étude au microscope électronique de l'ergastoplasme des glandes salivaires du rat. Mikroskopie, 8: 23–31.

Hally, A. D. 1958 The fine structure of the Paneth cell. J. Anat., 92: 268–277.

Ito, S. 1961 The endoplasmic reticulum of gastric parietal cells. J. Biophys. Biochem. Cytol., 11: 333–347.

Junqueira, L. C. U., H. A. Rothschild, and L. Vugman 1956 The action of atropine on pancreatic secretion. Brit. J. Pharmacol., 11: 71–73.

Kushida, H. 1959 On an epoxy resin embedding method for ultrathin sectioning. Electron Microscopy Japan, 8: 72 (In Japanese).

Leeson, C. R., and W. G. Booth 1961 Histological, histochemical, and electron-microscopical observations on the postnatal development of the major sublingual gland of the rat. J. Dent. Res., 40: 838–845.

Leeson, C. R., and F. Jacoby 1959 An electron microscopic study of the rat submaxillary gland during its post-natal development and in the adult. J. Anat., 93: 287–295.

Millonig, G. 1961 Advantages of phosphate buffer for OsO_4 solutions in fixation. J. Appl. Phys., 32: 1637.

Miller, F. 1960 Hemoglobin absorption by the cells of the proximal convoluted tubule in mouse kidney. J. Biophys. Biochem. Cytol., 8: 689–718.

Mollenhauer, H. H., and W. Zebrun 1960 Permangan in fixation of the Golgi complex and other cytoplasmic structures of mammalian testes. Ibid., 8: 761–775.

Palade, G. E. 1952 A study of fixation for electron microscopy. J. Exp. Med., 95: 285–298.

Parks, H. G. 1961 On the fine structure of the parotid gland of mouse and rat. Am. J. Anat., 108: 303–329.

Rauch, S. 1959 Die Speicheldrüsen des Menschen. Georg Thieme, Stuttgart.

Rawlinson, H. E. 1934 Certain histo-physiological aspects of gland secretion. McGill University Montreal. Quoted from Babkin (1950)

Rhodin, J 1958 Anatomy of kidney tubules. Int. Rev Cytol., 7 485–534.

Rubaschkin, W J 1906 Von den Kanälen des Drüsenepithels. Anat. Anz., 29 209–216.

Rutberg, U 1961 Ultrastructure and secretory mechanism of the parotid gland. Acta Odont. Scand., 19: Suppl. 30.

Scharrer E. 1938 On dark and light cells in the brain and in the liver. Anat. Rec., 72: 53–65.

Scott, B. L., and D C. Pease 1959 Electron microscopy of salivary and lacrimal glands of the rat. Am. J Anat., 104: 115–161.

Smith, C. A. 1956 Microscopic structure of the utricle. Ann. Otol. Rhinol. Laryngol., 65 450–470.

Smith, D. S., and V C. Littau 1960 Cellular specialization in the excretory epitheli of an insect, *Macrosteles fascifrons* Stål (Homoptera). J Biophys. Biochem. Cytol., 8 103–133.

Takahashi, N 1958 Electron microscopic stud ies on the ectodermal secretory glands in man. II. The fine structures of the myoepithelium in the human mammary and salivary glands. Bull. Tokyo Med. Dent. Univ., 5 177–192.

Tandler, B. 1962 To be published.

Thaysen, J H., N. A. Thorn and I. L. Schwartz 1954 Excretion of sodium, potassium, chloride and carbon dioxide in human parotid saliva. Am. J Physiol., 178 155–159

Watson, M. L. 1958a Staining of tissue sections for electron microscopy with heavy metals. II. Application of solutions containing lead and barium. J Biophys. Biochem. Cytol., 4: 727–730.

Zimmermann, K. W 1927 Die Speicheldrüsen der Mundhöhle und die Bauchspeicheldrüse. In Handbuch der Mikroskopischen Anatomie des Menschen, vol. 5, part 1. W von Möllendorff, ed. Berlin, pp 61–244

PLATE I

EXPLANATION OF FIGURE

4 The base of serous cell. Basal folds, sectioned in several different planes extend from the cell body to the basement membrane (*BM*) At I, the basal folds are shown in profile. At II, they have been sectioned longitudinally At III, fold has been sectioned longitudinally along its vertical axis. Note the lack of cytoplasmic organelles in the basal folds. A large nucleus, containing finely granular nucleoplasm, is at the left. Pores (arrow) are present in the nuclear envelope The cytoplasm between the basal folds and the ucleus contains endoplasmic reticulum (ER) A filamentous mitochondrion (M) extends across the lower border of the micrograph. *Methacryl te embedded.* × 37,000.

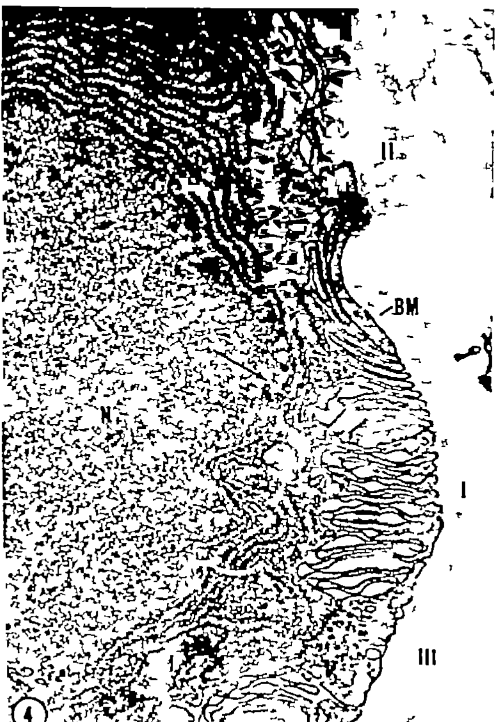

II
BM
N
I
III
4

PLATE 3

EXPLANATION OF FIGURES

6 The base of serous cell in methacrylate section A number of dense folds extend from the cell shown t the top of th micrograph to the basement membrane (BM) Alternating w th these folds, are discontinuous lighter folds, which come from adjoining cell of lesser density The wide separation of adjacent folds is haracteristic of the methacrylate embedded material. Vesicles and several invagina tions of the plasmalemma (arrows) filled with dense material, are present in some of the folds. × 80,000.

7 This micrograph shows the basal folds in an epon section. In this embedding medium, the space between adjacent f ld is con tant in width and is filled by dense substance which is not preserved in methacrylat embedded tissues. × 88,000.


BM
6

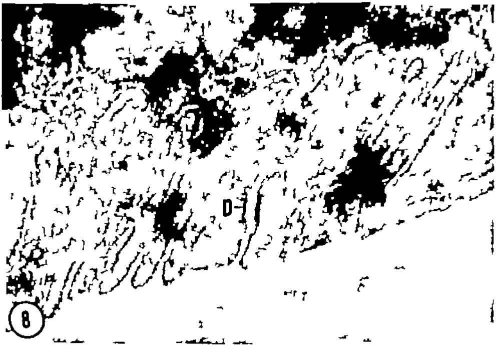

7

PLATE 4

EXPLANATION OF FIGURES

8 This micrograph shows an only rarely encountered desmosome-like structure (D) joining two basal folds. Epon embedded. × 70,000.

9 A serous cell sectioned parallel to the basement membrane at a level closer to the cell apex than that of figure 4. The cell is surrounded by corona of basal folds, cut in various planes. Mitochondria and elements of the endoplasmic reticulum are present in the cytoplasm. The cell is circumscribed by basement membrane. Methacrylate embedded. × 18,000.



8



9

PLATE 5

EXPLANATION OF FIGURE

10 Interdigitating basal folds of two serous cells fixed with potassium permanganate. The plane of section passes obliquely through the cells, being closer to the cell base at the bottom of the micrograph than at the top. The plasmalemma of the basal folds is resolved into unit membrane. The permanganate fixation has failed to preserve the RNP granules, resulting in their absence from the membranes of the endoplasmic reticulum (ER). Epon embedded. × 74 000.

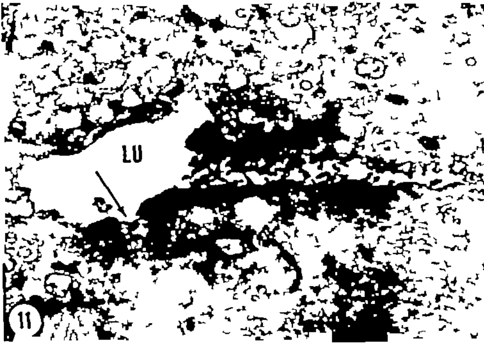

ER

PLATE 6

EXPLANATION OF FIGURES

11 A longitudinally sectioned secretory capillary (SC) is seen in direct continuity with the lumen (LU) of a serous acinus. The mouth of a second capillary is indicated by the arrow. The secretory capillaries are abundantly provided with microvilli. These structures are almost completely absent from the luminal surfaces of the serous cells. Methacrylate embedded. × 12,000.

12 A secretory capillary at high magnification. The microvilli are seen in longitudinal section and in profile. The unit membrane bounding these structures is resolved. Epon embedded. × 87,000.

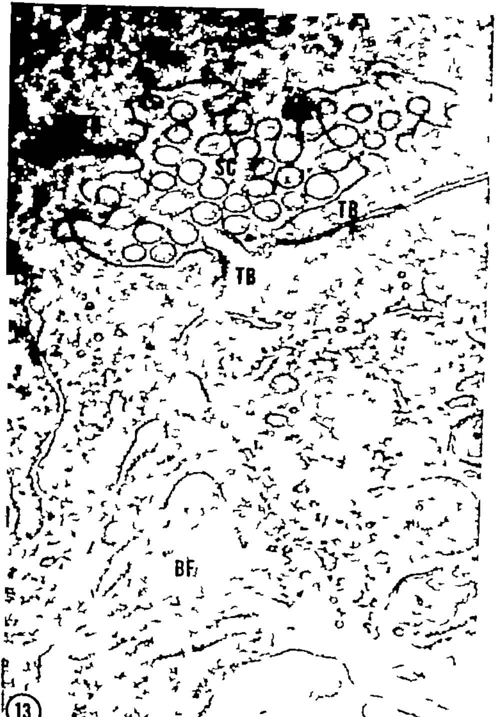

LU
11


12

PLATE 7

EXPLAN TION OF FIGURE

23 An oblique section passing through secretory capillary nd through the basal folds. The secretory capillary (SC) which extends parallel to the basement membrane is seen in cros section. Numerous profiles of microvilli re present in its lumen. The cells forming the capillary are joined by longitudinally oriented termin l bars (TB) here seen in profile The secretory capillary is urrounded by felt work of delicate fibril and is separ ted from the basal folds (BF) by two terminal bars. Methacryl te embedded. × 73,000


SC
TB
TB
BF
13

Abnormal Development Induced by the Maternal Administration of Phosphorus-32 after 14 or 17 Days of Gestation in the Rat

I. SKELETAL DEFECTS[1]

MELVIN R. SIKOV AND JAMES E. LOFSTROM
Department of Radiology Wayne State University College of Medicine and Receiving Hospital, Detroit, Michigan

The increasing possibilities for exposure to radioactive material emphasizes the need for more critical knowledge of the effects of maternally administered radioactive materials on prenatal development. It is also of theoretical interest to be able to sufficiently delineate the effects of the continuous radiation from an internally deposited isotope to permit a comparison with the extant data on acute external irradiation.

Although the effects of external radiation on the growth and morphology of the rodent fetus have been well defined, information obtained from studies using radioisotopes as radiation sources is much more limited. Finkel ('48) has reported that the *in utero* administration of radiostrontium or plutonium increased prenatal death in mice depressed growth and gave rise to various late effects. Burstone ('51) has demonstrated that P 32 injection in pregnant rats altered the development of the teeth of the offspring. Warren and Dixon ('49) have produced embryonic mortality and reduced hatching size by radiophosphorus administration in the chick although this treatment did not ind ce malformation.

The present report is part of a series of systematic quantitative studies on the effects of internal irradiation with phosphorus-32 throughout gestation and in the early life of the rat. As was indicated in earlier studies in this series (Sikov and Noonan '57 '58) P-32 administration during the first one-half of gestation produced effects which were qualitatively and quantitatively different than those found with acute external irradiation. In continuations of these studies (Sikov and Lofstrom, '57) the dosimetry and lethal effects of maternally administered phosphorus-32 were studied after injection during the last trimester of gestation.

As was indicated in the review by Russell ('54) pathology of the central nervous system is the usual morphologic finding after external radiation at this latter time of gestation. Only rarely has extraneural damage been reported, except in the case of the thymus although neonatal and post natal death and late pathology has been reported by several authors. Warkany and Schaffenberger ('47) found that irradiation with high doses of acute x rays produced a substantial number of skeletal malformations when administered during the period between 10 and 16 days of gestation in the rat. Levy et al. ('53) using a dose of 300 r to the mouse fetus at fifteen and one-half days of gestation found a reduction in the size of certain bones although the shapes were not altered.

It was therefore felt to be of value to determine the incidence of morphologic abnormalities in the fetuses which had been treated with P 32 during the last portion of gestation in our previous experiments. The skeleton was of particular interest since a *much greater radiation dose* is received by this system after P 32 administration than is possible to deliver using x-radiation.

---

[1] These studies were performed under Contract no. AT(11-1)-412 with the United States Atomic Energy Commission. Supported in part by the Receiving Hospital Research Corporation.

METHODS AND MATERIALS

Female rats of the Wistar albino strain weighing about 200 grams were caged with males of the same strain The presence of sperm in the vaginal smear was considered as presumptive evidence of mating. Nine o'clock A.M. of the day following mating was denoted as day one of gestation. As described previously (Sikov and Lofstrom '57) the pregnant females were intraperitoneally injected with graded doses of high specific activity P-32 in saline after 14 or 17 days of gestation. Control animals were injected with a comparable solution containing stable phosphorus

The animals were killed at intervals after injection by asphyxiation with natural gas. The rats were opened and the fetuses dissected free, weighed and examined under a low-powered stereoscopic microscope for gross malformations. The older fetuses and newborn rats obtained in this experiment were randomly distributed into several groups for more detailed study determination of radioactivity preparation of histologic slides and clearing and staining for study of skeletal development.

The latter fetuses were eviscerated and fixed in formalin. They were then stained with toluidine blue and alizarin red after maceration in potassium hydroxide according to the modification of the technique described by Guyer ('36) Several skeletal elements were measured including those structures reported upon by Levy et al ('53) and the resultant data analyzed in several ways Usually between six and twelve preparations were studied in each age-dose group Some of these measures are illustrated in figure 1 The skeletons were also examined for a variety of specific malformations and defects in ossification

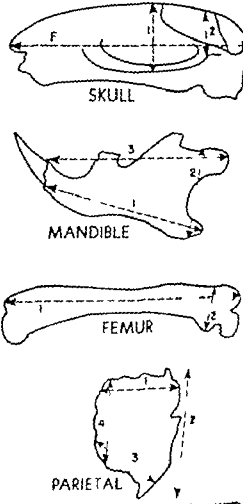


Fig. 1 Illustration of some of the measurements used in this study

OBSERVATIONS

It was found in these studies that there was a general reduction in the linear dimensions in the various skeletal elements of the more heavily irradiated fetuses Some representative sets of measurements of the various structures are presented in table 1 This decrease in skeletal size is perhaps more dramatically illustrated in figure 3 in which representative skeltons at birth both control and those receiving various doses of P 32 at 14 and 17 days of gestation are presented after being photographed simultaneously

As may be seen in table 1 the overall length of the skull was slightly reduced by the administration of two millicuries (mc) at 14 days of gestation but not by smaller doses of P 32. Not even the highest dose injected at 17 days had a substantial effect On the other hand there was a fairly marked effect in both of the two measures of skull height used in this study Injection of 2 mc at 14 days of gestation produced a marked decrease in skull height which could be noted as early as 19 days of gestation. One mc injected at this time produced only a slight and

TABLE 1

Size in mm of representative skeletal elements after injection of the dam with P-32 at 14 or 17 days of gestation

Fetal age at measurement	Control	14 Day injection 0.6	14 Day injection 1.0	14 Day injection 2.0 mc.	17 Day injection 0.6	17 Day injection 1.0	17 Day injection 2.0 mc.
			Length of skull				
18	9.6(0.5)	—	—	—	—	—	10.3
19	11.7(0.2)	11.5	11.5(0.5)	10.3(0.3)	11.1(0.5)	11.9(0.3)	11.6(0.4)
20	13.6(0.6)	12.8(0.3)	12.3(0.3)	10.5(0.3)	12.9(0.2)	12.8(0.7)	12.6(0.5)
21	14.3(0.5)	13.0(0.2)	13.3(0.6)	11.0(0.6)	13.2(0.5)	13.4(0.6)	12.9(0.4)
Birth	14.2(0.8)	14.3(0.4)	13.7(0.6)	12.2(0.4)	13.7(0.4)	12.9(0.5)	13.2(1.2)
			Height of skull (no. 2)				
18	4.4(0.2)	4.4	4.5(0.2)	4.4	—	4.7(0.4)	5.0(0.1)
19	5.2(0.2)	4.8(0.4)	5.0(0.2)	4.2(0.4)	5.0(0.4)	5.5(0.1)	5.2(0.2)
20	6.1(0.4)	5.2(0.7)	5.4(0.3)	4.4(0.3)	5.8(0.4)	5.6(0.3)	5.5(0.2)
21	5.7(0.3)	5.2(0.3)	5.3(0.2)	4.3(0.4)	5.6(0.3)	5.6(0.5)	5.0(0.2)
Birth	5.5(0.6)	5.4(0.2)	5.2(0.6)	4.4(0.3)	5.3(0.3)	5.3(0.2)	5.0(0.4)
			Parietal-length (no. 1)				
18	2.8(0.4)	2.8	—	—	—	3.2	3.0(0.2)
19	4.1(0.3)	3.7(0.5)	4.1(0.2)	3.8(0.2)	3.6(0.5)	4.1(0.2)	4.0(0.4)
20	4.4(0.4)	4.3(0.2)	4.3(0.2)	3.7(0.2)	4.4(0.3)	4.7(0.3)	4.4(0.4)
21	4.6(0.3)	4.2(0.2)	4.4(0.3)	3.6(0.2)	4.6(0.3)	4.7(0.3)	4.1(0.2)
Birth	5.1(0.4)	4.7(0.4)	4.3(0.4)	4.0(0.3)	4.9(0.4)	5.0(0.2)	4.5(0.4)
			Parietal width (no. 2)				
18	1.6(0.3)	1.2	1.7(0.2)	—	—	1.9(0.2)	1.9(0.4)
19	2.4(0.2)	2.3(0.2)	2.3(0.3)	2.1(0.2)	1.9(0.3)	2.3(0.2)	2.3(0.3)
20	3.2(0.2)	3.3(0.2)	3.1(0.2)	2.3(0.2)	3.1(0.3)	3.2(0.4)	2.9(0.3)
21	4.0(0.2)	3.6(0.2)	3.5(0.4)	2.5(0.3)	3.8(0.2)	3.6(0.3)	3.2(0.4)
Birth	4.2(0.4)	4.1(0.2)	3.7(0.4)	3.3(0.4)	3.9(0.2)	4.1(0.3)	3.7(0.7)
			Mandibular length				
18	4.7(0.6)	4.3(0.2)	4.6(0.4)	3.5(0.6)	—	4.8(0.2)	4.7(0.3)
19	6.0(0.2)	5.7(0.2)	6.3(0.3)	5.4(0.9)	5.4(0.5)	6.2(0.2)	6.0(0.3)
20	7.5(0.5)	7.3(0.3)	7.0(0.2)	6.6(0.5)	7.4(0.2)	7.4(0.4)	7.2(0.3)
21	8.8(0.4)	8.3(0.3)	8.2(0.6)	6.4(0.5)	8.4(0.2)	8.3(0.4)	7.5(0.4)
Birth	8.9(0.4)	9.1(0.2)	8.4(0.5)	8.0(0.3)	8.7(0.3)	9.1(0.2)	8.5(1.2)
			Mandibular height				
18	1.2(0.3)	1.3	1.2	1.3	—	1.1(0.1)	1.2
19	1.6(0.1)	1.6	1.8(0.2)	1.5(0.3)	1.4(0.2)	1.8(0.3)	1.5(0.1)
20	2.2(0.4)	2.4(0.3)	2.1(0.2)	1.6(0.3)	2.1(0.2)	2.1(0.2)	2.0(0.2)
21	2.3(0.2)	2.2(0.3)	2.5(0.2)	1.8(0.2)	2.6(0.2)	2.6(0.3)	2.0(0.2)
Birth	2.9(0.4)	2.8(0.2)	2.5(0.2)	2.1(0)	2.6(0.1)	2.8(0.1)	2.5(0.6)
			Femur length				
18	3.7(0.2)	3.2(0.3)	3.4(0.2)	3.1(0.3)	—	3.6(0.3)	3.4(0.2)
19	4.4(0.2)	5.0(0.3)	4.5(0.3)	4.0(0.6)	4.9(0.5)	4.7(0.3)	4.5(0.3)
20	5.9(0.4)	5.5(0.[illegible])	5.1(0.3)	4.8(0.2)	5.3(0.2)	5.4(0.2)	5.2(0.3)
21	6.1(0.4)	5.8(0.2)	5.9(0.3)	4.7(0.6)	6.0(0.3)	5.8(0.3)	5.2(0.2)
Birth	6.3(0.4)	6.3(0.4)	5.8(0.4)	5.0(0.4)	6.6(0.7)	6.1(0.4)	5.5(0.8)
			Femur width (no. 2)				
18	0.8(0.3)	0.4	0.4	0.4	—	0.4	0.4
19	0.8(0.2)	0.8	0.8(0.3)	0.6(0.2)	0.7(0.2)	0.8(0.2)	0.7(0.1)
20	0.8(0.4)	0.8(0.3)	0.8(0.2)	0.8(0.3)	0.8(0.2)	0.8(0.3)	0.7(0.1)
21	1.2(0.1)	1.0(0.2)	1.1(0.2)	0.7(0.2)	1.1(0.1)	1.1(0.6)	0.8(0.2)
Birth	1.2(0.2)	1.2(0.2)	1.1(0.2)	0.9(0.2)	1.2(0.1)	1.2(0.2)	1.1(0.2)
			Vertebral column length				
18	21.4(0.4)	26.5(1.5)	29.4(0)	24.2(2.1)	—	28.9(1.2)	29.6(1.1)
19	33.6(0.9)	33.6(1.7)	35.4(2.2)	30.1(2.4)	29.8(2.5)	36.6(1.8)	34.9(1.3)
20	43.6(1.8)	40.9(0.9)	37.8(3.6)	31.8(1.8)	41.2(0.9)	41.0(1.4)	39.3(2.6)
21	47.8(3.0)	41.0(0.7)	43.5(2.2)	33.3(2.8)	45.7(1.4)	45.1(2.8)	40.4(–0)
Birth	47.1(2.2)	48.3(2.3)	45.5(3)	40.0(3.2)	44.8(5.7)	46.7(3.4)	42.4(6.3)

Standard deviations presented in parentheses. S.D. values of less than 0.1 mm are deleted.

perhaps not significant, decrease in the height of the skull. Injection of 2.0 mc at 17 days of gestation produced a slight but definite decrease in the skull height at birth which for either measure could be detected at 21 days of gestation.

As illustrated in figure 1 four measurements of the parietal bone were obtained The administration of 2.0 mc at 14 days of gestation again produced the largest effect. However the earliest that any decrease in size could be noted was at 20 days of gestation Lesser effects were noted with 1 0 mc at this time and with 2.0 mc at 17 days of gestation The reduction in size was marked for certain of these measures while the diminution in others was minimal This led to a posterior narrowing of the skull in the present instance. Measurements of the mandible again similar to those of Levy et al. showed a symmetrical reduction in size This decrease was notable as early as 19 days of gestation

Both of the measures of the femur were decreased by the administration of 2 0 mc at 14 days It is notable that the decrease length was much more pronounced than the decrease in diameter In fact only length was reduced by 1 0 mc After the injection of 2 0 mc at 17 days a substantial decrease in length was evident at 21 days of gestation and at birth whereas only a slight transient decrease in thickness was noted

The generalized decrease in the size of the animals is perhaps most evident in terms of the measure of the length of the vertebral column With the injection of 2 0 mc of P 32 at 14 days of gestation a decrease in this measure is evident from 16 days of gestation onward this shortening is only transient with lower doses A decrease in size is evident in the skeletons measured at 21 days of gestation and at birth after the injection of 2 0 mc at 17 days. A decrease in the size of the tail, considered alone was also noted but this is less marked and is evident only later

Several qualitative abnormalities have been noted in these skeleton The most prominent of these is a rib defect which consisted of a sharp cephalad angulation at about the dorsal third of the posterior several ribs with hyperostosis at the apex of the angle (see fig 4) This condition appears similar to that produced by Warkany and Schraffenberger when x ray doses between 250 and 1 120 r were administered at about the same times of gestation In the present experiment, this condition was almost universally present in the fetuses treated with 2 mc at 14 days of gestation It was also found, but with lower incidence after 1 mc at this time as is shown in table 2. The angulation and hyperostosis was only found after treatment with 2 mc when injection is made at 17 days of gestation

As is also indicated in table 2, a number of ossification defects were noted in the membrane bones There was less marginal ossification in the parietal and intraparietal bones after treatment with 1 0 or 2.0 mc at 14 days of gestation than in the controls. This resulted in significantly greater unossified areas bordering upon the associated sutures (fig 5) It is also to be noted that there was a marked diminution of the density of the ossified areas in the more heavily treated animals as compared to the controls As is indicated in this table there were a number of areas of increased porosity as well as other areas in which frank faults in ossification were noted especially in the mandible

It was noted in several of the intact fetuses that a pronounced kyphosis or scoliosis was present This did not show in the final preparations because of the flexibility which resulted from the clearing process Similarly waviness and kinks of tails which were noted in the intact animals have been obliterated in the course of preparation

DISCUSSION

The specific skeletal effects of radiophosphorus injection in the present experiments have been found to be somewhat different than those which result from acute x radiation at the same times of gestation As we shall indicate these differences may be expected for a number of reasons.

Levy et al (53) using acute external radiation found a general reduction in the size of various skeletal elements although there was no change in the proportions or

TABLE 2

Abnormal growth patterns and ossification defects after maternal administration of P-32 at 14 or 17 days of gestation

Anomaly	14 Day injection		17 Day injection	
	1.0 mc	2.0 mc	1.0 mc	2.0 mc
Mis-angulation and hyperostosis	Noted at 21 days and birth in some — mild	Noted at 18 days et. seq. Uniform and severe incidence	Not seen	Noted in some only mild-moderate
Decreased prominence of greater trochanter of femur	Noted in some at birth	Notable at 21 days and birth	Not noted	Noted in some at 21 days and birth
Cranial bones	Decreased extent of ossification in many. Occasionally increased porosity	Uniformly decreased ossification and increased porosity	Increase of unossified area — mostly limited to parietals	Decreased extent of ossified area in many. Decreased density and increased porosity
Digits	Retardation of ossification	Retardation of ossification	Retardation of ossification	Retardation of ossification
Mandible	Occasional ossification faults	Ossification faults in most	None notable	None notable
Sternum	Slight retardation of ossification	Marked retardation of ossification	Slight (?) retardation of ossification	Moderate retardation of ossification
Misc.		Occasional uncharacterized defects of intravertebral discs		

in the rate of growth or relative growth. Similarly in the experiments of Warren and Dixon (49) P 32 in the chick embryo produced a generalized reduction in size without an alteration in the proportion of the birds. In the present experiments however P 32 administration, especially at 14 days of gestation, did alter the relative shape of specific bones as well as major skeletal elements. Thus, as was demonstrated above the effect of irradiation was to decrease the rate of linear increase in the femur although there was a much lesser effect on the increase in the diameter of this bone. Similarly the differential effect in the parietal bone and other structures led to skulls which were of approximately normal length although they were markedly lowered and narrowed. Unfortunately the narrow range over which measurements were obtained as well as the intrinsic variability made it impossible to construct allometric graphs with a high degree of accuracy. Despite this lack of accuracy such plots have confirmed the observations obtained by inspection and by comparison of the measurements. However they are probably not suitable for a direct comparison with the results of Levy and his associates.

When our results are compared to those of Warkany and Schraffenberger a number of similarities as well as differences are seen. Certain of the malformation reported by these workers such as angulation and hyperostosis of the ribs and decrease of tail size were observed in the present experiments. Other malformations such as reduction in the length of the jaws and the production of cleft palate were not seen. It should be noted also that these workers found that the long bones of the body were in general quite normal after irradiation during this stage of gestation although in the present experiments there were alterations in these structures.

We may also note that in the present studies the porosity of certain of the mem-

branous bones as well as the normal ossification pattern was altered by the administration of P-32. Although it is difficult to infer directly from such observations the mechanism by which this occurs a few tentative postulates may be advanced. It is known that the deposition of phosphorus is not uniform throughout a structure and that there are areas of greater and lesser specific activity The presence of definite ossification faults may possibly be related to areas of increased activity A generalized decrease in the ossification of a structure on the other hand may well be related to a generalized radiation to that structure

Not the least of the reasons for these differences is the markedly greater radiation doses received by the developing skeleton in the present experiments. As was demonstrated in a previous report (57) and shown in figure 2 the shape of the curves of accumulated radiation dose to the bone depends on whether injection is made at 14 or at 17 days of gestation. It is found that about 2,200 rep are received by the fetal skeleton by the time birth when 2.0 mc are administered at 4, days of gestation When the same

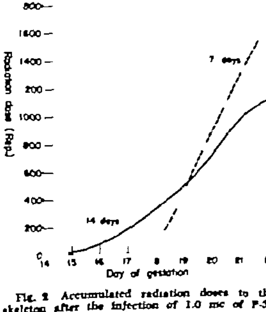


Fig. 2 Accumulated radiation doses to the skeleton after the injection of 1.0 mc of P-32 after 14 or 17 days of gestation.

amount of P 32 is injected at 17 days, greater than 3 000 rep are delivered to the skeleton by the time of birth At this dose level however it is to be noted that about 400 rep have been received by the skeleton by 17 days of gestation when injection is made at 14 days. Since the specific effects are much greater after injection at the earlier time we must conclude that as little as 400 rep over the three-day period between 14 and 17 days is capable of producing substantial damage to the developing skeleton.

Additionally we must consider two other important factors: dose rate and radiation energy As we have demonstrated recently (Sikov and Lofstrom '62) a decrease in dose-rate or an increase in radiation energy is capable of greatly reducing the amount of malformation produced by x radiation administered to the rat embryo. It is thus not remarkable that, despite the great magnitude of the radiation doses received by the skeleton the amount of damage is not even greater than was noted When injection is made at 14 days of gestation the average dose-rate to the skeleton is approximately 0 18 rep per minute and after injection at 17 days it approximates 0 41 rep per minute. These dose rates which are in the range studied in the above cited experiments, are quite low and would be expected to have a diminished teratogenic effect. Similarly the average beta energy from phosphorus-32 is substantially higher than the recoil-electron energy in the experiments of Levy et al. where 210 kvp x rays were used, possibly giving an RBE of less than one This difference would also be expected to tend towards producing a diminution of effect.

Levy et al. ('53) feel that their study and the literature indicate that skeletal differentiation in the mouse has been completed by 15 days of gestation. In the present experiments however injection of the rat at 14 days of gestation (which corresponds to about twelve and one-half days to 13 days in the mouse) and to a lesser extent at 17 days produces malformations as well as alterations in relative growth On the basis of the present experiments as well as from the results of

Warkany and Schraffenberger it is necessary to conclude that either the process of differentiation has not been completed at this time or that the skeleton is susceptible to the induction of malformations after the completion of differentiation.

SUMMARY

Pregnant female albino rats were given graded doses of radiophosphorus after 14 or 17 days of gestation and sacrificed at intervals after injection through birth. Randomly selected fetuses from each litter were cleared and stained. These specimens were examined for specific defects and several skeletal components were measured. A dose-dependent decrease in the overall size of the fetuses and of specific skeletal elements was noted this was more pronounced after injection at 14 days than at 17 Some alterations in relative growth as well as malformations and defects of ossification were observed These were more severe and frequent in those treated earlier in gestation The effects noted here have been compared to those obtained with acute external irradiation and the differences considered in terms of the greater radiation doses received by the skeleton using P-32.

ACKNOWLEDGMENT

The authors are grateful to Mrs. H Arndt and C. Resta for their technical assistance during the course of this study

LITERATURE CITED

Burstone, M. D. 1951 The effect of radioactive phosphorus upon the development of the embryonic tooth bud and supporting structures. Am. J Pathol 27 21–31

Finkel, M. P 1947 The transmission of radio-strontium and plutonium from mother to off spring in laboratory animals. Physiol. Zool. 20 405–421

Guyer M. F 1936 Animal Micrology University of Chicago Press Chicago, pp 117–119 157

Levy B M., R. Rugh, L. Lunin, N Chilton and M. Moss 1953 The effect of single subacute x-ray exposure to the fetus on skeletal growth; quantitative study J Morph 93 561–571.

Russell, L. B. 1954 The effects of radiation on mammalian prenatal development. In Radiation Biology A. Hollaender ed. McGraw-Hill Company Inc., New York, 1 Ch. 13.

Sikov M. R., and J E. Lofstrom 1957 The dosimetry and lethal effects of maternally administered phosphorus-32 after 14 and 17 days of gestation in the rat. Phys. Med. and Biol., 2: 157–168.

——— 1962 The influence of energy and dose-rate on the responses of embryonic rats to radiation. Radiology 79 302–309

Sikov M. R., J E. Lofstrom and T R. Noonan 1957 The effects of irradiation with phosphorus-32 on the viability and growth of rat embryos. Rad. Research., 7 541–550.

——— 1958 Anomalous development induced in the embryonic rat by the maternal administration of radio-phosphorus. Am. J Anat., 103 137–162.

Warkany J and E. Schraffenberger 1947 Congenital malformations induced in rats by roentgen rays. Skeletal changes in the offspring following single irradiation of the mother Am J Roentgenol. and Rad. Ther 57 455-463.

Warren, S., and F J Dixon 1949 Effects of continuous radiation on chick embryos and developing chicks. Radiology 52 714–729 869–850.

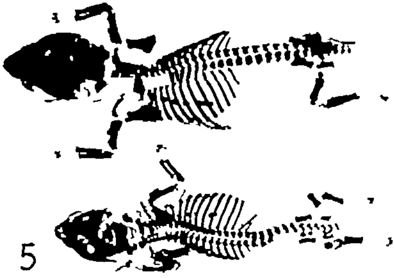


3 Representative 21 day fetuses — injected at 14 days. Reading from left: control, 0.6 mc, 1.0 mc, 2.0 mc. Females top row, males bottom row.

3b Representative 21 day fetuses — injected at 17 days. Reading from left: control, 0.6 mc, 1.0 mc, 2.0 mc. Females top row, males bottom row.
Note decrease in size and lessened ossification with increasing dose.



4



5

4 Control fetus at birth (at right) and representative fetuses which received 1.0 mc (center) and 2.0 mc (left) at 14 days of gestation. Note defect of ribs and decreased ossification, especially of the interparietals.

5 Control fetus at birth (above) and representative fetus which received 1.0 mc (below) at 14 days of gestation. Note increased porosity of cranial bones.

with a moderate increase in cornification. The squamous epithelium of the trigone was more dense than usual. The third case a 73-year-old woman received stilbestrol for two years which was stopped one year before death. Testosterone was then given for a year until two months prior to death. At this time stilbestrol therapy was resumed, 5 mg daily for the first month, and 20 mg daily thereafter Examination disclosed the epithelium of the vagina to be well differentiated and diffusely cornified. There was no squamous epithelium seen in the trigone; but squamous epithelium of the vesical neck and proximal urethra was well differentiated and cornified, which is unusual in patients of this age not receiving hormones.

My observations suggest that the basic characteristics of stratified squamous epithelium at the vesical neck, proximal urethra, and distal urethra, when such epi thelium is present at these sites, parallel those of the squamous epithelium of the vagina. This aspect of the study al though it does not include as many cases as the study of the trigone does include epresentative cases of pregnancy the cretory phase of the menstrual cycle and births and newborns where female sex hormone stimulus was high, as well as cases of other phases of the menstrual cycle and old age where such stimulus was low

Cornification has been specially studied with the Shorr (41) stain. The cornified cells stain orange in contrast to the green of the other epithelial cells Intraepithelial cornification can be seen in both trigone and vagina as reported by Cifuentes (47) and Dierks (27) (figs. 16 17) The corni fication process actually appears to start in the cells just above the basal cells and two cornified layers may be seen at times with non-cornified cells between them In one area three layers of cornification were observed in the vagina of one of the preg nant women (175 gm fetus) studied. In the trigone two layers of cornification are seen more rarely and the zone superficial to the cornified layer is relatively thinner This is interpreted as being at least partly due to processes such as urine washing the surface and expansion and contrac tion, which would remove the superficial cells more effectively than in the vagina In postmenopausal women a distinct intraepithelial layer of cornification may be present at times but frequently the corni fication in these cases is on the surface or is diffuse and patchy In the newborn cornification of the vagina is very diffuse rather than forming a dense layer These observations suggest that the cornification of the squamous epithelium of the vagina and trigone may be the result of estrogen stimulation which fluctuates with menses and is more constant late in pregnancy and in the postmenopause. Inasmuch as estrogens are thought to be capable of causing an increased cornification of vaginal cells (Shorr 40) this would seem to be the most likely explanation for variation in the site and degree of cornification. Whether the layer of cornification demarks the cells to be shed with menses as claimed by Dierks (27) is not certain; but it would seem that if the cornified layer were not largely shed two layers of cornification would be seen more frequently In some cases it appears that the cornified layer and deeper cells in some areas are shed during menses. This observation is consistent with the findings, concerning epithelial cells in urine sediments correlated with the menstrual cycle to be reported in another communication

DISCUSSION

Origin of stratified squamous epithelium in the trigone

There are at least three possibilities of origin of stratified squamous epithelium in the vesical trigone that should be considered. This squamous epithelium may result from metaplasia of preexisting transitional epithelium or develop from primitive cells capable of forming either transitional epithelium or squamous epithelium It may represent embryonically displaced squamous epithelium; or it may be that the squamous epithelium of the urethra extends into the bladder displacing the transitional epithelium.

By metaplasia is usually meant that the cell forming normal transitional epithelium can under certain circumstances form stratified squamous epithelium. Factors considered to be possible causes of this change are vitamin A deficiency pro-

longed irritation chronic infection, radiation, and hormonal stimulation such as by estrogens at high levels (Mostofi, '54 Zuckerman, 40)

The normal appearance of the epithelium would seem to be evidence against the theory of metaplasia, as nothing in the appearance of the stratified squamous epithelium suggests a pathologic condition. Intercellular bridges may not always be easily demonstrated (Cifuentes 47; Ney Ehrlich, '55) but in some they are readily apparent. They were particularly prominent in one of the pregnant women studied. Cornification and glycogen deposition also appear normal, suggesting normal metabolism. Adjacent transitional epithelium also appears normal. As Cifuentes ('47) has stated, squamous epithelium may occur in the trigone without inflammation being present clinically or histologically In none of the individuals having squamous epithelium in the trigone were there areas of similar epithelium present in other parts of the bladder or in the ureters or renal pelves. If a systemic factor were functioning to cause a metaplasia of the transitional epithelium, one might expect to see some evidence of metaplasia in these other locations. One factor which might cause metaplasia would be excessive estrogen stimulus. In the newborn in which estrogen stimulation is high, the squamous epithelium of the vagina, urethra, periurethral glands and parts of the prostate are often very prominent. The fact that no squamous epithelium was observed in the trigones of five male and 16 female newborns in which maternal estrogen stimulation is high indicates that the frequent presence of squamous epithelium in this location in females in later life is not simply the result of estrogen stimulation of transitional epithelium.

In considering the possibility that the squamous epithelium is embryonically displaced tissue a review of the pertinent embryology seems in order An attempt to evaluate the literature concerning the embryology of the lower urinary tract is difficult because of disagreements of experts. However certain of the concepts of Brockis ('52) and Wesson ('20) concerning the development of the trigone seem applicable and logical. The Wolffian duct is absorbed into the wall of the developing bladder until the ureteral bud also joins the bladder At this time the Wolffian ducts lie medial to the ureters. Then a relative craniolateral migration of the ureters, or possibly a caudal migration of the Wolffian ducts, takes place. The Wolffian ducts finally open into the male urethra at the lower end of the prostatic urethra and open distal or dorsal to the urethral meatus in the female embryo. This means that the trigone and urethra in the female are probably largely formed by either the Wolffian ducts or the ureters.

It has been noted by Brockis ('52) that the sites of ectopic ureteral orifices distal to the normal ureteral orifice can better be explained by a migration of the Wolffian ducts than by a migration of the ureters the ureter for the upper renal segment opening more distally A consideration of histologic features also seems consistent with this theory

Since the Wolffian ducts give rise not only to the ureters but also the epididymis, seminal vesicles (Moore '52) and possibly the prostate gland (Moullin, 1895) a structure formed by the Wolffian ducts themselves might be expected to have cells with various potentialities. Histologically the ureters and renal pelvis are lined by typical transitional epithelium. In the human, gland formation and squamous epithelium rarely if ever occur normally in these structures. On the other hand, the epithelium of most of the trigone and urethra has a different histologic appearance and apparently has various potentialities. It appears more dense more nuclear and less differentiated usually than the rest of the bladder and ureters. The epithelium of the urethra and lower trigone not rarely forms glandular structures. Johnson ('20) observes that the prostatic urethra in the embryo contains various types of cells. The embryonic origin of the glandular structures here is further supported by the finding of similar glands in the renal pelvis a Wolffian duct derivative under normal circumstances in certain animals (Johnson '37)

These observations suggest that the female urethra, prostatic urethra, and lower trigone in humans are more likely formed

from the Wolffian ducts than the ureters. This is consistent with Brockis's idea that the alteration in relationship of the Wolffian ducts and ureters during development is due to unequal absorption of the Wolffian ducts and active growth at their upper and outer lips rather than to a migration of the ureteral orifices (Brockis, '52). Considering the angle of entry of the ureter into the bladder and the development of an intravesical segment it may be that the ureteral orifices also migrate caudally but to a lesser degree than the Wolffian ducts.

As early as the eighth week of embryonic life the fused Mullerian ducts are in close proximity to the Wolffian ducts and appeared enveloped in the same tissue (Keith '33). The Mullerian ducts later open into the urethra, usually but not invariably distal to the openings of the Wolffian ducts (Lowsley '12). If the caudal migration of the Wolffian ducts is not complete at the time that the Mullerian ducts make contact with the urethra the stratified squamous epithelium in the urethra conceivably could come from the Mullerian ducts. The utriculus prostaticus or vagina masculinus, which is of Mullerian duct origin is lined by stratified squamous epithelium (Johnson '20). Comparison of the epithelium of this structure in the newborn, in which estrogen stimulus is high with that of the adult male is very suggestive of a profound estrogen influence similar to that in the vagina. Cifuentes ('47) notes Vilas's concept that the lining of the vagina is derived from the urogenital sinus and postulates that the islands of squamous epithelium in the trigone may come from embryonal residues of the mucosa of the urogenital sinus. Embryologists have also considered the possibility that urogenital sinus epithelium spreads onto the trigone (Hamilton, Boyd and Mossman '45). Zuckerman ('40) postulates that the caudal ends of the Mullerian and Wolffian ducts are invaded by epithelium from the urogenital sinus and that the caudal part of the sinus is infiltrated by ectodermal cells from the cloacal region. These ectodermal cells could be expected to produce squamous epithelium. The possibility that Mullerian cells could become displaced in the Wolffian ducts might also be considered in view of the possible similar origin of these structures (Hamilton, et al., '45). Also Wolffian ducts at times may connect with Mullerian ducts (Brockis, '52) so it does not seem unreasonable that on occasion Mullerian and Wolffian duct cells might become mixed. The presence of squamous cells of Mullerian, urogenital sinus, or cloacal origin in the Wolffian ducts could not only account for the squamous epithelium of the trigone and urethra but might also explain the presence of squamous epithelium in the vas deferens, seminal vesicles, and epididymis of the mouse (Zuckerman '40) and the seminal vesicles of rats following estrogen stimulation (Korenchevsky '41) and also the presence of leukoplakia and squamous cell epithelioma in the renal pelvis since these structures all develop from the Wolffian ducts. It is, of course possible that the problem of these rare pathologic conditions in the renal pelvis is unrelated. As far as the prostate gland is concerned, either Mullerian duct, Wolffian duct, or urogenital sinus origin could account for squamous epithelium being found in its substance since the prostate gland arises from the urethra, which is probably formed from the Wolffian ducts and the urogenital sinus (Johnson '20) with possibly some contribution from the Mullerian ducts.

From the study of the newborns, it would appear that in at least most cases there is no squamous epithelium initially in the trigone. However occasionally it may be found in patches in the proximal urethra. Its appearance, particularly in some junctional areas, suggests that this epithelium can spread and displace other cells particularly when it is being influenced by hormones. These factors suggest that the most likely origin of this epithelium is from a combination of embryonic inclusions and their ability to spread. In most instances the stratified squamous epithelium of the trigone has probably resulted from spreading of these cells from the urethra and vesical neck. In some it seems reasonable to postulate that similar embryonic inclusions may occur higher in the trigone.

CONCLUSIONS

1. Stratified squamous epithelium is commonly found in the trigone and vesical neck of adult women.

2. In basic characteristics of atrophy or maturation this epithelium usually resembles the vaginal epithelium in a given individual.

3. The squamous epithelium in the trigone and vagina both atrophy similarly with age, and they apparently respond similarly to hormonal influences as evidenced by their similarity to each other during the menstrual cycle and pregnancy.

4. The squamous epithelium of the female urethra and vagina are usually similar to each other in degree of differentiation and cornification, or atrophy in stillbirths and newborns and during young adult life, old age, and in pregnancy.

5. It seems possible that the stratified squamous epithelium on the trigone could result from inclusions of embryonic squamous epithelium in the proximal urethra and perhaps at times in the trigone. This epithelium perhaps develops differentiation and spreads to surrounding areas, particularly under hormonal influence until it occupies the areas where it is commonly found.

LITERATURE CITED

Brockis, J. G. 1952. The development of the trigone of the bladder with report of case of ectopic ureter. Brit. J. Urol., 24: 192–200.

Cifuentes, Luis. 1947. Epithelium of vaginal type in the female trigone. J. Urol., 57: 1028–1037.

Del Castillo, E. B., J. Argonz and C. G. Mainini. 1948. Cytological cycle of the urinary sediment and its parallelism with the vaginal cycle. J. of Clin. Endocrin., 8: 76–87.

Dierks, K. 1927. Der normale mensuelle Zyklus der Menschlichen Vaginal-Schleimhaut. Arch. f. Gyn., Bd. 130, S. 46–69.

Hamilton, W. J., J. D. Boyd and H. W. Mossman. 1945. Human Embryology (Prenatal Development of Form and Function) pp. 206, 211, 212. The Williams & Wilkins Company, Baltimore.

Heymann, A. 1906. Die Cystitis trigoni der Frau. Centralblatt f. d. Krkh. d. Harn u. Sex. Org., 16: 422, 1905. 17: 177.

Howard, F. S. 1947. Estrogen treatment of chronic urethritis in the female. California Medicine, 66: 352–354.

Johnson, F. P. 1920. The later development of the urethra in the male. J. Urol., 4: 447–502.

Johnson, F. R. 1957. Some proliferative and metaplastic changes in transitional epithelium. Brit. J. Urol., 29: 119–120.

Keith, Sir Arthur. 1933. Human Embryology and Morphology. 5th ed. pp. 66–67. William Wood & Co., Baltimore.

Korenchevsky, V. 1941. Some effects of sex hormones on the secondary sex organs of castrated male rats. J. of Path. & Bact., 52: 268–272.

Lencioni, L. J. 1953. Comparative and statistical study of vaginal and urinary sediment smears. J. of Clin. Endocrin. & Metab., 13: 263–270.

Lowsley, O. S. 1912. The development of the human prostate gland with reference to the development of other structures at the neck of the urinary bladder. Am. J. Anat., 13: 299–350.

Moore, T. 1952. Ectopic openings of the ureter. Brit. J. Urol. 24: 3–18.

Mostofi, F. K. 1954. Potentialities of bladder epithelium. J. of Urol., 71: 705–714.

Moullin, M. 1895. A contribution to the morphology of the prostate. J. Anat. and Physiol., 29: 201–204.

Ney, Charles, and J. C. Ehrlich. 1955. Squamous epithelium in the trigone of the human female urinary bladder. J. Urol., 73: 809–819.

Papanicolaou, G. N. 1933. The sexual cycle in the human female as revealed by vaginal smears. Am. J. Anat., 52, no. 3, supplement 519–637.

Salmon, U. J., R. I. Walter and S. H. Geist. 1941. The use of estrogens in the treatment of dysuria and incontinence in post-menopausal women. Am. J. Obst. & Gynec., 42: 845–851.

Shorr, E. 1940. Effect of concomitant administration of estrogens and progesterone of vaginal smears in man. Soc. Exper. Biol. & Med. Proc., 43: 501–506.

——— 1941. New technic for staining vaginal smears; single differential stain. Science 94: 545–546.

Shorr, E., G. N. Papanicolaou and B. F. Stimmel. 1938. Neutralization of ovarian follicular hormone in women by simultaneous administration of male sex hormone. Soc. Exper. Biol. & Med. Proc., 38: 759–762.

Smith, B. B., E. K. Brunner. 1934. The structure of the human vaginal mucosa in relation to the menstrual cycle and to pregnancy. Am. J. Anat., 54: 27–85.

Smith, B. G. 1929. Histological changes in the epithelium of human vagina correlated with the menstrual cycle. Anat. Rec., 43: 317–343.

Traut, H. F., P. W. Bloch and M. A. Kuder. 1936. Cyclical changes in the human vaginal mucosa. S. G. & O., 63: 7–15.

Wesson, M. B. 1920. An anatomical, embryological and physiological studies of the trigone and neck of the bladder. J. Urol., 4: 279–316.

Youngblood, V. H., E. M. Tomlin and J. B. Davis. 1957. Senile urethritis in women. J. Urol., 78: 150–152.

Zondek, B., and M. Friedman. 1936. Are there cyclic changes in the human vaginal mucosa. J. A. M. A., 106: 1051–1054.

Zuckerman, S. 1940. The histogenesis of tissues sensitive to estrogens. Biol. Rev. 15: 231–271.

PLATE 1

EXPLANATION OF FIGURES

All figures are from hematoxylin-eosin stained preparations, except figures 16, 17

2 A patch of squamous epithelium in the proximal urethra of newborn female. 150 ×

3 Urethra-vaginal septum of a term female fetus with the urethra t the left. Note the thickened squamous epithelium of the distal urethra as well as the vagina presumably due to maternal hormone influences. An apparently separated path of squamous epithelium in the proximal urethra (lower left hand corner) is enlarged in figure 4 8 ×

4 A patch of squamous epithelium with transitional epithelium proximally and distally in the proximal urethra of term female fetus. 75 ×

5 Immature squamous epithelium removed from the vesical neck *of an eight-year-old girl during* transurethral resection for vesical neck obstruction. 150 ×

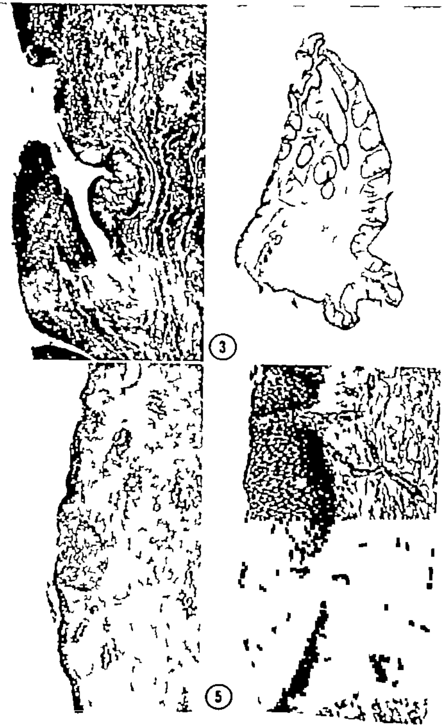

2
3
4
5

PLATE 2

EXPLANATION OF FIGURES

6 Stratified squamous epithelium in the vesical trigone of 41-year old woman in the early secretory phase of the menstural cycle as determined from the endometrium. 40 ×

7 Vagina of case in figur 6. 40 ×

8 Stratified squamous epithelium in the vesical trigone of 31 year-old woman in the early menses phase of the menstrual cycle. 40 ×

9 The vaginal epithelium f the same case as in figure 8 40 ×

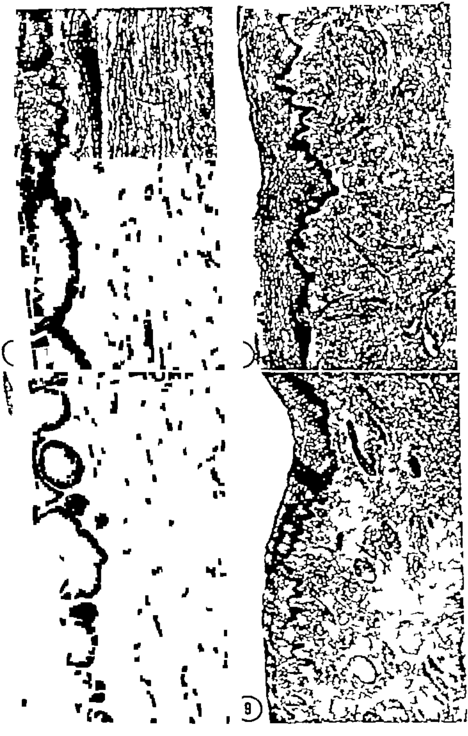

9

PLATE 3

EXPLANATION OF FIGURES

10 Stratified squamous epithelium in the vesical trigone f a 36-year old woman in the late menses and early proliferative phase of the menstrual cycle. 40 ×

11 V ginal epithelium of same case as in figure 10 40 ×

12 Stratified squamous epithelium in the trigone of 44-year-old woman in the proliferative phase of the menstrual cycle 40 ×

13 Vaginal epithelium f same case as in figure 12. There is probably moderate change due to utolysis in much of this section. Where preserved it is basically simil to the trigone squamous epithelium. 40 ×

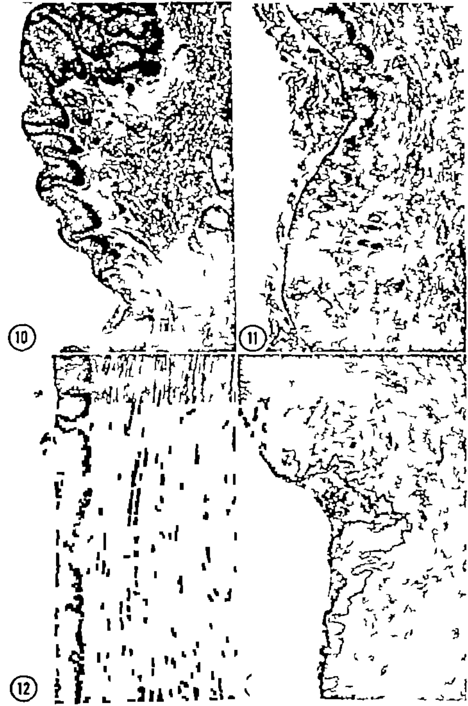

10
11
12

PLATE 4

EXPLANATION OF FIGURES

14 The thickened and vesicular stratified squamous epithelium in the vesical trigone of 17-year-old woman pregnant with 175 gram fetus. 40 ×

15 Vaginal epithelium from the same case as figure 14. 40 ×

16 Stratified squamous epithelium in the vesical trigone of 67 year-old woman which has distinct intraepithelial cornified layer. Shorr Stain. 40 ×

17 V ginal epithelium from the same case a figure 16 showing similar layer of intraepithelial cornification. Shorr Stain. 40 ×

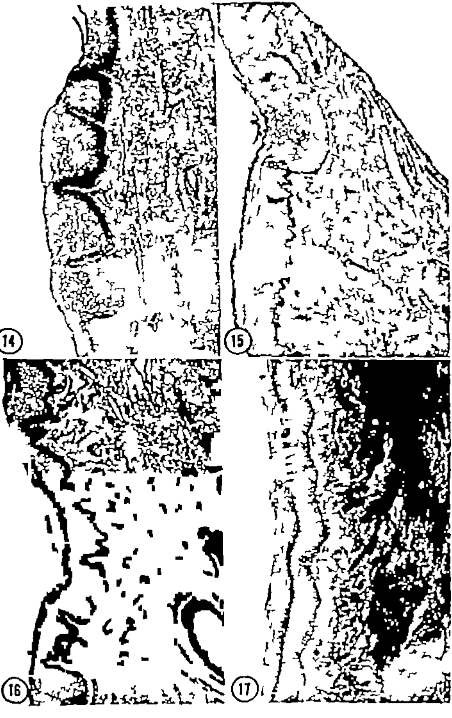

14
15
16
17

PLATE 5

EXPLANATION OF FIGURES

18 Atrophic stratified squamous epithelium in the vesical trigone of an 62-year-old woman. 40 ×

19 Atrophic vaginal epithelium from the same case as figure 18. 40 ×

20 Moderately atrophic stratified squamous epithelium in the vesical trigone of 58-year-old woman. 70 ×

21 Vaginal epithelium from the same case figure 20. 70 ×

SQUAMOUS EPITHELIUM IN TRIGONE
Donald E. Tyler



Index

H

I

K

L

M

O

P

Q

R